DOE/BC/14882-10
Distribution Category UC-122

RESPONSIVE COPOLYMERS FOR ENHANCED PETROLEUM RECOVERY

Second Annual Report

By
Charles McCormick
Roger Hester

May 1995

Work Performed Under Contract No. DE-AC22-92BC14882

Prepared for
U.S. Department of Energy
Assistant Secretary for Fossil Energy

Jerry Casteel, Project Manager
Bartlesville Project Office
P.O. Box 1398
Bartlesville, OK 74005

Prepared by
University of Southern Mississippi
Department of Polymer Science
Hattiesburg, MS 39406

DISCLAIMER

DISCLAIMER

Portions of this document may be illegible in electronic image products. Images are produced from the best available original document.

Nomenclature

Å	Angström
A	UV absorbance
A_2	Second viral coefficient
A_3	Third viral coefficient
a_i	Pre-exponential factor of ith component
B_j	Coefficients of the test model, Equation 1, **(Chapter 10)**
b_j	Coefficients of the coded test model, Equation 8, **(Chapter 10)**
$\underline{b}$	Vector containing b_j coefficients
C	Solution concentration
C*	Critical overlap concentration
C_1	Critical aggregation concentration
C_2	Critical mecille concentration
CMC	Critical micelle concentration
C_p	Polymer concentration
D_{app}	Apparent translational diffusion coefficient
D_{true}	True translational diffusion coefficient
D_e	Deborah Number
D_o	Diffusion coefficient
DP	Degree of polymerization
$\Delta\ell$	Incremental length of bed
ΔP	Fluid pressure drop
ΔX	Half of separation value between X independent variables
ΔY	Half of separation value between the Y independent variables
G'	Sstorage modulus
G"	Loss modulus
I_1/I_3	Ratio of first to third vibronic band in fluorescence emission spectrum of pyrene probe
I_E/I_M	Ratio of the intensity of naphthalene or pyrene excimer fluorescence emission to monomer fluorescence emission
K	Equilibrium constant
K	Light scattering optical constant **(Chapter 10)**
L	Path length
M	Polymer molecular weight
$\underline{\underline{M}}$	Matrix defined by Table II
$\underline{\underline{M}}^r$	Transpose of matrix $\underline{\underline{M}}$
M_W	Weight average molecular weight
M_1, M_2	Mean sequence length of M_1, M_2 repeat units in copolymer
M_1-M_1, M_2-M_2	Mole % blockiness of comonomer M_1-M_1, M_2-M_2
M_1-M_2	Mole % alternation in M_1-M_2 copolymer
M_w	Weight-average molecular weight
R	Gas law constant
R	Average response of all test conditions **(Chapter 10)**
$\underline{R}$	Vector containing R_i responses
R_e	Reynolds numbe

R_i	Average response at test condition i
R_g	Polymer radius of gyration
R_h	Polymer hydrodynamic radius
R_θ	Rayleigh ratio of light scattering intensities
S_{A2}	Standard error of the second viral coefficient
S_D	Standard error of the true diffusional coefficient
S_j	Estimated standard error associated with real space model coefficients
S_{MW}	Standard error of the weight average molecular weight
S_{RG}	Standard error of the radius of gyration from DLS
S_{Rg}	Standard error of the radius of gyration from SLS
S_{Rh}	Standard error of the hydrodynamic radius
T	Absolute temperature
T_1	Spin-lattice relaxation time
$\underline{\underline{V}}$	Variance-Covariance matrix
$\underline{X}$	Real space independent variable
$\overline{X}$	Average value of X independent variables
$\underline{Y}$	Real space independent variable
$\overline{Y}$	Average value of Y independent variables
d	Spherical particle diamater
f	Solution friction factor
f_s	Solvent friction factor
g	Index counter for Equation 11, **(Chapter 10)**
i	Index counter for experimental test conditions
j	Index counter for model coefficients
k	Spacing constant for Zimm Plot
k_B	Boltzman constant
m	Total number of test conditions
n	Refractive index
r	Adjusted correlation coefficient
r_1	Reactivity ratio of monomer 1 in a copolymerization
r_1r_2	Product of reactivity ratios r_1 and r_2
r_2	Reactivity ratio of monomer 2 in a copolymerization
s_e	Estimated experimental data
s_j	Estimated standard error associated with coded test model coefficients
tan δ	G"/G' = loss modulus/storage modulus
$t_{0.05}$	Student "t" distribution value at 90% confidence level
u	Dependent variable of Equation 20, **(Chapter 10)**
v_j	Variance associated with coded test model coefficients
x	Coded space independent variable
w_j	Independent variables of Equation 20, **(Chapter 10)**
y	Coded space independent variable
z	Number of measurements at a given test condition
α	Coefficient in Equations 40 and 42 **(Chapter 10)**
α	Ln (maximum normalized flow resistance) in the limit of zero polymer concentration **(Chapter 11)**
$1-\alpha$	Confidence level **(Chapter 10)**

β	Coefficient in Equations 40 and 43 **(Chapter 10)**
β	Change in 1n $\psi_{max}$with respect to a change in dimensionless polymer concentration
γ	Surface tension
δ	Coefficient in Equations 40 and 44 **(Chapter 10)**
ϵ	Elongation rate **(Chapter 11)**
κ	Proportionality constant in Equation 44 **(Chapter 10)**
λ	Wavelength
λ_0	Wavelength of light scattering radiation
η_{app}	Apparent viscosity
η_0	Solvent viscosity
η_{red}	Reduced viscosity
η_s	Solvent shear viscosity
$[\eta]$	Polymer intrinsic viscosity
θ	Scattering angle
ξ	Coefficient in Equations 40 through 45 **(Chapter 10)**
ρ	Fluid density
τ	Polymer coil response time
$[\tau]$	Average fluorescence lifetime
υ	Average fluid veloctiy **(Chapter 11)**
υ	Proportionality constant in Equation 45 **(Chapter 10)**
χ	Coefficient in Equation 40 **(Chapter 10)**
ψ	Normalized solution flow resistance
ψ_{max}	Maximum normalized solution flow resistance

CHAPTER ONE: BACKGROUND, OBJECTIVES, AND OVERVIEW OF RESEARCH DURING FY 1994

I. Introduction

Advanced copolymer and terpolymer systems are being studied under a coordinated research program in the Polymer Science Laboratories at the University of Southern Mississippi. In this report we described second year efforts in synthesis, characterization, and rheology to develop polymers with significantly improved efficiency in mobility control and conformance as compared to conventional systems. Key features of these microstructually tailored systems allow triggered response to environmental stimuli including pH, ionic strength, electrolyte concentration, and shear. Ampholytic and/or hydrophobic interactions between polymer chains can be designed for desired reological response. The polymers have potential to circumvent problems inherent in traditional EOR polymers where molecular weight must be compromised to allow sufficient permeation without plugging of the porous reservoir network. Most conventional polymers fail in high calcium, barium, or sodium concentrations, precluding use in high salinity fields or off-shore. By contrast, these advanced polymer systems would maintain high viscosities or behave as virtual gels under low shear conditions and at elevated electrolyte concentrations. At high fluid shear rates, associates would deaggregate yielding low viscosity solutions, reducing problems of shear degradation or face plugging during injection. Other promising polymer systems developed during the past year are polymeric surfactants with potential for use in higher salt, higher temperature reservoirs for mobilization of entrapped oil.

Since 1978, DOE-sponsored research projects in our laboratories have been directed at establishing unifying concepts regarding interrelationships between tailored polymer structures and fluid behavior under controlled salinity, pH, concentration, shear, and flow through porous media. We have demonstrated that nearly every significant behavioral characteristic of polymer solutions in mobility control can be related to macromolecular architecture and hydrodynamic volume. These include:

- concentrations required for mobility control
- viscosity in the presence of electrolytes
- phase stability as a function of ionic strength and temperature
- adsorption to porous media
- network pore clogging
- sweep efficiency and slug dispersion
- shear thinning effects
- molecular associations
- polymer/surfactant interactions

II. Overall Research Goals and Approach

The overall goal of this research is to prepare *advanced copolymers* for use as mobility control agents in EOR that rely on *microheterogeneous associations* (Scheme II-1) or *ampholytic associations* (Scheme II-2) to produce high viscosity in aqueous solutions yet are shear thinning. Such molecules would: (a) be efficient viscosifiers at low concentration and moderate molecular weight, (b) maintain or increase viscosity of the solution in the presence of mono- and/or multivalent electrolytes, (c) maintain or increase viscosity at higher temperatures or with pH changes, and (d) flow through relatively tight porous substrates under high shear stresses yet retard flow at low shear stress due to associative properties.

Scheme II-1. Proposed interaction of associative, hydrophobically modified polymers. Association is favored by addition of NaCl or other electrolytes and by increasing temperature. Dissociation is favored by application of a shearing stress. Work in our laboratories and at Exxon clearly demonstrates this effect. Additionally, dissolution in aqueous media can be enhanced and adsorption onto porous substrate reduced by incorporating charged carboxylate or sulfonate groups onto the copolymers.

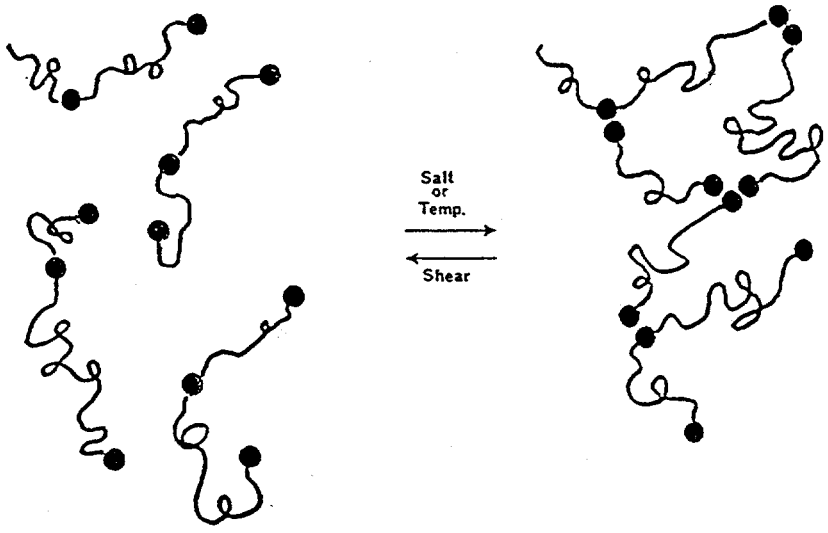

Scheme II-2. Polyampholyte expansion in salt solution. Copolymers with zwitterionic monomers or comonomer pairs exhibit low solution viscosity in water. As electrolyte is added expanded chain conformation results in enhanced viscosity. Gelation can occur with proper choice of monomers. This effect can be reversed.

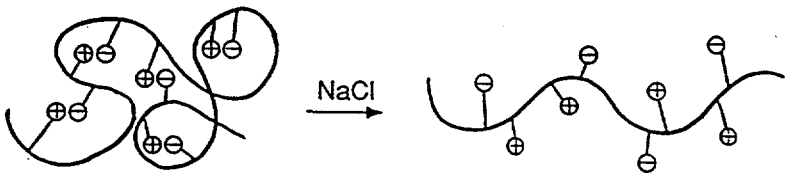

Compact Chain

Expanded Chain

A second major goal is to investigate the feasibility of utilizing a *hydrophobically modified polymer* as both the *surfactant* to emulsify oil and as a *viscosifying agent* (Scheme II-3) to increase sweep efficiency in EOR. The oil phase swells the polymer micelles which, in turn, would yield increased viscosity in the channels and pores. Such a polymer would eliminate the requirement of separate injections of a surfactant slug and a polymer slug and would avoid the attendant problems of polymer-surfactant mixing and slug dispersion normally encountered in micellar/polymer flooding.

Specific research objectives are

- Synthesis of advanced copolymers which rely on hydrophobic or ampholytic associations at low concentration for rheological control. Such associations are responsive to changes in pH and ionic strength.

- Synthesis and characterization of hydrophobically modified copolymers which can serve as both surfactant and viscosifier in EOR.

- Determination of hydrodynamic volume utilizing viscometry, low angle laser light scattering (LALLS), dynamic light scattering (DLS), and size exclusion chromatography (SEC) techniques.

- Development of predictive models based on interrelationships of molecular structure and solution behavior under operational conditions of temperature, shearing stress, concentration, and ionic strength.

- Technology transfer to the private sector for scale-up and field testing.

- Education and training of young scientists in innovative energy recovery research.

Scheme II-3. Polymeric surfactant-hydrophobic micelles swell upon contact with oil and interact coperatively resulting in oil emulsification and an increase in viscosity.

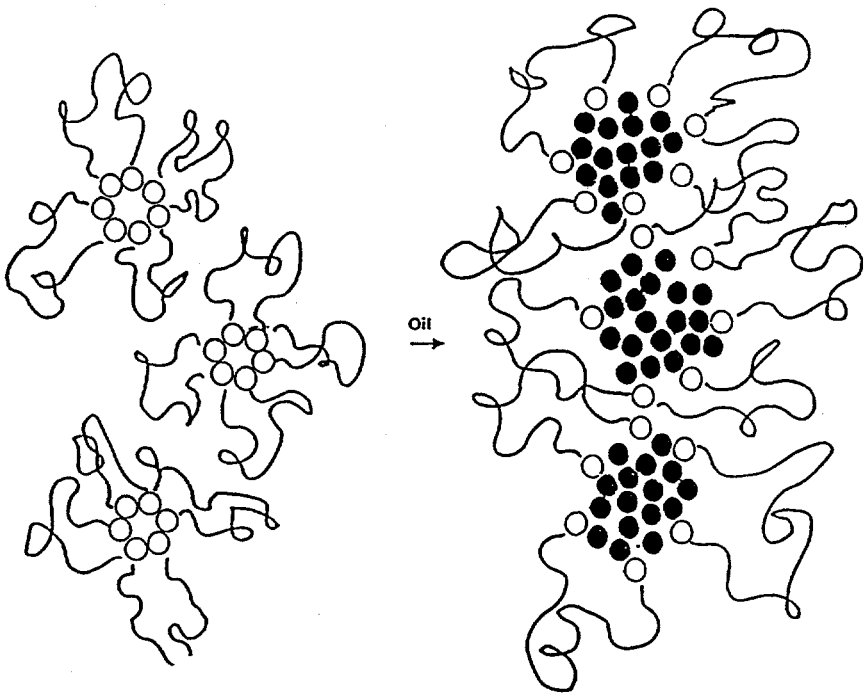

III. Advanced Copolymer Synthesis/Characterization/Solution Behavior

A. Conceptual Design

The three advanced copolymer systems conceptually illustrated in Scheme II-1 through II-3 have been prepared utilizing monomers shown in Scheme III-1 . Acronyms have been utilized to simplify nomenclature. Synthesis, characterization, and solution behavior of co- and terpolymers AM/NaAMB, AM/NaAMB/RAM, AM/NaAMB/AMPDAC, AM/AMPDAPS, and AM/APS are described in our First Annual Report, DOE/BC/14882-5 (August 1994).

Copolymers and terpolymers studied during the second year are overviewed in the sections of this chapter to follow. Details are found in Chapters Two through Eleven of this Annual Report.

Scheme III-1. Representative Monomers for Synthetically tailored EOR Polymers.

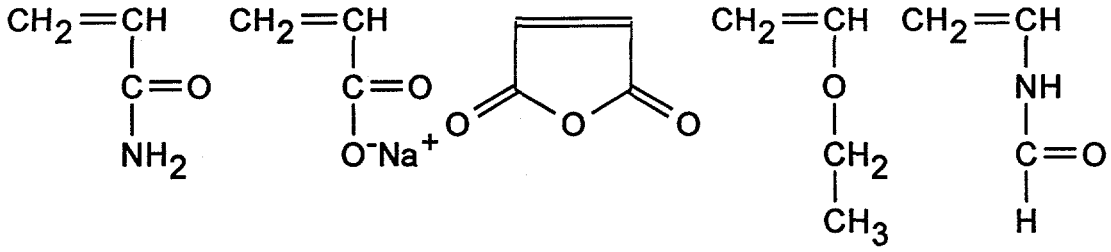

AM **NaA** **MA** **EVE** **NVF**

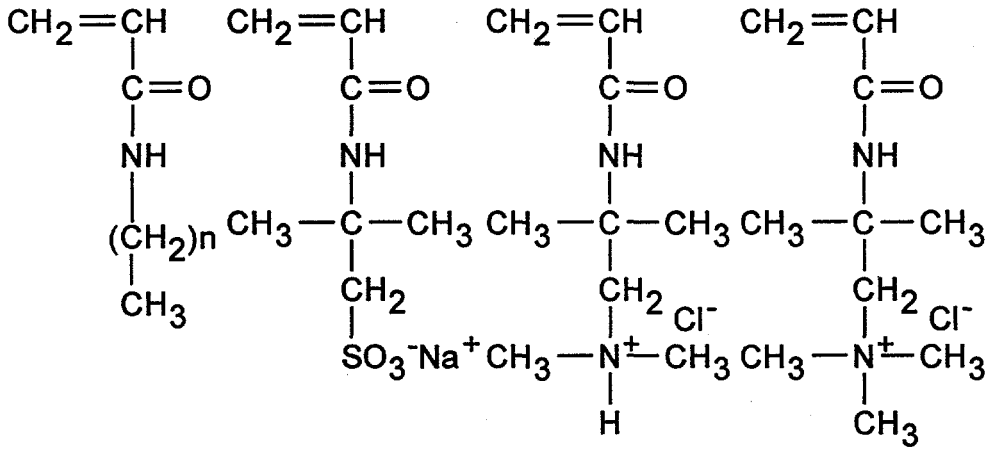

RAM **NaAMPS** **AMPDAC** **AMPTAC**

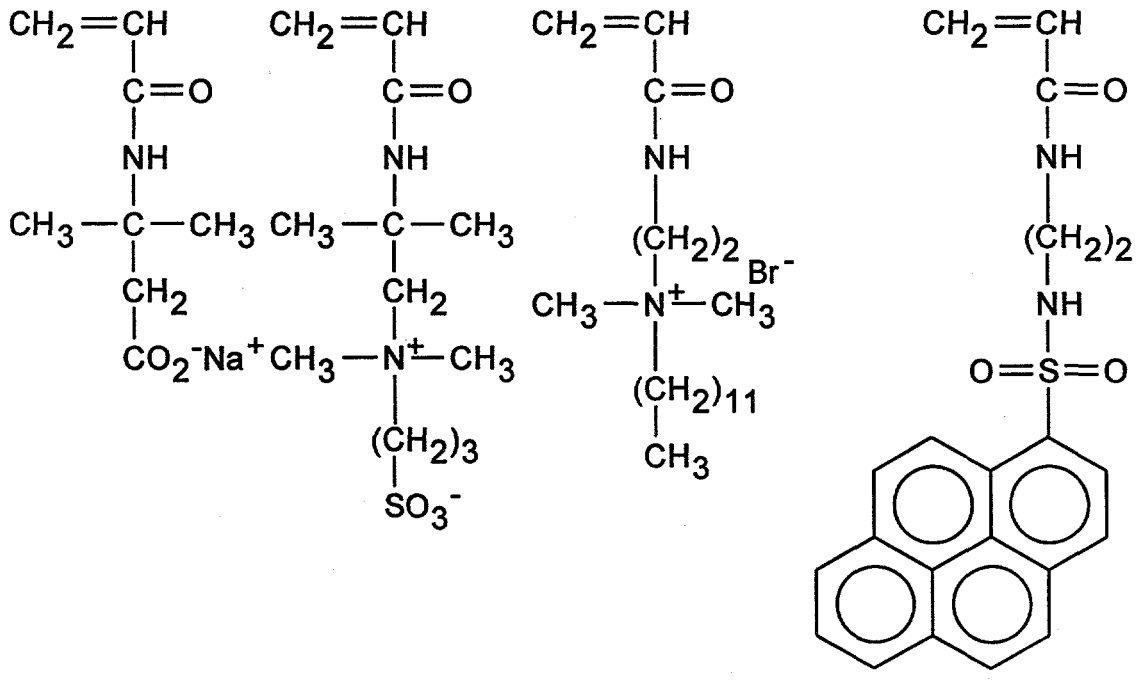

NaAMB **AMPDAPS** **DAMAB** **APS**

B. Terpolymers of AM/NaAMB/AMPTAC

Chapter Two describes zwitterionic terpolymers prepared from acrylamide (AM), sodium 3-acrylamido-3-methylbutanoate (NaAMB), and 2-acrylamido-2-methylpropanetrimethylammonium chloride (AMPTAC). The terpolymer with 10 mole% of NaAMB and 10 mole% of AMPTAC undergoes a 700% increase in intrinsic viscosity when NaCl concentration is increased from 0.05 to 1M. Such terpolymers offer potential as mobility control agents in EOR in high salinity conditions.

C. Copolymers of AMPDAPS and AM

Chapter Three describes a series of ampholytic copolymers which increase in viscosity upon addition of NaCl and $CaCl_2$ and upon increasing temperature from 25 to 60°C. The copolymers are prepared by free radical initiation of the sulfobetaine monomer 3-(2-acrylamido-2-methylammonio)-1-propane sulfonate (AMDAPS) and acrylamide (AM). These polymers, like those described in Chapter Two have potential as mobility control agents due to their electrolyte tolerance.

D. Copolymers of NVF

In Chapters Four and Five, fundamental studies of the reactivity of N-vinyl formamide (NVF), a water soluble comonomer, with the comonomers maleic anhydride (MA), acrylamide (AM), sodium acrylate (NaA), and n-butylacrylate are detailed. Reactivity ratios, structural compositions, and monomer distributions are proposed based on experimental data. NVF yields highly alternating compositions with AM, NaA, and n-butylacrylate.

E. Hydrophobically Associating Co-and Terpolymers

Chapters Six, Seven, and Eight describe our efforts during FY-1994 at synthesis of hydrophobically-associating polymers with high viscosity due to intermolecular chain interactions. Polymers of this type offer potential in EOR since they can a) associate with surfactants to enhance viscosity, b) act as polymeric emulsifiers, and c) undergo pH, salt, or shear reversible associations (viscosification).

In Chapter Six, synthesis of the monomer dimethyldodecyl(2-acrylamidoethyl) ammonium bromide (DAMAB) and its copolymer with acrylamide are described. The copolymer containing 10% DAMAB shows outstanding rheological properties. The onset of associations, C*, occurs at lower values of polymer concentration in aqueous solutions and the viscosity increases more rapidly above this value as compared to previously prepared n-alkylacrylamide/acrylamide copolymers. The interactions of the DAMAB copolymers with anionic, cationic, and non-ionic surfactants are described in Chapter Seven. The anionic surfactant has significant binding to the polycationic copolymer.

In Chapter Eight polymeric surfactants or "polysoaps" prepared by amidation (using alkylamines or naphthylamines) of preformed, alternating copolymers of maleic anhydride (MA) with ethyl vinyl either (EVE) are described. Photophysical and viscosity measurements have

been used to determine the pH-, and salt- responsive behavior of these polymers. Intramolecular associations are present which afford opportunities for hydrocarbon sequestration (emulsification) in EOR applications.

F. Characterization of HMW Acrylamide Copolymers by ^{13}C NMR

A new technique is described in Chapter Nine for characterizing high molecular weight, acrylamide copolymers using direct-polarization magic angle spinning ^{13}C nuclear magnetic resonance. The rapid technique providing analyses of copolymer compositions superior to those obtained conventional methods, has been applied to advanced EOR copolymers including polyelectrolytes, polyampholytes, and polysoaps.

G. Use of Factorial Experimental Design in Light Scattering Characterization of Water Soluble Polymers

When characterizing solutions of large, water soluble, random coil polymers by static light scattering or dynamic light scattering, regression is used to fit experimental data to linear relationships. These polynomial relationships contain two independent variables, sample concentration and scattering angle, and a response or dependent variable that is related to radiation intensities or intensity fluctuations. The coefficients of the terms in the polynomial are used to estimate parameters such as molecular weight and polymer coil radius of gyration. Because of dust in the samples, a high level of experimental noise is always in the scattering data. This makes it difficult to decide which polynomial model is appropriate. Chapter 10 discusses the use of a factorial experimental design data analysis technique to obtain the best model for fitting light scattering data. The molecular parameters obtained from this model are more accurate than would be obtained using conventional data analysis techniques.

H. Porous Medium Elongational Studies of NaAMB / AM Copolymer Solutions

In Chapter 11 the construction of a porous media rheometer is described. It was used to compare the fluid flow properties of AM / NaAMB copolymer solutions and acrylamide homopolymer solutions in beds of solid spheres. The polymer solutions were characterized by using the rheometer to collect the data necessary to plot a Normalized Solution Flow Resistance as a function of the Deborah Number. The Normalized Flow Resistance is directly related to the polymer coil elongation during flow through the converging and diverging cavities of the porous media. The Deborah Number describes the fluid extensional flow field in the porous media and is the ratio of polymer coil extensional response time to the flow field process time. Of all polymers examined using this technique, the AM / NaAMB 80 / 20 copolymer solutions had the largest resistance to flow. This copolymer is an excellent candidate for use as an advanced EOR polymer because this polymer can be highly extended in low velocity flow fields.

RELATED DISSERTATIONS

"^{23}NMR Studies of Ion-Binding Homopolyelectrolytes and Conformational Changes in Hydrophobically-Modified Polyelectrolytes," J. Kent Newman, 1993

"Synthesis, Characterization and Solution Behavior of Hydrophobically Modified Polyececctrolytes, Yihua Chang, 1993.

"Structurally Tailored Water Soluble Polymers for the Study of Drag Reduction," Pavneet S. Mumick, 1993.

"Investigations of Polymeric Drag Reduction: A Proposed Model and Experimetnal Evidence," James P. Dickerson, 1993.

RELATED PUBLICATIONS

1993

"Water Soluble Copolymers. XLII. Cationic Polyelectrolytes of Acrylamide and 2-Acrylamido-2-Methylpropanetrimethylammonium Chloride," C. L. McCormick and L. C. Salazar, *J. Poly. Sci.: Part A—Poly. Chem.*, *31*, 1099-1104 (1993).

"Water Soluble Copolymers 45. Ampholytic Terpolymers of Acrylamide with Sodium 3-Acrylamido-3-Methylbutanoate and 2-acrylamido-2-Methylpropanetrimethylammonium Chloride," C. L. McCormick and L. C. Salazar, *J. Appl. Poly. Sci., 1115-1120* (July 1993).

"Analysis of Hydrophobically Modified Copolymers Utilizing Spectroscopic Probes and Labels," Chapter 2 in *Macromolecular Complexes in Chemistry and Biology*, C. L. McCormick, K. D. Branham, R. Varadaraj, and J. Bock; Springer Verlag, NY 1993.

"Water Soluble Copolymers. 47. Copolymerization of Maleic Anhydride and N-Vinylformamide: Charge Transfer Complexation of the Monomers and Their Reactivity Ratios," Y. Chang and C. L. McCormick, *Macromolecules 26,* 4814-4817 (1993).

"Water Soluble Copolymers. 48. Reactivity Ratios of N-vinylformamide with Acrylamide, Sodium Acrylate, and n-Butyl Acrylate," Erich E.L. Kathmann and C. L. McCormick, *Macromolecules 26, 52-49-5252* (1993).

"Water Soluble Copolymers. 49. Effect of the Distribution of the Hydrophobic Cationic Monomer DAMAB on Solution Behavior of Associating Acrylamide Copolymers," Y. Chang and C. L. McCormick, *Macromolecules 26, 6121-6126* (1993).

CHAPTER TWO: AMPHOLYTIC TERPOLYMERS OF ACRYLAMIDE WITH SODIUM 3-ACRYLAMIDO-3-METHYLBUTANOATE AND 2-ACRYLAMIDO-2-METHYLPROPANETRIMETHYLAMMONIUM CHLORIDE

Abstract

Water soluble, low charge density polyampholytes have been synthesized by free radical terpolymerization of acrylamide (AM) with sodium 3-acrylamide-3-methylbutanoate (NaAMB) and 2-acrylamido-2-methylpropanetrimethylammonium chloride (AMPTAC). Terpolymer compositions obtained by ^{13}C NMR reflect monomer feed concentrations. Molecular weights and second virial coefficients range from 3.43 to 19.4 x 10^6 g/mol and 1.63 to 3.61 ml·mol/g^2 respectively as determined by low angle laser light scattering. Ionic associations were explored by investigating the dilute solution properties as a function of terpolymer concentration, terpolymer charge density and added electrolytes. Terpolymers with 0.5, 2.5 and 5.0 mole percent of both of the cationic (AMTAC) and anionic (NaAMB) monomers were soluble in deionized water while those with 10 and15 mole percent of each monomer required electrolyte addition. The higher density terpolymers undergo 700% increase in intrinsic viscosity upon changing NaCl concentration from 0.05M to 1M. Polyelectrolyte behavior could be induced by decreasing solution pH below the pKa of the NaAMB mer. Intermolecular ionic associations resulting in gel networks were studied utilizing dynamic mechanical analysis.

Introduction

Only a limited number of synthetic polyampholytes have been reported in the literature that possess the carboxylate moiety as the anionic group. Early studies incorporated methacrylic acid and various ammonium species that provided high charge density polymers that were polyampholytes at their isoelectric points[1-3]. The polymers were polyanions in alkaline solution and polycations in acid solution. Nonaka and Egawa[4] treated potassium polymethacrylate with 3-chloro-2-hydroxypropanetrimethylammonium chloride to obtain polymers with various amine/acid ratios. Merle, et al.,[5] compared polyampholytes prepared by the hydrolysis or acidolysis of poly(N,N-dimethylaminoethyl methacrylate to polymers made by the copolymerization of N,N-dimethylaminoethyl methacrylate and methacrylic acid.

Polyampholytes with regular structures have also been reported which incorporated the carboxylate group but solution properties were rarely mentioned.[6-8] Zwitterionic polyampholytes have been made with the carboxylate as part of a betaine functionality.[9] Wielma studied the synthesis and solubility of zwitterionic polymers with carboxylate moieties.[9] Varying degrees of ionization were achieved for the carboxylate groups by controlling the pH. At high pH values, the polymers behaved as polyampholytes whereas at low pH values polyelectrolyte behavior was observed.

Previously we reported ampholytic terpolymers containing the carboxylate group as the negatively charged moiety.[10-12] Sodium 3-acrylamido-3-methylbutanoate (NaAMB) was polymerized with 2-acrylamido-2-methyldimethylammonium hydrochloride (AMPDAC) and acrylamide (AM) as a neutral spacer. The superabsorbing terpolymers formed highly swollen gels even with added electrolytes due to strong intermolecular interactions. By contrast structurally homologous terpolymers synthesized with the sulfonate monomer were soluble in deionized water and exhibited viscosity increases as electrolytes were added.[13] Both intra- and intermolecular associations were observed in agreement with other literature reports on similar structures.[14] In this study we report electrolyte-soluble ampholytic terpolymers of acrylamide with the anionic monomer NaAMB and the cationic monomer AMPTAC.

Experimental

Materials and Monomer Synthesis

Sodium 3-acrylamido-3-methylbutanoate (NaAMB) monomer was synthesized via a Ritter reaction of equimolar amounts of 3,3-dimethylacrylic acid with acrylonitrile as reported by Hoke and Robins[15] and as modified by Blackmon.[16] Synthesis of 2-acrylamido-2-methylpropanetrimethylammonium chloride (AMPTAC) by a multistep procedure has been previously reported.[12,17] Briefly, 2-acrylamido-2-methylpropanedimethylamine was reacted with a ten-fold excess of methyl iodide in refluxing diethyl ether then ion-exchanged to yield AMPTAC.

Synthesis of Terpolymers of NaAMB with AMPTAC and AM

Terpolymers of AMPTAC with NaAMB and AM (the ATABAM series) were synthesized by free radical polymerization in a 0.5M NaCl aqueous solution under nitrogen at 30°C using 0.1 mol % potassium persulfate as the initiator. The feed ratio of AM:NaAMB:AMPTAC was varied from 99.0:0.5:0.5 to 70:15:15 mol % with the total monomer concentration held constant at 0.45M. The synthesis and purification procedures have been reported previously.[17,18] Table 2-I lists reaction parameters for the terpolymerization of AM with NaAMB and AMPTAC. IR: Terpolymer: ATABAM 15-15, N-H 3401-3200 cm^{-1} (s); C-H 2930 cm^{-1} (m); C=O 1685-1653 cm^{-1} (s); N^{+}-R_4 966 cm^{-1}. ^{13}C NMR: ATABAM 5-5 , AM C=O, 180.8 ppm; NaAMPS C=O, 176.9 ppm; AMPTAC C=O, 178.3 ppm; Chain CH, 43.1 ppm; Chain CH_2, 36.1 ppm; Gem CH_3, 27.9 ppm.

Terpolymer Characterization

Terpolymer compositions were determined from ^{13}C NMR by integration of the acrylamido carbonyl peaks.[19] ^{13}C NMR spectra were obtained using 10 wt/wt % aqueous (D_2O) polymer solutions with DSS as the reference. FTIR spectra were acquired using a Perkin-Elmer 1600 Series FT-IR spectrophotometer. Molecular weight studies were performed on a Chromatix KMX-6 Low Angle Laser Light Scattering instrument. Refractive index increments were obtained using a Chromatix KMX-16 Laser Differential Refractometer. A Langley-Ford Model LF1-64 channel digital correlator was used in conjunction with the KMX-6 to obtain quasielastic light scattering data. All measurements were conducted at 25°C in 1M NaCl.

Viscosity Measurement

A 1g/dL stock solution of each terpolymer was made in deionized water. Aliquots were taken and diluted with salt solutions to designated ionic strength and a polymer concentration of approximately 0.3 g/dL. These were further diluted to give polymer solutions with concentrations above and below C^* (0.025 to 0.3g/dL). After aging for 2-3 weeks, the solutions were analyzed with a Contraves LS-30 rheometer. Triplicate samples were prepared of each concentration to reduce experimental error. Intrinsic viscosities were evaluated using the Huggins equation.[20]

Dynamic Mechanical Analysis

A Rheometrics RMS-800 dynamic-mechanical spectrometer was used to examine G' (storage modulus) and G" (loss modulus) as a function of frequency for 1g/dL solutions of ATABAM 2.5-2.5 in various salt concentrations. Measurements where obtained using a Couette test geometry with 50% constant strain at 25°C.

Results and Discussion

The previously studied ADABAM terpolymer series that contained AM, NaAMB and AMPDAC (Figure 2-1) formed highly swollen gels in aqueous solutions even in the presence of electrolytes. Strong hydrogen bonding between the carboxylate and the tertiary ammonium hydrochloride groups led to intermolecular crosslinks that persisted even in 1*M* NaCl. Substitution of the protonated tertiary amine monomer AMPDAC by a quaternized monomer AMPTAC allows formation of soluble ampholytic terpolymers.

Compositional Studies

Compositions for the ATABAM series of terpolymers were determined by integration of ^{13}C NMR acrylamido carbonyl peaks (Table I). Much like the previously studied ATASAM series,[21] synthesis of the terpolymers in 0.5*M* NaCl led to random incorporation of the charged groups such that the resulting compositions approximate the feed compositions. The presence of added electrolytes during polymerization shields the charged groups from each other so that monomer pairing is not favored. Such random distribution of ionic mers along the backbone would be predicted to result in significantly different properties when compared to terpolymers with large numbers of neighboring group associations. The terpolymers ATABAM 10-5 and 5-10 were synthesized with charge imbalances in the feed resulting in polyelectrolyte solution behavior.

Light Scattering Studies

Low angle laser light scattering was employed to obtain the molecular weight and second virial coefficient (A_2) data shown in Table II. The molecular weights range from 3.43 to 19.4 x 10^6 g/mol for ATABAM 0.5-0.5 and ATABAM 10-5 respectively. The terpolymers ATABAM 10-10, 15-15, and 5-10 have very similar degrees of polymerization and therefore can be used for comparative structure/property assessments. Except for ATABAM 0.5-0.5, the A_2 values range from 1.63 to 2.06 x 10^{-4} ml mol/g^2 for the charle balanced systems. ATABAM 0.5-0.5 remains well solvated in 1*M* NaCl as indicated by the A_2 value of 3.63 ml·mol/g^2.

Quasieleastic light scattering was used to obtain the diffusion coefficients (D_o) and hydrodynamic volumes (d_o) shown in Table II. ATABAM 10-10 has the largest d_o value of 2160 Å reflecting good solvation and high molecular weight. ATABAM 5-5 possess a molecular weight and hydrodynamic volume approximately equal to that of ATABAM 0.5-0.5 although its second virial coefficient is much smaller. A similar effect is observed for ATABAM 10-5 which has 73 % the molecular weight of ATABAM 5-10, yet due to the presence of 3 times as much NaAMPS, has approximately the same hydrodynamic volume.

Viscometric Studies

Effects of Terpolymer Composition

The terpolymers ATABAM 2.5-2.5, 5-5, 10-10, and 15-15 exhibit polyampholyte behavior as expected for equal (or near equal) concentrations of NaAMB and AMPTAC. ATABAM 0.5-0.5, 2.5-2.5, and 5-5 have charge densities low enough to allow solubilization in the absence of added electrolytes. At slightly higher charge densities however, ATABAM 10-10 and 15-15 are insoluble in deionized water. The net charge of ATABAM 5-10 and 10-5 polyelectrolytes allow solubility in electrolyte free water.

Charge density also controls the type of macromolecular associations present. ATABAM 2.5-2.5 displays very strong intermolecular associations that "gel" semi-dilute polymer solutions at low ionic strengths. The high charge density ampholyte terpolymers possess both inter and intramolecular associations under the same conditions.

Effects of Added Electrolytes

Figure 2-2 displays the intrinsic viscosity of a number of the terpolymers as a function of NaCl concentration obtained using the Huggins equation.[20] The data are indicative of classic "antipolyelectrolyte" behavior. Increases in solution ionic strength disrupt intramolecular ionic associations thus producing increases in polymer hydrodynamic volume. ATABAM 10-10 undergoes a 700 % increase in intrinsic viscosity going from 0.05M to 1M NaCl. ATABAM 10-10 and 15-15, which have similar molecular weight attain the same intrinsic viscosity in 1M NaCl.

The data parallel the behavior observed for the previously examined ADASAM low charge density terpolymers.[13] For example, ADASAM 10-10 (76.7 mol % AM, 12.6 mol % NaAMPS, and 10.7 mol % AMPDAC) displayed a 330 % increase in intrinsic viscosity from deionized water to 1*M* NaCl. The complex solution behavior of the ATASAM terpolymers was not observed.[21]

Effects of pH

The reduced viscosities for ATABAM 10-10 obtained in neutral and acidic pH values are shown in Figure 2-3. Above pH 7.5 the polymers behave as polyampholytes since all NaAMB units possess a negative charge. Intramolecular charge-charge interactions initially constrict the coils but disappear as solvent ionic strength is increased. At pH 3 the polymers behave as polyelectrolytes. The NaAMB units are protonated so that only the cationic charge of AMPTAC remains. Like typical polyelectrolytes, the coils expand in the absence of added electrolytes but collapse in their presence.

It is interesting that the polyelectrolyte form of ATABAM 10-10 has smaller dimensions in 1M NaCl than the polyampholyte form. This may be due to the relative hydrophobicity of the acid form of NaAMB. For example, copolymers of NaAMB with AM precipitate from aqueous solution below pH 5.[12] The presence of this relatively hydrophobic monomer may constrict the polymer to dimensions smaller than those of a random coil thus producing the effect observed in Figure 2-3. Also the extent of counterion condensation may differ for the two forms at high NaCl concentrations.

Dynamic Mechanical Analysis

The intermolecular associations of ATABAM 2.5-2.5 are strong enough to produce gels with elastic properties in solvents of low ionic strengths. The storage modulus G′ and the loss modulus G″ were examined on a Rheometrics RMS-800 spectrometer using a couette test configuration. Solutions of varying ionic strengths at constant polymer concentrations (1 g/dL) were analyzed at 50 % strain in the frequency range of 0.1 to 100 radians/second. The frequencies at which G′ and G″ intersect, i.e., tan $\delta = G''/G' = 1$, are plotted as a function of ionic strength in Figure 2-4. At NaCl concentrations above 0.05M, the frequency at which tan δ is unity becomes independent of ionic strength. This implies the complete disappearance of intermolecular associations.

Conclusions

The ATABAM series of low charge density polyampholytes has been synthesized by free radical terpolymerization of AM with NaAMB and AMPTAC. Unlike the analogous terpolymers containing the tertiary amine hydrochloride monomer AMPDAC, this series dissolves in aqueous solutions provided enough salt is present to disrupt ionic associations. The terpolymers have been characterized by ^{13}C NMR, FT-IR, and classical and quasielastic low angle laser light scattering techniques. The terpolymer compositions reflect the monomer feed concentrations. Molecular weights range from 3.43 to 19.4 x 10^6 g/mol for the series.

Increases in solution ionic strength disrupt intramolecular ionic associations thus producing increases in polymer hydrodynamic volume. ATABAM 10-10 undergoes a 700 % increase in intrinsic viscosity going from 0.05M to 1*M* NaCl. Intermolecular ionic associations, studied utilizing dynamic mechanical analysis, were observed to be very sensitive to the presence of added electrolytes.

References

1. T. Alfrey and H. Morawetz, J. Am. Chem. Soc., 74, 436 (1952).

2. T. Alfrey, R. M. Fuoss, H. Morawetz and H. Pinner, J. Am. Soc., 74, 438 (1952).

3. G. Ehrlich and P. Doty, J. Am. Chem. Soc., 76, 3764 (1954).

4. T. Nonaka and H. Egawa, Bull. Chem. Soc. Jpn., 53, 1632 (1980).

5. Y. Merle, L. Merle-Aubry and E. Selegny, Polymeric Amine and Ammonium Salts, E. J. Goethals Ed., Pergamon Press, New York, 1980.

6. M. Vranken and G. Smets, J. Polym. Sci., 14, 521 (1954).

7. C. S. Marvel and W. W. Moyer, J. Am. Chem. Soc., 79, 4990 (1957).

8. C. S. Marvel and G. L. DeTommaso, J. Org. Chem., 25, 2207 (1960).

9. T. Wielma, Ph. D. Dissertation, University of Groningen, (1989).

10. C. B. Johnson, Ph.D. Dissertation, University of Southern Mississippi (1988).

11. C. L. McCormick and C. B. Johnson, Macromol. Sci., Chem., A27(5), 539 (1990).

12. L. C. Salazar, Ph.D. Dissertation, University of Southern Mississippi (1991).

13. C. L. McCormick and C. B. Johnson, Polymer, 31, 1100 (1990).

14. D. G. Peiffer and R. D. Lundberg, Polymer, 26, 1058 (1985).

15. D. Hoke and R. Robins, J. Polym. Sci., 10, 3311(1971).

16. C. L. McCormick and K. P. Blackmon, J. Poly. Sci., Polym. Chem. Ed., 24, 2635 (1986).

17. C. L. McCormick and L. C. Salazar, Water Soluble Co-Polymers 42. Cationic Polyelectrolytes of Acrylamide and 2-Acrylamido-2-Methylpropanetrimethylammonium Chloride.

18. C. L. McCormick and L. C. Salazar, Water Soluble Co-polymers 41. Copolymers of Acrylamide and Sodium 3-Acrylamido-3-Methylbutanoate.

19. C. L. McCormick and B. H. Hutchinson, Polymer, 27(4), 623 (1988).

20. M. L. Huggins, J. Am. Chem. Soc., 64, 2716 (1942).

21. C. L. McCormick and L. C. Salazar, Water Soluble Co-Polymers 44. Ampholytic Terpolymers of Acrylamide with Sodium 2-Acrylamido-2-Methylpropanesulfonate and 2-Acrylamido-2-Methylpropane-trimethylammonium Chloride.

TABLE 2-1

Reaction Parameters for Terpolymerization of Acrylamide (AM) with Sodium 3-acrylamido-3- methylbutanoate (NaAMB) and 2-Acrylamido-2-methylpropanetrimethylammonium Chloride (AMPTAC).

Sample Number	Feed Composition (mol %) AM:NaAMB:AMPTAC	Reaction Time (hr)	Conversion (%)	Terpolymer Composition[a] (mol %) AM:NaAMB:AMPTAC
ATABAM 0.5-0.5	99.0:0.5:0.5	2.5	20.8	99[b]:0.5[b]:0.5[b]
ATABAM 2.5-2.5	95.0:2.5:2.5	4.0	41.0	89.1:5.1:5.8
ATABAM 5.0-5.0	90.0:5.0:5.0	4.0	47.8	85.9:7.9:6.2
ATABAM 10-10	80.0:10.0:10.0	6.0	22.3	80.5:9.7:9.8
ATABAM 15-15	70.0:15.0:15.0	4.0	25.6	74.6:11.5:14.0
ATABAM 10-5	85.0:10.0:5.0	3.0	20.2	75.7:13.6:10.7
ATABAM 5-10	85.0:5.0:10.0	3.0	14.5	85.3:4.5:10.2

[a] Determined by ^{13}C NMR
[b] Theoretical

TABLE 2-2

Classical and Quasielastic Light Scattering Data for Terpolymers of Acrylamide (AM) with Sodium 3-Acrylamido-3-methylbutanoate (NaAMB) with 2-Acrylamido-2-methylpropanetrimethylammonium Chloride (AMPTAC).

Sample Number	dn/dc	Mw x 10^{-6} (g/mol)	A_2 x 10^4 (ml.mole/g^2)	D_o x 10^8 (cm^2/g)	d_o (Å)	DP x 10^{-3}
ATABAM 0.5-0.5	0.1543	3.43	3.61	4.98	1024	4.82
ATABAM 2.5-2.5	0.1372	13.9	1.66	3.13	1873	15.0
ATABAM 5-5	0.1386	3.45	1.63	4.76	1003	4.02
ATABAM 10-10	0.1395	10.8	2.06	2.64	2159	11.0
ATABAM 15-15	0.1308	12.2	1.75	3.13	1630	11.5
ATABAM 5-10	0.1460	11.2	1.84	3.61	1330	10.8
ATABAM 10-5	0.1399	19.4	1.85	3.89	1440	21.1

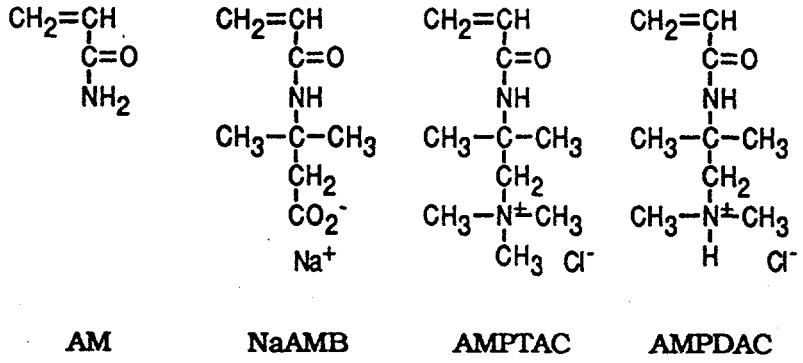

Figure 2-1. Structures for the monomers Acrylamide (AM), Sodium 3-Acrylamido-3-methylbutanoate (NaAMB), 2-Acrylamido-2-methylpropanetrimethylammonium Chloride (AMPTAC), and 2-Acrylamido-2-methylpropanedimethylammonium Hydrochloride (AMPDAC).

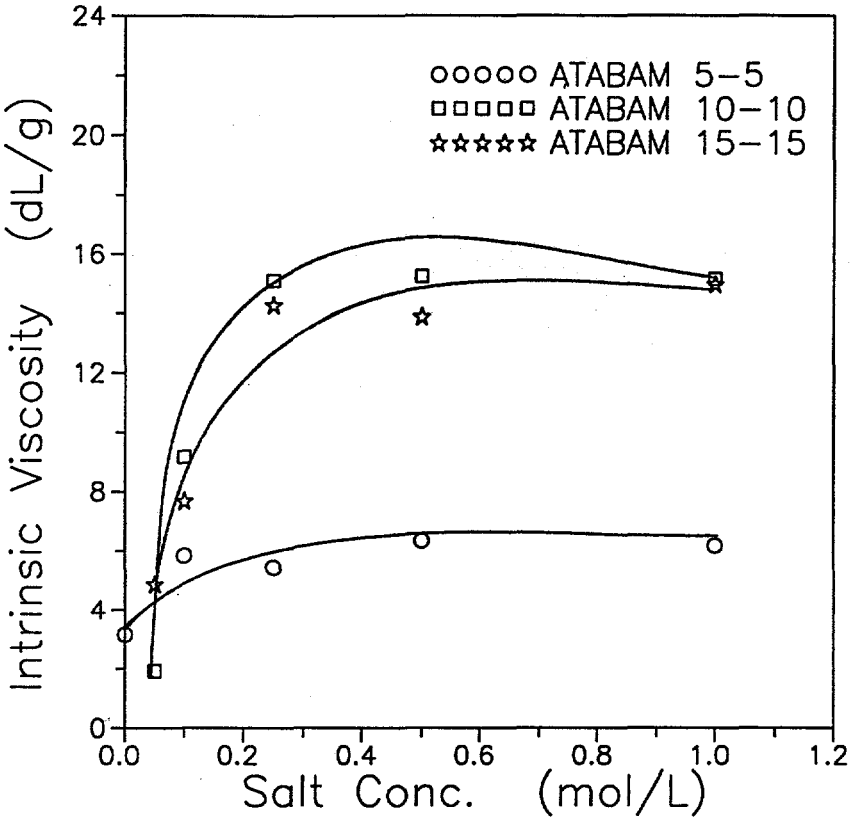

Figure 2-2. Intrinsic viscosities of ATABAM 5-5, 10-10, and 15-15 plotted as function of NaCl concentration determined at 25°C at a shear rate of 5.96 sec^{-1}.

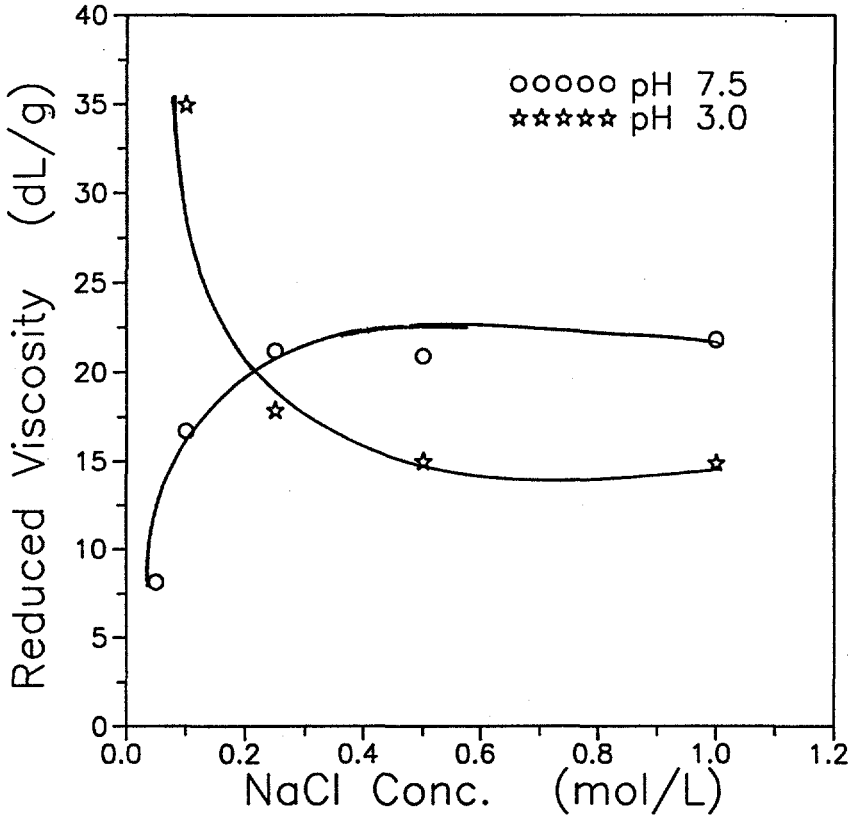

Figure 2-3. Reduced viscosity for ATABAM 10-10 in the polyampholyte form (pH = 7.5) and in the polyelectrolyte form (pH = 3.0). Determined with a polymer concentration of 0.10 g/dL at 25°C at a shear rate of 5.96 sec^{-1}.

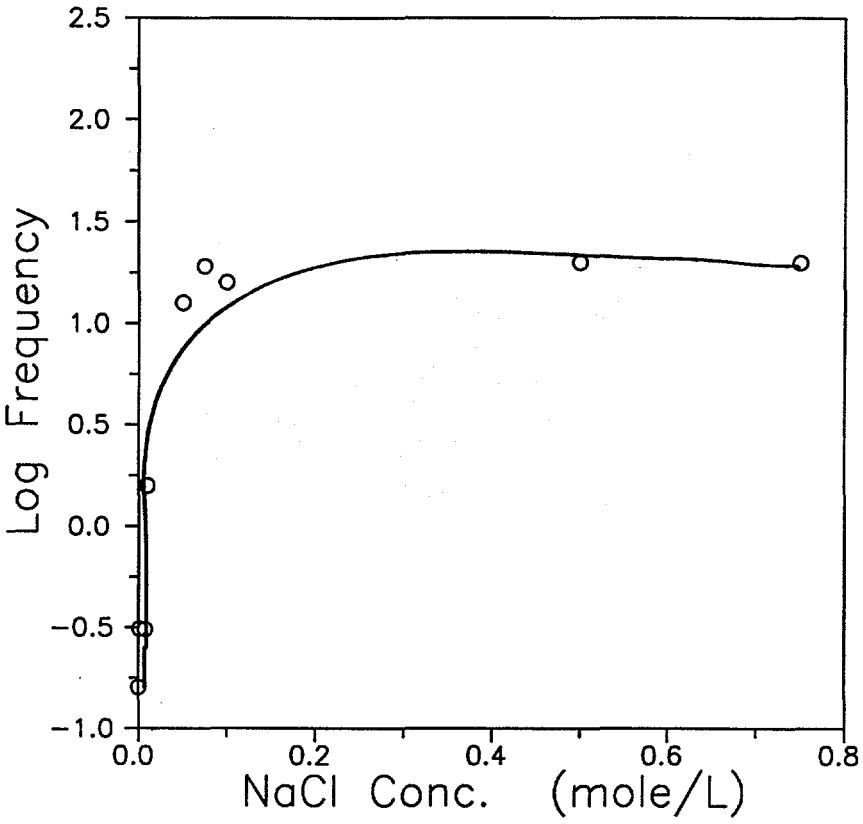

Figure 2-4. Log Frequency at which tan δ is unity as a function of NaCl concentration for 1 g/dL solutions of ATABAM 2.5-2.5.

CHAPTER THREE: HYDROPHILIC SULFOBETAINE COPOLYMERS OF ACRYLAMIDE AND 3-(2-ACRYLAMIDO-2-METHYLPROPANEDIMETHYLAMMONIO)-1-PROPANESULFONATE

Abstract

The free radical copolymerization of acrylamide (AM) with 3-(2-acrylamido-2-methylpropanedimethylammonio)-1-propanesulfonate (AMPDAPS) has been studied in the range from 99 to 25 % AM in the feed. Copolymer compositions obtained by elemental analysis and ^{13}C NMR reflect the monomer feed concentrations. The value of r_1r_2 has been determined to be 0.60 for the AM-AMPDAPS pair. Copolymer microstructures, including run numbers and sequence distributions, were calculated from the reactivity ratios. Molecular weights for the series range from 3.0 to 21.5 x 10^6 g/mol. Second virial coefficients decrease from 2.67 to 0.21 ml·mol/g^2 as charge density increases. Intrinsic viscosities decrease with increasing AMPDAPS content, but increase with increasing temperature (in the range of 25 to 60°C) and added electrolytes (NaCl and/or $CaCl_2$). The solution behavior of the homopolymer of AMPDAPS is independent of pH. The observed properties are consistent with the charge density of the polymers and the sulfobetaine structure of the AMPDAPS monomer.

Introduction

Synthetic polyampholytes can be prepared from zwitterionic monomers which exhibit the requisite net charge of zero at appropriate pH. The positive charge is provided by a quaternary ammonium functionality and the negative charge is provided by a carboxylate or sulfonate group (betaine and sulfobetaine). A number of investigations have focused on the unusual properties of zwitterionic polyampholytes.

Ladenheim and Morawetz reported the reaction poly(4-vinyl pyridine) with ethyl bromoacetate followed by hydrolysis of the ester to give high charge-density polyampholytes.[1] Hart and Timmerman prepared sulfobetaine polyampholytes by reacting poly(2-pyridine) with sultones or by polymerizing the sultone derivative of 4-vinylpyridine.[2] Salamone synthesized a variety of sulfobetaines based on vinylimidazole.[3]

Galin and coworkers conducted an elegant study of poly(sulfobetaines) with various structures.[4-7] They described the synthesis of a series of polyampholytes by the quaternization of vinylamines with 1,3-propanesultone. Utilizing the Mark-Howink-Sakurada relationship, the existence of specific dipolar intramolecular interactions between lateral zwitterions was established. They concluded that in the presence of electrolytes, a polyampholyte behaved like a random coil of moderate flexibility in a thermodynamically very poor solvent.

Schulz et al.[8] have examined the phase behavior and solution properties of the homopolymer of the commercially available monomer N-(3-sulfopropyl)-N-methacroyloxyethyl-N,N-dimethylammonium betaine (SPE). Negative A_2 values were found for the polyampholyte

in solutions of low ionic strength; positive values were found as the ionic strength increased. Highly alternating copolymers of N-vinylpyrrolidone (NVP) with SPE which showed polyampholyte behavior in solution were also researched.[9]

Wielma studied the synthesis and solution properties of zwitterionic betaine and sulfobetaine polymers with with one, two or three methylene units between the charged groups.[10] Varying degrees of ionization were achieved for the carboxylate groups by controlling the pH. At high pH values the polymers behaved as polyampholytes while at low pH values, polyelectrolyte behavior was observed. It was concluded that strong intramolecular coulombic interactions were the dominant factor in the solubility behavior of zwitterionic polymers.

Previous research in our laboratories focused on polyampholyte co- and terpolymers prepared by incorporation of cationic and anionic monomers.[11-15] Rheological characteristics, particularly pH and electrolyte responsiveness, can be readily changed by microstructural manipulation during synthesis. Recently we have initiated studies of polyampholytes prepared from zwitterionic monomers which would have similar structural characteristics.[15-19] In this paper we report the synthesis and characterization of a series of copolymers of acrylamide with the novel amphoteric monomer 3-(2-acrylamido-2-methylpropanedimethylammonio)-1-propanesulfonate (AMPDAPS).

Experimental

Materials and Monomer Synthesis

3-(2-Acrylamido-2-methylpropanedimethylammonio)-1-propanesulfonate (AMPDAPS) was synthesized by the ring opening reaction of 1,3-cyclopropanesultone (PS) with 2-acrylamido-2-methylpropanedimethylamine (AMPDA), Figure 3-1. 1,3-Cyclopropanesultone from Aldrich was used without further purification. The synthesis of AMPDA has been previously reported by our laboratories.[19] In a typical monomer synthesis, 0.144 mol AMPDA and 0.156 mol of PS were reacted in 500ml propylene carbonate under N_2 at 55°C for 4 days. During this period the product formed as a white precipitate. This was then filtered and washed with diethyl ether until all the propylene carbonate was removed. AMPDAPS (m.p. 220-224°C) was obtained in 80% yield. Anal. Calc. for $C_{12}H_{24}N_2O_4S$: C, 49.29%; H, 8.29%; N, 9.58%; S, 10.96%. Found: C, 49.07%; H, 8.27%; N, 9.56%; S, 11.12%. I.R.: N-H, 3280 cm^{-1}(m); C=C-H 2990 cm^{-1}; aliphatic C-H, 2940 cm^{-1}; amide C=O, 1660 cm^{-1}(s) and 1550 cm^{-1}(s); S-O, 1200 cm^{-1}(s). ^{13}C NMR:

Acrylamide (AM) from Aldrich was recrystallized twice from acetone and vacuum-dried at room temperature. Potassium persulfate from J.T. Baker was recrystallized twice from deionized water.

Synthesis of Copolymers of 3-(2-acrylamido-2-methylpropanedimethylammonio)-1-propanesulfonate with Acrylamide

The homopolymer of AMPDAPS and the copolymers of AMPDAPS with AM (the DAPSAM series) were synthesized by free radical polymerization in a 0.5M NaCl aqueous solution under nitrogen at 30°C using 0.1 mol % potassium persulfate as the initiator. The feed ratio of AM:AMPDAPS was varied from 99:1 to 25:75 mol % with the total monomer concentration held constant at 0.45M. The use of 0.5M NaCl as the reaction medium insured that polymers with high AMPDAPS content remained homogeneous during polymerization.

In a typical synthesis, specified quantities of each monomer were dissolved in small volumes of NaCl solution. The separate solutions were then combined and diluted to a 0.45M monomer concentration. After the pH was adjusted to 7, the reaction mixture was sparged with nitrogen for twenty minutes then initiated with 0.1 mol % potassium persulfate. A low conversion sample was always analyzed to allow reactivity ratio studies. The reaction was usually terminated at <30% conversion due to the high viscosity of the reaction medium and as a precaution against copolymer drift. The polymers were precipitated in acetone, redissolved in deionized water, then dialyzed using Spectra/Por 4 dialysis bags with molecular weight cutoffs of 12,000 to 14,000 g/mol. After isolation by lyophilization the polymers were stored in desiccators with a nitrogen atmosphere. When more than 40 mol % AMPDAPS was incorporated in the copolymers, swelling but not dissolution could be achieved in deionized water. These "hydrogels" were washed repeatedly with deionized water to remove any remaining salt or monomer and then lyophilized. Conversions were determined gravimetrically. Table I lists reaction parameters for the copolymerization of AMPDAPS with AM and the homopolymerization of AMPDAPS. IR: DAPSAM-100 homopolymer: N-H 3200 cm^{-1} (s); C-H 3050 cm^{-1} (m) and 2980 cm^{-1} (m); C=O 1650 cm^{-1} (s); S-O 1200 cm^{-1} (s). Typical copolymer: DAPSAM-75, N-H 3290 cm^{-1} (s); C-H 3050 cm^{-1} (m) and 2980 cm^{-1} (m); C=O 1670 cm^{-1} (s); S-O 1200 cm^{-1} (s).

Copolymer Characterization

Elemental analyses for carbon, hydrogen, and nitrogen were conducted by M-H-W Laboratories of Phoenix, AZ on both the low and high conversion copolymer samples. ^{13}C NMR spectra of the DAPSAM polymers were obtained using 5-10 wt % aqueous (D_2O) polymer solutions with DSS as the reference. The procedure for quantitatively determining copolymer compositions from ^{13}C NMR has been discussed in detail elsewhere.[20] FT-IR spectra for all materials synthesized were obtained using a Perkin-Elmer 1600 Series FT-IR spectrophotometer. Molecular weight studies were performed on a Chromatix KMX-6 Low Angle Laser Light Scattering instrument. Refractive index increments were obtained using a Chromatix KMX-16 Laser Differential Refractometer. For quasielastic light scattering a Langley-Ford Model LF1-64 channel digital correlator was used in conjunction with the KMX-6. All measurements were conducted at 25°C in 1M NaCl at a pH of 7.0 ± 0.1.

Viscosity Measurements

Stock solutions of sodium chloride were prepared by dissolving the appropriate amount of salt in deionized water in volumetric flasks. Polymer stock solutions were made by dissolving designated amounts of polymer in the salt solutions. The solutions were then diluted to appropriate concentrations and allowed to age for two to three weeks before being analyzed with a Contraves LS-30 rheometer. Triplicate samples were prepared of each concentration to reduce experimental error. Intrinsic viscosities were evaluated using the Huggins equation.[21] The Modified Einstein-Simha equation was used to calculate the intrinsic viscosities for DAPSAM-40-3 as a function of temperature.[22]

Results

Compositional Analysis

The copolymers of AMPDAPS with AM (the DAPSAM series) were synthesized by varying the feed ratios of AM:AMPDAPS from 99:1 to 10:90 mol %. Reaction parameters and the resulting compositions for the polymers are given in Table I. Copolymer compositions were determined from ^{13}C NMR and elemental analysis data. Integration of ^{13}C carbonyl peaks gave the mol % of AM and AMPDAPS in the copolymers which agrees favorably with that derived from elemental analysis. The copolymer compositions as a function of feed composition for the DAPSAM series are shown in figure 3-2. The copolymerization curve follows closely that of an ideally random system represented by the dashed line.

Reactivity Ratio and Microstructure Studies

Reactivity ratio values for the AMPDAPS series were determined from monomer feed ratios and resultant copolymer compositions obtained at low conversions. Fineman-Ross[23] and Kelen-Tüdös[24] methods were used to determine the monomer reactivity ratios. The Fineman-Ross method yielded reactivity ratios for AM and AMPDAPS of $r_1 = 0.79$ and $r_2 = 0.73$. The Kelen-Tüdös method gave reactivity ratios of 0.79 and 0.75 for r_1 and r_2 respectively and $r_1r_2 = 0.60$. The experimental data indicate random comonomer incorporation with a slight alternating tendency.

To elucidate the microstructural features of these copolymers, the equations of Igarashi [25] and Pyun[36] were employed. The fractions of AM-AM, AMPDAPS-AMPDAPS, and AM-AMPDAPS units (the mol % blockiness, the mol % alternation, and the mean sequence length) in the copolymers were calculated from the reactivity ratios and the copolymer compositions, Table II. The mean sequence lengths of AM and AMPDAPS reverse in value when the amount of AMPDAPS in the copolymers increases from 25 and 40 mol % to 60 and 75 mol %. This behavior is indicative of a random microstructure.

Low Angle Laser Light Scattering

Weight-average molecular weights were determined by classical low-angle laser light scattering. Table 3-3 shows the data obtained at 25°C in 1M NaCl. The molecular weights vary

from $1.3x10^6$g/mol to $21.5x10^6$g/mol. For polymers prepared under similar conditions (initiator concentration, reaction conversion, etc.), the more AMPDAPS in the feed, the lower the molecular weight of the resulting polymer. The similar molecular weights of DAPSAM-10 and -25, and DAPSAM-60 and -75 allow meaningful assessments of the effects of copolymer composition on solution behavior.

The second virial coefficients (A_2) decrease with increasing AMPDAPS content in the copolymers as shown in Figure 3-3. This is the opposite of polyelectrolytes which have increasing A_2 values with increasing charge density. In deionized water copolymers with compositions greater than 40 mol % AMPDAPS are insoluble. Solubility is achieved in the presence of electrolytes, however even in 1M NaCl, A_2 values are less than those of DAPSAM-1 which approximates a neutral polyacrylamide sample.

Quasielastic light scattering (QLS) data are presented in Table 3-3 and illustrated in figures 3-4 and 3-5. The mean polymer diffusion coefficients (D_o) and diameters (d_o) for all copolymer systems in 1M NaCl show some dependence on the degree of polymerization and on the weight-average molecular weight. As degree of polymerization and molecular weight increase, D_o values decrease (d_o increase). The scatter in the data is, of course, due to solvation differences with compositional changes - clearly supported by A_2 values.

Dilute Solution Properties

Effects of Copolymer Composition

The effects of copolymer composition on the intrinsic viscosities of the DAPSAM copolymers (Table 3-2) in 0.514-M NaCl are shown in figure 3-6. The decrease in the intrinsic viscosities is due to decreases in molecular weight as well as increasing intramolecular interactions which constrict the polymer coils. The presence of the AMPDAPS monomer units is responsible for the latter as demonstrated by the second virial coefficients. For DAPSAM-60 and -75, which have similar molecular weights and degrees of polymerization, increasing AMPDAPS concentration decreases the respective intrinsic viscosities. Schulz and Peiffer postulated these interactions to be based on electrostatic attractions between opposite charges of different sulfobetaine units.[8] One might expect such effects to be especially strong as microheterogeneous associations lead to local decreases in dielectric constant of the domains.

Effects of Added Electrolytes

The effects of sodium chloride on the intrinsic viscosities of the DAPSAM copolymers and the AMPDAPS homopolymer were determined at a shear rate of 1.25 sec^{-1} as shown in Figure 3-7. The polymer solutions show increasing intrinsic viscosities as the amount of salt in the solutions increases. Some of the polymers do not dissolve unless salt is present. DAPSAM-60 and DAPSAM-75 require 0.0428-M NaCl, and DAPSAM-100 needs 0.257-M NaCl for dissolution. Attempts to remove the salt from the polymers by dialysis result in phase separation of the polymers from solution.

The initial decreases in intrinsic viscosity for DAPSAM-10 and DAPSAM-25 are due to the elimination of intermolecular molecular interactions with increasing ionic strength. This behavior has been observed with other polyampholyte systems.[1,15,17,18] DAPSAM-40 which

possesses a higher charge density experiences a disruption of intramolecular interactions with increasing ionic strength. In all cases the intrinsic viscosities increase significantly.

Figure 3-8 demonstrates the effects of adding the divalent salt calcium chloride to solutions of the DAPSAM copolymers and the AMPDAPS homopolymer. DAPSAM-60, -70, and the AMPDAPS homopolymer are insoluble up to a critical concentration.

A number of studies by other research groups have attempted to find evidence for the existence of hydrophobic domains within polyampholytes. For sulfobetaine and betaine polyampholytes, it is conceivable that intramer and intramolecular charge-charge associations may lead to such domains. Galin et al. utilized reporter anionic probes to find a polyampholytic environment with the same relative hydrophobicity of methano.[7] Wielma was unsuccessful in using fluorescent labels on polysulfobetaines to relate macroscopic behavior, such as increases in solution viscosity, to changes in the microenvironment along the polyampholyte backbone.[10]

Our research group is currently active in developing fluorescence probe and label technology.[27,28] For this study however a simple approach was utilized to assess the presence of hydrophobic domains in the DAPSAM polymers. Urea is a water structure breaker which solubilizes certain molecules by disrupting hydrophobic domains. It follows that if hydrophobic domains exist within polyampholytes, the presence of urea should alter solution behavior.

Solutions of the copolymers DAPSAM-10-3 and DAPSAM-40-3 were studied in deionized water, 1M NaCl, 1M urea, and a mixture of 1M NaCl and 1M urea. Figures 3-9 and 3-10 show the reduced viscosity for each copolymer as a function of polymer concentration. For each copolymer, the solution in deionized water has lowest viscosity. The addition of 1M urea increases reduced viscosity by only a small amount relative to that produced by the addition of 1M NaCl. The combination of NaCl and urea yields the same viscosity increase as that attained by 1M NaCl alone. As a reference, homo-polyacrylamide solution shows no change in viscosity in the presence of salt or urea. The slight increase in reduced viscosity for both DAPSAM-10-3 and DAPSAM-40-3 in the presence of urea is most likely due to enhanced hydrogen bonding between the polymers and the solvent. The major effect dominating rheological behavior appears to be charge screening upon addition of NaCl yielding better solvated chains. Transition from dilute to semidilute behavior is more readily observed for the DAPSAM-10-3 sample which is initially less compact than DAPSAM-40-3.

Effects of Temperature

Intrinsic viscosities for DAPSAM-40-3 increase with increasing temperature (Figure 3-11). The copolymer was tested in deionized water in the range of 25°C to 60°C. Most neutral polymers and polyelectrolytes exhibit reductions in viscosity as a function of increasing temperature. In deionized water this betaine exists in a compact conformation as evidenced by second virial coefficients and viscosity data. Temperature increases obviously allow accessibility to more extended conformations and better solvation. Copolymers which were insoluble in deionized water however could not be solubilized by the application of heat apparently due to strong intramolecular ionic effects. Interestingly, the DAPSAM copolymers are phase stable to 100°C in the presence of added electrolytes.

Effects of pH

Although acrylamide can be used as a comonomer to obtain very high molecular weights, hydrolysis can be problematic. Figure 3-12 shows the effects of pH on DAPSAM-25 in deionized water and in 0.512M NaCl. At high pH the acrylamide unit is hydrolyzed to the carboxylate ion and a corresponding increase in viscosity is observed for the polymer in deionized water. The presence of salt negates the polyelectrolyte effect and disrupts zwitterionic intramolecular interactions. The solution viscosities of the DAPSAM-100 homopolymer are independent of pH in 0.514M NaCl. Resistance of the AMPDAPS monomer to hydrolysis is due to the presence of geminal methyl groups next to the amide functionality. This protecting group has been used in other hydrolytically stable monomers such as sodium 2-acrylamido-2-methylpropanesulfonate (NaAMPS)[29] and sodium 3-acrylamido-3-methylbutanoate (NaAMB).[30]

Conclusions

The new sulfobetaine monomer 3-(2-acrylamido-2-methylpropanedimethylammonio)-1-propanesulfonate (AMPDAPS) has been synthesized and incorporated into a series of copolymers (the DAPSAM series) with AM as the comonomer. The polymers were examined by C-13 NMR, FT-IR, elemental analysis and low angle laser light scattering. Elemental analysis data from low conversion samples gave r_1r_2 = 0.60 for the AM-AMPDAPS monomer pair. Copolymer microstructures were statistically determined from reactivity ratios and found to be random with a slight alternating tendency. Weight-average molecular weights in the range of $1.3x10^6$ to $21.5x10^6$ g/mol have been determined for the polymers. Second virial coefficients were found to decrease in value as the zwitterion content of the copolymers increased.

Increasing concentrations of AMPDAPS decrease the intrinsic viscosities of the copolymers. Terpolymers containing greater than 40 mol % AMPDAPS are insoluble in deionized water but readily dissolve in the presence of NaCl. The copolymers display increases in viscosity upon the addition of NaCl and $CaCl_2$. Description of intramolecular interactions are responsible for this effect. Intrinsic viscosities increase in the temperature range of 25-60°C.

References

1. H. Ladenheim and H. Morawetz, *J. Polym. Sci., 26(113)*, 251 (1957).

2. R. Hart and D. Timmerman, *J. Polym. Sci., 28(118)*, 638 (1958).

3. J. C. Salamone, W. Volksen, S. C. Israel, A. P. Olson and D. C. Raia, *Polymer, 18*, 1058 (1977).

4. V. M. Monroy Soto and J. C. Galin, *Polymer, 25*, 121 (1984).

5. V. M. Monroy Soto and J. C. Galin, *Polymer, 25*, 254 (1984).

6. M. Galin, E. Marchal, A. Mathis, B. Meurer, V. M. Monroy Soto and J. C. Galin, *Polymer, 28*, 1937 (1987).

7. Y. L. Zheng, R. Knoesel and J. C. Galin, *Polymer, 28*, 2297 (1987).

8. D. N. Schulz, D. G. Peiffer, P. K. Agarwal, J. Larabee, J. J. Kaladas, L. Soni, B. Handwerker and R. T. Garner, *Polymer, 27*, 1734 (1987).

9. D. N. Schulz, K. Kitano, J. A. Danik and J. J. Kaladas, *Polym. Mat. Sci. Eng., 147*, 149 (1987).

10. T. Wielma, Ph.D. Dissertation, University of Groningen, (1989).

11. C. L. McCormick and C. B. Johnson, Macromolecules, 21, 686 (1988).

12. C. L. McCormick and C. B. Johnson, Macromolecules, 21, 694 (1988).

13. C. L. McCormick and C. B. Johnson, Polymer, 31, 1100 (1990).

14. C. L. McCormick and C. B. Johnson, Macromol. Sci., Chem., A27(5), 539 (1990).

15. L. C. Salazar, Ph. D. Dissertation, University of Southern Mississipp (1991).

16. C. L. McCormick, L. C. Salazar, and E. E. Kathmann, ACS Polym. Preprints, 32(1), 98 (1991).

17. C. L. McCormick and L. C. Salazar, ACS Symp., 467, p. 119 (1991).

18. C. L. McCormick and L. C. Salazar, Polymer Preprints, 30(2), 344 (1989).

19. C. L. McCormick and K. P. Blackmon, Polymer, 27, 1971 (1986).

20. C. L. McCormick and B. H. Hutchinson, Polymer, 27(4), 623 (1988).

21. M. L. Huggins, J. Am. Chem. Soc., 64, 2716 (1942).

22. J. C. Salamone, C. C. Tsai, A. P. Olsen and A. C. Watterson, in Advances in the Chemical Sciences: Ions in Polymers, Vol. 187, ACS, 1980, p. 337.

23. M. Fineman and S. Ross, J. Polym. Sci., 5(2), 259 (1950).

24. T. Kelen and F. Tüdös, J. Macromol. Sci. Chem., A9, 1, (1975).

25. S. Igarashi, J. Polym. Sci., Polym. Lett. Ed., 1, 359 (1963).

26. C. W. Pyun, J. Polym. Sci., A2(8), 1111 (1970).

27. M. C. Clark, Ph.D. Dissertation, University of Southern Mississippi (1990).

28. S. A. Ezzell, Ph.D. Dissertation, University of Southern Mississippi (1990).

29. C. L. McCormick and G. S. Chen, *J. Polym. Sci., Polym. Chem. Ed.*, *20*, 817 (1982).

30. C. L. McCormick and K. P. Blackmon, *J. Poly. Sci., Polym. Chem. Ed.*, *24*, 2635 (1986).

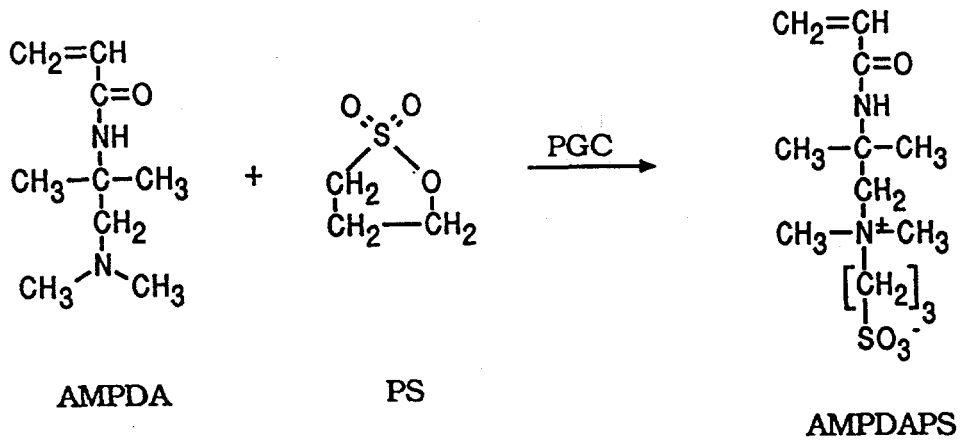

Figure 3-1. Synthesis of 3-(2-acrylamido-2-methylpropane-dimethylammonio)-1-propanesulfonate (AMPDAPS).

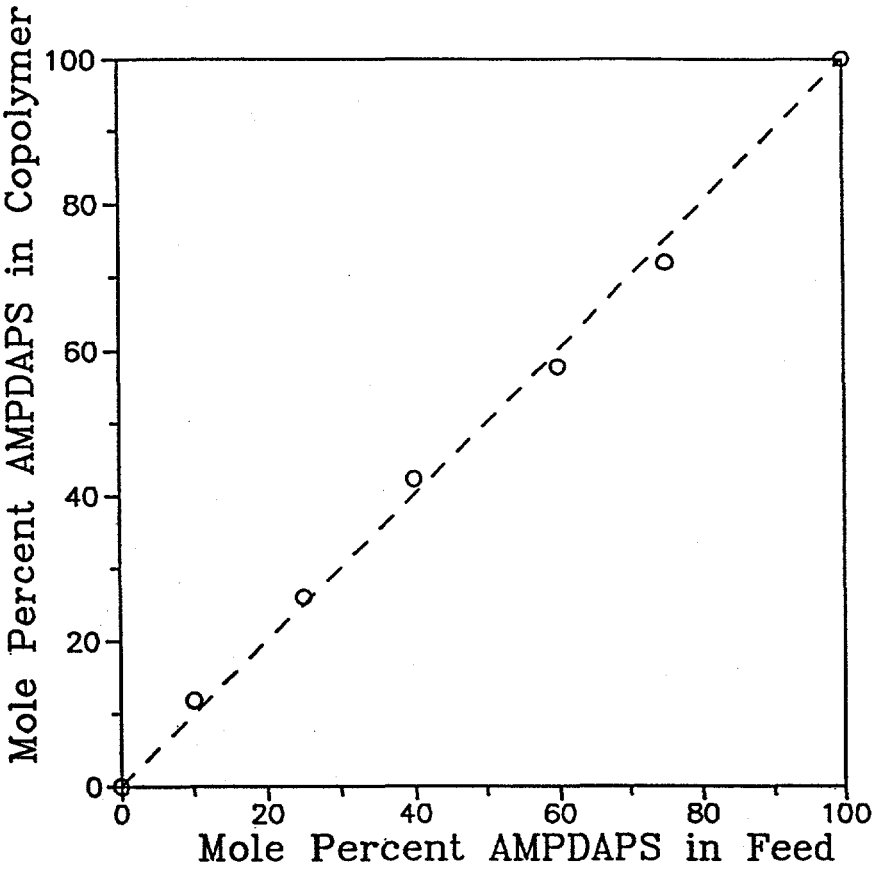

Figure 3-2. Mole percent AMPDAPS incorporated into the copolymers as a function of comonomer feed ratio.

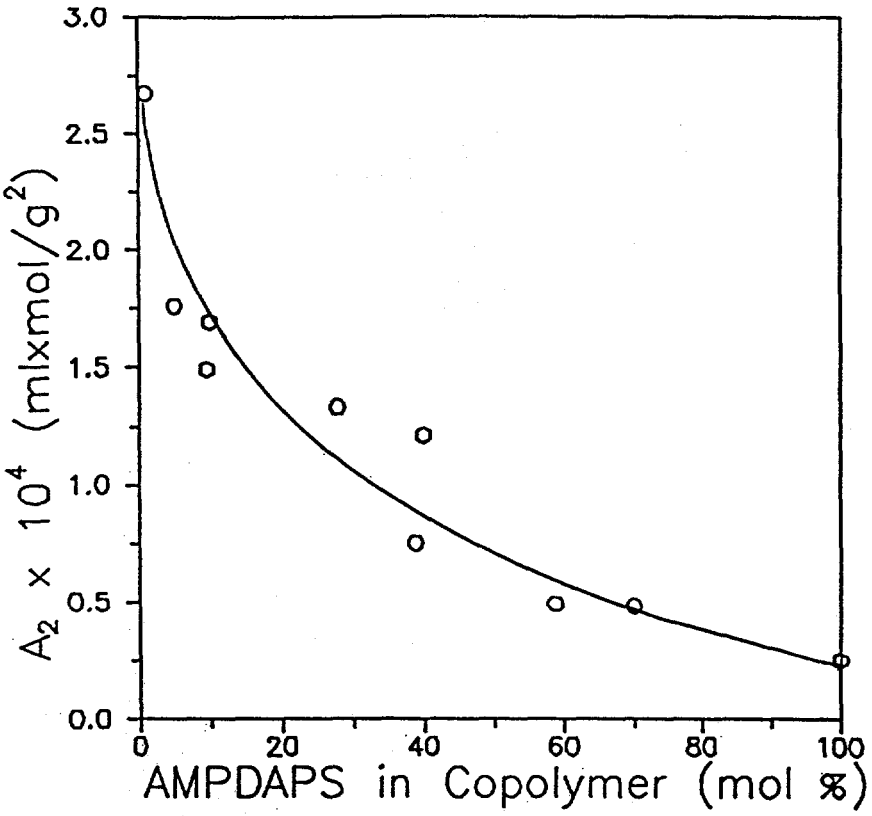

Figure 3-3. Dependence of the second virial coefficient on the composition of the DAPSAM polymers as determined in 1M NaCl at 25°C.

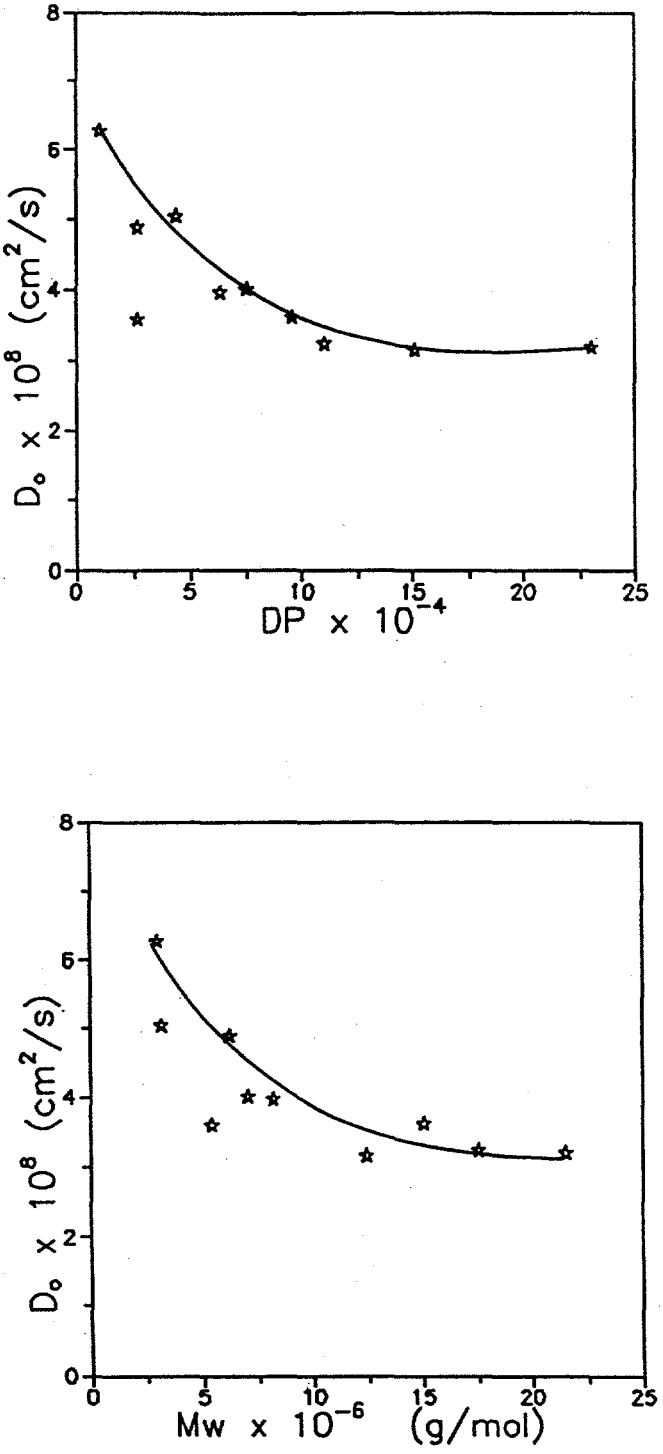

Figure 3-4. Dependence of the diffusion coefficient (D_o) on molecular weight and degree of polymerization of the DAPSAM copolymers as determined by QLS in 1M NaCl at 25°C.

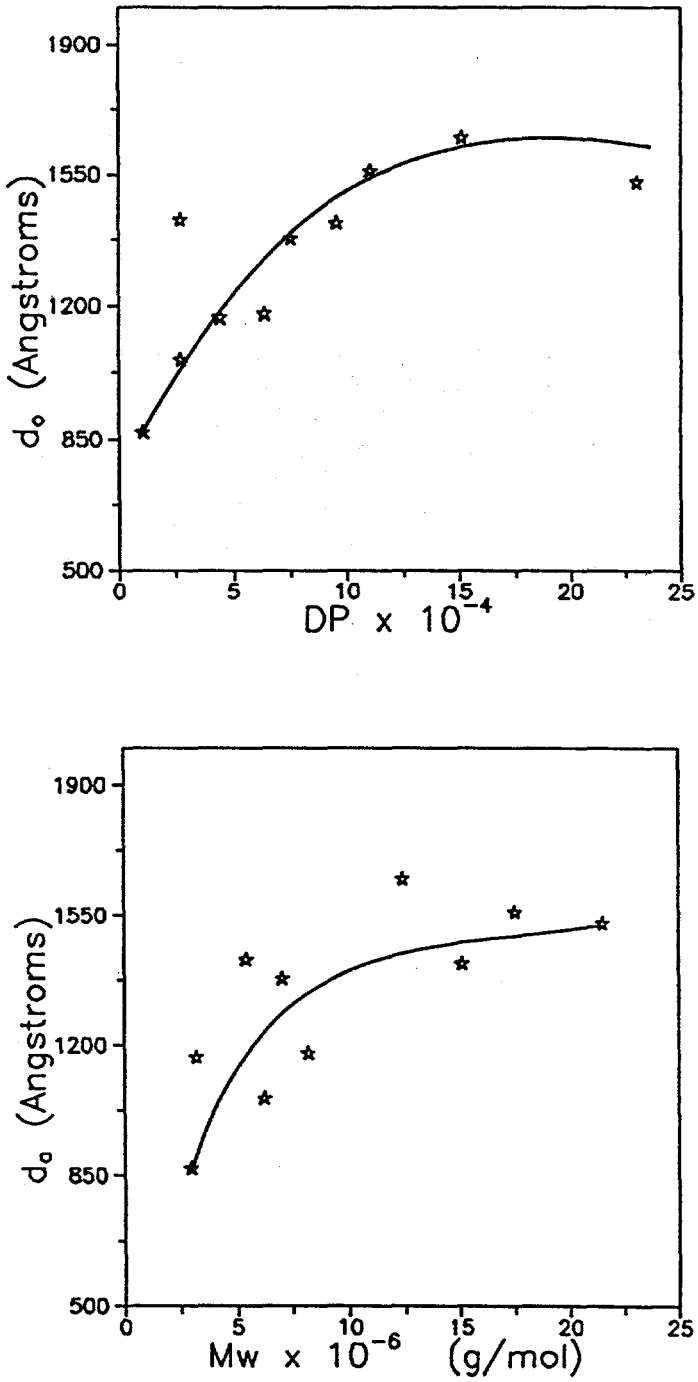

Figure 3-5. Dependence of copolymer mean diameter (d_o) on degree of polymerization and molecular weight as determined by QLS in 1M NaCl at 25°C.

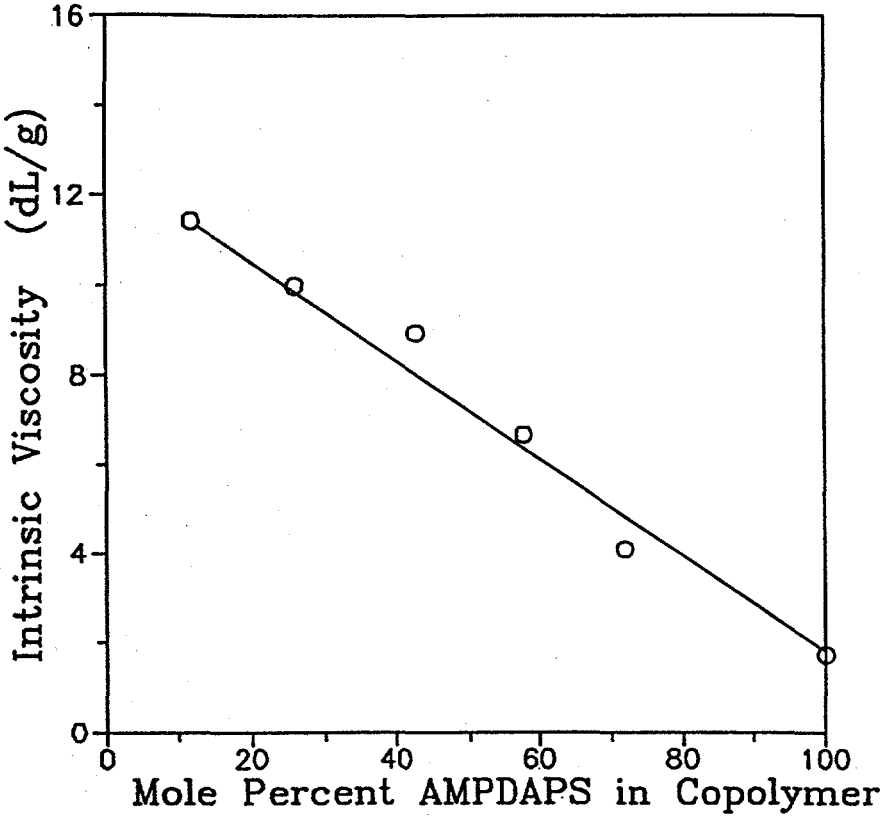

Figure 3-6. Intrinsic viscosity of DAPSAM copolymers as a function of mole percent AMPDAPS incorporated. (Determined in 0.514M NaCl at a shear rate of 1.25 sec^{-1}.)

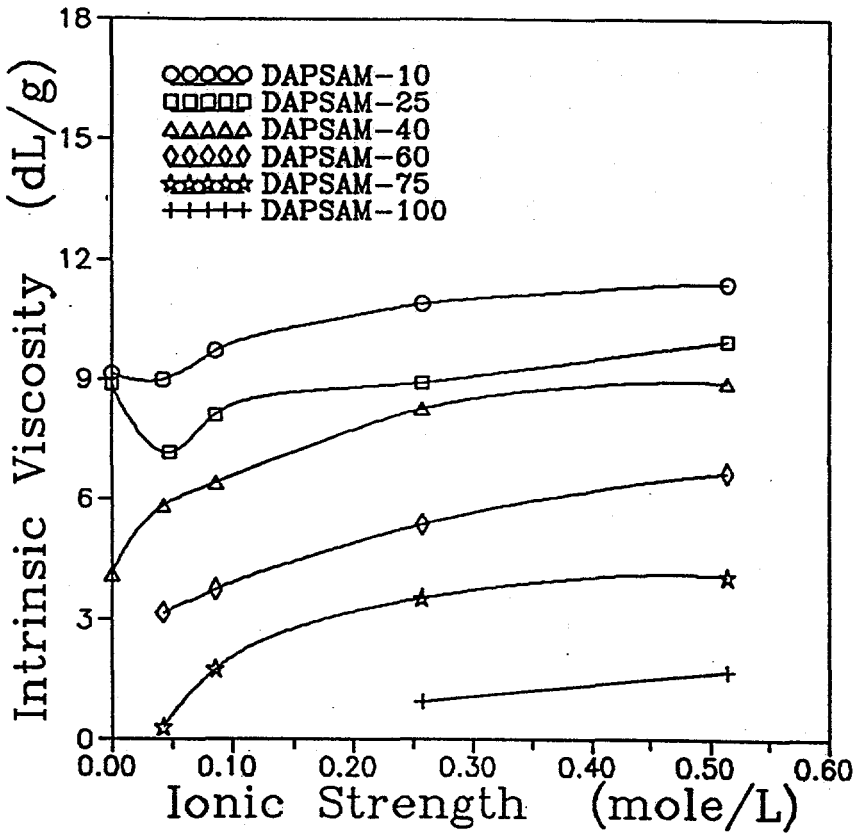

Figure 3-7. Dependence of the intrinsic viscosity of DAPSAM copolymers on NaCl ionic strength determined at 25°C at shear rate of 1.75 sec^{-1}.)

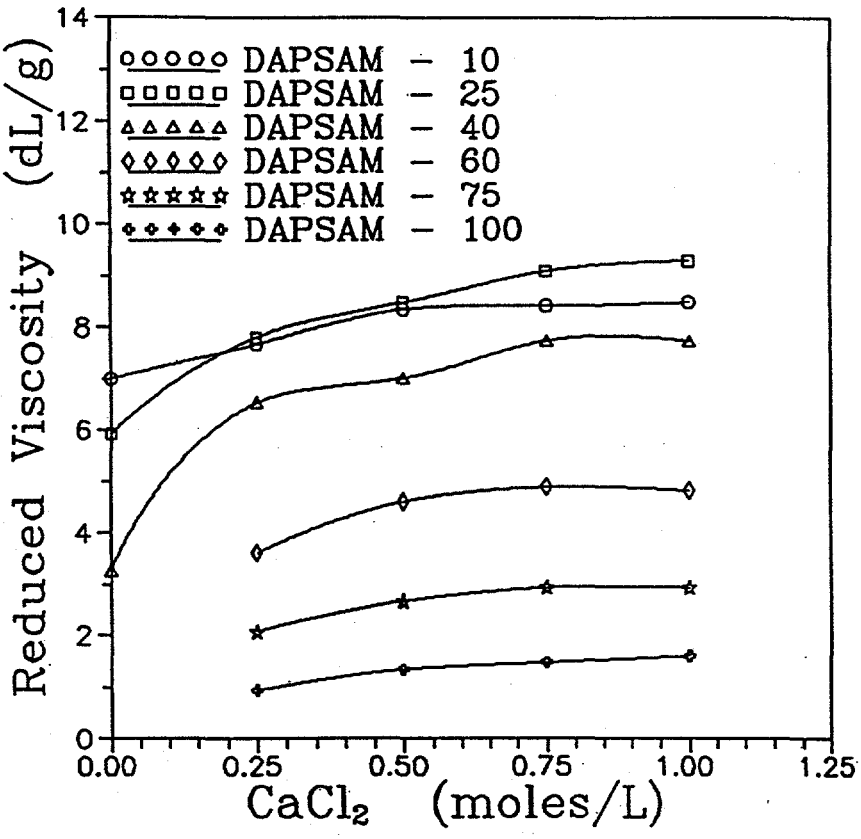

Figure 3-8. Reduced viscosity of DAPSAM copolymers as a function of $CaCl_2$ concentration. (Determined at 25°C at shear rate of 1.75 sec^{-1}.)

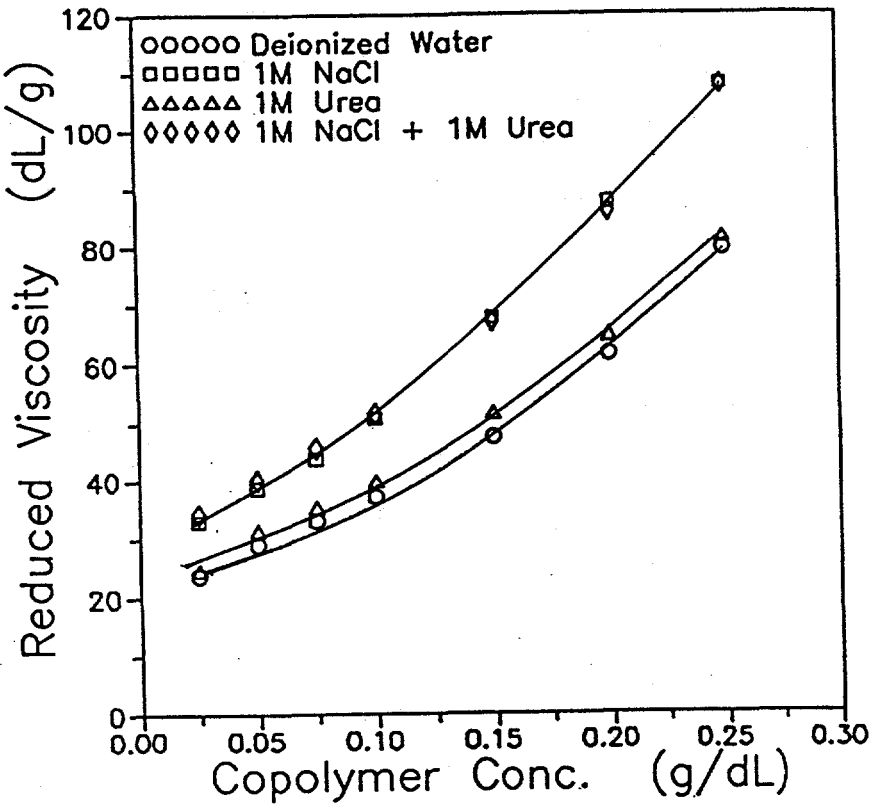

Figure 3-9. Changes in reduced viscosity of DAPSAM-10 as a function of solvent determined at 25°C with a shear rate of 5.96 sec^{-1}.

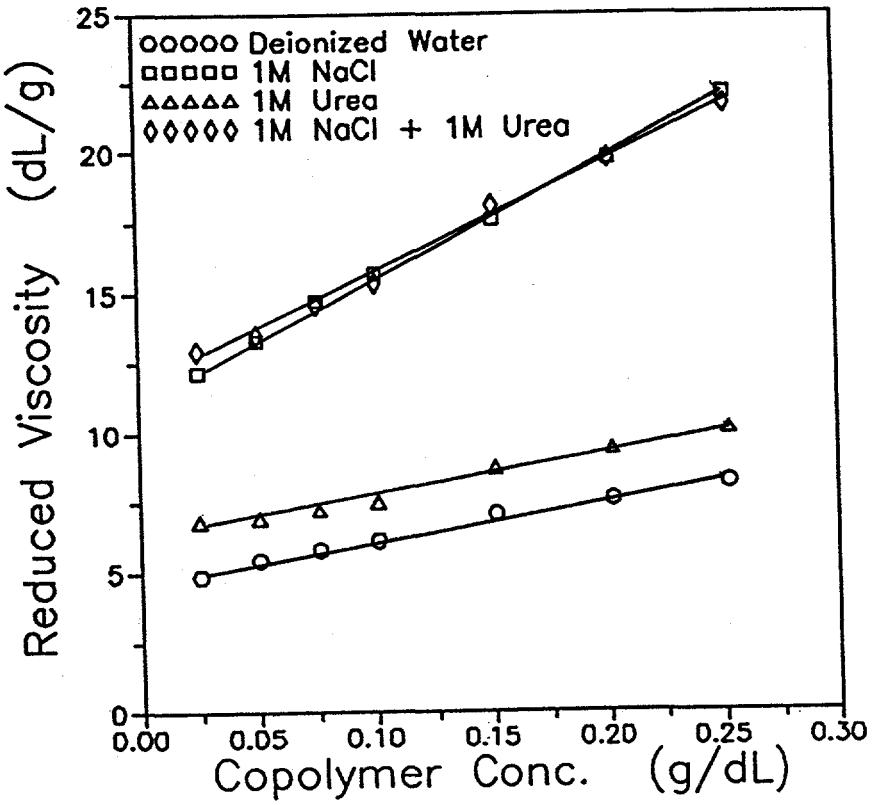

Figure 3-10. Changes in reduced viscosity of DAPSAM-40 as a function of solvent determined at 25°C with a shear rate of 5.96 sec^{-1}.

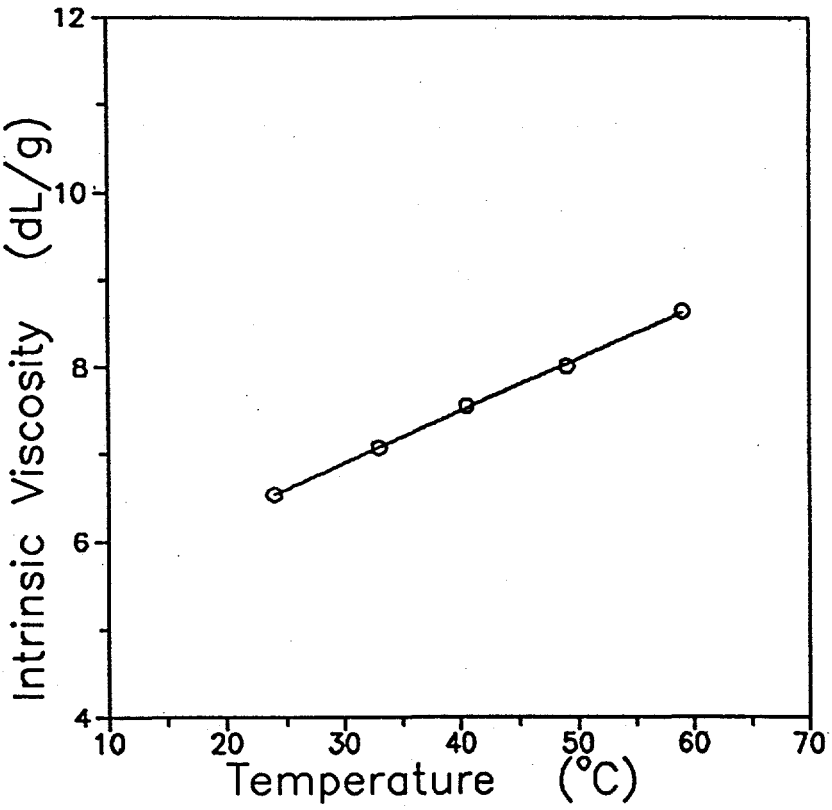

Figure 3-11. Intrinsic viscosity of the DAPSAM-40-3 copolymer as a function of temperature determined in deionized water at a shear rate of 5.96 sec^{-1}.

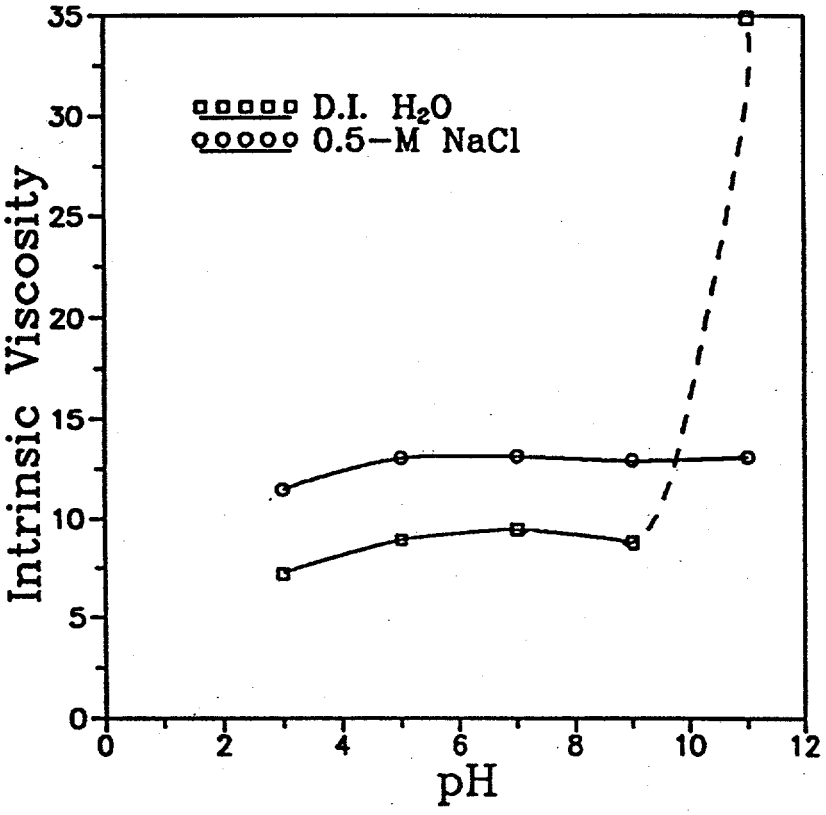

Figure 3-12. Intrinsic viscosity of DAPSAM-25 as a function of pH in D.I. H_2O and in 0.5M NaCl determined at 30°C with a shear rate of 1.25 sec^{-1}.

CHAPTER FOUR: COPOLYMERIZATION OF MALEIC ANHYDRIDE AND N-VINYLFORMAMIDE: CHARGE TRANSFER COMPLEXATION OF THE MONOMERS AND THEIR REACTIVITY RATIOS

Abstract

The free radical copolymerization of maleic anhydride (MA) and N-vinylformamide (NVF) in homogeneous solution has been studied in the range from 10 to 90 mole % NVF in the feed. The copolymer compositions have been determined from elemental analysis and ^{13}C NMR. Reactivity ratios were calculated by Fineman-Ross, Kelen-Tudos and nonlinear least square methods, and indicate that the monomer pair has strong tendency to alternate. MA and NVF were found to form a charge transfer complex in both chloroform and THF. The equilibrium constant and composition of the charge transfer complex were calculated from the modified Benesi-Hildebrand equation.

Introduction

Maleic anhydride (MA) does not homopolymerize by normal free radical polymerization but can readily form alternating copolymers with electron-donor monomers such as styrene[1], vinyl ethers[2] and vinylacetate.[3] N-vinylformamide (NVF), on the other hand, can homopolymerize and copolymerize to high molecular weight.[4,5] Here we report the synthesis and characterization of the copolymers derived from MA and NVF. The possibility of complexation of MA and NVF has also been investigated.

Experimental

Materials

Maleic anhydride was recrystallized from chloroform and vacuum dried at room temperature (mp 55-55.5°C). N-Vinylformamide, supplied by Air Products Inc., was distilled twice under reduced pressure prior to use (bp 60-61°C at 0.5 mm-Hg). AIBN was recrystallized from ethanol. THF and chloroform were spectroscopic grade and used as received.

Measurements

Infrared spectra were obtained from a Mattson Model 2020 FTIR. ^{1}H and decoupled ^{13}C NMR spectra of the copolymer samples were recorded on Bruker 200 MHz and 300 MHz instruments, using DMSO-d_6 as solvent. Classical light scattering studies were performed with a Chromatix KMX-6 low-angle laser light scattering spectrophotometer with a 2-mW He-Ne laser operating at 633 nm. Refractive index increments (dn/dc) were obtained using a Chromatix KMX-16 differential refractometer. NVF purity was determined with a Hewlett-Parkard 5890 Series II GC instrument. The UV absorption of all samples was measured with a Hewlett-Parkard 8452A UV/VIS spectrophotometer at room temperature. Elemental analyses were conducted by M-H-W Laboratories of Phoenix, AZ.

Copolymerization. MA and NVF were copolymerized by free radical polymerization in THF under nitrogen at 65--67°C using 0.1 mole % AIBN as the initiator. The feed ratio of NVF/MA was varied from 10/90 to 90/10 (Table 4-1).

In a typical synthesis involving 60 mole % NVF in the feed, MA (8.06 g, 0.0822 mole), NVF (8.90 g, 0.125 mole), AIBN (0.0340 g, 2.07×10^{-4} mole) and THF (100 ml) were placed in a 250 ml flask equipped with magnetic stirrer, nitrogen inlet, and a condenser. The mixture was purged with pre-purified nitrogen for 30 minutes and then immersed in an oil bath at 65°C. Copolymerization was allowed to proceed to about 10% conversion. The copolymer was then precipitated in ether, filtered, purified by successive precipitations in ether from DMF, and then dried under vacuum at room temperature for 24 hours.

Determination of Charge Transfer Complex Formation Between MA and NVF

The stock solutions of MA in two different solvents, chloroform and THF, were prepared in 500 ml volumetric flasks. The solutions of MA and NVF were obtained by adding appropriate amount of NVF to 20 ml of MA stock solution. The initial concentrations of MA and NVF in such solutions ranged in chloroform from 0.00427 to 0.00483 M and from 0.492 to 2.14 M, respectively, (Table 4-3) and in THF from 0.00438 to 0.00482 M and from 0.508 to 1.760 M (Table 4-4).

Results and Discussion

Monomer Purification and Copolymerization

NVF, as supplied, contains 4% formamide and other impurities. Initial attempts at purification of NVF, involving successive extraction of formamide with small amount of water from a benzene solution, led to a 98.8% pure product. However, the yield from this method was only about 10%. Multiple vacuum distillations proved to be more efficient. The purity of NVF was 98.2% after two distillations with 78% recovery..

Copolymerizations of MA and NVF were carried out in four organic solvents: benzene, DMF, THF and ethyl acetate. Copolymerization in benzene yielded a light orange precipitate which gradually became tacky in the air and was difficult to purify. The product obtained in DMF was precipitated into ether as a light brown solid. MA and NVF copolymerized most effectively in THF and ethyl acetate. The polymers precipitated as white or slightly yellow solids. Dissolution in DMF and reprecipitation from ether yielded white substances.

Copolymer Composition and Reactivity Ratios

Distinct carbonyl resonances from MA and NVF occur at 173-175 ppm and 160-165 ppm, respectively, in ^{13}C NMR spectra and are useful for the estimation of copolymer composition. The mole fraction of each monomer in the respective copolymers was obtained by integration of the ^{13}C carbonyl resonances of MA and NVF as shown in Table 4-1. Compositional information from NMR agreed favorably with that obtained from elemental analysis utilizing the following equation

$$wt.\ \%N = \frac{14.01 m_1}{71.02 m_1 + 98.06 (1 - m_1)} \times 100$$

where wt.% N represents the weight percentage of nitrogen in the copolymers and m_1 is the mole fraction of NVF units.

The reactivity ratios for NVF (M_1) and MA (M_2) were calculated by the graphical methods of Fineman-Ross[6] and Kelen-Tudos[7], and by a nonlinear least square method[8]. The results are summarized in Table 4-2.

To ascertain copolymer copolymerization behavior, the mole fraction of NVF in the copolymers was plotted as a function of the mole fraction of NVF in the feed. The curve in Figure 4-1 illustrates that the copolymers contain equimolar ratios of the monomers over a wide range of the composition of the feed, which suggests the formation of alternating structure. The alternating tendency of the comonomer pair is also indicated by their r_1r_2 product which approaches zero.

Studies of Charge Transfer Complex Between MA and NVF.

Several monomers that copolymerize with MA in an alternating manner through a free radical mechanism form charge transfer complexes. A charge transfer complex might be expected to exist in the MA/NVF system. For MA and NVF to form a charge transfer complex (CTC), an equilibrium would exist

$$MA + n\,NVF \rightleftharpoons CTC \qquad (1)$$

for which the equilibrium constant is defined as

$$K = [CTC]/([MA][NVF]^n) \qquad (2)$$

where [CTC], [MA] and [NVF] are the concentrations of the CTC, MA and NVF, respectively. The degree of association of the complex is n. Values for K and n can be determined via a modified Benesi-Hildebrand technique. In the classical Benesi-Hildebrand method[9], the absorbance of the complex at given wavelength can be determined by Beer-Lambert equation, provided the electron-donor monomer (D), electron-acceptor monomer (A) and the solvent do not absorb at this wavelength

$$A_{CTC,\lambda} = \epsilon_{CTC,\lambda} L[CTC] \qquad (3)$$

$\epsilon_{CTC,\lambda}$ is the molar absorptivity of the CTC, and L is the path length of the sample.

If the donor molecules are in large excess,

$$[D] >> [A], \text{ i.e., } [D] \approx [D]_o \quad (4)$$

the following relationship can be written:

$$L[A]_o/A_{CTC,\lambda} = 1/\epsilon_{CTC,\lambda} + (1/\epsilon_{CTC,\lambda})(1/K_o)(1/[D]_o^n) \quad (5)$$

where $[A]_o$ is the initial concentration of the acceptor and K_o is the equilibrium constant between the monomer pair and the charge transfer complex. By choosing a proper n value, a plot of $L[A]_o/A_{CTC,\lambda}$ against $1/[D]_o^n$ should yield a straight line. $\epsilon_{CTC,\lambda}$ and K can be calculated from the slope and intercept, respectively.

When there is competition between the solvent and the electron donor monomer for the acceptor sites, experimental approaches become more difficult and a more complicated mathematical equation[10] has to be solved to obtain n and K values. Examination of the recent literature provides no information about possible charge transfer complex formation between MA and THF. However, Caze and Loucheux have shown that MA does not form a complex in chloroform.[10] We have studied the absorption of the MA/NVF systems in both chloroform and THF.

The absorption of MA/NVF in chloroform was measured at 340 nm. For this wavelength, there are weak absorptions of MA and NVF at the concentration studied (Table 4-3), so the classical Benesi-Hildebrand method is not applicable in this case. Careful studies indicate that the absorptions of all components in solution obey the Beer-Lambert relationship under the experimental conditions. The total absorbance $A_{T,\lambda}$ is

$$A_{T,\lambda} = \epsilon_{CTC,\lambda}L[CTC] + \epsilon_{MA,\lambda}L[MA] + \epsilon_{NVF,\lambda}L[NVF] \quad (6)$$

Noticing that

$$[MA] = [MA]_o - [CTC] \quad (7)$$

and $$[NVF]_o >> [MA]_o, \text{ i.e., } [NVF] \approx [NVF]_o \quad (8)$$

the Benesi-Hildebrand method may be applied using (1), (2), (6), and (8)

$$L[MA]_o/A^* = 1/\epsilon^* + (1/\epsilon^*)(1/K)(1/[NVF]_o^n) \quad (9)$$

where $[MA]_o$ and $[NVF]_o$ are the initial molar concentrations of MA and NVF, respectively, and

$$A^* = A_{T,\lambda} - \epsilon_{MA,\lambda}L[MA]_o - \epsilon_{NVF,\lambda}L[NVF]_o,$$
$$\epsilon^* = \epsilon_{CTC,\lambda} - \epsilon_{MA,\lambda}$$

A plot of $L[MA]_o/A^*$ vs $1/[NVF]_o$ yields a straight line (Figure 4-2), and the n, K and $\epsilon_{CTC,\lambda=340\ nm}$ values are summarized in Table 4-5.

MA in THF exhibits almost the same molar absorptivity as in chloroform indicating no complex formation between MA and THF. The n, K values of the MA/NVF system in THF were determined at wavelengths of 340 and 360 nm in a similar manner. The experimental data are summarized in Table 4-4, and plotted in Figures 4-3 and 4-4. $\epsilon_{CTC,\lambda}$, n and K are listed in Table 4-5. The composition of the charge transfer complex of MA and NVF is 1:1, as indicated by the n values of one in both THF and chloroform.

Copolymerization Mechanism

Molar concentrations of charge transfer complex in the copolymerization systems are calculated based on the equilibrium constant, and listed in Table 4-1. The copolymerization rate is not proportional to the concentration of charge transfer complex. Rather, the copolymerization rate increases with increasing NVF concentration. The above suggests that the alternating copolymerization results from the cross-addition of MA and NVF monomers to the propagating chain rather than the homopolymerization of charge transfer complex and that reaction of the maleic anhydride radical with the NVF monomer is the rate-determining step.

Conclusions

MA and NVF form a 1:1 charge transfer complex in both chloroform and THF. Copolymerization of MA and NVF was performed in THF using AIBN as the initiator. The copolymer composition was determined by integration of ^{13}C carbonyl resonances of the monomer units. The reactivity ratios were calculated by three different methods and these values indicate that the monomer pair has strong tendency to form alternating copolymer. The involvement of the charge transfer complex in the alternating copolymerization is excluded since no direct relationship between the copolymerization rate and the concentration of the complex has been found. However, the data are not sufficient to ascertain at this point that whether the complex is involved in the copolymerization.

References

1. Seymour, R. B.; Garner, D. P. *J. Coatings Technology* **1976**, 48, 41.

2. Baldwin, M. G. *J. Polym. Sci.* **1965**, A3, 703.

3. Seymour, R. B.; Garner, D. P.; Sanders, L. J. *J. Macromol. Sci. Chem.* **1979**, A13, 173.

4. Kondo, S.; Inagaki, Y.; Ozeki, M.; Tsuda, K. *J. Polym. Sci., Part A: Polym. Chem.* **1989**, 27(10), 3383.

5. Badesso, R. J.; Lai, T. W.; Pinschmidt, R. K.; Sagl, D. J.; Vijayendran, B. R. *Polym. Prep.* **1991**, 32(2), 110.

6. Fineman, M.; Ross, S. *J. Polym. Sci.* **1950**, 5(2), 259.

7. Kelen, T.; Tudos, F. *J. Macromol. Sci. Chem.* **1975**, A9, 1.

8. Tidwell, P. W.; Mortimer, G. A. *J. Polym. Sci. Part A* **1965**, 3, 369.

9. Benesi, H. A.; Hildebrand, J. H. *J. Am. Chem. Soc.* **1949**, 71, 2703.

10. Caze, C. Loucheux, C. *J. Macromol. Sci., Chem.* **1973**, A7(4), 991.

TABLE 4-1
Copolymerization of NVF and MA

NVF_I[a] (M_1) (Mole %)	NVF_E[b] (M_1) (Mole %)	$[NVF]_E$[c] (M)	[CTC] (M)	t (min.)	Conversion (Mole %)	NVF_C[d] (m_1) (Mole %)	$M_w \times 10^{-4}$
10.1	6.60	0.0751	0.055	240	3.0	46.9	
20.6	15.6	0.169	0.10	480	10.3	47.7	
30.6	25.7	0.293	0.16	420	9.7	49.4	
40.4	37.7	0.460	0.24	210	8.8	50.3	
50.2	52.4	0.675	0.32	110	7.8	50.6 51.8[e]	
60.4	65.0	0.932	0.32	70	9.0	52.3	8.5
70.1	77.2	1.15	0.27	30	9.8	53.8	
80.0	88.0	1.76	0.28	20	6.7	57.6 55.9[e]	8.0
89.9	97.0	2.24	0.31	15	6.0	63.3	

a. Initial mole fraction of NVF in the feed.
b. Mole fraction of NVF at equilibrium.
c. Equilibrium concentration of NVF.
d. Mole fraction of NVF in the copolymers.
e. From elemental analyses.

TABLE 4-2
Reactivity Ratios of NVF and MA

	r_1	r_2	r_1r_2
F-R	$2.2 \times 10^{-2} \pm 0.002$	-0.16 ± 0.01	
K-T	$4.1 \times 10^{-2} \pm 0.003$	$1.1 \times 10^{-2} \pm 0.001$	4.5×10^{-4}
NLS	$2.8 \times 10^{-2} \pm 0.026$	$1.0 \times 10^{-2} \pm 0.025$	2.8×10^{-4}

Table 4-3
NVF/MA System in Chloroform at λ = 340 nm

$C_{MA} \times 10^2$ (M)	C_{NVF} (M)	A_{MA}	A_{NVF}	A_T	A^*
0.483	0.492	0.0182	0.0580	0.100	0.023
0.479	0.713	0.0180	0.0847	0.133	0.030
0.472	0.850	0.0178	0.1010	0.153	0.034
0.463	1.12	0.0174	0.136	0.193	0.040
0.454	1.36	0.0171	0.169	0.228	0.042
0.447	1.57	0.0168	0.192	0.256	0.047
0.440	1.75	0.0165	0.218	0.284	0.050
0.427	2.14	0.0160	0.259	0.333	0.058

TABLE 4-4
NVF/MA System in THF

$C_{MA} \times 10^2$ (M)	C_{NVF} (M)	A_{MA} 340/360 nm	A_{NVF} 340/360 nm	A_T 340/360 nm	A* 340/360 nm
0.482	0.508	0.0178/0	0.06055/0.00555	0.3411/0.1250	0.2578/0.1195
0.470	0.855	0.0173/0	0.09420/0.00883	0.4882/0.1802	0.3767/0.1714
0.461	1.120	0.0170/0	0.1220/0.01141	0.5580/0.1995	0.4190/0.1881
0.452	1.363	0.0165/0	0.1479/0.01433	0.6269/0.2297	0.4625/0.2154
0.438	1.762	0.0161/0	0.1889/0.01789	0.7326/0.2520	0.5271/0.2341

Table 4-5
K and $\epsilon_{CTC,\lambda}$ of NVF/MA System in Chloroform and THF

Solvent	λ (nm)	$\epsilon_{CTC,\lambda}$ ($cm^{-1}M^{-1}$)	n	K (M^{-1})
$CHCl_3$	340	27	1	0.533
THF	340	214	1	0.680
THF	360	99	1	0.672

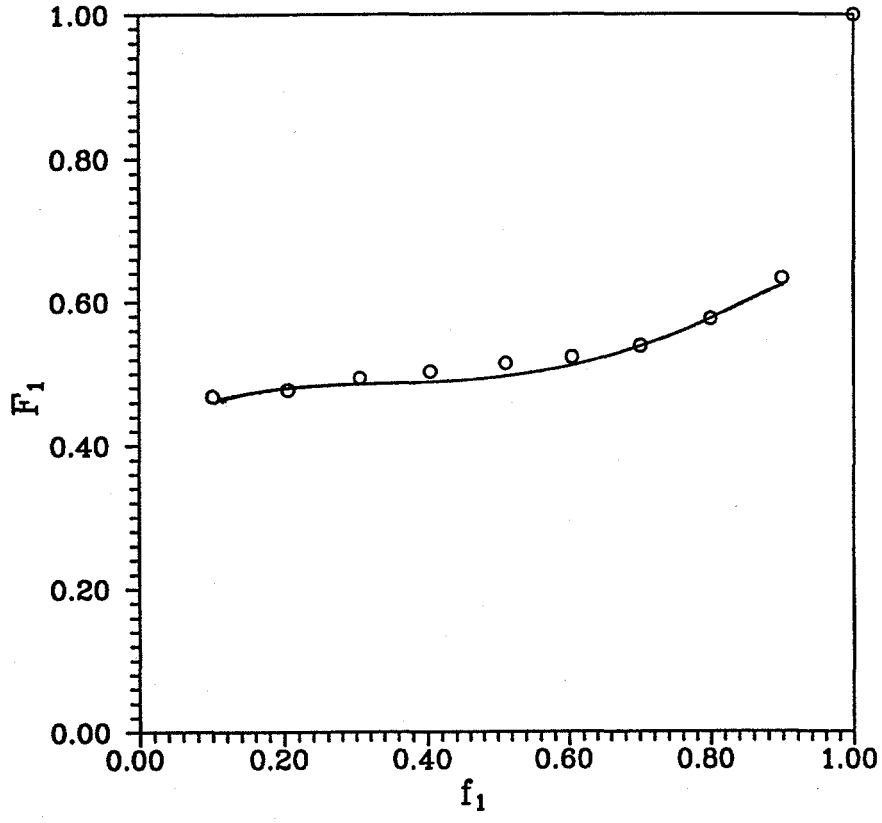

Figure 4-1. Mole percent NVF in the NVF/MA copolymer as a function of comonomer feed ratio.

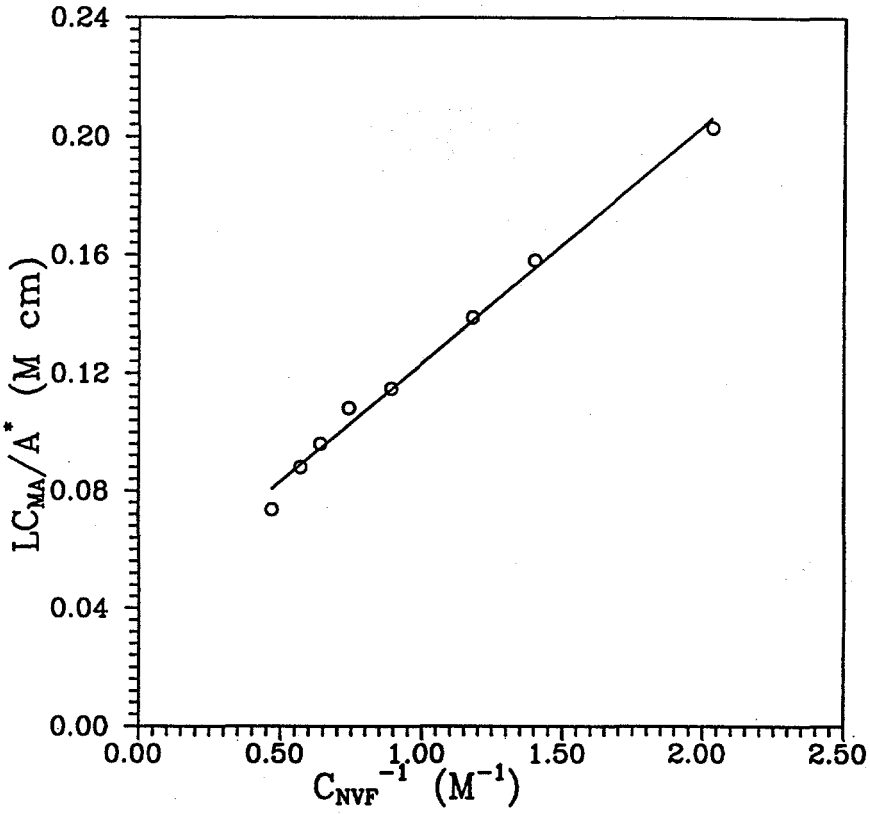

Figure 4-2. A modified Benesi-Hildebrand plot of LC_{MA}/A^* vs. $1/C_{NVF}^{-1}$ for NVF/MA solution in chloroform. (λ = 340 nm)

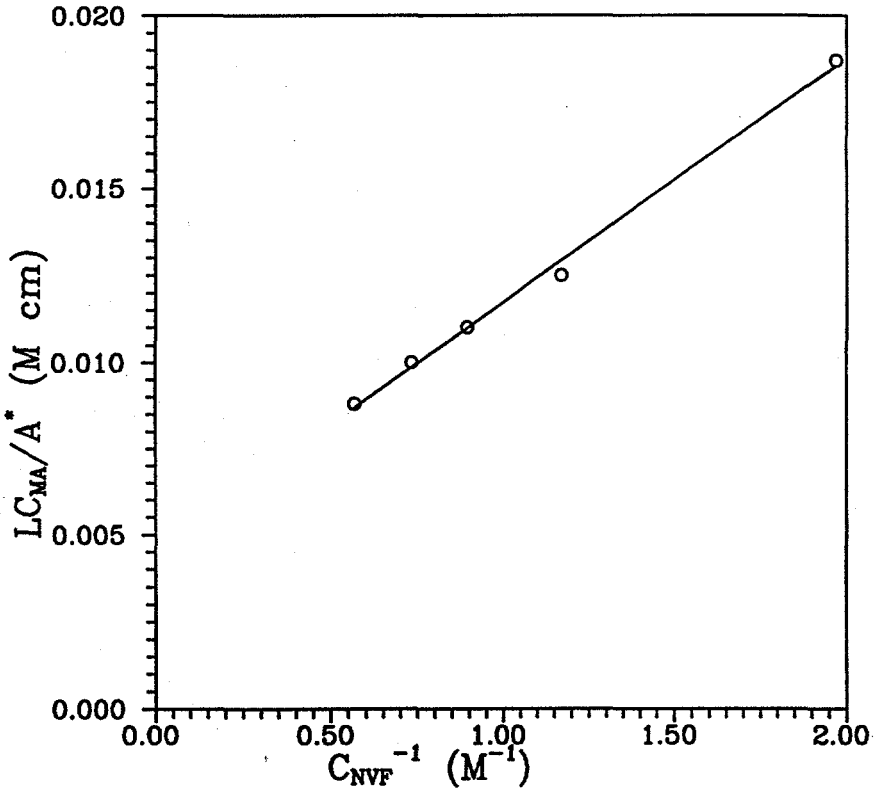

Figure 4-3. A modified Benesi-Hildebrand plot of LC_{MA}/A^* vs. $1/C_{NVF}^{-1}$ for NVF/MA solution in THF. (λ = 340 nm)

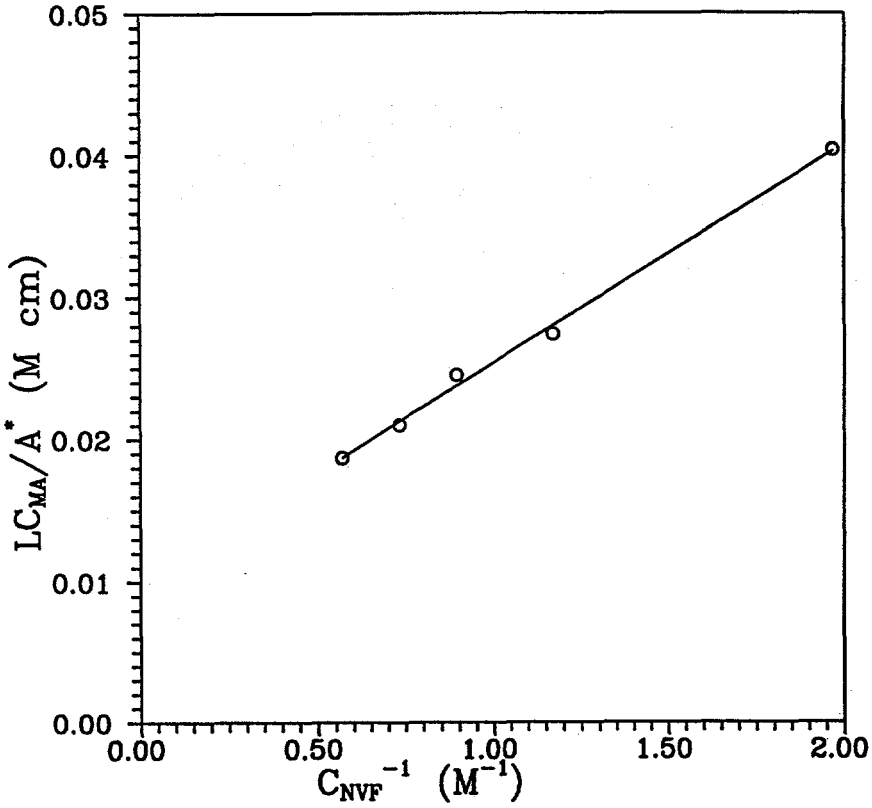

Figure 4-4. A modified Benesi-Hildebrand plot of LC_{MA}/A^* vs. $1/C_{NVF}^{-1}$ for NVF/MA solution in THF. (λ = 360 nm)

CHAPTER FIVE: REACTIVITY RATIOS OF N-VINYLFORMAMIDE WITH ACRYLAMIDE, SODIUM ACRYLATE, AND N-BUTYL ACRYLATE

Abstract

Copolymers of N-vinylformamide (NVF) with acrylamide (AM), sodium acrylate (NA), and n-butyl acrylate (BA) have been prepared by free radical polymerization in homogeneous solutions. Copolymer compositions were obtained by ^{13}C NMR. Reactivity ratios and microstructures of the resulting copolymers were determined. The reactivity ratios calculated by the method of Kelen-Tudos for NVF(M_1)/AM(M_2) were r_1=0.046 and r_2=0.51; for NVF(M_1)/NA(M_2), r_1=0.22 and r_2=0.52; and for NVF(M1)/BA(M2), r_1=0.071 and r_2=0.55. Microstructural data calculated by the method of Igarashi indicated that all three copolymer series exhibit high degrees of alternation.

Introduction

Water-soluble polymers have become increasingly important in industrial applications over the past several decades. In particular, cationic polyelectrolytes are commonly utilized in commercial processes as flocculating agents in water treatment and additives in papermaking.[1] Polyvinylamine, one of the more simple polybases, has recieved little attention in the literature mainly because of the difficulty involved in preparing the polymer.[2] Recently, however, a considerable patent literature has appeared on the purification and polymerization of N-vinylformamide.[3-6] N-vinyl-formamide, once sufficiently purified, may be readily polymerized and subsequently hydrolyzed to attain high molecular weight polyvinylamine.[7]

N-vinylformamide may also be copolymerized with various acrylic monomers. In tailoring copolymers for specific applications, it is useful to know the reactivity ratios of comonomer pairs. Once the reactivity ratios are calculated, a copolymer of known composition may be synthesized by simply adjusting the feed ratio of each monomer before polymerization.

Copolymers of N-vinylformamide with acrylamide, sodium acrylate, and n-butylacrylate were synthesized with a variety of compositions. The reactivity ratios were determined and then used to statistically predict the microstructures of the resulting copolymers. The synthesis and characterization of these copolymer series are discussed in this paper.

Experimental

Materials

N-vinylformamide (NVF) from Air Products and Chemicals Inc. was vacuum distilled prior to use (72° C @ 5 Torr). Acrylamide from Aldrich Chemical Co. was recrystallized three times from acetone and vacuum-dried at room temperature prior to use (mp 83-84° C). Acrylic acid and n-butyl acrylate from Aldrich Chemical Co. were vacuum distilled prior to use. 2,2'-Azobis(N,N'-dimethyleneisobutyramidine) dihydrchloride (VA-044) from Wako Chemicals USA, Inc. and 2,2'Azobisisobutyro-nitrile were employed as the initiators. THF was UV grade and used as received.

Poly(N-vinylformamide-co-acrylamide)

The copolymers of N-vinylformamide (NVF) and acrylamide (AM) were prepared in an aqueous solution at 50° C using 0.1 mol % VA-044 as the initiator. Each reaction was conducted in a 250 mL, three necked flask equipped with a mechanical stirrer and a nitrogen inlet tube. Designated amounts of NVF and AM was dissolved in 145 mL of deionized water. The reaction mixture was then deaerated with oxygen-free nitrogen for 30 minutes and placed in a water bath at 50° C. After the reaction mixture had equilibrated, 0.0485 g of VA-044 dissolved in 5mL of deionized water was injected into the stirring solution. The total monomer concentration was held constant at 1.0 M in each reaction. After a designated time (15-40 mins), the resulting polymer solution was precipitated into a liter of reagent grade acetone. The polymers were further purified by reprecipitation into acetone followed by vacuum drying for 2 days. Conversions were determined gravimetrically. Table 5-2 lists reaction parameters for the copolymerization of NVF with AM.

Poly(N-vinylformamide-co-sodium acrylate)

The copolymers of N-vinylformamide (NVF) and sodium acrylate (NA) were prepared in an aqueous solution at 45° C using 0.075 mol % VA-044 as the initiator. Each reaction was conducted in a 250 mL, three necked flask equipped with a mechanical stirrer and a nitrogen inlet tube. A designated amount of acrylic acid was dissolved in deionized water. To this solution was added an equimolar concentration of sodium hydroxide and the pH adjusted to 8.5. The appropriate amount of NVF was added and the mixture was then deaerated with oxygen-free nitrogen for 30 minutes and placed in a water bath at 45° C. After the reaction mixture had equilibrated, 0.0485 g of VA-044 dissolved in 5mL of deionized water was injected into the stirring solution. The total monomer concentration was held constant at 2.5 M in each reaction. After a designated time, the resulting polymer solution was precipitated into a liter of reagent grade acetone. The polymers were further purified by reprecipitation into acetone followed by vacuum drying for 2 days. Conversions were determined gravimetrically. Table 5-4 lists reaction parameters for the copolymerization of NVF with NA.

Poly(N-vinylformamide-co-n-butyl acrylate)

The copolymers of N-vinylformamide (NVF) and n-butyl acrylate (BA) were copolymerized by free radical polymerization in THF under nitrogen at 65-67°C using 0.1 mol% AIBN as the initiator. The feed ratio of NVF/BA was varied from 10/90 to 90/10. Each reaction was conducted in a 250 ml, three necked flask equipped with a magnetic stirrer, nitrogen inlet, and a condenser. A designated amount af NVF and BA was dissolved in THF and deaerated with oxygen-free nitrogen for 30 minutes and placed in an oil bath at 65-67°C. After the reaction had equilibrated, 0.013 g of AIBN dissolved in 7 ml of THF was injected into the stirring solution. The total monomer concentration was held constant at 1.0M in each reaction. After a designated amount of time (30-60 mins), the resulting polymer was precipitated into petroleum ether/ethyl ether (4/1 v/v). The polymers were further purified by dissultion in acetone followed by precipitation into petroleum ether. After vacuum drying, conversions were determined gravimetrically. Table 5-6 lists reaction parameters for the copolymerization of NVF with BA.

^{13}C Nuclear Magnetic Resonance Spectroscopy

^{13}C NMR spectra of the NVF/AM , NVF/NA and NVF/BA were obtained at 50.3 MHz on a Bruker AC 200 Spectrometer using 10-15 wt % polymer solutions in 5-mm tubes. A recycle delay of 5 s, 90° pulse length, and gated decoupling to remove all NOE was used for quantitative spectral analysis.

Results and Discussion

Reactivity Ratio Studies

Poly(N-vinylformamide-co-acrylamide)

The feed ratios of monomers and the resultant copolymer compositions as determined from ^{13} C NMR (Table 5-2) were used to calculate the reactivity ratios for the NVF (M1) / AM (M2) copolymer series. Figure 5-1 shows a typical ^{13}C NMR spectrum of a copolymer of NVF and AM (NVF/AM6). The Fineman-Ross[8] method and the Kelen-Tudos[9] method were employed to determine the monomer reactivity ratios at low conversion. The Fineman-Ross method yielded values of $r_1 = 0.053 \pm 0.023$ and $r_2 = 0.534 \pm 0.111$ while the Kelen-Tudos method generated values of $r_1 = 0.046 \pm 0.035$ and $r_2 = 0.517 \pm 0.065$. A comparison of the reactivity ratios obtained by the two methods is given in Table 5-1. In Figure 5-2, a copolymer composition plot of mol % NVF found in the copolymer versus mol % NVF in the feed is shown. The NVF / AM comonomers, with r_1 and r_2 both less than 1 and $r_1 r_2 < 0.03$, possess a strong inherent tendency to form alternating copolymers. The calculation of the statistical distribution of monomer sequences, M_1-M_1, M_2-M_2, and M_1-M_2 was performed for the NVF / AM copolymers by the method of Igarashi.[10] Table 5-3 lists the structural data for the copolymers. The calculated mol % of M_1-M_2 linkages is very high, again indicating a definite alternating tendency. Also, the relatively low mean sequence length values are a further indication of the alternating tendency in the NVF / AM copolymers.

The alternating tendency of the copolymers suggests that there is some donor-acceptor character between N-vinylformamide and acrylamide. NVF is expected to be a mildly electron-

donating monomer while acrylamide, due to the strong electron withdrawing amide group, is a mildly electron-accepting monomer. Similar behavior has been observed by Schulz et al.[11] for copolymers of N-vinylpyrrolidone with various monomers possessing an acrylamido functionality. Comparable behavior has been found with the NVF / AM copolymers and would be anticipated due to the similar electronic nature of the formamide and N-pyrrolidone groups.

Poly(N-vinylformamide-co-sodium acrylate)

The feed ratios of monomers and the resultant copolymer compositions as determined from ^{13} C NMR (Table 5-4) were used to calculate the reactivity ratios for the NVF (M1) / NA (M2) copolymer series. The Fineman-Ross[8] method and the Kelen-Tudos[9] method were employed to determine the monomer reactivity ratios at low conversion. The Fineman-Ross method yielded values of $r_1 = 0.29 \pm 0.11$ and $r_2 = 0.65 \pm 0.03$ while the Kelen-Tudos method generated values of $r_1 = 0.22 \pm 0.09$ and $r_2 = 0.52 \pm 0.05$. A comparison of the reactivity ratios obtained by the two methods is given in Table 5-1. In Figure 5-3, a copolymer composition plot of mol % NVF found in the copolymer versus mol % NVF in the feed is shown. The calculation of the statistical distribution of monomer sequences, M_1-M_1, M_2-M_2, and M_1-M_2 was performed for the NVF / NA copolymers by the method of Igarashi.[10] Table 5-5 lists the structural data for the copolymers.

The copolymers of NVF and NA also display an alternating tendency; however, the cause for alternation is likely due to electrostatic repulsions between the sodium acrylate units. Unlike acrylamide, sodium acrlylate possesses a carboxylate functionality which actually donates electron density into the vinyl bond. Thus, NVF and NA both bearing a partial negative charge in the vinyl bonds should repel each other to some extent. However, the repulsion between sodium acrylate units is greater since these monomer units carry a full negative charge. If sodium acrylate is the pendent unit on the growing chain, the activation energy to add a NVF monomer will be slightly lower than the addition of a sodium acrylate due to the absence of electrostatic repulsion. Once NVF is the pendant group, the addition of sodium acrylate will be favored since the NA radical is more stable than the NVF radical. This same alternating tendency has been observed in sodium acrylate/acrylamide copolymers; however, a decrease in alternation is observed if the polymerization is carried out in 1 M NaCl[12]. This behavior is expected since in the presence of added electrolytes, electrostatic repulsions are screened. Therefore the structural composition of these copolymers is significantly affected by the polymerization medium which in turn will affect the physical behavior of the resulting copolymers.

Poly(N-vinylforamide-co-n-butyl acrylate)

The feed ratios of monomers and the resultant copolymer compositions as determined from ^{13} C NMR (Table 5-6) were used to calculate the reactivity ratios for the NVF (M1) / BA (M2) copolymer series. Elemental analyses were also performed on two copolymers, NVF/BA2 and NVF/BA4, and agreed favorably with the information obtained by ^{13}C NMR. The Fineman-Ross[8] method and the Kelen-Tudos[9] method were employed to determine the monomer reactivity ratios at low conversion. The Fineman-Ross method yielded values of $r_1 = 0.061 \pm 0.02$ and $r_2 = 0.54 \pm 0.09$ while the Kelen-Tudos method generated values of $r_1 = 0.071 \pm 0.03$ and $r_2 = 0.55 \pm 0.06$. A comparison of the reactivity ratios obtained by the two methods is given in Table 5-1. In Figure 5-4, a copolymer composition plot of mol % NVF found in the copolymer versus mol

% NVF in the feed is shown. The NVF / BA comonomers, with r_1 and r_2 both less than 1 and $r_1r_2 < 0.04$, also possess a strong inherent tendency to form alternating copolymers. The calculation of the statistical distribution of monomer sequences, M_1-M_1, M_2-M_2, and M_1-M_2 was performed for the NVF / BA copolymers by the method of Igarashi.[10] Table 5-7 lists the structural data for the copolymers. The calculated mol % of M_1-M_2 linkages is very high, again indicating a definite alternating tendency. Also, the relatively low mean sequence length values are a further indication of the alternating tendency in the NVF / BA copolymers.

Conclusions

Copolymers of N-vinylformamide with acrylamide, sodium acrylate, and n-butyl-acrylate were prepared by free radical polymerization. ^{13}C NMR was used to determine the copolymer compositions by integration of the carbonyl peaks. The reactivity ratios were determined by two methods and indicate a strong alternating tendency in all copolymerizations. This alternating tendency was further confirmed by determining the copolymer microstructures by the method of Igarashi.

References

(1) Jones, G. D., in Polyelectrolytes, K. C. Frisch, D. Klemper, and A. V. Patsis, eds., Technomic Publishing Co., Inc., Westport, CT., **1976**, pp144-176.

(2) Molyneux, P., *Water-Soluble Synthetic Polymers: Properties and Behavior, Vol. II,* CRC Press, Boca Raton, Fl., **1984**.

(3) U.S. Pat. 4,772,359 Linhart, F., Degen, H., Auhorn, W., Kroener, M., Hartmann, H., and Heide, W., **1988**.

(4) U. S. Pat. 4,774,285 Pfohl, S., Kroener, M., Hartmann, H., and Denzinger, W., **1988**.

(5) U. S. Pat. 4,795,770 Lai, T. and Vijayendran, B., **1989**.

(6) U. S. Pat. 4,814,505 Kroener, M., Schmidt, W., Proll, T., and Hartmann, H., **1989**.

(7) Badesso, R.J., Lai, T. W., Pinschmidt, R. K., Sagl, D. J., and Vijayendran, B. R., *Polymer Preprints,* **1991**, *32(2)*, 110.

(8) Fineman, M.; Ross, S. *J. Polym. Sci.*, **1950**, *5,* 259.

(9) Kelen, T.; Tudos, F. *J. Macromol. Sci., Chem.,* **1975**, *A9*, 1.

(10) Igarashi, S. *J. Polym. Sci., Polym. Lett. Ed.*, **1963**, *1,* 359.

(11) Schulz, D. N.; Kitano, K.; Danik, J. A.; Kaladas, J. J. *Polymers in Aqueous Media: Performance Through Associatons;* Glass, J. E., Ed.; Advances in Chemistry 223; American Chemical Society; Washington D.C. **1989**, 165.

(12) Ponratnam, S.; Kapur, S. L. *Makromol. Chem.*, **1977**, *178*, 1029.

TABLE 5-1.
REACTIVITY RATIOS FOR N-VINYLFORMAMIDE WITH VARIOUS COMONOMERS

Comonomer Pair	Fineman-Ross	Kelen-Tudos
N-Vinylformamide (M1) and Acrylamide (M2)	$r_1 = 0.053 \pm 0.023$ $r_2 = 0.534 \pm 0.111$	$r_1 = 0.046 \pm 0.035$ $r_2 = 0.517 \pm 0.065$
N-Vinylformamide (M1) and Sodium Acrylate (M2)	$r_1 = 0.29 \pm 0.11$ $r_2 = 0.65 \pm 0.03$	$r_1 = 0.22 \pm 0.09$ $r_2 = 0.52 \pm 0.05$
N-Vinylformamide (M1) and n-Butyl Acrylate (M2)	$r_1 = 0.061 \pm 0.02$ $r_2 = 0.54 \pm 0.09$	$r_1 = 0.071 \pm 0.03$ $r_2 = 0.55 \pm 0.06$

TABLE 5-2.
REACTION PARAMETERS FOR THE COPOLYMERIZATION OF N-VINYLFORMAMIDE (M1) WITH ACRYLAMIDE (M2)

Sample Number	Feed	% Conversion	M1 in Copoly.[a]
NVF/AM1	9.40 : 90.60	16.0	14.1 ± 0.9
NVF/AM2	23.60 : 76.40	18.4	25.0 ± 1.5
NVF/AM3	38.40 : 61.60	9.6	41.0 ± 2.5
NVF/AM4	58.30 : 41.70	8.3	41.1 ± 2.5
NVF/AM5	74.10 : 25.90	9.4	49.7 ± 3.0
NVF/AM6	89.40 : 10.60	13.5	57.6 ± 3.5

(a) Determined by ^{13}C n.m.r.

TABLE 5-3.
STRUCTURAL DATA FOR THE COPOLYMERS OF N-VINLYFORMAMIDE (M1) WITH ACRYLAMIDE (M2)

Sample Number	M1 in Copoloymer (mol %)	Blockiness Mole % M1-M1	M2-M2	Alternation Mole % M1-M2	Mean Seq. Length M1	M2
NVF/A M1	14.10	0.07	71.87	28.07	1.00	5.99
NVF/A M2	25.00	0.29	50.29	49.42	1.01	2.67
NVF/A M3	41.00	1.83	19.83	78.33	1.03	1.83
NVF/A M4	41.10	1.86	19.66	78.48	1.06	1.37
NVF/A M5	49.70	6.38	6.98	86.64	1.13	1.18
NVF/A M6	57.60	17.40	2.20	80.39	1.39	1.06

TABLE 5-4.
REACTION PARAMETERS FOR THE COPOLYMERIZATION OF N-VINYLFORMAMIDE (M1) WITH SODIUM ACRYLATE (M2

Sample Number	Feed	% Conversion	M1 in Copoly.[a]
NVF/NA1	90.0 : 10.0	13.0	77.1 ± 4.6
NVF/NA2	75.0 : 25.0	4.7	60.7 ± 3.6
NVF/NA3	60.0 : 40.0	13.0	48.3 ± 2.9
NVF/NA4	50.0 : 40.0	8.8	40.8 ± 2.5
NVF/NA5	40.0 : 60.0	10.7	38.7 ± 2.3
NVF/NA6	25.0 : 75.0	14.6	27.6 ± 1.7
NVF/NA7	10.0 : 90.0	18.0	18.5 ± 1.1

(a) Determined by ^{13}C n.m.r.

TABLE 5-5.
STRUCUTRAL DATA FOR THE COPOLYMERS OF N-VINYLFORMAMIDE (M1) WITH SODIUM ACRYLATE (M2)

Sample Number	M1 in Copoloymer (mol %)	Blockiness Mole % M1-M1	M2-M2	Alternation Mole % M1-M2	Mean Seq. Length M1	M2
NVF/NA1	77.10	55.20	1.00	43.80	3.00	1.06
NVF/NA2	60.70	26.49	5.09	68.43	1.67	1.17
NVF/NA3	48.30	11.05	14.45	74.53	1.33	1.35
NVF/NA4	40.80	5.82	24.22	69.96	1.22	1.52
NVF/NA5	38.70	4.82	27.42	67.76	1.15	1.78
NVF/NA6	27.60	1.67	46.47	51.87	1.07	2.56
NVF/NA7	18.50	0.58	63.58	35.84	1.02	5.67

TABLE 5-6.
REACTION PARAMETERS FOR THE COPOLYMERIZATION OF N-VINYLFORMAMIDE (M1) WITH n-BUTYL ACRYLATE (M2)

Sample Number	Feed	% Conversion	M1 in Copoly.[a]
NVF/BA1	90.0 : 10.0	9.5	59.5 ± 3.6
NVF/BA2	75.0 : 25.0	11.2	48.2 ± 2.9 49.2[b]
NVF/BA3	60.0 : 40.0	12.0	47.5 ± 2.8
NVF/BA4	50.0 : 50.0	13.5	42.2 ± 2.5 41.6[b]
NVF/BA5	40.0 : 60.0	9.9	38.2 ± 2.3
NVF/BA6	25.0 : 75.0	10.1	24.5 ± 1.5
NVF/BA7	10.0 : 90.0	8.0	14.9 ± 0.9

(a) Determined by ^{13}C n.m.r.

(b) Defined by elemental analysis

TABLE 5-7.
STRUCTURAL DATA FOR THE COPOLYMERS OF N-VINYLFORMAMIDE (M1) WITH n-BUTYL ACRYLATE (M2)

Sample Number	M1 in Copoloymer (mol %)	Blockiness Mole % M1-M1	M2-M2	Alternation Mole % M1-M2	Mean Seq. Length M1	M2
NVF/BA1	59.50	21.60	2.60	75.80	1.64	1.06
NVF/BA2	48.20	6.62	10.22	83.15	1.21	1.18
NVF/BA3	47.50	6.07	11.07	82.85	1.11	1.36
NVF/BA4	42.40	3.25	18.45	78.29	1.07	1.55
NVF/BA5	38.20	2.00	25.60	72.39	1.05	1.82
NVF/BA6	24.50	0.44	51.44	48.12	1.02	2.64
NVF/BA7	14.90	0.12	70.32	29.56	1.01	5.92

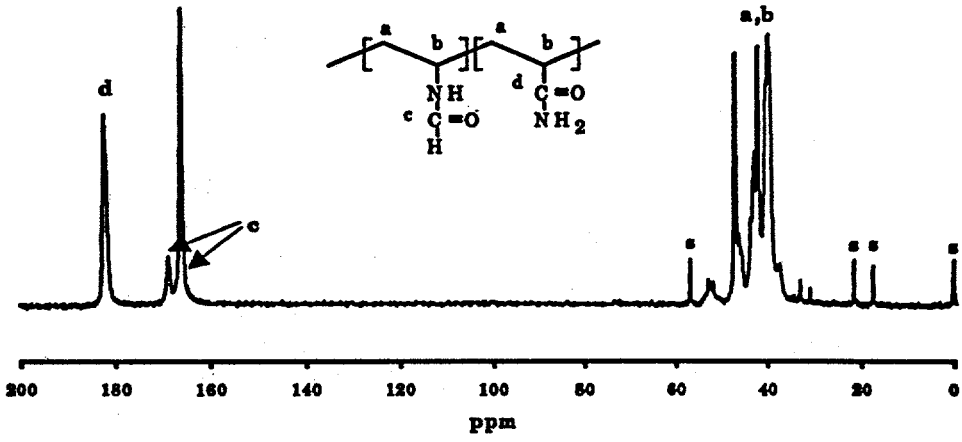

Figure 5-1. Typical ^{13}C NMR spectrum of N-vinylformamide with acrylamide.

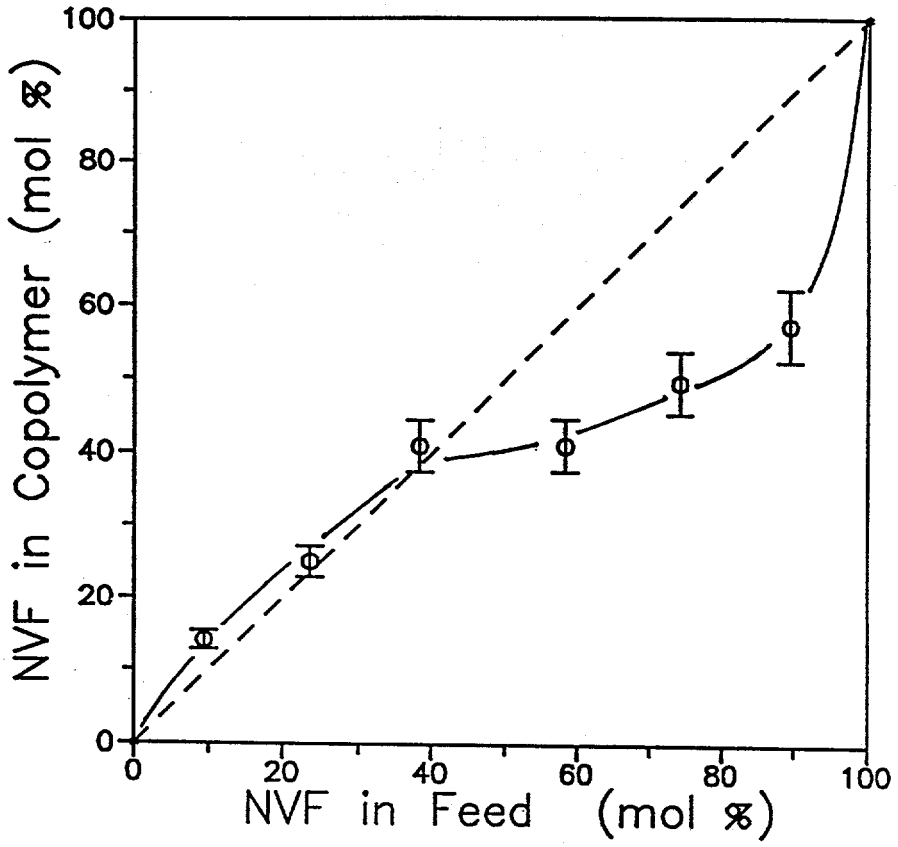

Figure 5-2. Mole percent NVF incorporated into the NVF/AM copolymers as a function of comonomer feed ratio. The dashed line represents ideal random incorporation.

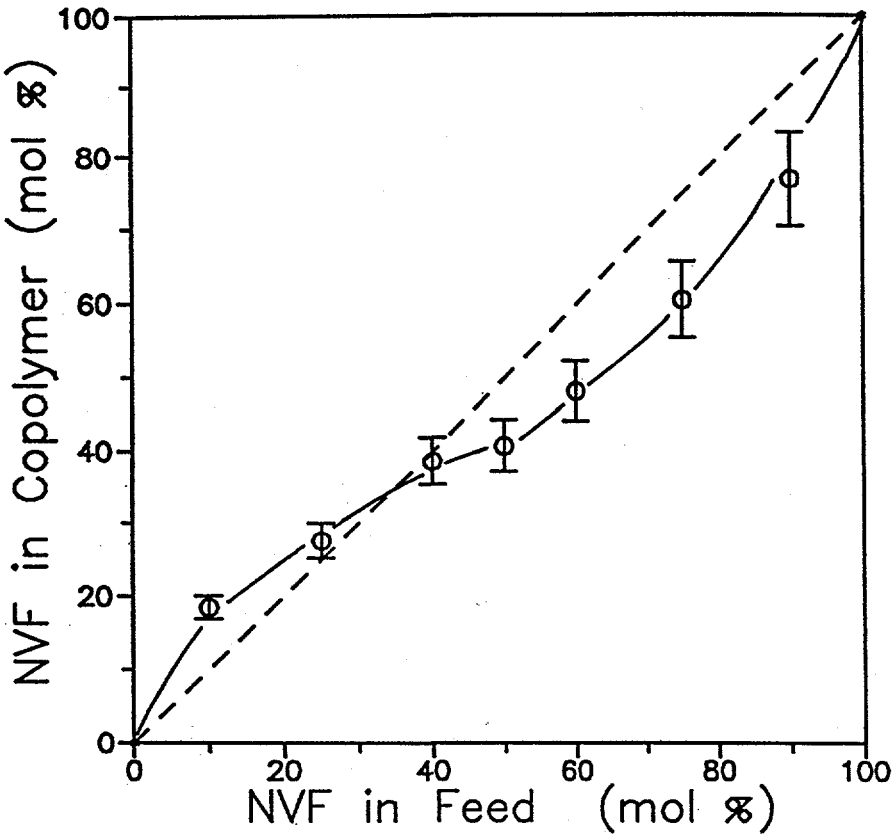

Figure 5-3. Mole percent NVF incorporated into the NVF/NA copolymers as a function of comonomer feed ratio. The dashed line represents ideal random incorporation.

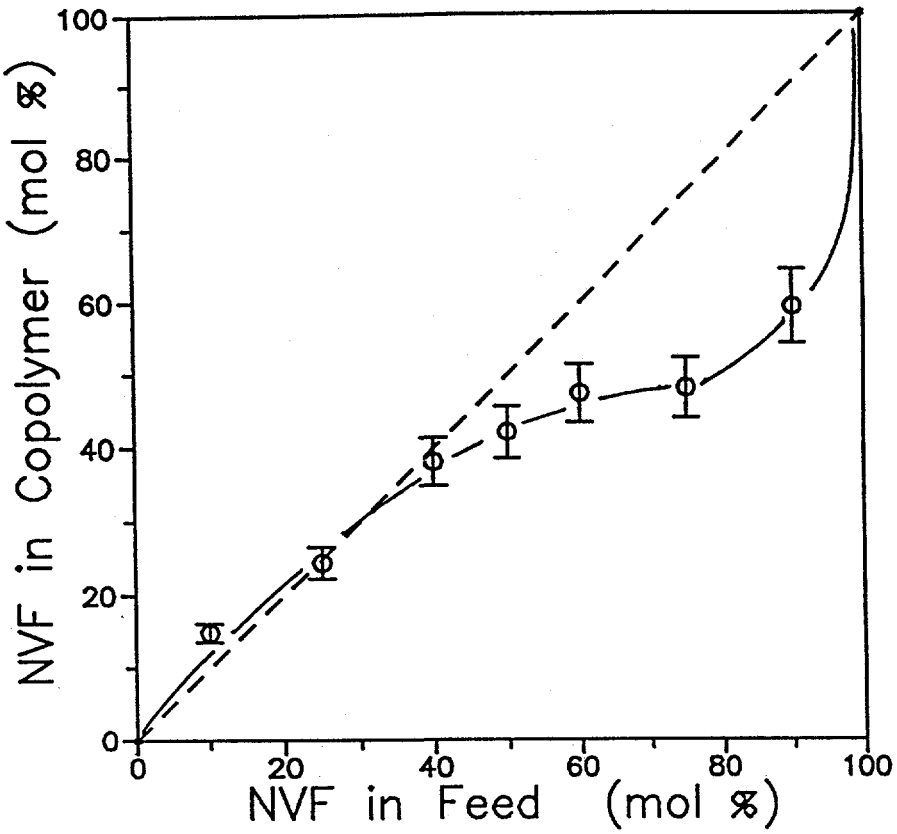

Figure 5-4. Mole percent NVF incorporated into the NVF/BA copolymers as a function of comonomer feed ratio. The dashed line represents ideal random incorporation.

CHAPTER 6: EFFECT OF THE DISTRIBUTION OF THE HYDROPHOBIC CATIONIC MONOMER DIMETHYLDODECYL(2-ACRYLAMIDOETHYL)AMMONIUM BROMIDE ON THE SOLUTION BEHAVIOR OF ASSOCIATING ACRYLAMIDE COPOLYMERS

Abstract

A novel water soluble monomer, N,N-dimethyl-N-dodecyl-N-(2-acrylamidoethyl) ammonium bromide (DAMAB), was synthesized. This monomer possesses a CMC of 4.9×10^{-3} M. A series of copolymers of DAMAB with acrylamide (AM) have been prepared by radical copolymerization by micellar and solution techniques. The rheological properties of the copolymers were strongly affected by their microstructures. A random copolymer with 5 mole % of DAMAB obtained by solution polymerization in t-butanol showed a tendency for intramolecular hydrophobic association, while microheterogeneous copolymerization of AM with 5 and 10 mole % of DAMAB in water yielded microblocky structures which promoted intermolecular association of hydrophobes. The intermolecular association was enhanced by increasing the length of the hydrophobic block and/or the number of blocks in the polymer chain. Evidence of hydrophobic microdomains was obtained utilizing pyrene probe fluorescence.

Introduction

Hydrophobically modified polymers have been the subject of considerable research beginning with the classical studies of Strauss.[1] These amphipathic polymers exhibit unusual aqueous solution behavior, arising from hydrophobic associations that occur in order to minimize water-hydrophobe contact.[2-6] Such associations determine the macromolecular conformation, which in turn, controls the rheological properties of aqueous fluids. These polymers have potential applications in such diverse fields as enhanced oil recovery, fluid modification, controlled drug release, personal care formulation and frictional drag reduction.[7,8]

Certain hydrophobically-modified polymer systems exhibit intermolecular association in aqueous solution[2,3] while others show a preference for intramolecular association[1,4]. The number of the hydrophobic groups incorporated within the amphipathic polymers has been suggested to play an important role in determining the polymer conformation adopted in aqueous solution. Several polymer systems containing either hydrocarbon[9] or fluorocarbon[10] pendent chains show viscosity maxima with increasing hydrophobic group content, implying a transition from intermolecular to intramolecular association. Recent studies in our laboratory have indicated that the distribution of the hydrophobic groups along the polymer chain also significantly affects the conformation of such copolymers.[11,12] When the hydrophobic groups in pyrene labeled acrylamido copolymer systems are arranged in a block-like fashion with long intervening hydrophilic sequences, the hydrophobic interactions promote intermolecular association. Polymers with a random distribution of the same units, on the other hand, exhibit intramolecular associative behavior.

Although many hydrophobically modified polymer systems have been reported, much less attention has been focused on the control of the type of association by altering the polymerization process. As well, structure-property relationships for amphipathic copolymers in aqueous solution are not well established. This paper describes the synthesis and solution properties of copolymers of acrylamide and N,N-dimethyl-N-dodecyl-N-(2-acrylamidoethyl)ammonium bromide. The blockiness of the hydrophobic sequences can be controlled utilizing mixed micelle polymerization. Introduction of cationic groups into the polymers increases water solubility and allows arrangement of hydrophobes in block-like structures using simple solution polymerization techniques. The length of hydrophobic blocks can be controlled under selected conditions. For comparison, a copolymer of identical composition but random hydrophobe distribution was prepared by solution polymerization in t-butanol. The effect of random hydrophobe incorporation versus block hydrophobe incorporation on solution behaviors was investigated. Changes in the run number of blocks were also examined. These data are interpreted in terms of inter- versus intra-molecular associations.

Experimental

Materials

Acrylamide was recrystallized twice from acetone prior to use. Water was deionized to a conductance of 1×10^{-17} mho/cm. Other materials were used as received.

Monomer Synthesis

Scheme 6-1 illustrates the synthesis of the hydrophobically-modified acrylamido monomer N,N-dimethyl-N-dodecyl-N-(2-acrylamidoethyl) ammonium bromide. Into a 250 ml 3-neck round-bottom flask were added methylene chloride (82 ml), N,N-dimethylethylenediamine (8.82 g, 0.100 mole), and 6N sodium hydroxide (25 ml). The mixture was placed in an ice bath and agitated by a magnetic stirrer under nitrogen atmosphere. When the temperature dropped below 5°C, acryloyl chloride (9.36 g, 0.104 mole) in 20 ml of methylene chloride was added slowly from an addition funnel such that the temperature was maintained below 10°C. The mixture was stirred for an additional 30 minutes after complete addition of acryloyl chloride. The organic layer was then separated, washed twice with water, once with concentrated NaCl solution, and dried over anhydrous sodium sulfate. The solvent was removed on a rotary evaporator to yield a slightly yellow oil (11.67 g, 80% yield). The crude product was purified by vacuum distillation in the presence of a small amount of phenothiazine as an inhibitor. A colorless oil was collected at 88-90°C under vacuum of 0.5 mm-Hg. IR (KBr) 3284 (N-H), 1655 (C=O) cm^{-1}; ^1H NMR ($CDCl_3$) δ 2.23 (s, 6 H), 2.46 (t, 2 H), 3.42 (m, 2 H), 5.55-5.60 (m, 2 H), 6.25-6.27 (m, 4 H); 7.53 (br, 1 H); ^{13}C NMR ($CDCl_3$) δ 36.45, 44.43, 57.29, 124.61, 130.59, 165.05.

Freshly distilled N-(N,N-dimethylaminoethyl)acrylamide (5.0 g, 0.035 mole) was then treated with dodecylbromide (13 g, 0.052 mole) under nitrogen at room temperature for 48 hours. Excess dodecylbromide was decanted and the transparent gel precipitated into a white solid on cooling. The resulting material was washed with two portions of ether and dried under vacuum. Further purification of the final product was accomplished by recrystallization from a 1 : 1 mixture of acetone and ether. Yield: 13.26 g (96%). m.p. 70.5--72°C ^1H NMR ($CDCl_3$) δ 0.88

(t, 3 H), 1.25-1.34 (br m, 20 H), 1.76 (m, 2 H) 3.42 (s, 6 H), 3.82 (m, 4 H), 5.63-5.74 (m, 1 H), 6.28-6.6.48 (m, 2 H), 8.79 (br. 1 H); ^{13}C NMR ($CDCl_3$) δ 13.18, 21.71, 21.97, 25.36, 28.36, 28.55, 28.65, 30.94, 33.18, 50.89, 51.18, 64.39, 165.56.

Copolymerization in the Absence of External Surfactant

To a 1000 ml 3-necked round bottom flask equipped with a mechanical stirrer, a condenser, and a nitrogen inlet were added acrylamide (AM) and N,N-dimethyl-N-dodecyl-N-(2-acrylamidoethyl) ammonium bromide (DAMAB) in the desired ratio, and 500 ml deionized water. The total concentration of the comonomers was kept constant at 0.21 M. The solution was heated to 50°C in a water bath with a small nitrogen stream passing through the system. Polymerization was then initiated by addition of $K_2S_2O_8$ (0.0262 g, 9.71×10^{-5} mole in 3 ml of deionized water) via a syringe. Polymerization was conducted continuously at 50°C for 6 hours and then the reaction stopped by precipitating the polymer in 800 ml of acetone. The precipitated polymer was washed twice with acetone and vacuum dried. Conversion was 60-72%. Further purification was accomplished by redissolving the polymer in water and dialyzing for a week against water using a 12,000-14,000 molecular weight cut-off dialysis tubing. The polymer was recovered by freeze drying.

Copolymerization in the Presence of External Surfactant

Equimolar amounts of cetyltrimethylammonium bromide and DAMAB monomer were added with acrylamide to the polymerization system. The same procedure as in the previous case was followed for polymerization and polymer purification.

Solution Polymerization

A copolymer containing 5 mole % DAMAB in the feed was prepared via homogeneous solution polymerization. AM (23.3 g, 0.328 mole) and DAMAB (6.79 g, 0.0173 mole) were dissolved in 300 ml t-butanol. The solution was purged with nitrogen for 30 minutes at 50°C. AIBN (0.056 g, 3.4×10^{-4} mole) was then added to initiate the polymerization. Polymerization was conducted for 10 hours. In this case, the copolymer precipitated from solution as polymerization continued. Purification procedure was as described for the polymerization in water. A quantitative yield was obtained.

Characterization

^1H and ^{13}C NMR spectra were recorded using a Bruker AC-300. A Mattson 2020 Galaxy Series FTIR was used to obtain infrared spectra. The critical micelle concentration of DAMAB was determined by surface tension measurements with a Kruss processor tensiometer K12 instrument using the DeNouy ring method at 25°C. Viscosity measurements were conducted with a Contraves LS-30 low shear rheometer at a constant shear rate of 6 reciprocal seconds at 25°C. Classical light scattering studies were performed on a Chromatix KMX-6 low-angle laser light scattering spectrophotometer with a 2-mW He-Ne laser operating at 633 nm. Refractive index increments (dn/dc) were obtained using a Chromatix KMX-16 differential refractometer. Steady-state fluorescence measurements were made with a Spex Fluorolog-2 fluorescence spectrometer.

Elemental analyses to determine bromine content were conducted by MHW Laboratories of Phoenix, Arizona.

Results and Discussion

Monomer Structure and Micellar Formation

In devising synthetic strategies for ionic monomers, it is generally better to generate the ionic structure in the last synthetic step to minimize any isolation and purification problems.[13] In our DAMAB monomer synthesis, the polymerizable group was attached to the organic framework, followed by a single reaction which connecting the hydrophobic group to the monomer and simultaneously generating the ionic structure. This two-step process proved to be very convenient and the yield and purity of the product is quite satisfactory. The DAMAB monomer provides a quaternary ammonium group which enhances the solubility as well as the dodecyl group for hydrophobic association. The acrylamido functionality of the monomer provides a competitive copolymerization rate with acrylamide. Furthermore, this monomer has an amphipathic structure analogous to cationic surfactants; hence it will form micelles at concentrations above the critical micelle concentration. The CMC of this monomer was measured to be 4.9×10^{-3} M. Negligible change in the CMC was observed on addition of 0.21 M acrylamide. Kinetic studies have demonstrated that monomers of this type possess much higher polymerization rates due to aggregation of the monomers in water.[12] In our case, formation of micelles provide a high concentration of the reactive acrylamido groups near the micelle-water interface, facilitating the formation of the block-like structures during the copolymerization with acrylamide.

Copolymer Synthesis

DAMAB and AM monomers were copolymerized successfully in water and in the presence of external surfactant (Scheme 6-2). Incorporation of cetyltrimethyl ammonium bromide as the cationic cosurfactant should dilute the number of DAMAB molecules in each micelle; therefore, the blocks or "runs" of hydrophobic monomer units in the copolymer are expected to be shortened.

The solution polymerization was designed to yield a random copolymer. Copolymerization studies of AM (M_1) and DAMAB (M_2) in t-butanol indicate that two monomers tend to undergo random, nearly ideal, copolymerization with $r_1 = 1.14 \pm 0.06$ and $r_2 = 0.88 \pm 0.04$. The degree of DAMAB incorporation in each of the copolymers was determined by elemental analysis for bromine content. The resulting compositions are summarized in Table 6-1.

The copolymers are named according to their microstructures. The random and microblocky copolymers are distinguished by having R for random and B for blocky at the beginning of their names. C12 indicates that hydrophobes involved in the copolymers are dodecyl groups. The concentration of the hydrophobic groups in the copolymers are identified by the last number. For instance, R-C12-5.1 is a random copolymer containing 5.1 mole %

dodecyl groups and SB-C12-4.3 is a microblocky copolymer which was prepared in the presence of external surfactant and contains 4.3 mole % dodecyl groups.

Light Scattering Studies

For hydrophobically associating copolymers (BS-C12-4.3, B-C12-4.7, R-C12-5.1, and B-C12-10.5), methanol was used as a co-solvent in the light scattering measurement to disrupt hydrophobic associations and to keep the copolymers from interacting with the filter. As shown in Figure 6-1, for example, R-C12-5.1 in the methanol/water mixture (50/50 by volume) shows a higher viscosity than in deionized water. This is believed to be a result of breakage of intramolecular hydrophobic associations. Lack of hydrophobic associations for the copolymers in the mixted solvent is further demonstrated by studying the response of viscosity of the copolymer solution to changes in shear rate. As shown in Figure 6-2, a region in which the viscosity of R-C12-5.1 in water increases with increasing shear rate is observed. Below and above the region, the copolymer exhibits Newtonian flow. This shear thickening behavior has been reported by other researchers[3] and can be explained by changes in intra- and intermolecular associations with shear. The intramolecular associations are disrupted above a certain shear stress and the chain extension results in an increase in the number of intermolecular associations. The viscosity of the same polymer in the methanol/water mixture only increases slightly with increasing the shear rate, indicating a much less intramolecular hydrophobic association.

The weight average molecular weight data for the copolymers are presented in Table 6-1. The copolymer synthesized in t-butanol has a substantially lower molecular weight than those that were prepared in water. However, the difference in the molecular weight for the two types of copolymers should not be taken alone as the reason for their different association behaviors.

Copolymer Solubility

Copolymers formed in the absence and presence of the cationic co-surfactant exhibit different solubilities. DAMAB monomer concentrations of 1, 5 and 20 mole % in the feed, respectively, result in complete water solubility. The copolymer with 25 mole % DAMAB monomer is only partially soluble, probably because of multiple associations. The effect is more pronounced for the copolymer containing a higher level of hydrophobe. Increasing DAMAB monomer concentration to 40 mole % results in total insolubility.

Dilute Solution Properties

Viscometry is a convenient and reliable method for determining associative properties of amphipathic copolymers in aqueous solution. A typical intramolecular associating polymer in aqueous solution is characterized by a lower viscosity compared to its parent polymer containing no hydrophobic group. The viscosity will increase gradually with polymer concentration due to an increase in the hydrodynamic volume occupied by the macromolecules. If a rapid increase in apparent viscosity occurs at a critical concentration, C^*, the polymer is then described as intermolecularly associative in nature.

Associating properties of the copolymers can also be investigated by fluorescence spectroscopy method using pyrene as a probe. The ratio of the pyrene fluorescence intensities of band I to band III (I_1/I_3) serves as an indicator of the polarity of the micro-environment. A lower value of I_1/I_3 indicates a more hydrophobic environment as experienced by the probe.[14]

Effect of copolymer composition

Before discussing the viscosity properties of the copolymers as a function of the copolymer composition, it is necessary to emphasize that since the copolymers are made at relatively high conversions, they are expected to have somewhat broad molecular weight distributions and copolymer compositions. Studies in Candau's group have shown that in the micellar copolymerizations both the molecular weight and hydrophobic content in the copolymers decrease as copolymerization runs to higher conversion.[15] In our experiments, the copolymerizations were terminated at 60-72% conversion and the DAMAB concentration remains above its CMC even at the highest conversion. Therefore, the number of the hydrophobic blocks in the copolymers may decreases as the copolymerization proceeds, but the sequence length of the blocks should remain relatively constant.

Figure 6-3 illustrates the effect of polymer composition on solution properties. Viscosity increases with increasing DAMAB content. The copolymer containing 0.32 mole % of DAMAB (R-C12-1) displays viscosity behavior that is similar to that of polyacrylamide prepared under the same conditions; there are no significant hydrophobic associations in the concentration range investigated. Copolymers with higher DAMAB content show a significantly greater dependence of the viscosity on concentration, similar to the previously reported behavior of AM and n-alkylacrylamide copolymer systems.[2] The copolymer with 10.5 mole % DAMAB (B-C12-10.5) possesses a lower C^* and a steeper slope beyond C^* than the copolymer with 4.7 mole % DAMAB (B-C12-4.7). This is attributed to stronger intermolecular associations in the former. The C^* values of AM-DAMAB copolymers are generally higher than that of an AM and dodecylacrylamide copolymer containing 0.25 mole % dodecyl groups. This may be attributed to the presence of charged groups in the polymer chain. It is noteworthy, however, that no polyelectrolyte effect is observed for these systems in dilute regime due to the low DAMAB concentration.

Addition of a cationic surfactant to the polymerization system containing 5 mole % DAMAB results in a lower slope gradient in the viscosity profile of the resulting polymer (BS-C12-4.3) relative to the one without external surfactant (B-C12-4.7) (Figure 6-4). This is consistent with formation of shorter blocks and/or a more random distribution of DAMAB units, decreasing the tendency of intermolecular association.

A completely different viscosity profile for the copolymer with 5.1 mole % DAMAB prepared by solution polymerization (R-C12-5.1) is observed (Figure 6- 4). The reduced viscosity decreases with increasing polymer concentration, indicating that hydrophobic associations are largely intramolecular in nature. This point will be addressed further in the discussion of fluorescence data and solvent effects.

Fluorescence Studies

Figure 6-5 depicts the dependence of I_1/I_3 values of pyrene steady state fluorescence spectra on polymer concentration in aqueous solutions of the copolymers. I_1/I_3 values for BS-C12-4.3, B-C12-4.7 and B-C12-10.5 copolymers remain almost constant at 1.36-1.38 in the concentrations above 0.05 g/dL upon dilution. Further decreases in the copolymer concentrations result in rapid increases in I_1/I_3 values. The data suggest that pyrene molecules initially reside inside the hydrophobic microdomains formed through association of the hydrophobic groups. These hydrophobic microdomains vanish as polymer molecules are diluted to concentrations below 0.05 g/dL such that pyrene probes are exposed to a more aqueous environment. This behavior is consistent with intermolecular hydrophobic association. Furthermore, increase in I_1/I_3 occurs at concentrations well below C^*. This implies that hydrophobic interactions at the microscopic level take place at much lower concentration than reflected by macroscopic properties.

Pyrene fluorescence spectra for the R-C12-5.1 copolymer are consistent with classical water-soluble polymeric surfactant behavior[16] (Figure 6-5). A low I_1/I_3 value of pyrene throughout the copolymer concentration range is observed. This indicates that the R-C12-5.1 copolymer provides hydrophobic microdomains and acts as a host. The presence of hydrophobic microdomains is independent of copolymer concentration, consistent with intramolecular association.

I_1/I_3 values in the R-C12-1 copolymer solution decrease continuously with increasing polymer concentration (Figure 6-5). A similar behavior is observed in polyacrylamide solutions. There is no well-defined transition point in the I_1/I_3 vs. copolymer concentration curve, suggesting the absence of hydrophobic interactions between long alkyl chains capable of sequestering a pyrene probe from the aqueous environment. This information agrees favorably with that obtained from viscosity studies.

Effect of solvent

Hydrophobic associations are induced by the water-structuring effect. Change in the water structure by addition of additives or cosolvents can either enhance or reduce hydrophobic interactions, depending on the nature of the additive. Controlled studies of changes in the rheological properties of polymer solutions in different aqueous media provide information on polymer conformation. In this work, NaBr is used as a water-structure forming agent[17] and 1,4-dioxane as a water-structure breaking agent[18]. The R-C12-1 copolymer is soluble in both 0.05 M NaBr aqueous solution and a water/dioxane mixture in a ratio of 10 to 1 by volume. However, solubility of the copolymers with higher hydrophobe content is affected significantly by added external electrolyte. Addition of NaBr results in precipitation from solution due to a "salting out" effect[17]. The latter copolymers are soluble in the water/dioxane mixture.

Figure 6-6 shows the effect of solvent on the viscosity of the R-C12-5.1 copolymer. The reduced viscosity increases upon addition of 10% dioxane. This is attributed to the decrease in the extent of intramolecular association resulting in the expansion of the polymer coil. Intermolecular association is also disrupted as dioxane is introduced into BS-C12-4.3 and B-C12-4.7 copolymer solutions. The viscosity of the BS-C12-4.3 copolymer shows less concentration dependence due to reduced intermolecular association tendency (Figure 6-7). It is interesting to

note that this copolymer possesses a higher reduced viscosity in the lower concentration range in the water/dioxane mixture than in deionized water. A similar behavior is also observed for B-C12-4.7 copolymer. A possible explanation is that there are some intramolecular associations of hydrophobic groups in the low concentration regime which are disrupted upon addition of dioxane. This indicates that hydrophobic associations undergo a transition from intermolecular to intramolecular when the solution is diluted. A similar observation was reported by Siano, et al[19] in a study of acrylamide and n-octylacrylamide copolymers using 8-anilino-1-naphthalene sulfonic acid as a fluorescence probe. Schulz, et al[20] also observed such a transition for the copolymer of acrylamide and a nonionic surfactant monomer. However, such an intramolecular association at low concentration was not seen in pyrene probe studies. This suggests that while polymer solution properties may be influenced considerably by the presence of hydrophobic interactions, aggregates may not be of sufficient size to protect pyrene molecules from the bulk aqueous solution. I_1/I_3 values of pyrene fluorescence in such cases fail to "report" the presence of hydrophobic interactions.[21] The viscosity profile of the R-C12-1 copolymer is essentially invariant with addition of NaBr or dioxane, again indicating the lack of hydrophobic interactions in this system (Figure 6-8).

Conclusions

Rheological and fluorescence studies of amphipathic copolymers of AM and DAMAB have demonstrated that the associating behavior of the copolymers is governed by the arrangement of DAMAB units along the polymer chains. A random copolymer with 5 mole % of DAMAB shows a tendency for intra-molecular hydrophobic association, while a microblocky copolymer of identical composition results in intermolecular association of hydrophobes. The intermolecular hydrophobic associations are enhanced by increasing the length of the hydrophobic block and/or the number of the blocks in the polymer chain.

References

1. Strauss, U. P.; Gershfeld, N. L. *J. Phys. Chem.* **1954**, 747.

2. McCormick, C. L.; Johnson, C. B.; Nanaka, T *Polymer* **1988**, 29, 731.

3. Bock, J.; Siano, D. B.; Valint, P. L. Jr.; Pace, S. L. In *Polymers in Aqueous Media*; Glass, J. E., Ed.; Advances in Chemistry Series No. 223; ACS Washington, D C **1989**; p 411.

4. Morishima, Y.; Kobayashi, T.; Nogakura, S. *Polym. J.* **1989**, 21(3), 267.

5. Tanford, C *The Hydrophobic Effect: Formation of Micelles and Biological Membranes*; 2nd Ed.; John Wiley & Sons: New York, **1980**.

6. Franks, F. In *Water: A Comprehensive Treatise*; Franks, F., Ed.; Plenum Press: New York, **1975**; Vol. 4.

7. McCormick, C. L.; Bock, J.; Schulz, D. N. In *Encyclopedia of Polymer Science and Engineering*; John Wiley & Sons: New York, **1989**; Vol. 17; p 730.

8. McCormick, C. L.; Johnson C. B. In *Polymers in Aqueous Media*; Glass, J. E., Ed.; Advances in Chemistry Series No. 223; ACS Washington, DC **1989**; p 437.

9. Landoll, L. M. *J. Polym. Sci. Chem.* **1982**, 20, 443.

10. Zhang, Y. X.; Da, A. H.; Hogen-Esch, T. E.; Butler, G. B. *J. Polym. Sci. Lett.* **1990**, 28, 213.

11. Ezzell, S. A.; McCormick, C. L. *Macromolecules* **1992**, 25, 1881.

12. Ezzell, S. A.; McCormick, C. L. *Macromolecules* **1992**, 25, 1887.

13. Hamid, S. M.; Sherrington, D. C. *Polymer* **1987**, 28, 325.

14. Kalyanasundaram, K.; Thomas, J. K. *J. Am. Chem. Soc.* **1977**, 99, 2039.

15. Biggs, S; Hill, A.; Selb, J.; Candau, F. *J. Phys. Chem.* **1992**, 96, 1505.

16. Laschewsky, A.; Zerbe, I. *Polymer* **1990**, 32, 2081.

17. Schild, H. G.; Tirrell, D. *J. Phys. Chem.* **1990**, 94, 4352.

18. Schild, H. G.; Muthukumar, M.; Tirrell, D. A. *Macromolecules* **1991**, 24, 948.

19. Siano, D. B.; Bock, J.; Myer, P.; Valuit, P. L. Jr. In *Polymers in Aqueous Media*, Glass, E. J., Ed.; Advances in Chemistry Series No. 223; ACS Washington, DC **1989**; p 425.

20. Schulz, D. N.; Kaladas, J. J.; Maurer, J. J.; Bock, J.; Pace, S. J.; Schulz, W. W. *Polymer* **1987**, 28, 2110.

21. Clark, M. Ph. D. Dissertation, The University of Southern Mississippi, Hattiesburg, MS 39406, **1990**.

TABLE 6-1. STRUCTURAL PARAMETERS OF THE COPOLYMERS

Copolymer	DAMAB Content (mole %)	$M_w \times 10^{-6}$
PAM	0	1.12[a]
R-C12-1	0.32	0.74[a]
BS-C12-4.3	4.3	0.95[b]
B-C12-4.7	4.7	1.04[b]
R-C12-5.1	5.1	0.46[b]
B-C12-10.5	10.5	1.12[b]

a. Measurement was taken in deionized water.
b. Measurement was taken in MeOH/H_2O mixture (50/50 by volume).

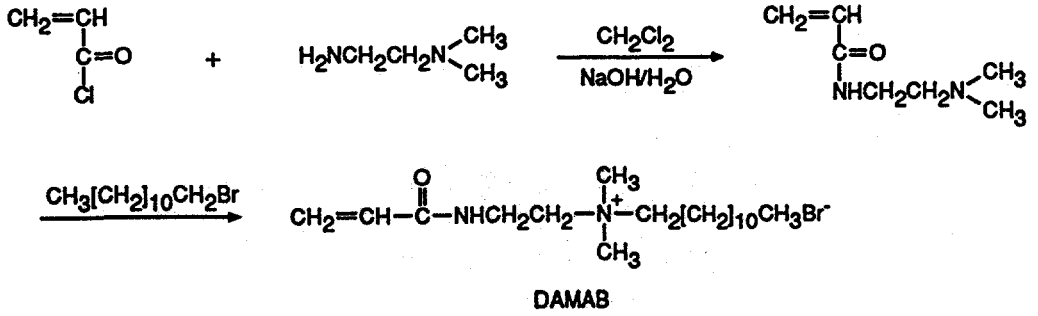

DAMAB

Scheme 6-1. Synthesis of DAMAB Monomer

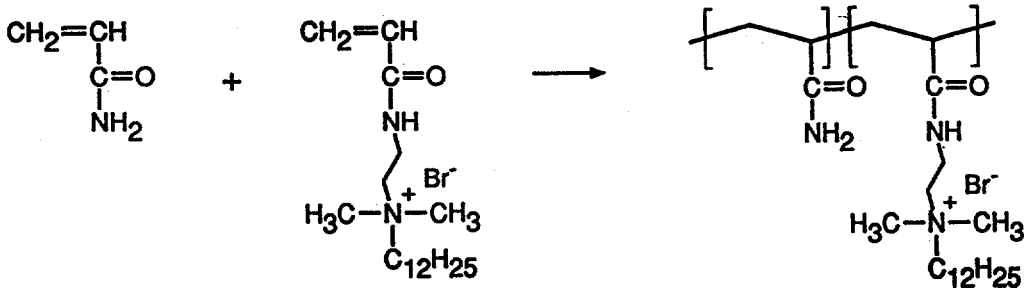

Scheme 6-2. Copolymerization of AM and DAMAB

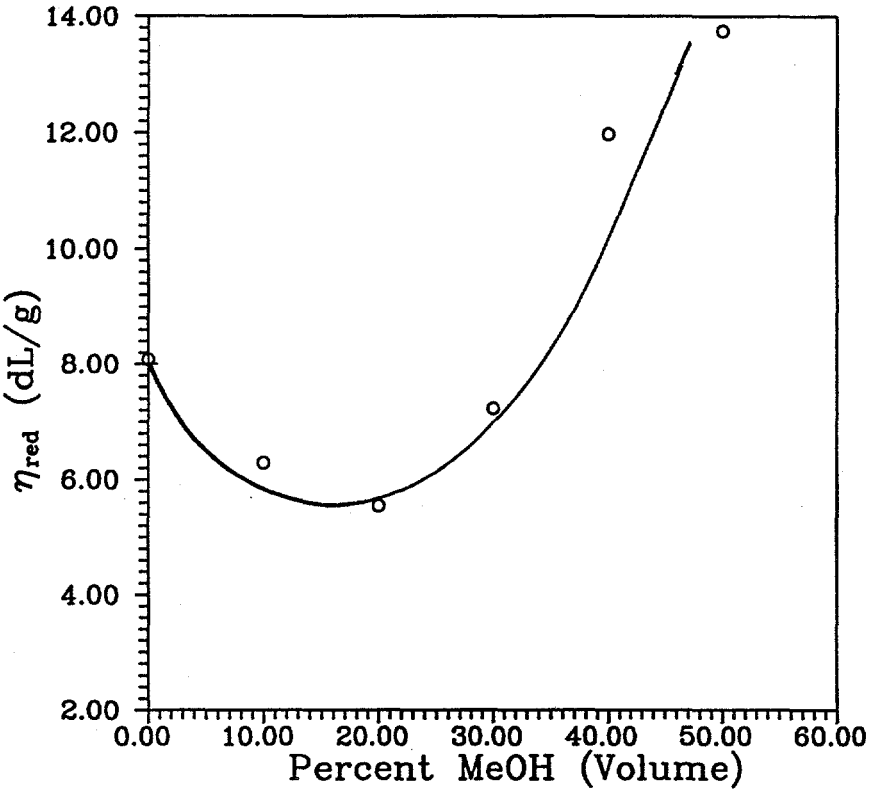

Figure 6-1. Effect of solvent on the η_{red} of R-C12-5.1 copolymer. The copolymer concentration is 0.127 g/dL.

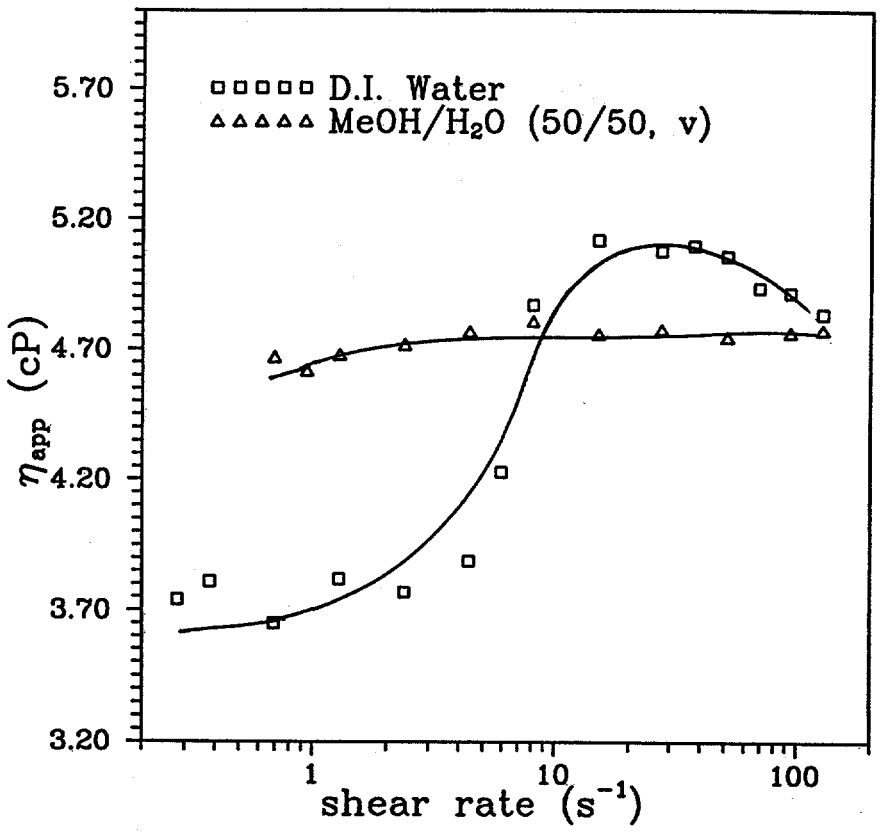

Figure 6-2. Effect of the shear rate on the viscosity of R-C12-5.1 at 0.484 g/dL.

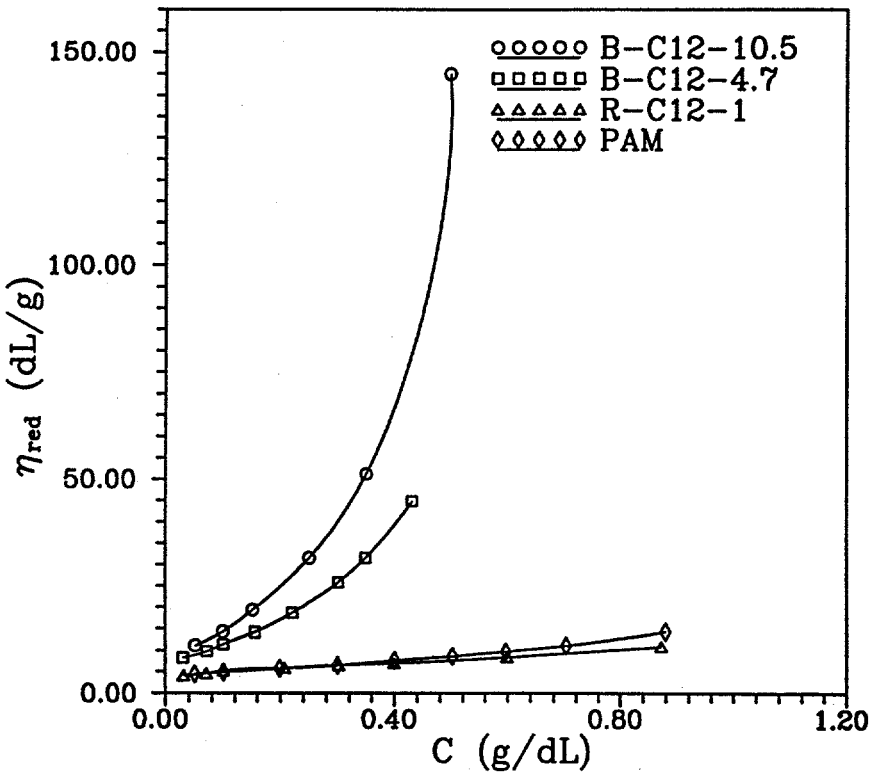

Figure 6-3. Effect of concentration on η_{red} for the copolymers with various hydrophobic group contents in D.I. water.

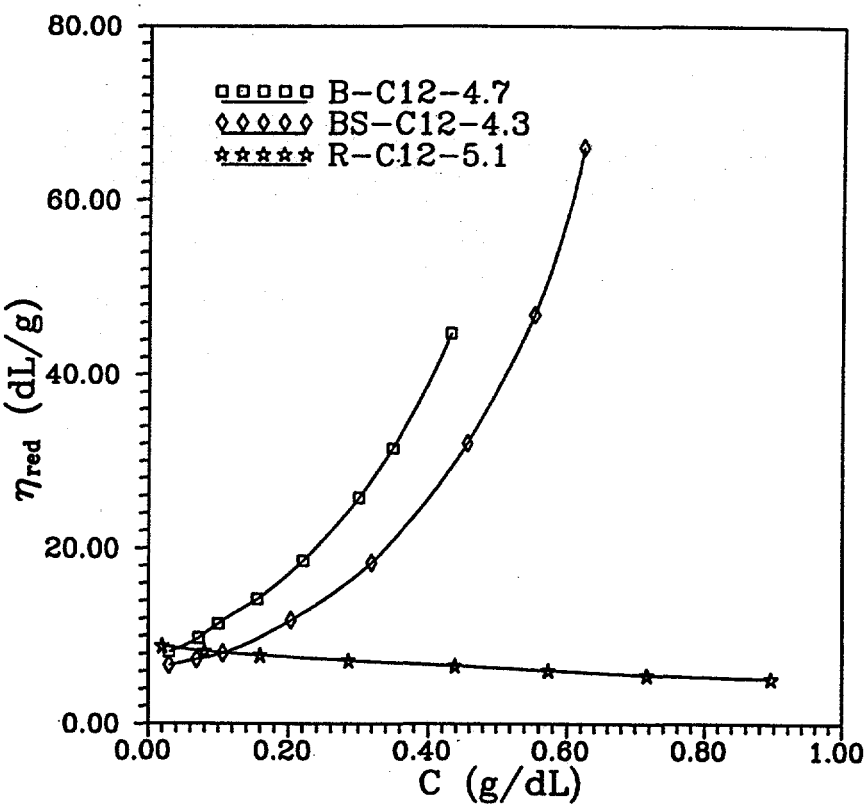

Figure 6-4. Effect of polymer concentration on η_{red} for copolymers containing various hydrophobic sequence length in D.I. water.

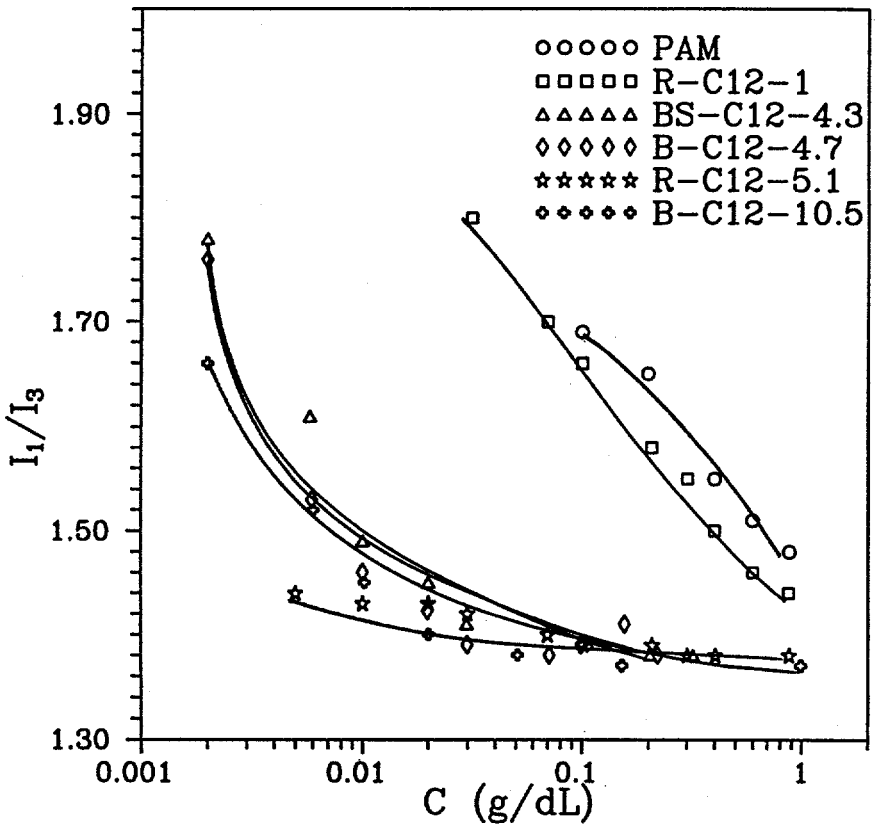

Figure 6-5. I_1/I_3 as a function of polymer concentration for various copolymers in D.I. water.

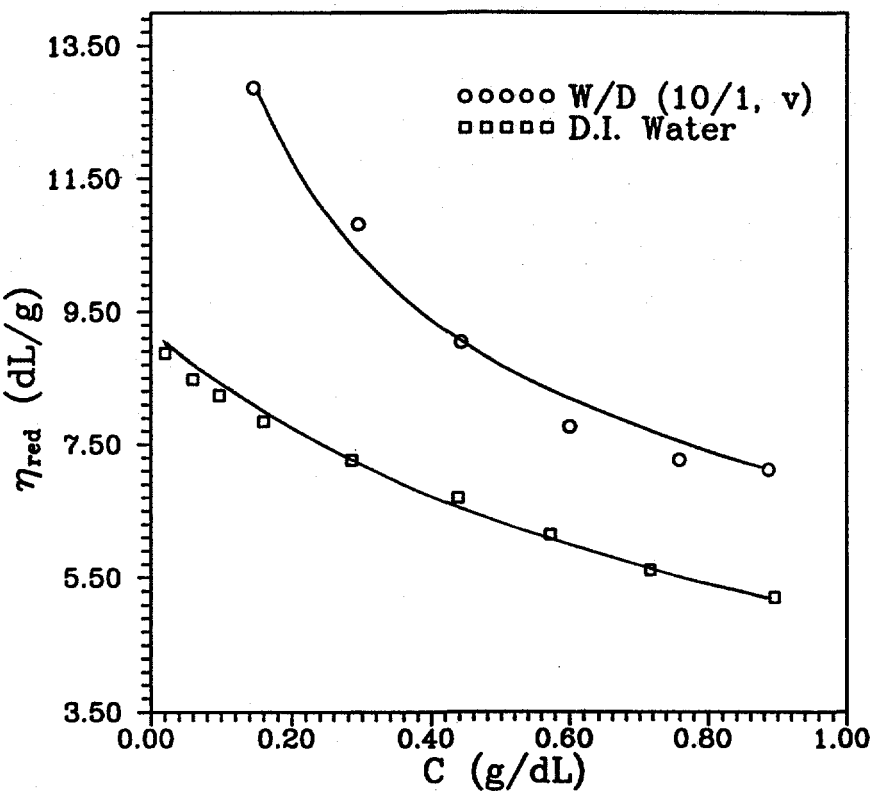

Figure 6-6. Effect of solvent on η_{red} of R-C12-5.1 copolymer.

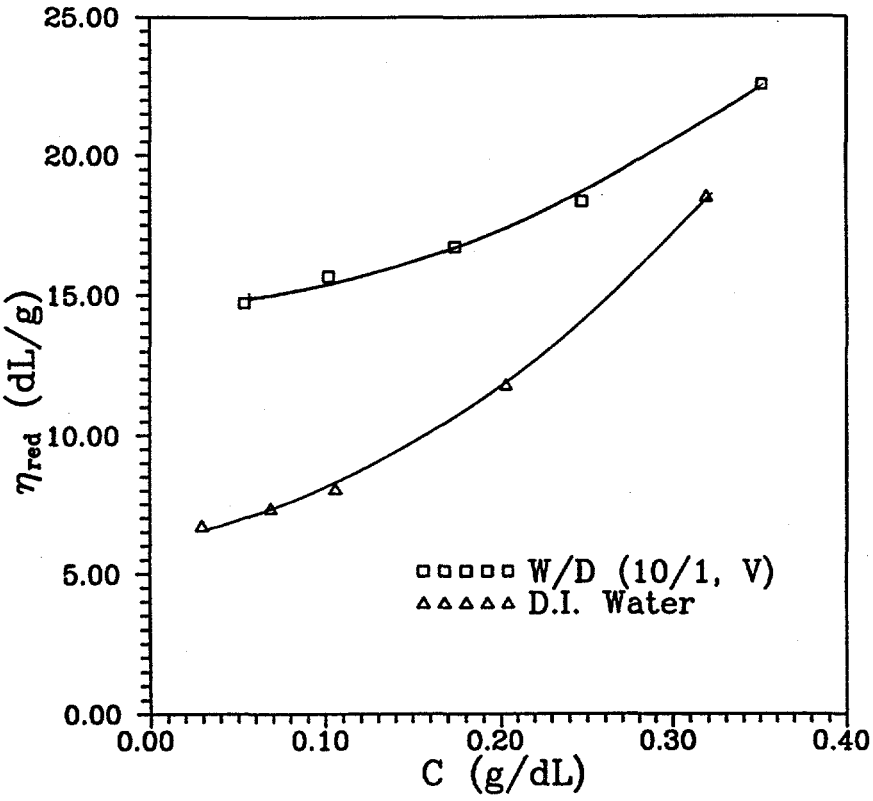

Figure 6-7. Effect of solvent on η_{red} of BS-C12-4.3 copolymer.

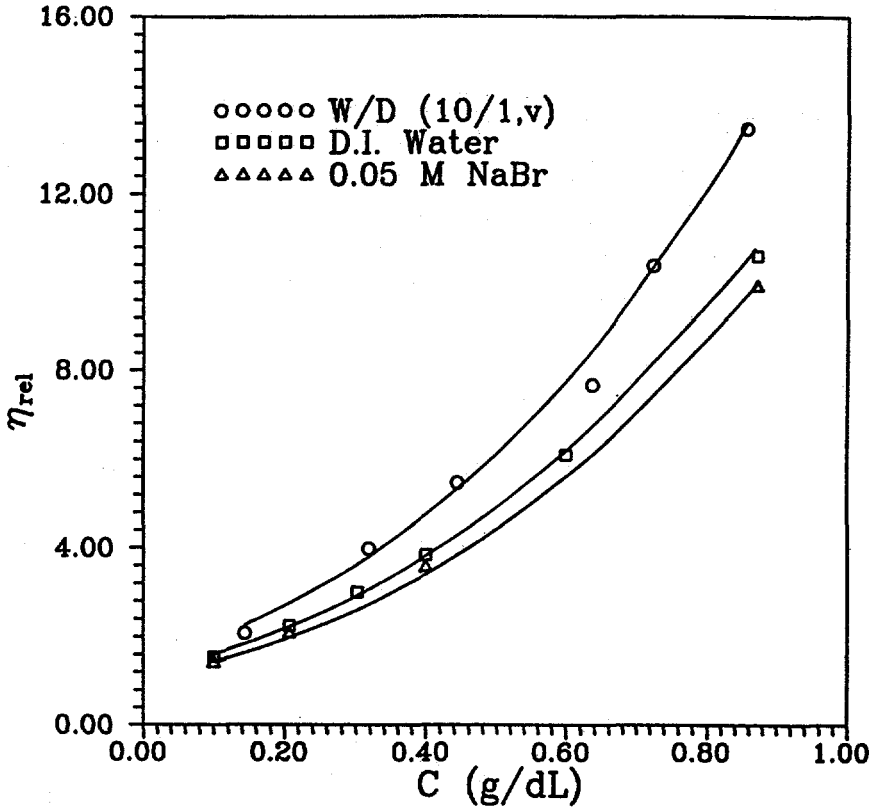

Figure 6-8. Effect of solvent on η_{red} of R-C12-1 copolymer.

CHAPTER SEVEN: EFFECT OF SURFACTANTS ON THE SOLUTION PROPERTIES OF AMPHIPATHIC COPOLYMERS OF ACRYLAMIDE AND N,N-DIMETHYL-N-DODECYL-N-(2-ACRYLAMIDOETHYL)AMMONIUM BROMIDE

Abstract

The interactions of surfactants sodium dodecyl sulfate (SDS), trimethyltetradecylammonium bromide (TTAB), and Triton X-100 with amphiphilic copolymers of acrylamide and dimethyldodecyl(2-acrylamidoethyl) ammonium bromide (DAMAB) have been investigated in aqueous solutions. The rheological properties of the copolymer/surfactant systems is affected by both the microstructures of the copolymers and the nature of the surfactant. Addition of nonionic surfactant, Triton X-100, resulted in a large increase in the reduced viscosity for the microblocky copolymers with 5 mole % DAMAB, while a random copolymer with the same composition exhibited a collapsed conformation in the presence of the cationic surfactant., TTAB. A strong viscosity enhancement was observed when SDS was added to the solution of a copolymer containing 0.32 mole % DAMAB. Evidence of mixed micelles formed by surfactant molecules and the hydrophobic groups of the copolymers was obtained utilizing surface tension, pyrene probe fluorescence and viscometry.

Introduction

The solution properties of aqueous media can be dramatically changed by utilizing combination of amphiphilic copolymers and simple surfactants.[1] However, there is presently an inadequate understanding of the mechanism of the interactions between macromolecules and surfactants.[2] Aqueous solutions comprised of polymers and surfactants have been studied by a variety of experimental techniques including viscometry, surface tension, dialysis equilibrium, NMR, ESR, neutron scattering, and fluorescence. In general, the surfactant molecules form micelle-like clusters associated with the polymer chains. The behavior of these systems can be described by two critical surfactant concentrations, namely the critical aggregation concentration (C_1) and the apparent critical micelle concentration (C_2). C_1 is defined as the surfactant concentration required to induce surfactant binding to the polymer, and C_2 is the concentration at which all the polymer sites available for interaction with surfactant are saturated; further increase in surfactant concentration will lead to the formation of classical micelles.[3,4] C_1 and C_2 are always located, respectively, below and above the CMC of the corresponding surfactant in pure water solution. C_1 is largely independent of the polymer concentration, while the maximum amount of polymer-bound surfactant in the system increases linearly with the total polymer concentration in the solution.[5]

Interactions between polyelectrolytes and charged surfactants in aqueous solution are governed primarily by coulombic forces and dipole-ion interactions. For example, polyelectrolytes interact strongly with oppositely charged surfactants which can lead either to a large increase in solution viscosity[6,7] or in some cases to phase separation[8]. Often the associations between polyelectrolytes and surfactants are quite weak or absent mainly because of the unfavorable electrostatic repulsions.[2b,9] When polyelectrolytes are hydrophobically modified,

the situation becomes more complicated. In addition to the forces operating in simple polyelectrolyte/surfactant systems, hydrophobic interactions between the amphiphilic groups on the polymer chains and the surfactant molecules also play the important roles. For instance, a C_{12}-grafted hydroxyethylcellulose[10] exhibits strong association with SDS while its parent polymer[11], hydroxyethylcellulose, interacts only weakly with SDS.

Another major consideration affecting amphiphilic polymer/surfactant interactions is the chemical microstructure of the polymer, particularly the "mer" distribution resulting from the method of polymerization[19,29,30]. Change in the compositional distribution can dramatically alter the association of surfactant with the polymer. Addition of SDS to an aqueous solution of hydrophobically modified poly(sodium acrylate) has been shown to cause a marked viscosity enhancement[13]. The viscosity passes through a pronounced maximum in the region of the critical micelle concentration. This viscosity increase is observed only when the polymer concentration is in the semi-dilute regime and it is attributed to mixed micelle liasons between the hydrophobic elements of the chains. The decrease in viscosity above the CMC arises from stoichiometry, since the mixed micelles eventually will contain, on average, only one polymer alkyl chain per micelle, and crosslinking will be lost because there is no longer any stoichiometric requirement for the polymer hydrophobes to share micelles. However, studies for the hydrophobically modified acrylamide copolymers in the presence of SDS suggest that the surfactant disrupts intermolecular association of the hydrophobic groups, causing a decrease in solution viscosity[14,15]. In viscometric studies, Goddard, et al.[6] investigated the effect of the polymer structure on the interactions of cationic polymers and an anionic surfactant system. Their studies indicated that addition of SDS to a cationically-modified cellulosic terpolymer leads to intermolecular association between polymer chains via bound surfactant at high polymer concentrations (1% by weight), but intramolecular association at low concentration (0.1%). A similar investigation of the interaction of SDS with poly(acrylamide-co-β-methacryloxyethyltrimethyl ammonium chloride) showed no detectable change in viscosity over the same SDS concentration range and it was concluded that the latter polymer maintained a constant conformation during binding of the surfactant. In analogous study, Hayakawa et. al[16] investigated the interaction of trimethyldodecylammonium bromide with polystyrene sulfonate and dextran sulfate. The equilibrium binding constant is higher for polystyrene sulfonate than for dextran sulfate, but, surprisingly the co-operativity of the binding is higher for the more hydrophilic dextran sulfate. Thus higher hydrophobicity in a polymer does not necessarily result in enhanced micellar clustering of surfactant on the polymer; other factors such as linear charge density and flexibility of the polymer must also be taken into account.

In a previous work, we described the synthesis and solution properties of copolymers of acrylamide and dimethyldodecyl(2-acrylamidoethyl)ammonium bromide (Figure 7-1).[17,29] These copolymers contain various amounts (up to 10 mole %) of dodecyl groups and show very interesting hydrophobic associative properties in aqueous solutions. Associative behavior of the copolymers is affected to a large degree by the arrangement of the hydrophobic groups along the copolymer chains. When the hydrophobic groups in such copolymer are arranged in a block-like fashion, the hydrophobic interactions promote intermolecular association when the copolymer concentration is above C^*. A random copolymer with the same composition exhibits intramolecular associative behavior and reaches C^* at much higher concentration. The

intermolecular interactions can be enhanced by increasing the length of the hydrophobic blocks and/or the number of blocks in the copolymer.

In this paper we report studies of the effects of sodium dodecylsulfate trimethyltetradecyl ammonium bromide, and Triton X-100 on the solution properties of acrylamide with dimethyldodecyl(2-acrylamidoethyl)ammonium bromide. Surfactant concentrations were chosen to span a range from below to above the cmc of the surfactants in pure water. Rheological behavior as a function of the type of surfactant and the distribution of the hydrophobic groups is investigated. Complementary data obtained by surface tension and pyrene probe fluorescence will also be presented.

Experimental

Materials

Deionized water used in this study had a resistance of 18 MΩ and a surface tension of 70.8 mN/m. All surfactants were purchased from Aldrich (purity: SDS, 98%; TTAB, 99%; Triton X-100, containing less than 3% polyethylene glycol). The syntheses of the copolymers have been described elsewhere.[17] Microblocky copolymers were prepared by free radical polymerization in aqueous solution with the surfactant monomer concentration above CMC (BS-C12-4.3, B-C12-4.7). Two random copolymers were synthesized via solution polymerization techniques: one in t-butanol (R-C12-5.1) and the other in water with the surfactant monomer concentration below the CMC (R-C12-1). The compositions of the copolymers are summarized in Table 7-1. The DAMAB content was determined by elemental analyses and the weight average molecular weights of the copolymers were measured on a Chromatix KMX-6 low angle laser light scattering in methanol/water mixture (50/50 by volume).

Methods

Surface tension measurements were performed with a Kruss Processor Tensiometer K12 instrument at 25°C using a Pt DeNouy ring. Viscosity measurements were conducted on a Contraves LS-30 low-shear rheometer at 25°C and a shear rate of 6 s^{-1}. Elemental analyses were conducted by MHW Laboratories of Phoenix, AZ. Stead-state fluorescence spectra were obtained with a Spex Fluorolog 2 fluorescence spectrophotometer equipped with a DM3000F data system. Classical light scattering studies were performed with a Chromatix KMX-6low-angle laser light scattering spectrophotometer with a 2-mW He-Ne-Ne Laser operating at 633 nm. Refractive index increments for classical studies were obtained on a Chromatix KMX-16 laser differential refractometer. A Spectra-Physics 127 laser operating at 632.8 nm was used for dynamic light scattering studies. Data were collected using a Brookhaven Instruments Model BI-2000SM automatic goniometer interfaced with a Brookhaven Instruments personal computer. Studies were performed at 90°, and the signals were processed with a Brookhaven Instruments Model BI-2030AT autocorrelator. Data were analyzed using the algorithm CONTIN and associated software provided by the manufacturer. Polymer solutions of 2.0 x 10^{-4} g/mL in 0.5 M NaCl were filtered in a Tygon tubing filter loop using Millipore 0.45 μm filters to remove dust. Typical filtration times were 14-48 h. Multiple analyses were performed to ensure reproducibility.

Results and Discussion

Anionic Surfactant

Solubility

The solubility diagram for the copolymer R-C12-1/SDS system in deionized water is shown in Figure 7-2. At low polymer concentrations (C_p < 1%), the system exhibits several distinguishable solubility zones. When SDS is initially added to the copolymer solution, turbid two-phase dispersions are observed. Continued addition of the surfactant results in macroscopic phase separation in which one clear phase is on top of the other clear phase. The precipitate is resolubilized in the presence of excess surfactant and the resulting solutions are clear and fluid. This solubility behavior is similar to that reported by Goddard et al.[18] Note that the transition occurs at the CMC of SDS. Initial precipitation of the copolymer in this case is caused by interaction of SDS with the copolymer by opposite ion-charge interaction between surfactant and polymer ions and this simultaneously increases hydrophobicity of the copolymer. At the higher surfactant concentrations, however, it is likely that the SDS forms micelle-like clusters around hydrophobic groups attached to the polymer and the copolymer is resolublized.

When the copolymer concentrations are above 1%, a gel phase is observed at the surfactant concentrations between the precipitating zone and the resolubilizing zone. Apparently, a physical crosslinking network is requiring association between SDS and the copolymer; no such a gel formation is observed in the pure copolymer solutions.[19]

Phase separation occurs when SDS is mixed with B-C12-4.3, B-C12-4.7, and R-C12-5.1 copolymer solutions throughout the copolymer concentration ranges. Dubin, et al.[20] have shown that the degree of ion pairing between high charge density polyelectrolytes and oppositely charged micelles is very extensive so that complexation leads to the rapid and irreversible formation of an amorphous solid, much as the mixing of oppositely charged strong polyelectrolytes produces water-insoluble "polyelectrolyte complexes"[21]. In our study precipitation of the copolymers upon addition of SDS may be caused by this strong ion-pair interaction. Because of solubility limits, studies of the interaction of SDS and copolymers were focused on SDS/R-C12-1 systems.

Surface Tension

Surface tension measurements show a classical "cross-over" of the "with- and without-polymer" surface tension curves for the SDS solutions[22] (Figure7-3). The surface tension of the SDS solution in the absence of the copolymer displays a pronounced minimum in the region of the CMC. This has been previously reported as a result of the presence of a lauryl alcohol impurity in the surfactant[23].

The concentration, C_1, at which the surfactant begins to interact with the polymer and the concentration, C_2, at which the normal micelles begin to form are conspicuous in Figure 7-3. It is interesting to note that in the presence of the copolymer, the surface tension curve shows no-minimum. It can be inferred, from the shape of the curve, that lauryl alcohol is co-micellized in the polymer-surfactant complex in preference to being adsorbed at the air-liquid interface. When regular micelles form, the measured surface tensions are slightly higher in the presence of copolymer. This may be an artifact of the DeNouy method, arising from visco-elastic recoil of the solubilized copolymer. The lower value of the copolymer curve at surfactant concentrations

below C_1 can be explained by the surface activity of the copolymer. Adsorption of copolymer at the surface would necessarily compress the available area available for surfactant adsorption, which would increase the surface excess surfactant concentration and, consequently, cause a lowering of the surface tension. The higher surface tension at the surfactant concentration around the CMC clearly demonstrates binding of the surfactant to the copolymer and concomitant depletion of surfactant from the air/water interface. C_1 in this case is 4.5×10^{-4} M. The surfactant adsorption on the polymer reaches a limit at a surfactant concentration of 9.7×10^{-3} M, corresponding to 60 SDS molecules per DAMAB monomer. This agrees well with the value of 50-60 surfactant molecules per micelle cluster reported in previous literature.[24]

Viscosity and Fluorescence measurements

Figure 7-4 illustrates the dependence of the reduced viscosity profile of R-C12-1 copolymer on the SDS concentration. Initial addition of SDS causes a slight decrease in the viscosity, presumably due to the loss of the copolymer from the solution which could arise from mixed micelle formation within each single amphiphilic copolymer molecule in solution. On the other hand, I_1/I_3 decreases in the region until a constant value is reached at a surfactant concentration of 5.1×10^{-3} M, a concentration significantly lower than the CMC of SDS (8.3×10^{-3}). It is noteworthy that I_1/I_3 decreases gradually with increasing SDS concentration over a large surfactant concentration range, indicating that the binding of charged surfactant occurs by a noncooperative mechanism[25]. It is likely that surfactant molecules first adsorb on DAMAB monomers units at low surfactant concentrations to form loosely packed hydrophobic clusters. Continuous addition of the surfactant results in the increase in the cluster size and a tightly packed hydrophobic microdomain is formed at the critical concentration of 5.1×10^{-3} M. The ratio of SDS molecule to DAMAB monomer in each microdomain is 34 as estimated from fluorescence data in Figure 7-4. This value is lower than that determined from surface tensiometry-but it is reasonable. It appears that not all of the polymer hydrophobes are co-micellized at C_1. Some of the hydrophobes are buried inside the polymer coil that are not available for association with the surfactant. As the surfactant are adsorbed onto the copolymer chains to form the mixed micelles, the chains are uncoiled due to the electrostatic repulsion between the mixed micelles, allowing more surfactant molecules to associate with the hydrophobes that were initially not available. The transition point of the curve corresponds to the surfactant concentration at which the precipitate begins to resolubilize. This clearly implies that micelle type aggregates are responsible for redissolution of the precipitate.

At the CMC of SDS, further addition of surfactant dramatically enhances the solution viscosity. The curve reaches a plateau value at 18 mM of SDS. This viscosity behavior differs from the observation of Leung and Goddard[6] for a system involving a cationic cellulose ether and SDS. In the latter case, the highest viscosity was observed in the precipitation zone and the viscosity dropped sharply in the resolubilization zone. In our system the increase in viscosity may be ascribed to association of surfactants and DAMAB of the copolymer in the mixed hydrophobic microdomains. It is reasonable to assume that the adjacent hydrophobic microdomains combine with increasing SDS concentration. Large clusters then form which may contain DAMAB units belonging to two or more distinct polymer chains. Taking into account that the copolymer concentration studied in the semidilute regime, these microdomain clusters serve as sites where hydrophobic groups from adjacent polymer chains associate intermolecularly.

Formation of intermolecular association in the system can be seen more clearly by studying the viscosity behavior of the mixture at fixed surfactant concentrations. As shown in Figure 7-5, a sharp upturn of the viscosity profile occurs within a narrow concentration range in the system containing 8.32 mM SDS, typical of intermolecular association. Such viscosity enhancement is not observed for polyacrylamide (Figure 7-6). Obviously, this interchain association is facilitated by interactions between SDS and DAMAB. It is interesting to note that the viscosity upturn occurs at the concentration where a constant limiting value of I_1/I_3 is reached. This value is very close to the one in Figure 7-4, suggesting that pyrene molecules locate in similar mixed micelles.

Clearly, two effects promote DAMAB association with SDS, hydrophobic and ionic associations. Hydrophobic association reduces the contacts of the hydrophobic groups of the copolymer with water and consequently lowers the free energy of the system.[26] Ionic attractions between SDS molecules and the cationic groups of the copolymer also contribute to the formation of mixed micelles. Each micelle apparently contains two or more DAMAB moieties belonging to different polymer chains.

Nonionic Surfactant

Surface Tension

It has been shown that in a system composed of a nonionic surfactant and a polymer having long hydrocarbon pendant groups, surfactant molecules form micelle-like clusters adsorbed to each hydrocarbon chain.[2a,14,28] Such associations also occur when Triton X-100 is added to the R-C12-1 copolymer solution (Figure 7-7). C_1 is 0.032 mM and C_2 is 0.40 mM.

Viscosity and Fluorescence Studies

The effects of nonionic surfactant on the viscosity of C12-1 copolymer solution are shown in Figure 7-8. Contrary to behavior in SDS, addition of Triton X-100 to R=C12-1 solutions results in no observable change in the reduced viscosity. The hydrodynamic size of the polymer oil remains nearly constant ($d_o \approx$77-79 nm) over a range of added surfactant concentration from 0.2 to 0.8 mM. However, I_1/I_3 decreases with increasing surfactant concentration, passing through a minimum and then increasing (Figure 7-8). The surfactant concentration at which I_1/I_3 shows the lowest value is very close to C_2. The initial decrease in I_1/I_3 is due to the formation of hydrophobic microdomains through association between surfactant molecules and hydrophobic groups of the copolymer. It is necessary to emphasize that the decrease in I_1/I_3 does not result from adsorption of surfactant to the pyrene molecules since the surfactant solution in the absence of the copolymer at the cmc shows a much higher I_1/I_3 of 1.44. When the limit of adsorption of the surfactant molecules onto the polymer is reached, further increase in surfactant concentration will result in the formation of normal surfactant micelles. Apparent I_1/I_3 values in such a system depend on the partitioning of pyrene molecules into two hydrophobic regions. By knowing the cmc of Triton X-100 in the system to be 0.3 mM and the C1 of 3.2 X 10-2mM, the number of surfactant molecules around each DAMAB unit is calculated to be ~3. Since there are no interactions between hydrophobes in the absence of surfactant, condensation of the surfactant on the R-C12-1 polymer does not alter the polymer conformation, and the viscosity of the polymer solution is essentially invariant throughout the surfactant concentration range.

The effect of a nonionic surfactant on the viscosity of the polymer solution with higher hydrophobic content was investigated using the microblocky copolymer B-C12-4.3 (Figure 7-9). The polymer shows a higher viscosity in the presence of 0.264 mM Triton X-100 than in the absence of the surfactant. Apparently, this surfactant promotes intermolecular associations.

Cationic Surfactant

Surface Tension

No definite cross-over is observed for the R-C12-1/trimethyltetradecylammonium bromide (TTAB) mixture (Figure 7-10). However, the system shows much more pronounced surface activity at very low surfactant concentrations and the curve of the mixture levels off below the CMC. Apparently, hydrophobic interaction overcomes the ionic repulsion between DAMAB moiety and TTAB surfactant molecules, resulting in the formation of the surface active complex. The polymer/surfactant association is also observed in R-C12-5.1/TTAB system. In this case, however, the complex is less surface-active as compared with R-C12-1/TTAB. This may be explained by the collapsed conformation of R-C12-5.1 upon addition of TTAB as discussed below. The dramatic decrease in the surface tension in both R-C12-1 and R-C12-5.1 solutions around CMC of surfactants is not due to the exclusion of the copolymers from solutions to the air-liquid interface as a result of increased ionic strength. This is verified by only the slight decrease in surface tensions in both system with increasing the NaBr concentration (Figure 7-11). Addition of TTAB to microblocky copolymer solutions (B-C12-4.3, B-C12-4.7 and B-C12-10.5) results in polymer precipitation, probably due to the "salting-out" effect[24].

Viscosity and Fluorescence Studies

Addition of TTAB does not change the rheological properties of R-C12-1 copolymer. However, a significant decrease in viscosity is observed when TTAB is mixed with R-C12-5.1 copolymer (Figure 7-12). In this case, TTAB acts as a cosurfactant associating with the polymer coils which become much more compact. The hydrophobic effect is apparently too strong in this system for the polymer coil to expand; the reduced viscosity remains essentially unchanged upon dilution. In other words the copolymer behaves like a highly collapsed coil.

Conclusions

Effects of small surfactants on the rheological properties of the copolymers depend on the type of surfactant and the nature of the hydrophobic association (intermolecular vs. intramolecular). Addition of SDS results in a slight decrease in the solution viscosity of R-C12-1 at surfactant concentration below the CMC and then a rapid increase at the CMC. The curve reaches a plateau at 18mM SDS. This viscosity behavior can be explained by the association of SDS around each hydrophobic group along the polymer chain to form mixed micelles and subsequent polymer chain extension due to the ionic repulsion between the mixed micelles. The copolymers with higher hydrophobic content precipitate from the solution in the presence of SDS. In contrast, no significant viscosity change has been observed when the nonionic surfactant is added to the solution of R-C12-1 although the surface tension measurement and fluorescence studies indicate that association of surfactant with the copolymer does occur. An initial decrease and then an increase in the I_1/I_3 value can be explained by the partitioning of pyrene molecules

between the homo-micelles of Triton X-100 and the mixed micelles formed by hydrophobic groups of the copolymer and Triton X-100. Addition of nonionic surfactant to the SB-C12-4.3 solutions results in a large increase in the viscosity. In the case of TTAB cationic surfactant, R-C12-5.1 exhibits a collapsed conformation while the viscosity of R-C12-1 is hardly affected. However, R-C12-1 forms a more surface-active complex with CTAB than does R-C12-5.1. Macrophase separation occurs for the microblocky copolymers solutions in the presence of this cationic surfactant.

References

1. For reviews, see *Polymers in Aqueous Media*; Glass, J. E., Ed.; Advances in Chemistry Series 223; American Chemical Society: Washington, DC **1989**.

2. For reviews, see (a). Goddard, E. D. *Colloids and Surfaces* **1986**, 19, 255. (b). Goddard, E. D. *Colloids and Surfaces* 1986, 19, 301.

3. Jones, M. N. *J. Colloid Interface Sci.* **1967**, 23, 36.

4. Cabane, B.; Duplessix, R. *Colloids and Surfaces* **1985**, 13, 19.

5. Thalberg, K.; Lindman, B. *Langmuir*, **1991**, 7, 277.

6. Leung, P. S.; Goddard, E. D. *Colloids and Surfaces* **1985**, 13, 47.

7. Hayakawa, K.; Kwak, J. C. T. *J. Phys. CHem.* **1983**, 87, 506.

8. Goddard, E. D.; Hannan, R. B. *J. Colloid Interface Sci.* **1976**, 55, 73.

9. Methemitis, C.; Morcellet, M.; Sabbadin, J.; Francois, J. *Eur. Polym. J.* **1986**, 22, 619.

10. Steiner, C. A. *J. Appl. Polym. Sci.* **1991**, 42, 1493.

11. Goddard, E. D.; Hannan, R. B. In *Micellization, Solubilization, and Microemulsions*; Mittal, K. L., Ed.; Plenum Press: New York, **1977**; Vol. 2; p 835.

12. Biggs, S.; Selb, J.; Candau, F. *Langmuir* **1992**, 8, 838.

13. Iliopoulos, I.; Wang, T. K.; Audebert, R. *Langmuir* **1991**, 7, 617.

14. McCormick, C. L.; Nonaka, T.; Johnson, C. B. *Polymer* **1988**, 29, 731.

15. Schulz, D. N.; Kaladas, J. J.; Maurer, J. J.; Bock, J.; Pace, S. J.; Schulz, W. W. *Polymer* **1987**, 28, 2110.

16. (a) Huyakawa, K.; Santerre, J. P.; Kwak, J. C. T. *Macromolecules* **1983**, 16, 1642. (b) Hayakawa, K.; Santerre, J. P.; Kwak, J. C. T. ACS Symp. Ser. 253, **1984**, 225.

17. Chang, Y.; McCormick, C. L. *Polym. Prep.* **1992**, 33(2), 202.

18. Goddard, E. D.; Hannan, R. B. *J. Am. Oil Chem. Soc.* **1977**, 54(12), 561.

19. Goddard, E. D.; Leung, P. S.; Padmanabhan, K. P. A. *J. Soc. Cosmat. Chem.* **1991**, 42,

20. Dubin, P. L; Vea, M. E. Y.; Fallon, M. A.; The, S. S.; Rigsbee, D. R.; Gan, L. M. *Langmuir* **1990**, 6, 1422.

21. Smid, J.; Fish, D. In *Encyclopedia of Polymer Science and Technology*; Wiley-Interscience: New York, **1988**; Vol. 11; 720.

22. Jones, M. N. *J. Colloid Interface Sci.*, **1967**, 23, 36.

23. Ananthapadmanabhan, K. P. In *Interaction of Surfactant with Polymers and* Proteins, Goddard, E. D. and Ananthapadmanabhan, K. P., Ed.; CRC Press, Boca Raton, **1993**; p 14.

24. Wennerstrom, H.; Lindman, B. *Phys. Rep.* **1979**, 52, 1.

25. Winnik, F. M.; Ringsdorf, H.; Venzmer, J. *Langmuir* **1991**, 7, 905.

26. Tanford, C. *The Hydrophobic Effect: Formation of Micelles and Biological Membranes*; 2nd Ed.; John Wiley & Sons: New York, **1980**.

27. Cabane, B. J. *J. Phys. Chem.* **1977**, 81, 1639.

28. Holtzscherer, C.; Candau, F. *J. Colloid Interface Sci.* **1988**, 125(1), 97.

TABLE 7-1. COMPOSITION OF COPOLYMERS

Copolymer	DAMAB Content (Mole%)	M_w x 10^{-6}
PAM	0	1.12
R-C12-1	0.32	0.74
BS-C12-4.3	4.3	0.95
B-C12-4.7	4.7	1.04
R-C12-5.1	5.1	0.47
B-C12-10.5	10.5	1.12

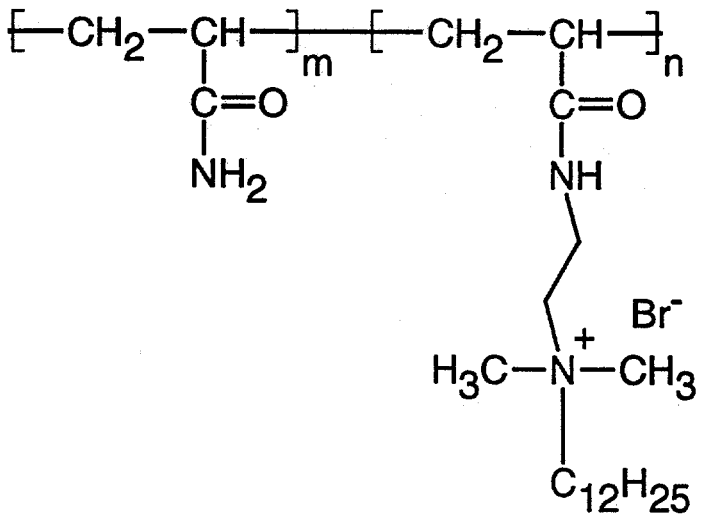

Figure 7-1. Structure of AM/DAMAB copolymers

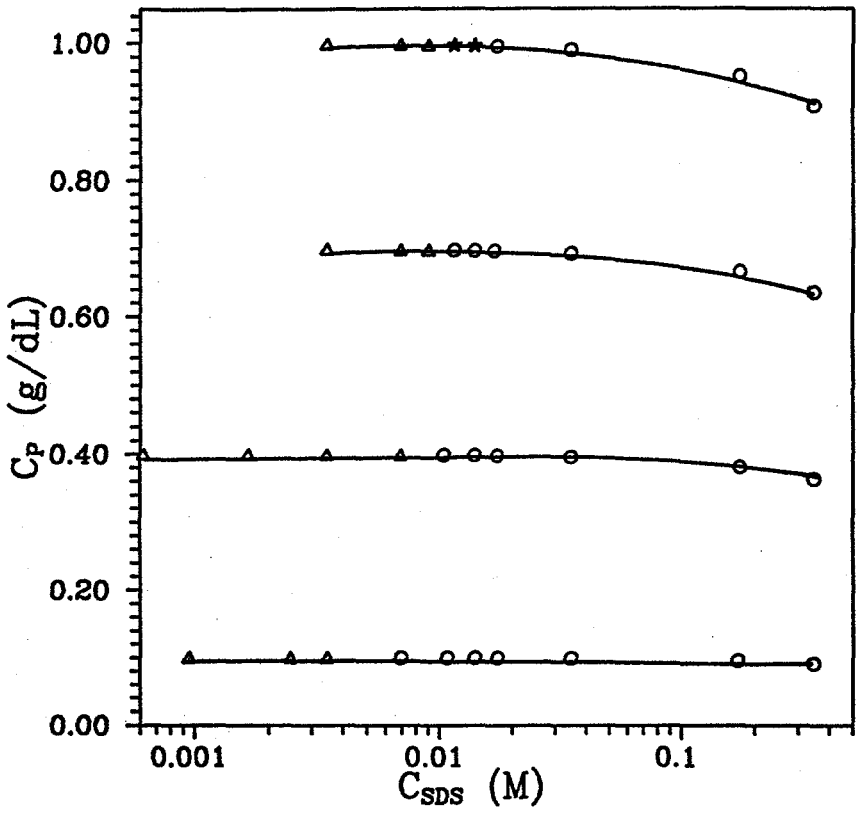

Figure 7-2. Solubility diagram of R-C12-1/SDS: two phases (Δ(; clear solution (O); gel (★).

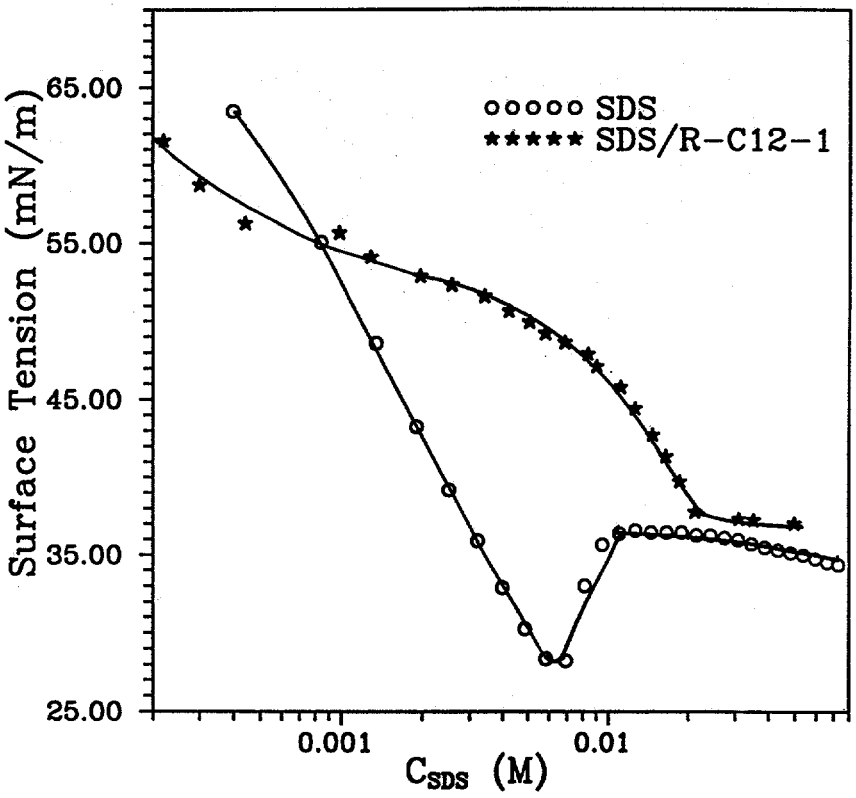

Figure 7-3. Surface tension measurements of SDS in the presence and absence of R-C12-1 copolymer (C_p = 0.33 g/dL).

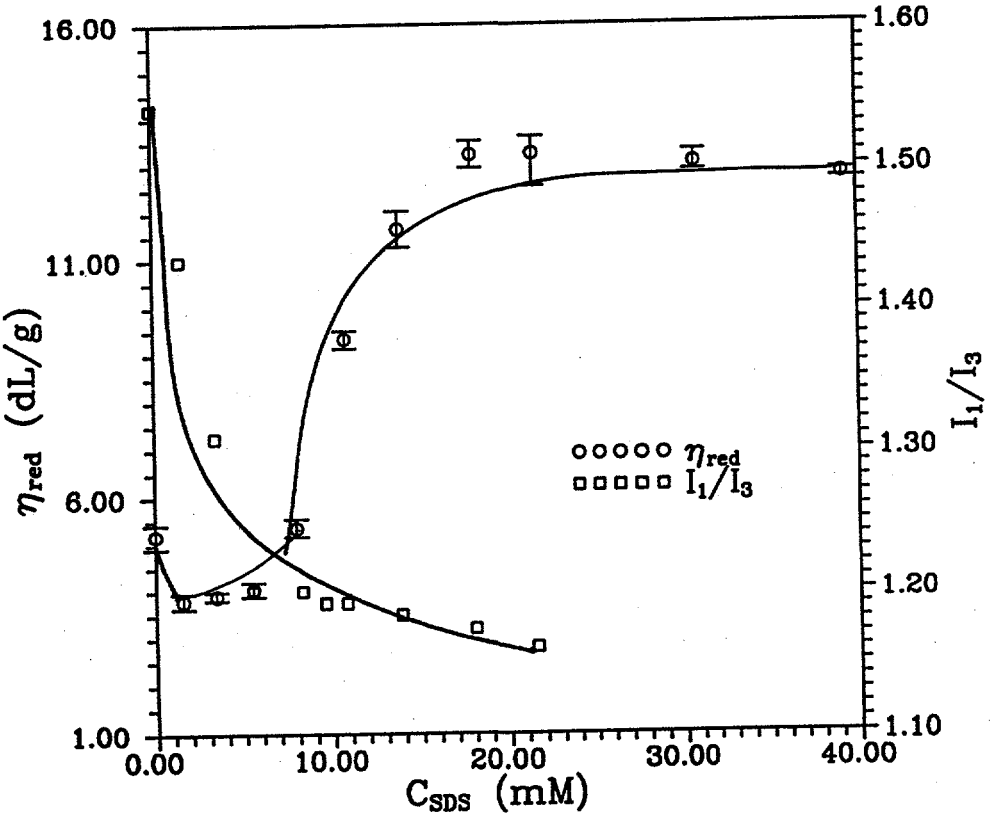

Figure 7-4. η_{red} and I_1/I_3 as a function of SDS concentration for R-C12-1 copolymer at a concentration of 0.33 g/dL ($C_{pyr} = 10^{-6}$ M).

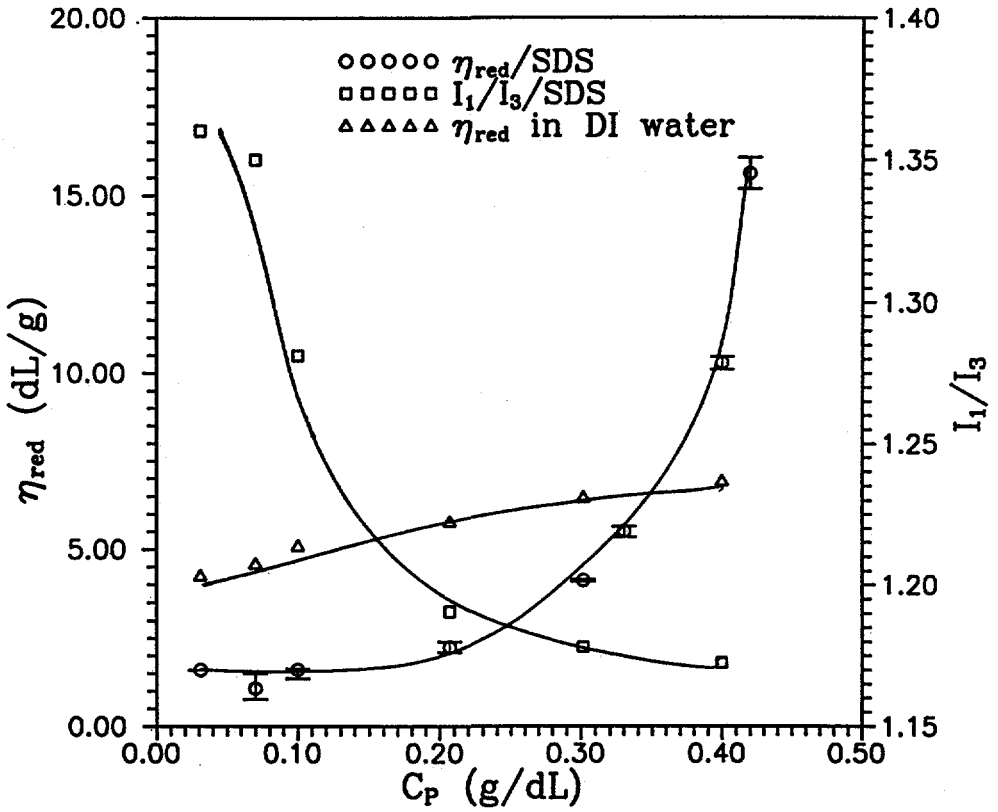

Figure 7-5. η_{red} and I_1/I_c as a function of concentration of R-C12-1 copolymer in deionized water and 8.32mMSDS aqueous solution.

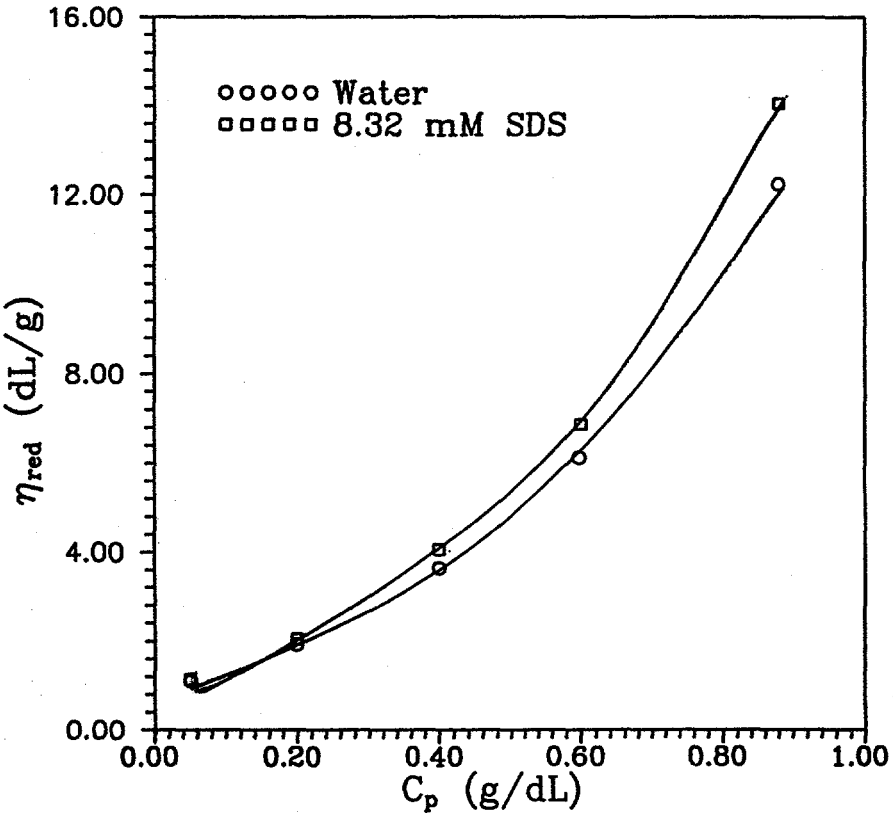

Figure 7-6. Effect of SDS on the ηred of homopolyacrylamide.

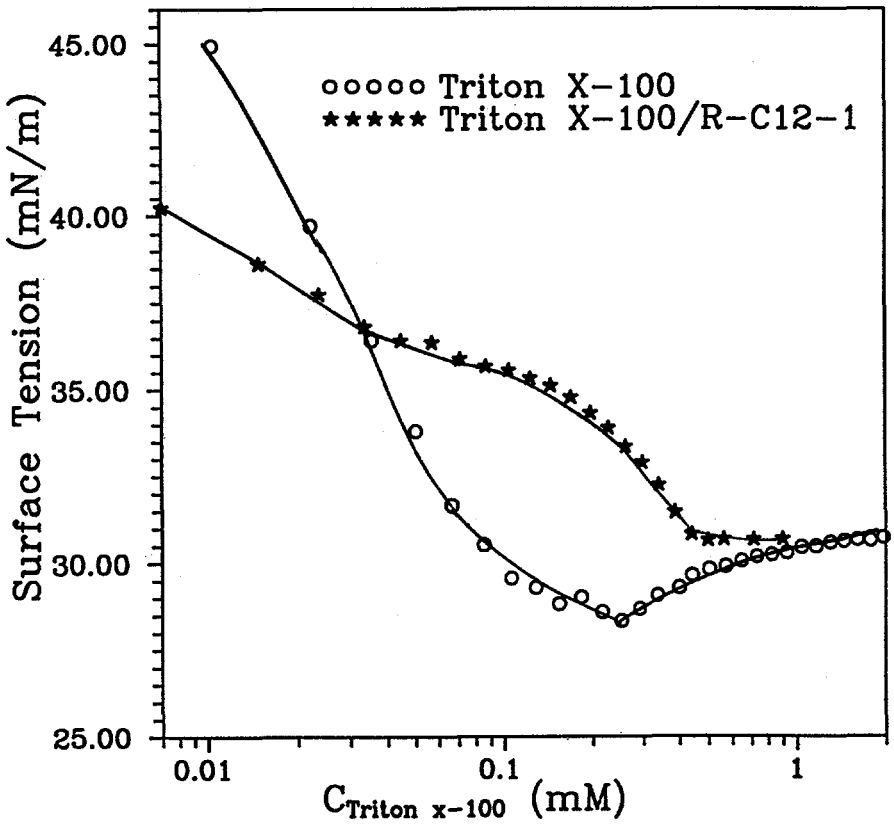

Figure 7-7. Surface tension measurements of Triton X-100 in the presence and absence of R-C12-1 copolymer (C_p = 0.33 g/dL).

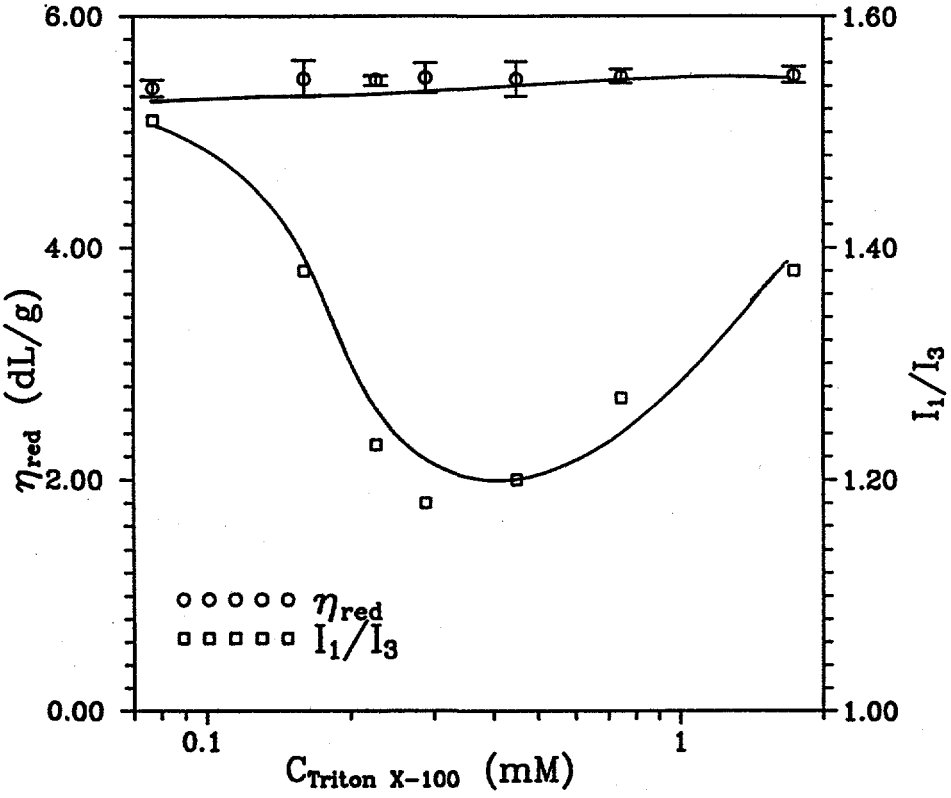

Figure 7-8. η_{red} and I_1/I_3 as a function of Triton X-100 concentration for R-C12-1 copolymer at concentration of 0.33 g/DL (C_{pyr} - 10^{-6} M).

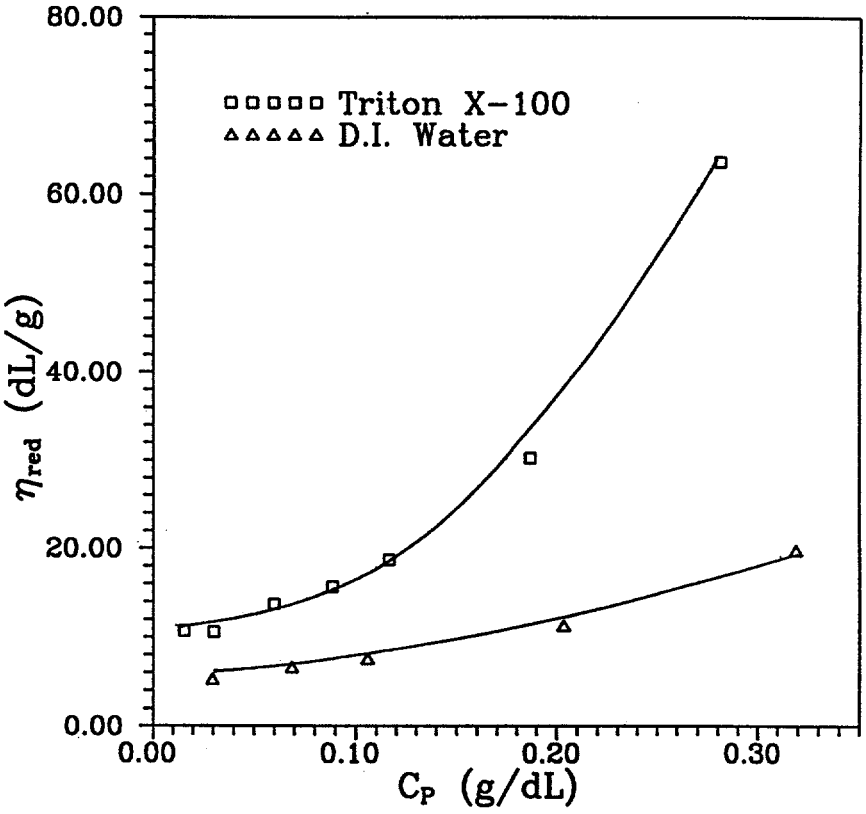

Figure 7-9. Viscosity behavior of B-C12-4.3 copolymer in 0.264 mM Triton X-100 aqueous solution and in deionized water.

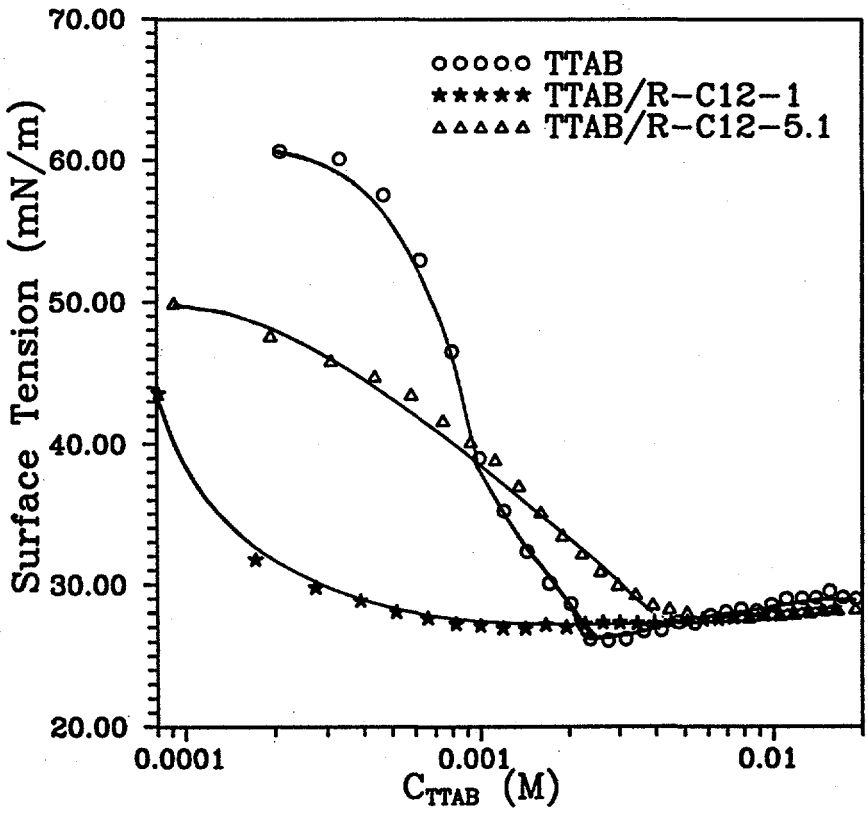

Figure 7-10. Surface tension behavior of TTAB in the presence of R-C12-1 and R-C12-5.1 copolymers (C_p = 0.33 g/dL).

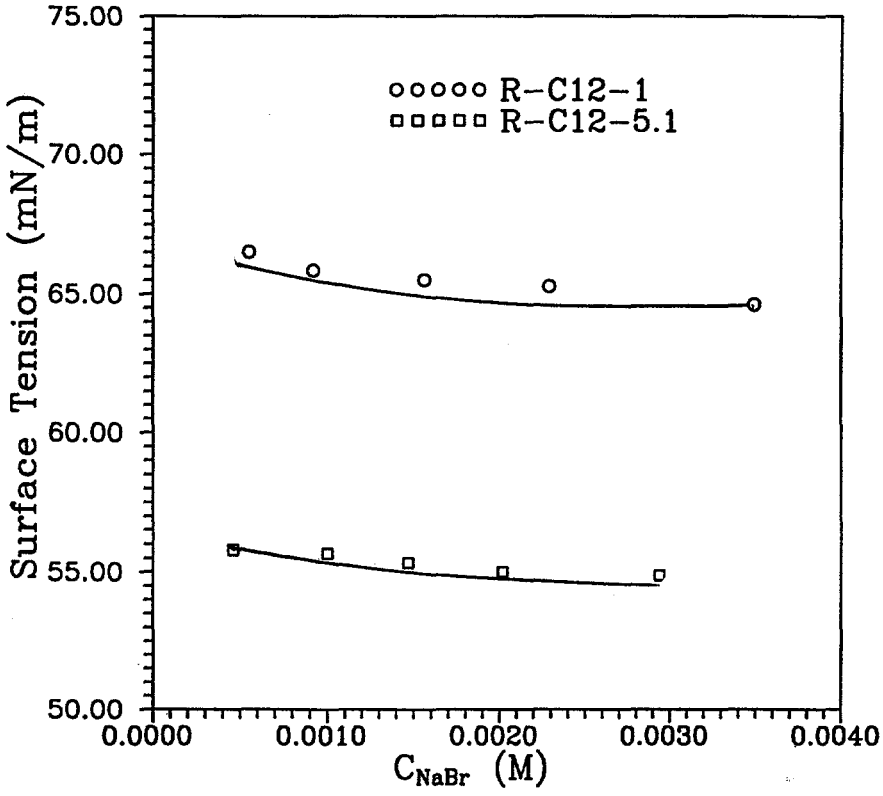

Figure 7-11. Effect of NaBr concentration on the surface tension of R-C12-1 and R-C12-5.1 solutions (C_p = 0.33 g/dL).

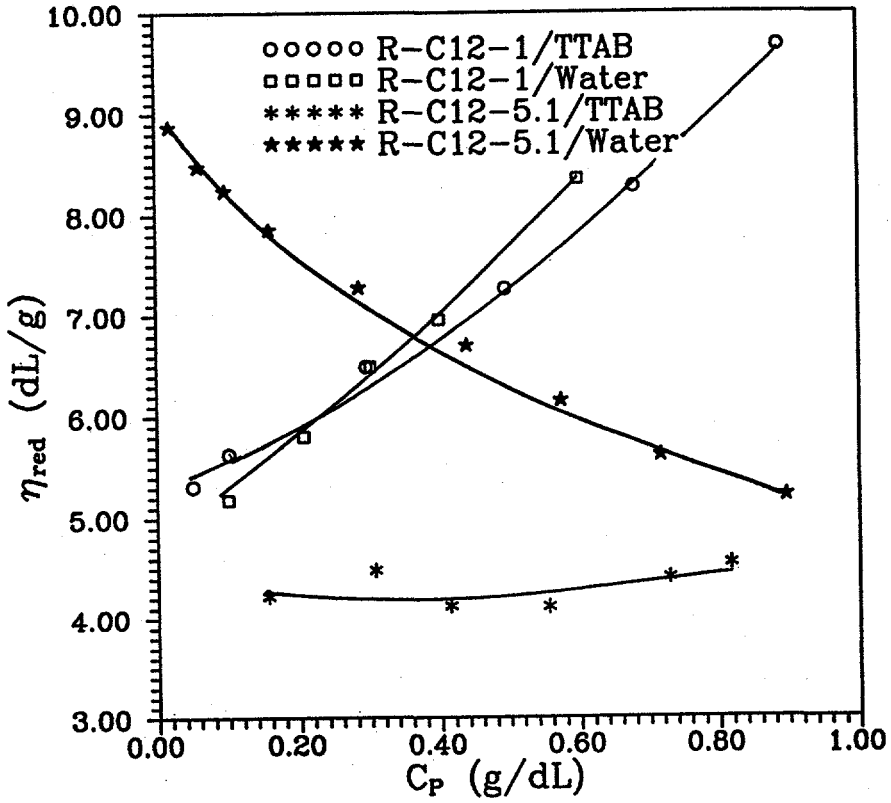

Figure 7-12. Effects of surfactants on η_{red} of R-C12-1 and R-C12-5.1 copolymers in the presence of 0.3 mM TTAB.

CHAPTER EIGHT: ASSOCIATIVE INTERACTIONS AND PHOTOPHYSICAL BEHAVIOR OF AMPHIPHILIC TERPOLYMERS PREPARED BY MODIFICATION OF MALEIC ANHYDRIDE/ETHYL VINYL ETHER COPOLYMERS

Abstract

A series of amphiphilic terpolymers were prepared by sequentially copolymerizating maleic anhydride and ethyl vinyl ether, adding octyl, dodecyl or naphthyl amines, and then hydrolyzing the remaining anhydride units. Viscosity studies indicate that these amphiphilic systems form intramolecular associations in dilute and semidilute solutions at various values pH and ionic strength. The dodecyl terpolymers show more pronounced hydrophobic associations than do the octyl analogs. Change in solution pH or addition of NaCl lowers significantly the viscosity of the polymer solutions, indicating a more collapsed conformation. Fluorescence lifetimes increase with increasing hydrophobe content. The lifetime of the monomer emission decreases with increasing pH, demonstrating a more hydrated environment experienced by the probe within the polymer coil. I_E/I_M values of the terpolymers with low hydrophobe content decrease with increasing pH from 3 to 10 while the terpolymers with moderate hydrophobe content exhibit a maxmium I_E/I_M in the same pH range. Systems with high hydrophobe content show little pH dependence. These results are interpreted in terms of the relative concentration of the chromophore in the hydrophobic domains as well as the change in the mobility of the naphthyl labels.

Introduction

Intramolecular associative polymers, also called polymeric micelles or "polysoaps" due to their surfactant properties, were first studied as models to mimic conformational behavior of proteins. Strauss and coworkers[1,2] demonstrated the formation of intramolecular micelles using the random copolymers of N-ethyl-4-vinylpyridinium bromide and N-dodecyl-4-vinylpyridinium bromide. The intrinsic viscosity decreased dramatically with increasing dodecyl group content and reached a minimum value of 0.04 dL/g at a hydrophobe content of 28.5 mole%. This value is of same order of magnitude as that observed for globular proteins, indicating a highly collapsed conformation. The transition from extended to compact coils was reported to occur at a critical hydrophobe concentration of approximately 11 mole%. The Huggins constant exhibited an almost 25-fold increase as the dodecyl group content was changed from 0 to 37 mole%, verifying the increased compaction of the polymer coils in aqueous media.

Loucheux et al[3] studied the solution properties of poly(4-vinylpyridine) modified with alkyl bromides utilizing viscometry and NMR techniques. Their data showed that the conformational transition occurred only when the alkyl groups contained more than eight carbon atoms. The critical hydrophobe concentration shifted to lower value with increasing alkyl group length.

Another widely studied associative polymer is based on hydrolyzed alternating copolymers of maleic anhydride and n-alkyl vinyl ethers. These copolymers with moderate concentration of alkyl sidechains (alkyl = butyl, pentyl, hexyl, and octyl) in aqueous solutions undergo conformational transitions from hypercoil to random coil as the degree of ionization is increased.[4-12] The transition, however, is shifted to a higher value of ionization with increasing alkyl group size.[7] The conformation of the copolymers with longer hydrophobic chains (alkyl = decyl, cetyl) is essentially independent of the degree of ionization since these copolymers remain in a collapsed conformation at all values of pH.[13-15]

A series of studies have been conducted in our laboratories to further investigate the nature of intramolecular associations of various amphiphilic water soluble polymers. Clark et al[16] demonstrated the pH dependence of the chain associations in a 20:80 mole% copolymer of 2-(1-naphthylacetyl) acrylate (NAEA) and methacrylic acid (MAA). The copolymer adopts a highly collapsed conformation at low pH due to the hydrophobic interactions of both methyl and naphthyl groups. At high pH, the copolymer remains in the micelle-like conformation with the naphthyl groups forming a hydrophobic core surrounded by a charged shell of methacrylic acid units. Such a conformation is attributed to the presence of large quantity of the naphthyl groups in the copolymer and the relatively long spacer between the naphthyl groups and the polymer backbone.

In this paper, we report synthesis and solution properties of copolymers of maleic anhydride and ethyl vinyl ether reacted with controlled amounts of octyl- and dodecylamines. A small concentration (~1 mole%) of naphthalene labels with long spacer groups is incorporated. Hydrolysis of the remaining anhydride groups yielded water-soluble terpolymers with degrees of amidation ranging from 8 to 50 mole%. Key features of this study include variation in hydrophobe length and content, maintenance of a small quantity of naphthyl groups to avoid perturbation of the parent copolymers, and presence of comparatively large hydrophobes relative to naphthyl label. These terpolymers provide useful models for elucidating the nature of hydrophobic associations in systems having a random distribution of the hydrophobic groups. Changes in polymer conformation upon altering the concentration and length of the hydrophobic groups as well as the solution pH and ionic strength are examined by viscosity and fluorescence studies.

Experimental

Materials

Chemicals were obtained from Aldrich Chemical Company and used as received. Benzene was dried over CaH_2 and distilled under nitrogen prior to use. Other solvents were reagent grade and used without further purification. Water was deionized to a conductance of 1×10^{-17} mho/cm.

Synthesis of Naphthalene-Containing Fluorescence Label 3 (Scheme 8-1).

1-(6-Hydroxyhexyloxymethyl)naphthalene 1.

1,6-Hexanediol (100.0 g, 0.846 mol) was placed in a 1000 ml, round-bottomed flask equipped with a mechanical stirrer, and heated to melt at 55°C. Sodium hydride (4.06 g, 0.169 mol) was added and the mixture was stirred at 70°C for 4 hours until all NaH reacted. A precipitate was formed immediately upon addition of chloromethylnaphthalene (30.0 g, 0.169 mol). The mixture was stirred vigorously at 80°C for 3 hours. Thin layer chromotography (TLC) indicated that most of chloromethylnaphthalene had been reacted. The reaction was allowed to proceed for another three hours. Excess hexanediol was then removed at 106°C/0.5 mm-Hg. The residue was diluted with 150 ml of acetone and the precipitate was filtered. The concentrated filtrate was distilled under reduced pressure to yield a colorless oil. bp 166.5°C at 0.5 mm-Hg. Yield: 41 g (94%). GC purity was determined to be > 99.9%. ^{1}H NMR ($CDCl_3$) δ 1.22-1.70 (m, 8 H), 2.01 (s, 1 H), 3.47-3.55 (2t, 2 H), 4.91 (s, 2 H), 7.39-8.15 (m, 7 H); ^{13}C NMR ($CDCl_3$) δ 25.5, 25.9, 29.7, 32.6, 62.6, 70.3. 71.4, 124.0, 125.1, 125.7, 126.0, 126.3, 128.5(2), 131.7, 133.7, 133.9; FTIR 3383 (O-H), 1597, 1510, 1460 (aromatic C-C stretch), 1099 (C-O-C), 794, 775 (aromatic C-H bend) cm^{-1}.

1-(6-Cyanohexyloxymethyl)naphthalene 2.

A modified literature procedure[17] was used in the preparation of 2. Methanesulfonyl chloride (28.6 g, 0.250 mol) was added dropwise at 8-15°C to a solution of hydroxyhexyloxymethylnaphthalene (51.7 g, 0.200 mol) and trimethylamine (30.4 g, 0.300 mol) in 150 ml of ether. After addition was complete, the mixture was stirred at room temperature for 1 hour. The precipitate was filtered and washed twice with 50 ml of anhydrous ether. A light yellow oil was obtained from the filtrate upon removal of the solvent. ^{1}H NMR ($CDCl_3$) δ 1.29-1.73 (m, 8 H), 2.90 (s, 3 H), 3.52 (t, 2 H), 4.13 (t, 2 H), 4.91 (s, 2 H), 7.36-8.12 (m, 7 H); ^{13}C NMR δ 25.1, 25.6, 29.0, 29.5, 37.0, 70.1(2), 71.3, 124.0, 125.2, 125.7, 126.0, 126.3, 128.3(2), 131.7, 133.7, 134.0.

The oil was heated at 75°C with sodium cyanide (15.5 g, 0.300 mol) in 200 ml anhydrous DMSO for 3.5 hours in a 500 ml round-bottomed flask. TLC confirmed the disappearance of the starting compound. The solution was cooled and poured into 800 ml of water. The product was extracted with 200 ml of methylene chloride three times. The organic extracts were combined and dried with $MgSO_4$. A dark red oil was obtained upon removal of the solvent. Vacuum distillation yielded a slightly yellow oil; bp 186-188°C at 0.5 mm-Hg. Yield: 49.7 g (93%). ^{1}H NMR ($CDCl_3$) δ 1.20-1.66 (m, 8 H), 2.11 (t, 2 H), 3.46 (t, 2 H), 4.87 (s, 2 H), 7.32-8.11 (m, 7 H); ^{13}C NMR ($CDCl_3$) δ 16.8, 25.2, 25.3, 25.5, 28.2, 29.3, 69.9, 71.4, 124.0, 125.2, 125.7, 126.0, 126.3, 128.5(2), 131.7, 133.7, 133.9; FTIR 2245 (C≡N), 1597, 1510, 1462 (aromatic C-C stretch), 1099 (C-O-C), 801, 777 (aromatic C-H bend) cm^{-1}.

1-(7-Aminoheptyloxymethyl)naphthalene 3

$LiAlH_4$ (0.789 g, 0.0196 mol) in 40 ml of anhydrous ether was placed in a 100 ml flask equipped with a thermometer, an addition funnel and a magnetic stirring bar. When the mixture was cooled to 0°C, cyanohexyloxymethylnaphthalene (5.00 g, 0.0187 mol) in 5 ml of ether was

added slowly at such a rate that the temperature did not exceed 5°C. After addition was complete, 1 ml of water was added slowly (caution: very vigorous reaction), followed by 1 ml of 20% NaOH solution and additional 3 ml of water. The ether layer was decanted from the white, granular inorganic residue. This residue was washed once with 20 ml of ether. The organic solution was dried with Na_2SO_4. Removal of ether yielded a slightly yellow oil. GC indicated that the product contained about ~6% of 1-(6-hydroxyhexyloxymethyl)naphthalene **1**. To remove unreacted alcohol, the oil was dissolved in 10 ml of ether and 20 ml of 1 M HCl ether solution was added. The ammonium salt was precipitated as an off-white solid which was filtered, washed with ether and dried under vacuum. Recrystallization in acetone gave pure white crystals. The solid was dissolved in water and solution pH was adjusted to about ~12. The free amine was extracted with ether. The organic phase was dried with Na_2SO_4 and the solvent was removed to yield a slightly yellow oil. Yield: 3.68 g (73%). HPLC purity was determined to be > 99.8%. ^{1}H NMR ($CDCl_3$) δ 1.03 (b, 2 H), 1.19-1.70 (m, 10 H), 2.62 (t, 2 H), 3.52 (t, 2 H), 4.92 (s, 2 H), 7.34-8.16 (m, 7 H); ^{13}C NMR ($CDCl_3$) δ 22.9, 26.2, 26.8, 29.3, 29.7, 33.8, 42.3, 70.5, 71.4, 124.1, 125.1, 125.7, 126.0, 126.2, 128.5(2), 131.8, 133.7, 134.1; FTIR 3374, 3300 (N-H), 1597, 1512, 1464 (aromatic C-C stretch), 1101 (C-O-C), 792, 777 (aromatic C-H bend) cm^{-1}.

Succinic Acid N-[7-(1-Naphthylmethoxy)heptyl]Monoamide (4)

The synthesis of naphthalene-labelled model compound 4 is illustrated in Scheme 8-2. 1-(7-Aminoheptyloxymethyl)naphthalene 3 (1.00 g, 3.69 mmol) in 10 ml of anhydrous DMF was placed in a 25 ml flask equipped with a condenser, addition funnel, and N_2 inlet and outlet. Succinic anhydride (0.380 g, 3.80 mmol) in 5 ml of DMF was added at 0°C with stirring. The reaction was conducted at room temperature for 30 min. and at 65°C for additional 30 min. TLC confirmed disappearance of the amine. The product was precipitated in water. The light yellow solid was filtered, washed with 10 ml water and dried under vacuum. Yield: 1.19 g (87%). The product was recrystallized in ethyl acetate to yield a pale yellow solid. mp 78-79.5°C. ^{1}H NMR ($CDCl_3$) δ 1.10-1.84 (m, 10 H), 2.39 (t, 2 H), 2.59 (d, 2 H), 3.09 (d, 2 H), 3.51 (t, 2 H), 4.90 (s, 2 H), 6.43 (b, 1 H), 7.31-8.19 (m, 7 H), 10.07 (b, 1 H); ^{13}C NMR ($CDCl_3$) δ 26.0, 26.7, 28.9, 29.1, 29.5, 30.0, 30.7, 39.7, 70.4, 71.3, 124.0, 125.2, 125.7, 126.1, 126.4, 128.5(2), 131.7, 133.7, 133.9, 172.6, 176.1; FTIR (KBr) 3460-2370 (O-H), 3319 (N-H), 1696 (acid C=O), 1643 (amide C=O), 1596 (aromatic C-C stretch), 1537 (amide II band), 1120 (C-O-C), 797, 767 (aromatic C-H bend) cm^{-1}.

Synthesis of Sodium Salt of Hydrophobically Modified, Maleic Anhydride and Ethyl Vinyl Ether Copolymers 7 (Scheme 8-3). Copolymerization of Maleic Anhydride (MA) with Ethyl Vinyl Ether (EVE).

Maleic anhydride (10.77 g, 0.110 mol) and benzoyl peroxide (0.0451 g, 1.86×10^{-4} mol) were dissolved in 100 ml of benzene in a 250 ml 3-neck round bottomed flask equipped with a magnetic stirring bar. The flask was sealed and fitted with a thermometer, a condenser, a long gas delivery needle and a short needle on the top of condenser to serve as a gas escape valve. Dry, oxygen-free nitrogen was purged through the flask for 45 min. The short needle was then removed and ethyl vinyl ether (9.11 g, 0.121 mol) was injected into the solution. The system was heated at 59--61°C for 8 hours resulting in a white precipitate which was filtered and dried

under vacuum. Copolymer 5 was purified by repeated precipitation in dry diethyl ether. The polymer was filtered and dried under vacuum.

Synthesis of Naphthalene-Labelled, Hydrophobically Modified Maleic Anhydride and Ethyl Vinyl Ether Terpolymers 6.

Synthesis of naphthalene-labelled MA/EVE terpolymer containing 20 mole% octyl groups is described below. Other terpolymers were prepared by same procedure but differing in amounts of alkylamines in the feed. Aminoheptyloxymethylnaphthalene (0.162 g, 5.99×10^{-4} mol) 3 and octylamine (1.55 g, 1.20×10^{-2} mol) were added dropwise to a rapid stirring solution of poly(maleic anhydride-alt-ethyl vinyl ether) (10.2 g, 5.99×10^{-2} mol) 5 in 100 ml of ethyl acetate at room temperature under nitrogen. The reaction was allowed to proceed at 60°C for 10 hours. The polymer was then precipitated into 300 ml of diethyl ether. The precipitate was stirred in another 200 ml of diethyl ether overnight, filtered and dried under vacuum.

Hydrolysis of Hydrophobically Modified Maleic Anhydride and Ethyl Vinyl Ether Copolymers.

The hydrolysis of the terpolymers 6 was performed in aqueous NaOH solution. A dilute NaOH solution containing an appropriate amount of dry polymer was placed on an orbital shaker at room temperature to facilitate the hydrolysis of the anhydride groups.

Characterization. Naphthalene Derivatives.

1H and ^{13}C NMR spectra were recorded using a Bruker AC-200. A Mattson 2020 Galaxy Series FTIR was used to obtain infrared spectra. GC analysis was performed on a Hewlett Packard 5890 Series II Gas Chromatograph equipped with an Alltech Capillary Column AT-5. A Hewlett Packard Model 1050 HPLC was used to determine the purity of solid samples. A waters Bondapak C18 column was employed with methanol as the mobile phase. The sample effluent was typically monitored at 280 nm.

Terpolymer Solution Preparation.

The appropriate amount of dried terpolymer **7** was weighed and then dissolved in water in a volumetric flask from which further dilutions of this stock solution could be made. The solutions were allowed to stand for two weeks prior to viscosity measurement. The pH value of each solution was obtained with a Corning 130 pH meter at room temperature.

UV Analysis

Ultraviolet spectroscopy was used in determining the naphthalene content in the terpolymers. All spectra were recorded with a Hewlett Packard 8452A Diode Array Spectrophotometer. Beer-Lambert plots were obtained for model compound, sodium salt of succinic acid, N[7-(1-naphthylmethoxy)heptyl] mono-amide (**4**), in water and compared with polymer absorption.

Fluorescence Analysis.

The concentrations of terpolymer solutions were 0.05 g/dL. The concentration of naphthyl moieties in these solutions varied from 2.5×10^{-6} to 3.0×10^{-6} M. Sample solutions were degassed by gentlely bubbling with helium. All the samples were excited at 280 nm, and monomer intensities were measured at 330 nm. Emission spectra of the terpolymers were recorded with a Spex Fluorolog-2 fluorescence spectrometer. Fluorescence decays were measured with a Photochemical Research Associates (PRA) single-photon-counting instrument equipped with a H_2-filled 510-B flashlamp. A nonlinear iterative deconvolution technique was used to fit the decay curves.

Low Angle Laser Light Scattering

Classical light scattering studies were performed with a Chromatix KMX-6 low-angle laser light scattering spectrophotometer with a 2-mW He-Ne laser operating at 633 nm. Refractive index increments (dn/dc) were obtained using a Chromatix KMX-16 differential refractometer. Molecular weight of hydrolyzed poly(maleic anhydride-alt-ethyl vinyl ether) was measured in 1 M NaCl solution.

Viscometry

Viscosity measurements were conducted with a Contraves LS-30 low shear rheometer at a constant shear rate of 1.28 reciprocal seconds at 25°C. A constant pH of 9-9.5 was used during the measurement, unless otherwise noted.

Results and Conclusions

One synthetic objective of this work was to prepare the amphiphilic water-soluble polymers with controlled placement of fluorescence labels. The random incorporation of the labels was achieved by first synthesizing a functionalized naphthalene derivative shown in Scheme 8-1. The synthesis 1-(7-aminoheptyloxymethyl)naphthalene 3 proved to be facile with satisfactory yields. The spacer length (in this case, heptyl) can be altered to decouple the naphthalene from the polymer backbone. A model compound, succinic acid, N-[7-(1-naphthylmethoxy)heptyl] mono-amide (4) (Scheme 8-2), was designed for fluorescence studies. The sodium salt form is soluble in aqueous media.

Terpolymer Synthesis and Characterization

Hydrophobically modified MA/EVE terpolymers 7 were prepared utilizing the synthetic procedures shown in Scheme 8-3. Terpolymers are designated by the number 7 followed by C8 or C12 designating octyl or dodecyl substitution. The final number represents the mole% incorporation. Initially, MA/EVE copolymer 5 was prepared in benzene. Characteristic of the free radical copolymerization is virtually complete alternation with little tendency of either monomer to homopolymerize.[18] The M_w of the copolymer obtained by light scattering in this study was 2.4×10^5 g/mol. The ^{13}C NMR spectrum of the MA/EVE copolymer is shown in Figure 8-1.

Initial attempts to induce the reaction of the MA/EVE copolymer 5 with alkyl amines and naphthalene label 3 were performed in methylethyl ketone (MEK). The color of the products varied from pink to purple as the degree of incorporation of the hydrophobic groups increased from 8 to 50 mole%.

To ascertain the possibility of charge-transfer complexation between the amine and anhydride functionality of the MA/EVE copolymer 5, we examined some model reactions. Reaction of succinic anhydride (SA) (**8**) with dodecylamine (**9**) yielded the corresponding amide **10** (Scheme 8-4) identified by NMR and FTIR. However, the solution of succinic anhydride and dimethyldodecylamine (DMDA) in MEK exhibited a color change from pink to brown at room temperature with increasing reagent concentration. It is known that pyridine can promote the hydrolysis of anhydride group by forming a zwitterionic intermediate.[19,20] Kluger and Hunt[21] detected the formation of succinyl-4-(dimethylamino)pyridinium ion in the reaction of succinic anhydride with 4-(dimethylamino) pyridine. It is likely that the reported color change in succinic anhydride and dimethyldodecylamine solution is due to the formation of an analogous switterion. We also observed a similar color change for the reaction of the copolymer 5 with dimethyldodecylamine. UV spectra of the solutions of SA/DMDA mixture and the products from the reactions of the MA/EVE copolymer 5 with primary and tertiary amines exhibit the same absorption maximum at 556 nm (Figure 8-2), suggesting the presence of similar switterionic species in these three systems. The absorption intensity of tertiary solution is stronger for the same feed ratio of amine to acid anhydride. This observation may be explained by partial dodecylamine conversion to the amide. This is consistent with the increase in intensities of the absorption at 562 nm for dodecylamine-modified terpolymers **7** as the degree of amidation varies from 8 to 50 mole% (Figure 8-3).

Reactions of the MA/EVE copolymer **5** with octyl and dodecylamine in ethyl acetate exhibit no color changes and ^{13}C NMR studies demonstrate that the products are the expected amide and carboxylic acid derivatives (Figure 8-4). In this solvent homogeneous conditions should allow uniform, random incorporation of the hydrophobic groups along the polymer chain. The hydrophobe concentration in the terpolymers can be easily controlled by the amount of the amine added to the reaction. To ensure complete conversion, the reactions were carried out at 80°C for 10 hours. It has been shown that 4-butylaniline reacts efficiently (100%) with the maleic anhydride and ethyl vinyl ether copolymer under the same reaction conditions.[22] Since the octyl and dodecyl amines used in this study are more reactive toward the anhydride group than aromatic amines, we feel confident that a complete reaction is also achieved. This is supported by the fact that the naphthalene content in the terpolymers is the same as in the reaction mixture, about 1 mole%. The compositions of the terpolymers are summarized in Table 8-1.

The hydrolysis of the remaining anhydride groups of the modified terpolymers was performed in aqueous NaOH solutions at room temperature with the NaOH concentration varying from 0.1 to 0.5 M depending upon the degree of substitution. To completely dissolve the polymer with higher hydrophobe content, low NaOH concentration was necessary to avoid high ionic strength of the medium during neutralization. Complete hydrolysis was demonstrated by the FTIR spectra with disappearance of the C=O stretching vibration of the acid anhydride; it is

assumed that no hydrolysis of the amide bond occurs since in previous work none was observed.[22] 7-C12-50 failed to dissolve completely in 0.01 M NaOH solution even over an extended period of time.

Solution Properties

The solution properties of amphiphilic water-soluble polymers are controlled by specific structural characteristics, molecular weight and the solvent quality. The structural parameters including concentration and distribution of hydrophobic groups, hydrophilic segment length, and fixed ionic groups are among many which may be changed to yield the desired properties. For example, hydrophobic interactions of long chain hydrocarbons incorporated along the polymer backbone can greatly affect the degree to which the polymer coil may expand or collapse. Changes in the degree of ionization and solvent characteristics such as ionic strength and pH alter the polymer conformations as well. In this study, influences of these parameters on the solution behavior of the terpolymers 7 are examined by viscosity and fluorescence measurements.

Viscosity Studies

Aging Effects

Hydrophobically modified, water-soluble polymers often show time-dependent reorganization in solution.[23] To properly assess the effects of terpolymer composition, pH and added electrolytes on solution behavior, aging studies were first conducted. Figure 8-5 shows the aging effects for the 7-C12-10 and 7-C12-40 polymers. Both terpolymers dissolve completely in deionized water within 24 hours. The apparent viscosity of P-C12-10 decreases only slightly before reaching a constant value within 3 days. A more pronounced aging effect was observed for 7-C12-40. Apparently, the stronger hydrophobic interactions require a longer period of time to reach equilibrium. Furthermore, freshly prepared 7-C12-40 solution exhibits intermolecular associating behavior (Figure 8-6). In contrast, intramolecular association was observed for the same solution at equilibrium. This indicates that the 7-C12-40 terpolymer undergoes a conformational transition from intermolecular to intramolecular during the aging process. No such a conformational transition was observed for 7-C12 terpolymers at lower hydrophobe levels or for all 7-C8 terpolymers.

Effects of Hydrophobic Groups

To assess the effects of hydrophobic monomer content on viscosity behavior in deionized water, it was first necessary to determine intrinsic viscosity utilizing the Fuoss relationship[24]. Figure 8-7 shows the intrinsic viscosities of 7-C8 and 7-C12 terpolymers as a function of composition. The intrinsic viscosities decrease dramatically as the hydrophobe concentration in the terpolymers increases from 0 to 50 mole%. A larger quantity of hydrophobic groups effectively enhances the hydrophobic interactions, resulting in collapse of the polymer coil. A sharp drop in the intrinsic viscosity is observed at hydrophobe concentrations between 20 and 30 mole% for both 7-C8 and 7-C12 terpolymers. Similar observations have been reported for other intramolecular associative copolymers[2-5] and have been attributed to a transition from random coil to tighter hypercoil. Dodecyl terpolymers possess more compact structure than their octyl analogs at constant hydrophobe levels as indicated by the slightly lower intrinsic viscosities of the former (Figure 8-7).

Effect of pH

The amphiphilic terpolymers contain a large number of carboxyl functionalities as the major hydrophilic component. Variation in pH can impart significant change in solution properties. Figure 8-8 illustrates the viscosity behavior of the terpolymers containing varying n-octyl concentration at selected pH values. The reduced viscosities of all the polymer solutions initially increase with increasing pH and then decrease. The maximum value of reduced viscosity for all 7-C8 polymers is observed about pH 9.5. Changes in the reduced viscosity are qualitatively similar to those observed for maleic anhydride and alkyl vinyl ether copolymers[7,9-11]. The degree of ionization of the terpolymers increases with increasing pH, disrupting intramolecular associations. The terpolymers reach maximum charge density at the pH at which the highest reduced viscosity is achieved. Further increase in pH increases the concentration of sodium ions in the solution; therefore, the interaction between the charged groups along the polymer backbone is shielded, causing the polymer coil collapse.

When the pH of the solution is below the pKa of the carboxylic acid, most, if not all, of the charges carried by the terpolymers are neutralized. Therefore, there are not enough charged groups on the surface of polymer coil to prevent macromolecular aggregation and macrophase separation occurs. For example, the terpolymers with 40 and 50 mole% octyl groups precipitate below pH 4 and 5, respectively.

Effect of Electrolyte Addition

The effect of NaCl on the viscosity of the terpolymer solutions were investigated using 7-C8 series (Figure 8-9). The reduced viscosity decreases for all terpolymers as the NaCl molarity increases due to the shielding of ionic interactions of the carboxylate groups. The terpolymers with high hydrophobe content such as 7-C8-50 precipitate at high salt concentration (~0.5 M).

Effect of Shear Rate

The effect of shear rate on the apparent viscosity of 7-C8-10, 7-C8-30 and 7-C8-50 terpolymers were investigated in pure water at both low and high polymer concentrations. Unlike some of the reported systems which showed shear thickening behavior[25], the terpolymers at 0.05 g/dL exhibit Newtonian behavior over the shear rate regime. Similar behavior was observed for the terpolymers at 0.5 g/dL.

Photophysical Studies

Fluorescence measurements were conducted in attempts to evaluate associative properties of the terpolymers in aqueous solutions. Naphthalene lifetimes and excimer to monomer ratios (I_E/I_M) were recorded to monitor the changes of terpolymer conformation.

Effects of Hydrophobic Groups

A significant change in the fluorescence decay of monomer fluorescence (330 nm) was observed upon altering the hydrophobe content (Figure 8-10). The decay profiles of the terpolymers are complex but could be approximately fit by a sum of two exponentials composed

of a longer-lived component and a shorter-lived component. Table 8-2 summarizes the values of the average lifetime[26] defined by the following equation:

$$[\tau]=\Sigma a_i\tau_i^2/\Sigma a_i\tau_i$$

where a_i is the preexponential factor of the ith component and τ_i is the corresponding lifetime.

Multi-exponential fits have been reported for other associative polymers in aqueous media[16,27] and are probably due to labels in different environments contributing to the emission. It is noteworthy in our case that the values of $[\tau]$ increase with increasing hydrophobe concentration. The lifetimes of the naphthalene-labelled model compound 4 in solutions of THF, ethanol, methanol, and 50/50 methanol/water are 68.1, 47.2, 30.7, and 21.8 ns, respectively, demonstrating the effect of microenvironmental polarity on the decay of the excited state of the naphthalene label. Therefore, the increase in the average lifetime at higher hydrophobe content is consistent with coil collapse. Also, the 7-C12 series polymers have higher $[\tau]$ values than the 7-C8 analogs with the same hydrophobe mole%. Longer side chains effectively enhance the hydrophobic effect, providing shielding of the naphthyl label from water. These results are similar to those previously reported for hydrophobically modified poly(allylamine)s.[28]

In addition to changes in the average lifetime, terpolymers also show a dramatic hydrophobe concentration dependence of I_E/I_M. As indicated in Figure 8-11, I_E/I_M values of the terpolymers increase as the hydrophobe concentration varies from 10 to 30 mole%. Further increase in the hydrophobe concentration results in a decreases in I_E/I_M. It is unlikely that excimer formation is due to nearest neighbor interactions since the number of naphthyl groups are small and they are separated over a large distance along the polymer backbone. The initial increase in I_E/I_M may be attributed to the increased compaction of the polymer coil, which facilitates the formation of the excimer due to the reduced separation of the chromophore within the hydrophobic microdomain. When the hydrophobe concentration is above 30 mole%, the large hydrophobe quantities within the polymer coil separate the naphthyl labels. Furthermore, the highly compact hydrophobic microdomains limit the mobility of the chromophores, preventing orientation in a manner favorable for excimer formation. The latter effect has been observed previously by our group[16] and elsewhere[29] for naphthalene-labelled methacrylic acid copolymers. The negligible formation of excimer in 7-C8-50 and 7-C12-40 which have high hydrophobe concentrations, lends credence to these arguments.

Effect of pH

The effect of solution pH on the conformation of the terpolymers was first examined by the lifetime measurement at 330 nm of the monomer decay of 7-C8 systems. Decrease in $[\tau]$ indicates the expansion of the hydrophobic domains upon increasing pH (Table 8-2). The highly hydrophobic terpolymers such as 7-C8-40 and 7-C8-50 remain in the rather compact conformations at high pH as evidenced by the large $[\tau]$ values.

Figure 8-12 depicts the pH dependence of I_E/I_M for 7-C8 polymers in the aqueous solutions. For the 7-C8-10 and 7-C8-20 polymers, I_E/I_M decreases in the pH range 3 to 10 and then increases slightly at higher pH. This is consistent with the rheological response of the

terpolymers. As the pH is increased, the polymer coil expands and the naphthyl groups are separated, leading to decreased I_E/I_M. The lowest I_E/I_M occurs at the pH where maximum expansion of the polymer coil occurs. A slight rise in I_E/I_M at higher pH is attributed to an increase in ionic strength. 7-C8-20 exhibits a higher I_E/I_M value at constant pH than does 7-C8-10 due to a more compact structure of the former.

The 7-C8-30 polymer exhibits a different dependence of I_E/I_M on the pH. The curve first rises and then drops rapidly upon increasing the pH. The initial increase in the values of I_E/I_M may be explained by increased mobility of the naphthyl groups in the hydrophobic microdomains upon coil expansion. At pH 3, the terpolymer adopts a highly collapsed conformation, indicated by the very low reduced viscosity. The mobility of the chromophore is largely restricted. The probability of two chromophores approaching each other in a coplanar or sandwich manner, a necessity for the excimer formation, is small. As pH is increased, chain expansion decreases polymer coil density. The relatively large separation of the naphthyl moieties from the polymer backbone allows the chromophores to maintain proximity to one another upon moderate expansion; this, coupled with increased mobility of the chromophores, leads to the increased I_E/I_M. Further increase in the coil size at higher pH, however, results in the long range separation of the chromophores and I_E/I_M decreases rapidly. This behavior is significantly different from that observed previously by our group[16] for naphthalene labelled poly(methacrylic acid). In this case, I_E/I_M increased rapidly at pH of 7.5 but exhibited no decrease thereafter. Relatively large quantities of naphthyl labels and long spacers in that copolymer were reported to allow association even in a highly expanded coil. For the 7-C8-30 terpolymer, however, each naphthyl group is surrounded by comparatively large neighboring octyl groups upon coil expansion[6,7], resulting in a decrease in I_E/I_M. Interestingly, the I_E/I_M maximum is observed at lower pH than the reduced ivscosity maximum (Figure 8-8), indicating that significant chromophore separation occurs before the polymer chain reaches its maximum expansion.

The terpolymer 7-C8-40 also shows an increase in I_E/I_M, but to a lesser extent. This can be attributed to the increased difficulty of two chromophores approaching each other in a large hydrophobe concentration within the polymer coil. This is consistent with the observation that the 7-C8-40 polymer always exhibits a lower I_E/I_M value than 7-C8-30 at a constant Ph.

Values of I_E/I_M for 7-C8-50 change little with pH. In this case, very high hydrophobe concentration within the polymer coil results in almost complete diminution of the naphthyl group interactions. Each naphthyl label is surrounded by a large number of octyl groups even in the expanded coil. Therefore, low I_E/I_M values are observed throughout the pH range.

Effect of Electrolyte Addition

Table 8-3 lists the average lifetimes of the monomer emission for 7-C8 polymers at different NaCl concentrations. Increased average lifetime is consistent with the compaction of polymer coil with increasing the salt concentration. The terpolymers with higher hydrophobe content are less sensitive to the ionic strength as indicated by the reduced curvature of the data. The reduced sensitivity may be explained by the already very compact conformation adopted by the terpolymers in the salt-free solution as well as the decreased quantity of charged groups along the terpolymer chain.

Conclusions

A series of naphthalene-labelled poly(maleic anhydride-alt-ethyl vinyl ether) copolymers containing pendent octyl and dodecyl groups has been synthesized. The Fluorescence and viscosity behavior of the terpolymers have been studied as a function of the length and concentration of the hydrophobic groups, electrolyte concentration, and the solution pH. In all the cases investigated, the terpolymers exhibit a tendency toward intramolecular association in dilute and semidilute aqueous solutions at specifically varied conditions of pH and ionic strength. The terpolymers with longer alkyl groups and/or higher alkyl group content tend to be more compact and exhibit lower viscosity in deionized water. Addition of either acid or base results in decreased solution viscosity. Addition of NaCl lowers significantly the viscosity of the polymer solutions, indicating a more collapsed conformation at higher ionic strength. Photophysical data parallel the rheological responses. I_E/I_M values of naphthyl moieties from steady-state fluorescence increase initially, reach a maximum, and then decrease upon increasing the hydrophobe concentration from 10 to 50 mole%. Extended lifetime of the monomer fluorescence decay with increasing hydrophobe level indicates increased compaction of the polymer coil. As the pH values change from 3 to 10, significant decrease in the I_E/I_M values is observed for the terpolymers with low hydrophobe content due to the coil expansion. I_E/I_M values of the terpolymers with moderate hydrophobe content rise initially and then decrease continuously over same pH range. Systems with high hydrophobic content show little dependence on pH. These results are explained by considering the relative concentration of the chromophore in the hydrophobic microdomains as well as the change in the mobility of the naphthyl moieties with the compactness of the polymer coils. The lifetime of the monomer emission decreases with increasing pH, indicating a more hydrated environment experienced by the probe within the polymer coil.

References

1. Strauss, U. P.; Gershfeld, N. L. *J. Phys. Chem.* **1954**, 747.

2. Strauss, U. P.; Gershfeld, N. L.; Crook, E. H. *J. Phys. Chem.* **1956**, 577.

3. Ghesquiere, D.; Chachaty, C.; Ban. B.; Loucheux, C. *Makromol. Chem.* **1976**, 177, 1601.

4. Strauss, U. P.; Vesnaver, G. *J. Phys. Chem.* **1975**, 79, 1558.

5. Strauss, U. P.; Vesnaver, G. *J. Phys. Chem.* **1975**, 79,2428.

6. Strauss, U. P.; Schlesinger, M. S. *J. Phys. Chem.* **1978**, 82, 571.

7. Strauss, U. P.; Schlesinger, M. S. *J. Phys. Chem.* **1978**, 82, 1627.

8. Ito, K.; Ono, H.; Yamashita, Y. *J. Colloid Sci.* **1964**, 19, 28.

9. Dubin, P.; Strauss, U. P. *J. Phys. Chem.* **1967**, 71, 2757.

10. Dubin, P.; Strauss, U. P. *J. Phys. Chem.* **1973**, 77, 1427.

11. Dubin, P.; Strauss, U. P. *J. Phys. Chem.* **1970**, 74, 2842.

12. Martin, P. J.; Strauss, U. P. *Biophys. Chem.* **1980**, 11, 397.

13. Binana-Limbele, W.; Zana, R. *Macromolecules* **1987**, 20, 1331.

14. Binana-Limbele, W.; Zana, R. *Macromolecules* **1990**, 23, 2731.

15. Chu, D.-Y.; Thomas, J. K.; In *Polymers in Aqueous Media. Performance Through Association*; Glass, J. E. Ed.; Advances in Chemistry Series No. 223, ACS, Washington, DC, **1989**; p 325.

16. McCormick, C. L.; Hoyle, C. E.; Clark, M. D. *Macromolecules* **1990**, 23, 3124.

17. Newman, M. S.; Otsuka, S. *J. Org. Chem.* **1958**, 23, 797.

18. Baldwin, M. G. *J. Polym. Sci.* **1965**, A3, 703.

19. Fersht, A. R.; Jencks, W. P. *J. Am. Chem. Soc.* **1970**, 92, 5432.

20. Castro, C.; Castro, E. A. *J. Org. Chem.* **1981**, 46, 2939.

21. Kluger, R.; Hunt, J. C. *J. Am. Chem. Soc.* **1989**, 111, 3325.

22. McCormick, C. L.; Hoyle, C. E.; Clark, M. D. *Polymer* **1992**, 33, 243.

23. McCormick, C. L.; Nonaka, T.; Johnson, C. B. *Polymer* **1988**, 29, 731.

24. Fuoss, R. M.; Cathers, G. I. *J. Polym. Sci.* **1949**, 4, 96.

25. Bock, J.; Siano, D. B.; Valint, P. L. Jr.; Pace, S. L. In Polymers in Aqueous Media; Glass, J. E., Ed.; Advances in Chemistry Series No. 223; ACS Washington, D C **1989**; p 411.

26. Bai, F.; Chang, C.-H.; Webber, S. E. *Photophysics of Polymers*; Hoyle, C. E., Torkelson, J. M., Ed.; ACS Symposium Series 358; American Chemical Society: Washington, DC, **1987**.

27. Ezzell, S. A.; Hoyle, C. E.; Creed, D.; McCormick, C. L. *Macromolecules* **1992**, 25, 1887.

28. Morishima, Y.; Kobayashi, T.; Nozakura, S.; Webber, S. E. *Macromolecules* **1987**, 20,807.

29. Seo, T.; Take, S.; Akimoto, T.; Hamada, K.; Iijima, T. *Macromolecules* **1991**, 24, 4801.

TABLE 8-1. TERPOLYMER COMPOSITIONS

Terpolymers	Hydrophobe Content (Mole %)	Naphthalene Content (Mole %)
7-C8-10	10	1.05
7-C8-20	20	1.01
7-C8-30	30	0.995
7-C8-40	40	1.04
7-C8-50	50	1.04
7-C12-10	10	0.986
7-C12-20	20	1.00
7-C12-30	30	1.02
7-C12-40	40	1.06

TABLE 8-2 FLUORESCENCE LIFETIME [τ] (ns) OF MONOMER EMISSION DECAY FOR 7-C8 TERPOLYMERS IN AQUEOUS SOLUTIONS

pH	7-C8-10	7-C8-20	7-C8-30	7-C8-40	7-C8-50
3	44.3	52.5	57.1	58.8	60.8
5	41.2	44.3	49.1	54.1	58.1
7	34.5	34.8	43.7	49.8	54.3
8	28.9	31.4	40.1	48.5	52.6
10	24.1	28.3	36.6	44.3	51.6

TABLE 8-3. FLUORESCENCE LIFETIME [τ] (ns) OF MONOMER EMISSION DECAY FOR 7-C8 TERPOLYMERS IN NaCl AQUEOUS SOLUTIONS

C_{NaCl} (M)	P-C8-10	P-C8-20	P-C8-30	P-C8-40	P-C8-50
0.1	49.3	54.5	60.1	65.3	68.6
0.2	55.2	58.7	64.5	67.6	69.5
0.3	58.9	62.4	67.5	69.9	72.4
0.4	61.2	63.5	69.8	71.3	74.1

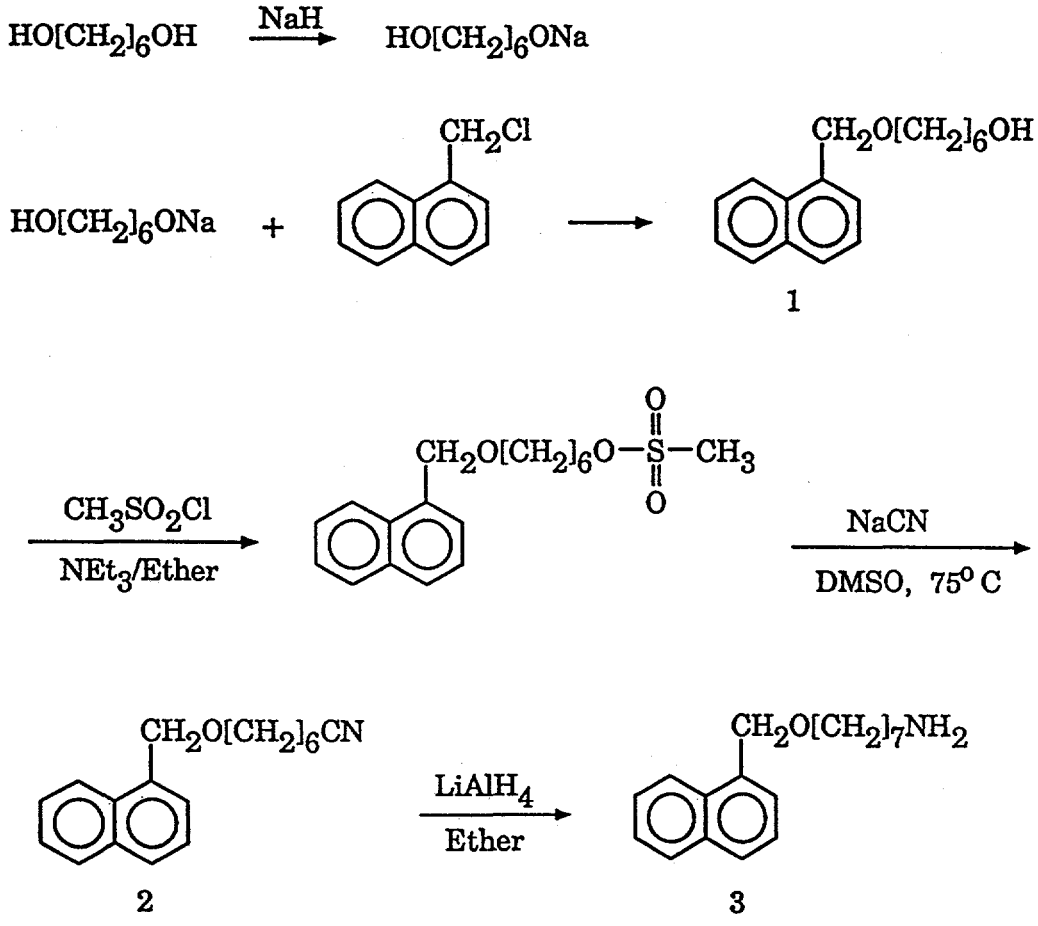

Scheme 8-1. Synthesis of 1-(7-aminoheptyloxymethyl)naphthalene **3**.

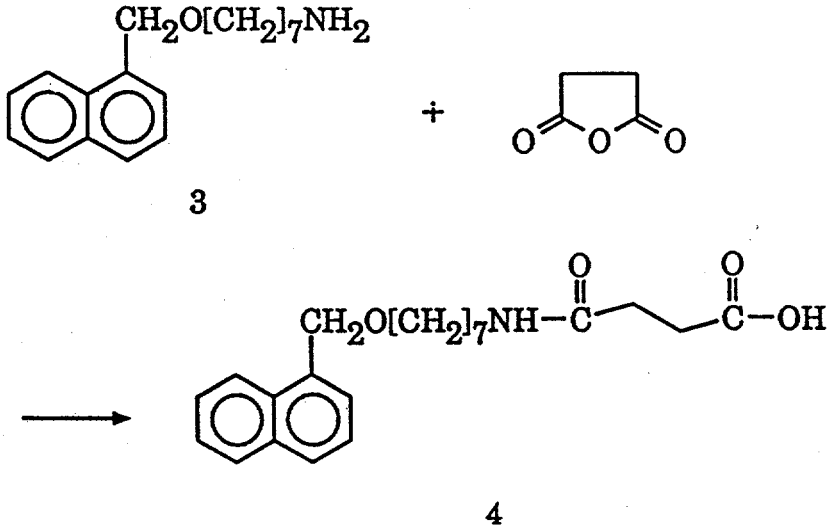

Scheme 8-2. Synthesis of naphthalene-containing model compound **4**.

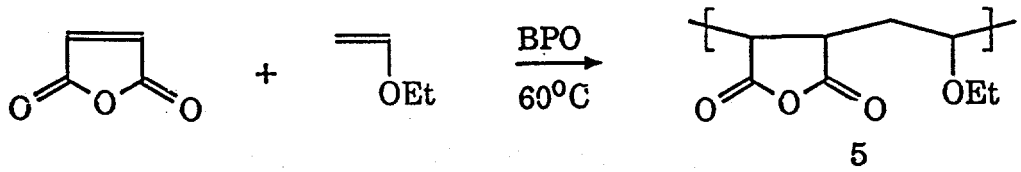

5

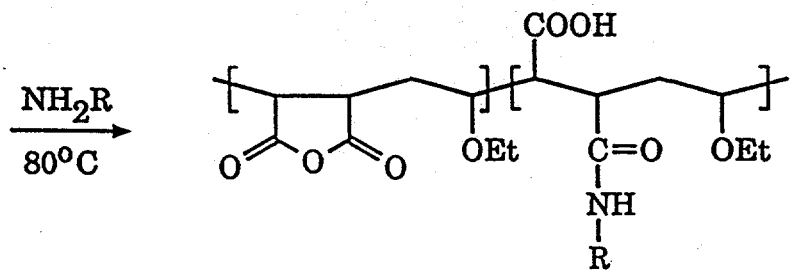

6

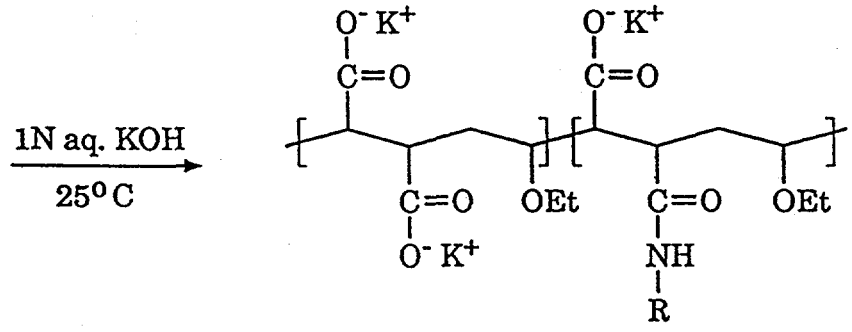

7

R: $[CH_2]_7CH_3$, $[CH_2]_{11}CH_3$

Scheme 8-3. Synthesis of hydrophobically modified maleic anhydride and ethyl vinyl ether based terpolymers 7.

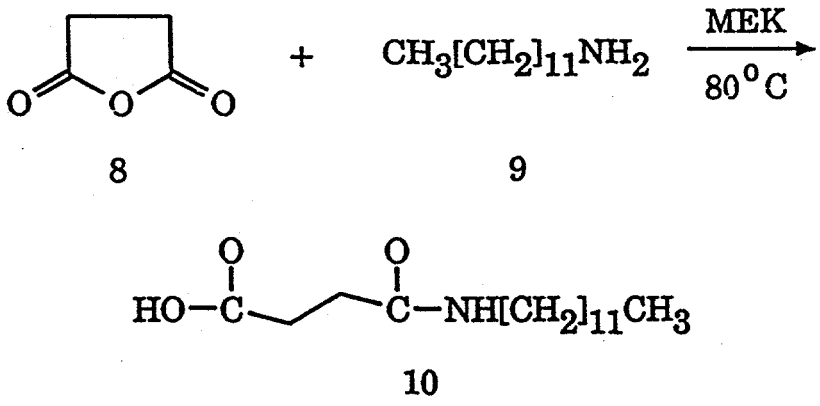

Scheme 8-4. Model reaction of succinic anhydride and dodecylamine.

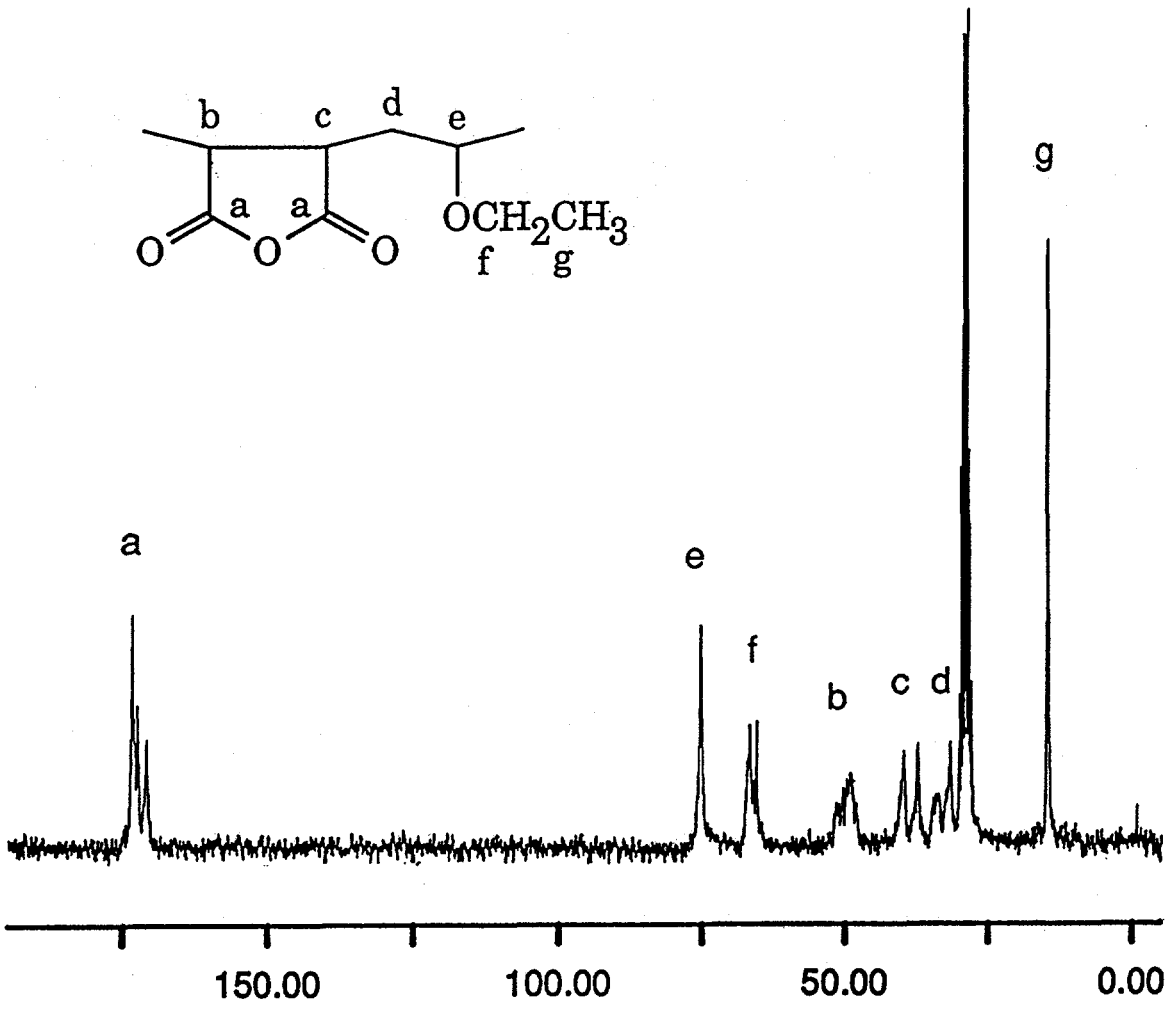

Figure 8-1. ^{13}NMR spectrum of MA/EVE copolymer 5. Solvent: acetone-d_6.

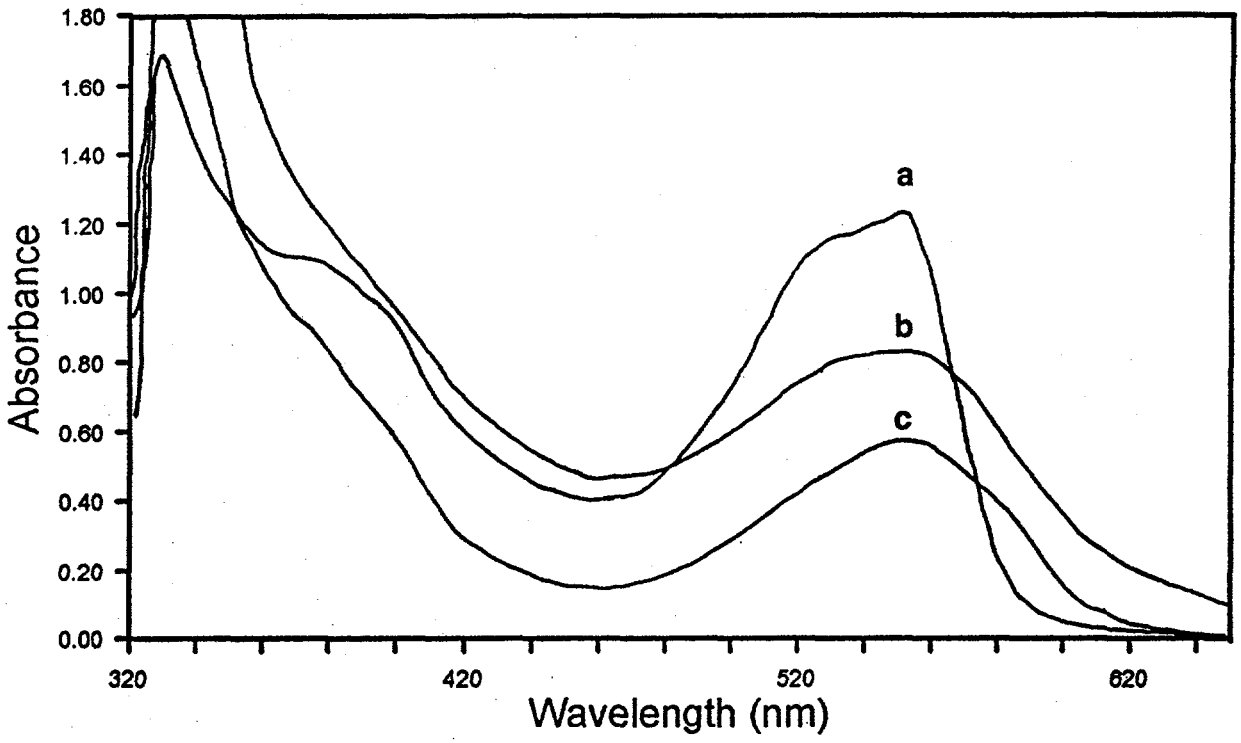

Figure 8-2. UV absorption of 5/DMDA (a, 0.0036 g/ml), SA/DMDA (b, 0.036 g/ml), and 5/dodecylamine (c, 0.036 g/ml) obtained in MEK. Note that all three samples exhibit adsorption maxima at 556 nm.

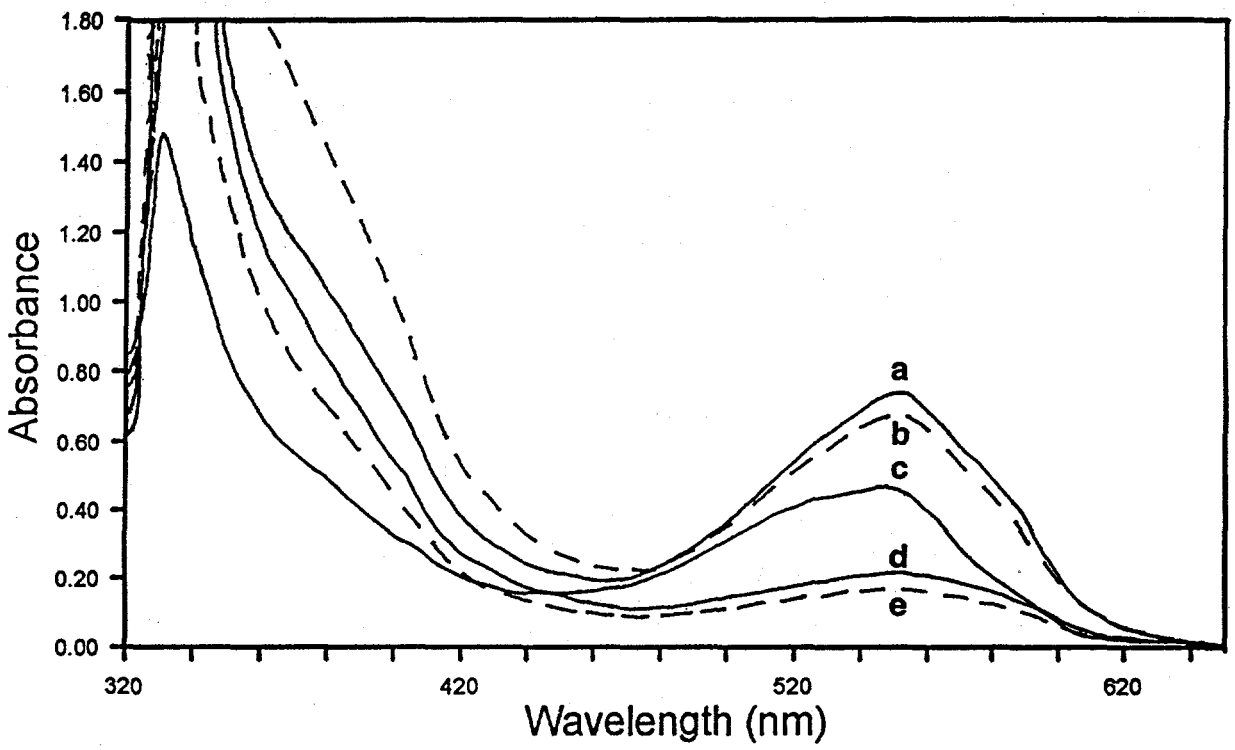

Figure 8-3. UV adsorption of 7-C12 terpolymers obtained in MEK. Sample concentration: 0.036 g/ml. (a) 7-C12-50; (b) 7-C12-40; (c) 7-C12-25; (d) 7-C12-16; (e) 7-C12-8.

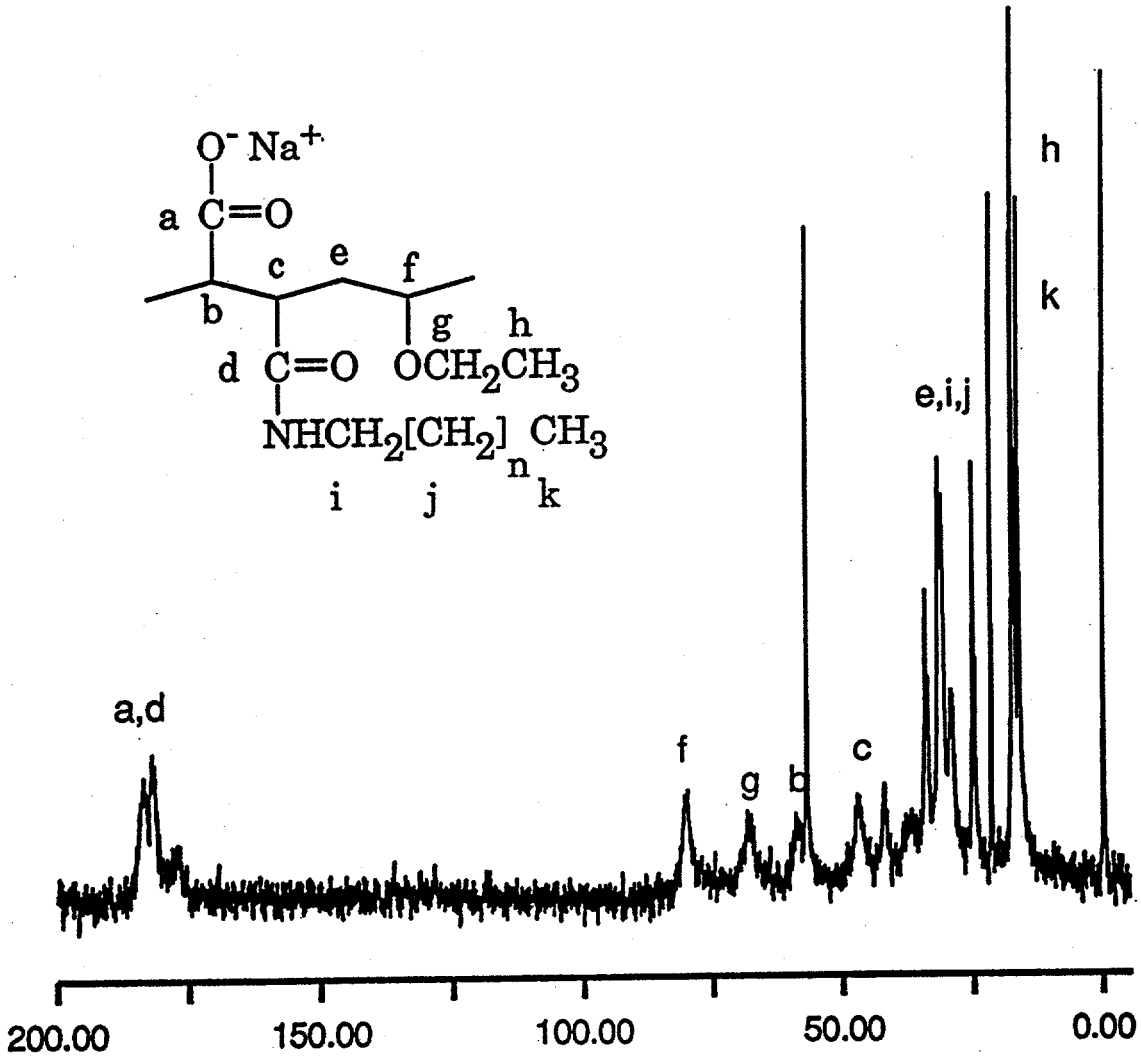

Figure 8-4. ^{13}NMR spectrum of 7-C12-40 terpolymer. Solvent: D_20.

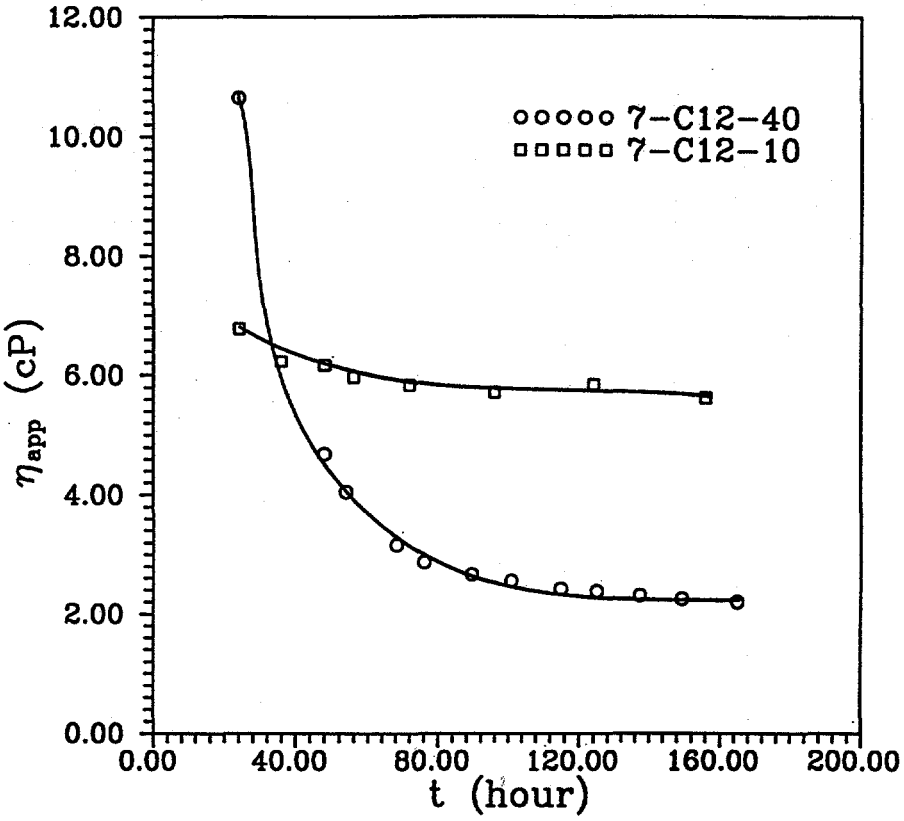

Figure 8-5. Aging effect for 7-C12-10 and 7-C12-40 polymers at 25°C in deionized water. C_p = 2.0 g/dL. shear rate: 1.28 s^{-1}.

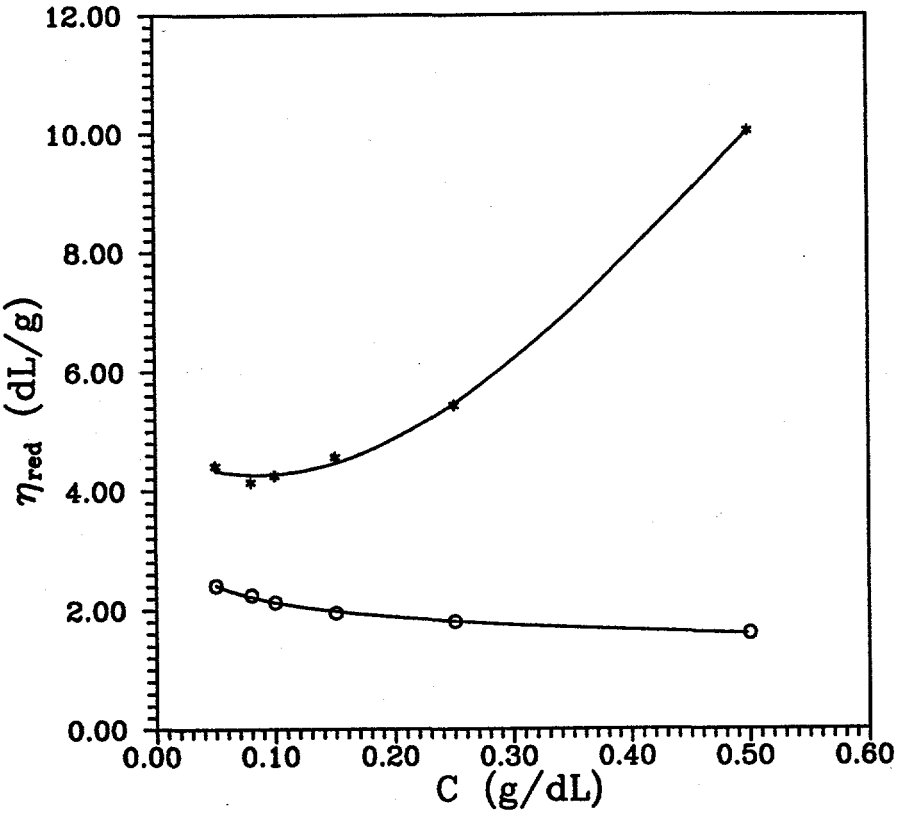

Figure 8-6. Comparison of viscosity behavior of 7-C12-40 terpolymer at 25°C in deionized water at different times. (*) one day after sample preparation; (o) 20 days after sample preparation. shear rate: 1.28 s^{-1}.

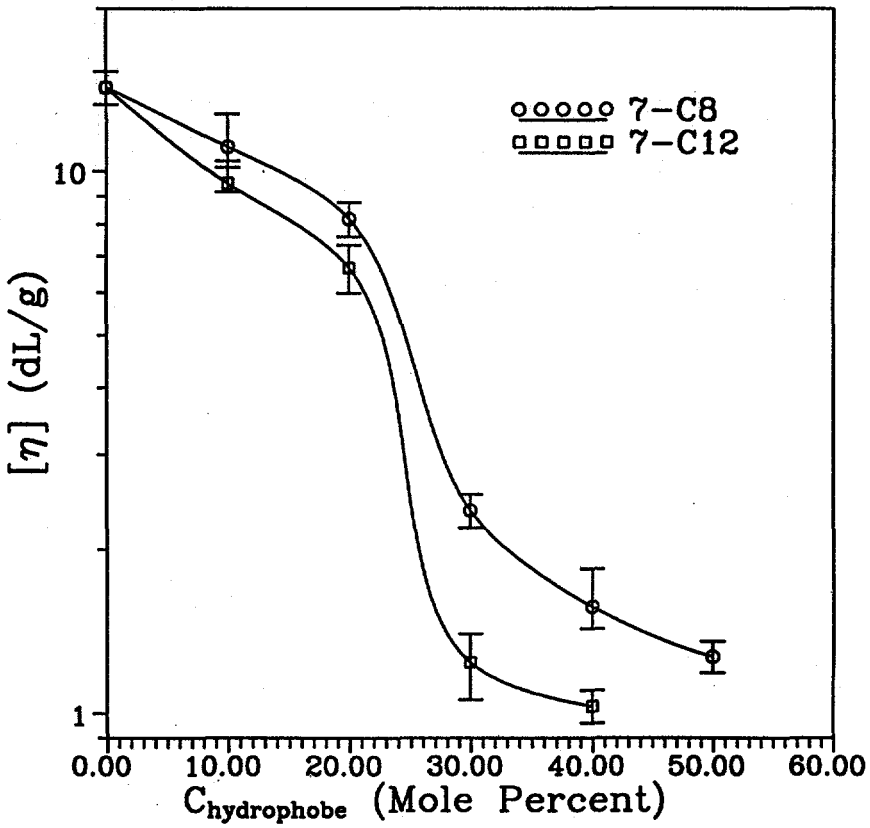

Figure 8-7. Effects of n-octyl and n-dodecyl groups content on the intrinsic viscosity of 7-C8 and 7-C12 terpolymers in deionized water.

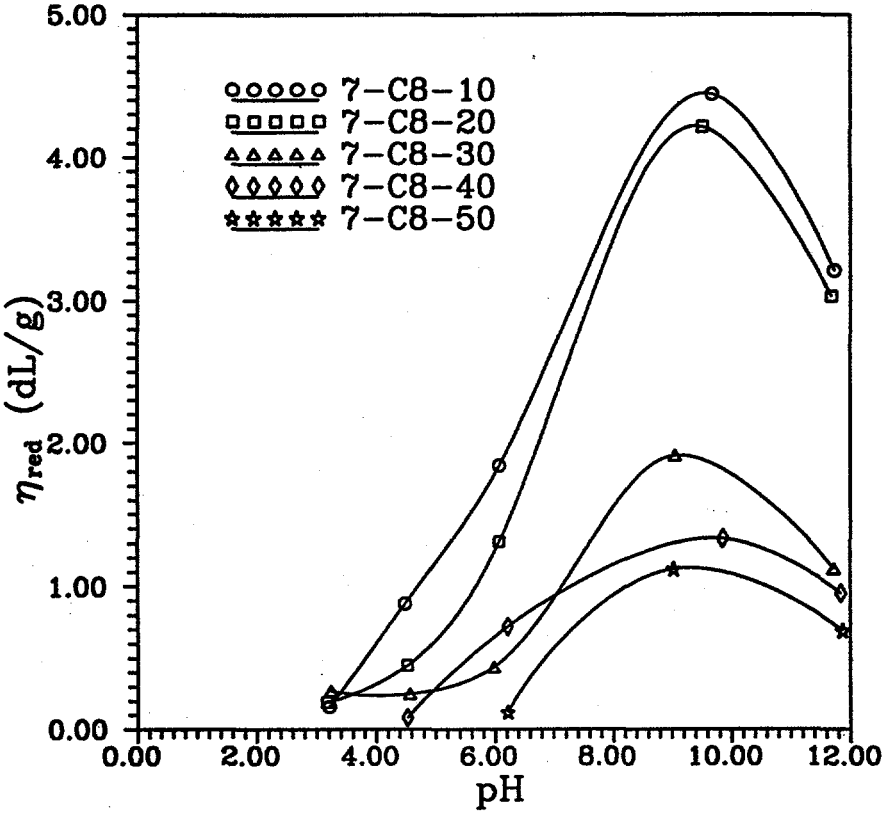

Figure 8-8. Effect of solution pH on η_{red} for 7-C8 polymers at 25°C. C_p = 0.5 g/dL. shear rate: 1.28 s^{-1}.

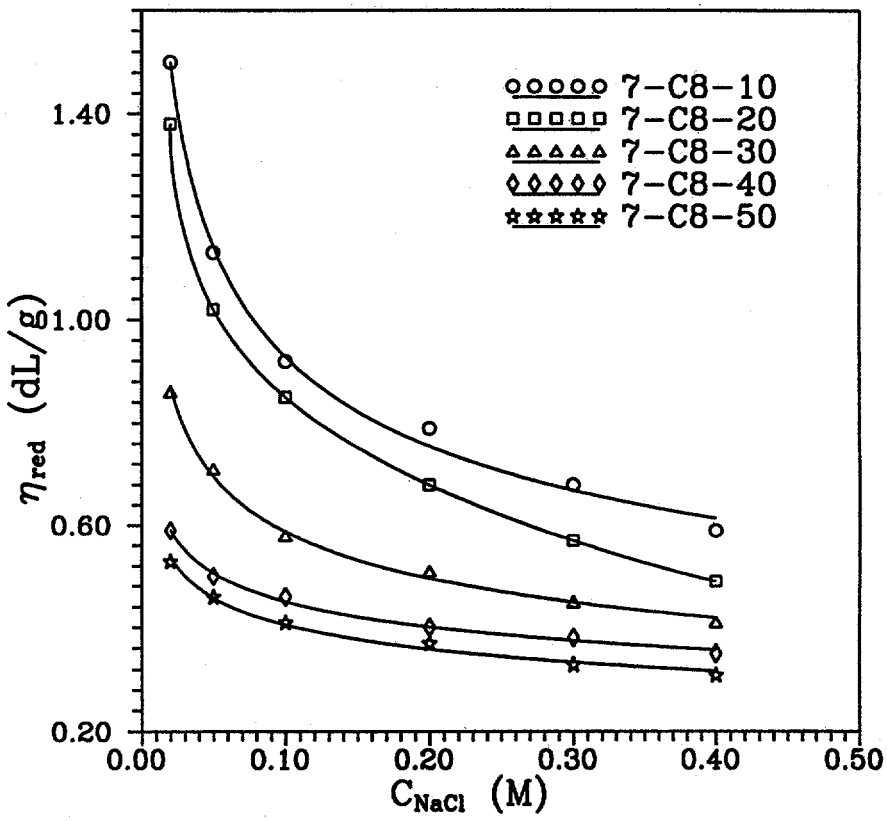

Figure 8-9. Effect of salt concentraion on η_{red} of 7-C8 polymers at 25°C. C = 0.15 g/dL. shear rate: 1.28 s^{-1}.

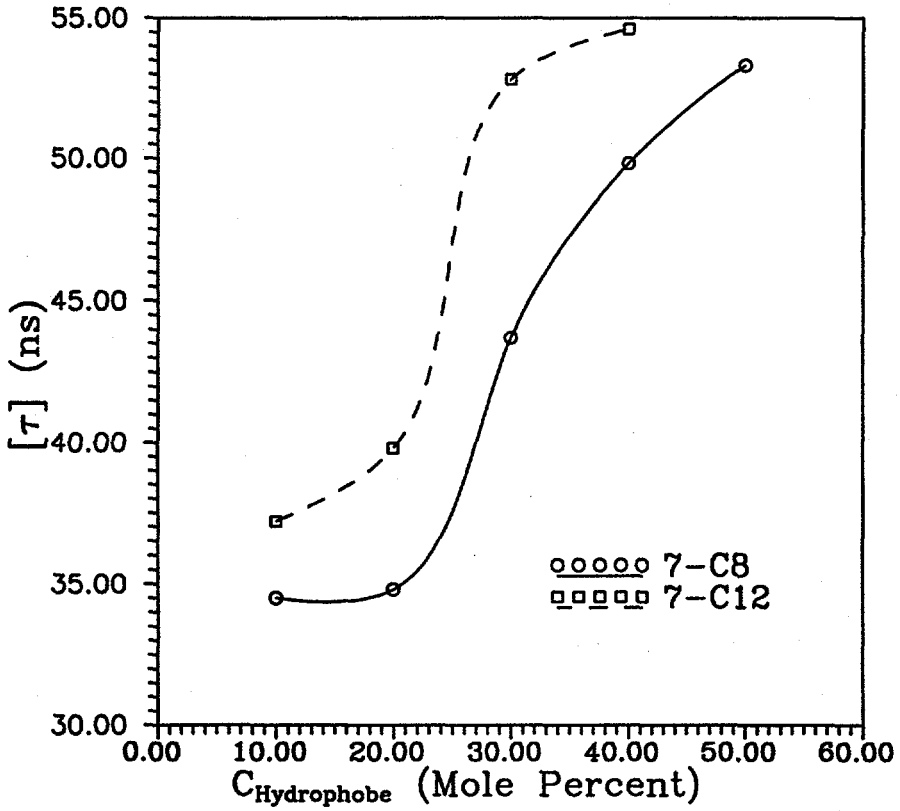

Figure 8-10. Dependence of average lifetime for monomer emission on the hydrophobe content.

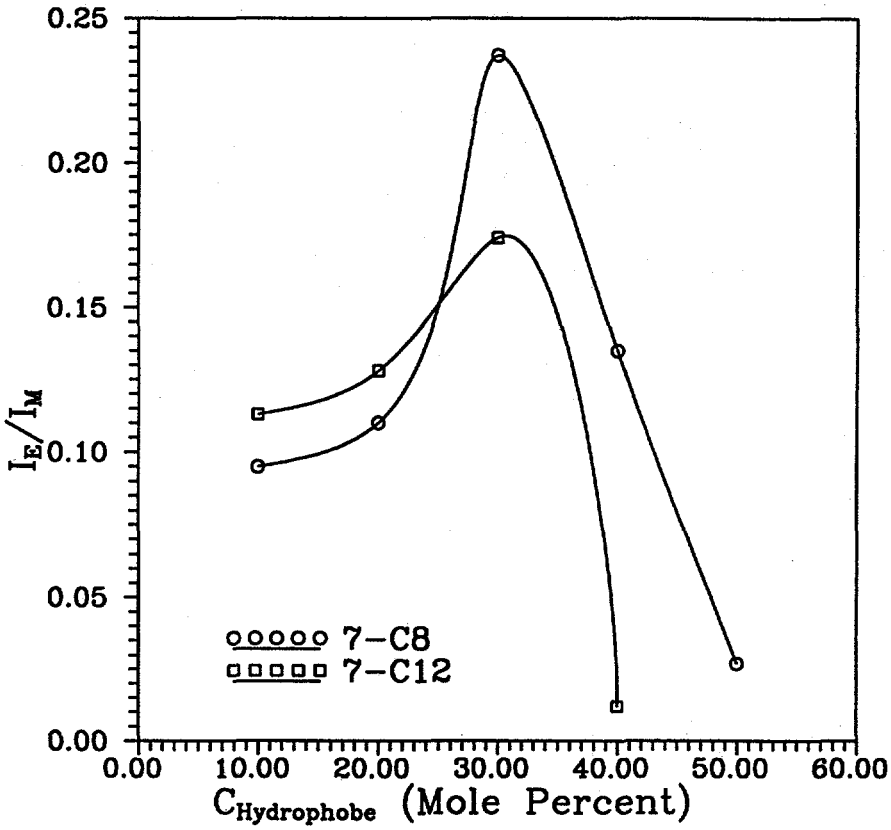

Figure 8-11. Dependence of I_E/I_M for both 7-C8 and 7-C12 polymers on the hydrophobe content at pH 7.

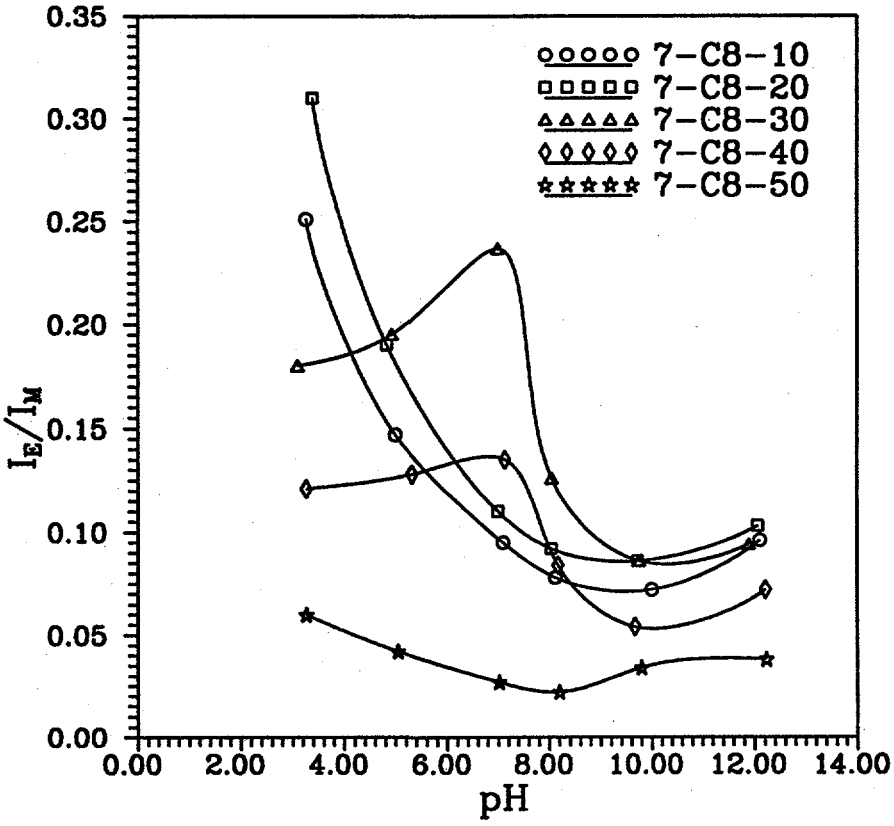

Figure 8-12. Dependence of I_E/I_M on solution pH for 7-C8 polymers. C_p = 0.05 g/dL.

CHAPTER 9: COPOLYMER COMPOSITIONS OF HIGH-MOLECULAR-WEIGHT FUNCTIONAL ACRYLAMIDO WATER-SOLUBLE POLYMERS USING DIRECT-POLARIZATION MAGIC-ANGLE SPINNING ^{13}C NUCLEAR MAGNETIC RESONANCE

Abstract

Compositions of several high-molecular-weight (>10^6g mol^{-1}) water-soluble copolymers have been determined using direct-polarization magic-angle spinning (d.p.m.a.s.) ^{13}C nuclear magnetic resonance (n.m.r.). Comonomers were studied that comprised acrylamide and sodium 3-acrylamido-3-methylbutanoate, sodium 2-acrylamido-2-methylpropanesulfonate, diacetone acrylamide or isopropylacrylamide. A copolymer of sodium 2-acrylamido-2-methylpropanesulfonate and 2-acrylamido-2-methlypropanetrimethylammonium chloride was also included. The technique is rapid and provides copolymer compositional analysis with accuracies close to those obtained by conventional elemental analysis and solution n.m.r. techniques. Spectral resolution is excellent and d.p.m.a.s. n.m.r. allows shorter acquisition times and smaller sample size. The technique is applied to a variety of acrylamide copolymers including polyelectrolytes, polyampholytes and hydrophobically associating polymers. The results are compared to copolymer compositions obtained from elemental analysis and solution ^{13}C n.m.r. spectroscopy.

Introduction

Copolymer characterization of polymer systems is a necessary requirement for the determination of reactivity ratios and interpretation of observed solution properties. For high-molecular-weight (HMW) acrylamide-based polymers, techniques such as elemental analysis require careful drying to remove adsorbed water; samples are usually submitted to outside laboratories for analysis. Additionally, analysis by ^1H nuclear magnetic resonance (n.m.r.) spectroscopy may not be possible owing to broad, overlapping spectral lines resulting from high molecular weights.

Solution ^{13}C n.m.r. has been employed extensively in the characterization of HMW acrylamide-based polymers that are routinely synthesized in our laboratories and has been shown to yield copolymer compositions consistent with those obtained by elemental analysis1,2. However the technique is time-consuming, often requiring 12-15 h of scanning time to yield a proper signal-to-noise ratio for accurate determination of copolymer ratios. In addition, the solution technique necessitates concentrations of 5-20% w/w in H_2O/D_2O, requiring several days for complete dissolution of high-molecular-weight polymers (>10^6 g mol^{-1}) to obtain quality solution spectra.

Recently, solid-state ^{13}C direct-polarization magic-angle spinning (d.p.m.a.s.) n.m.r. studies have been performed on hydrated polymer samples[3] and solvent-swollen gels[4,5]. The high solids content (<75% w/w solvent) along with considerable segmental mobility of the solvent-swollen polymer chains can yield ^{13}C m.a.s. n.m.r. spectra rivalling those obtained at the lower concentrations employed in solution n.m.r. The gel-state regime that lies between that of an

uncrosslinked solid and a dilute solution involves considerable chain entanglement that restricts overall tumbling of the polymer. The averaging of the molecular motions necessary for narrow lines in n.m.r. spectra is often not achieved in conventional solution spectroscopy. However, magic-angle spinning at moderate rates combined with high-power decoupling can impart a considerable decrease in linewidths[3-7].

D.p.m.a.s. spectra of a superabsorbing hydrolysed starch-*g*-acrylonitrile with minimal hydration of the polymer have been reported[3]. The dynamic behavior of the polymer chain as a function of hydration was studied by monitoring changes in longitudinal relaxation times and nuclear Overhauser enhancements (NOE). Clearly resolved spectra were obtained at polymer concentrations in water exceeding 50% w/w. Similar behaviour has previously been observed in synthetic polymers[6] and biopolymers[7].

The quantitative analysis of polymers by conventional ^{13}C n.m.r. has been well documented[8,9] and continues to be a routine technique for copolymer characterization[2,10]. Certain requirements must be met in order to obtain quantitative information from ^{13}C n.m.r. A delay of at least $5T_1$ after the excitation pulse is needed for more than 90% of the nuclei to return to the ground state. Additionally, the effect of the NOE must be reduced if the system is not outside the extreme narrowing regime where the NOE values may reach their maximum of 1,998[11]. For almost all of the systems of this study, the extreme narrowing condition is violated, resulting in varying NOE values depending on the backbone segmental motion and the motions of the pendent side chains[1]. This problem can be circumvented by employing gated decoupling. Since the ^{13}C-^{1}H decoupling is essentially instantaneous compared to the build-up of the NOE[11], the benefits of decoupled spectra are realized without NOE.

Previous ^{13}C n.m.r. studies in our laboratories on sodium 2-acrylamido-2-methylpropanesulfonate (NaAMPS) and diacetone acrylamide (DAAM) polymers have demonstrated short relaxation times (>1.25s) and near-equivalence of the T_1 and NOE values for the respect carbonyl moieties[2]. Thus, integration of the carbonyl peaks yielded copolymer compositions in agreement with those obtained from elemental analysis. Subsequent studies of the recycle times demonstrated that relaxation delays of as low as 2s could be employed without introducing significant error in the integration of the carbonyl peaks.

In this work, we describe a d.p.m.a.s. technique appropriate for compositional analysis of highly concentrated copolymer samples that allows much shorter acquisition times by employing highly concentrated samples. The copolymer compositions determined in this manner are compared with those obtained from elemental analysis to establish the validity of the technique. Gated decoupling and short relaxation delays of less than $5T_1$ were utilized to minimize instrument time. N.m.r. spectra were obtained by employing a 90° pulse angle, gated decoupling and relaxation delays of 2 and 10s. The technique is much faster than solution techniques owing to the highly concentrated samples, and generally requires less sample. Several random copolymers of acrylamide with ionic, hydrophobic and ampholytic moieties are reported.

Experimental

The syntheses of the polymers characterized in this work have been previously reported[12-15]; however, a brief description will be provided here. The appropriate amount of comonomer -- sodium 3-acrylamido-3-methylbutanoate (NaAMB), sodium 2-acrylamido-2-methylpropanesulfonate (NaAMPS), diacetone acrylamide (DAAM), or isopropylacrylamide (IPAM) -- with acrylamide (AM) is dissolved in water at 30°C and $K_2S_2O_8$ added as an initiator under nitrogen. NaAMB-25 refers to the polymer obtained from a 25/75 NaAMB/AM mixture in the feed. The ATAS polyampholyte is a copolymer of NaAMPS and 2-acrylamido-2-methylpropanetrimethylammonium chloride (AMPTAC). ATAS-50 refers to a 50/50 copolymer. The polymers were precipitated into acetone, redissolved in water, dialysed and freeze-dried. All polymers were vacuum dried at 40°C overnight before use. Samples were prepared by placing approximately 0.1 g of polymer in 0.6 ml centrifuge tubes and adding an equivalent amount of water (50% w/w). The samples were placed in a desktop centrifuge and allowed to spin overnight. Complete dissolution of the samples proved unnecessary as excellent spectra were obtained on samples that were clearly not completely dissolved. Most samples were essentially hydrogels that could be easily handled although some of the samples were highly viscous and would flow given sufficient time.

Copolymer compositions were determined by solid-state ^{13}C n.m.r. spectroscopy on a Bruker MSL-400 operating at 100.6 MHz ^{13}C frequency. Direct-polarization magic-angle spinning spectroscopy employed for solid samples yielded high-resolution spectra with low signal-to-noise ratios. The sample was placed in a 7mm ZrO rotor and spun at 2kHz. Spinning of the samples was relatively easy since the samples quickly conform to the rotor and are essentially self-balancing. A recycle time of 2s was employed with a flip angle of 90°. Generally, only 2000 scans were necessary to yield excellent signal-to-noise ratio. The spectra were resolution-enhanced by the Lorentzian method using a line-broadening factor of 6HZ and integrated to yield the copolymer ratio. The approximate error of the d.p.m.a.s. technique based on repetitive measurements is ± 2%.

Results and Discussion

Table 9-1 lists feed compositions as well as copolymer compositions obtained from elemental analysis and d.p.m.a.s. n.m.r. for copolymers described in the 'Experimental' section. The structures of the polymers are given in *Figures 9-1 thru 9-5* with representative spectra from each polymer group. The peak assignments are also provided for each polymer in the figures. In general, the agreement between the elemental analysis and n.m.r. data is excellent. The types of polymers investigated were selected to provide a cross-section of the acrylamide based water-soluble copolymers routinely synthesized in our laboratory. NaAMPS and NaAMB are sulfonate- and carboxylate-containing polyelectrolytes, respectively. The DAAM and IPAM series represent a class of hydrophobically associating copolymers, and ATAS is a polyampholyte.

In *Figure 9-1*, the d.p.m.a.s. spectrum is shown for NaAMB-25. The feed ratio in the polymerization was 25 mol% of the NaAMB monomer. The peak labelled 3, 8 is due to the acrylamido and carboxylate functionalities in NaAMB and peak 4 is due to the acrylamide carbonyl moiety. The backbone methine (2) and methylene (1) peaks are broadened due to their

hindered motion. The side-chain peaks (5, 6 and 7) are considerably sharper due to less restricted motion. The copolymer characterization is obtained by integration of the peaks at 176 ppm (acrylamide) and 180 ppm (NaAMB). However, the acrylamido peak and the carboxylate peak from the NaAMB moiety overlap. This problem is circumvented by integration of the peak area at 53 ppm (the quarternary carbon) and subtraction from the peak area at 180 ppm. The copolymer ratio is therefore the ratio of the peak area at 176 ppm to the corrected area at 180 ppm. The technique yields a value of 21 mol% NaAMB in the polymer compared with 22 mol% from the elemental analysis data. In *Table 9-1*, d.p.m.a.s. and elemental analysis data are presented for NaAMB copolymers with 5 to 75mol% compositions.

In *Figure 9-2*, a representative spectrum of a copolymer from the NaAMPS copolymer series is shown. The feed ratio employed in this polymerization was 20 mol% NaAMPS. Assignment of the spectrum is similar to that for NaAMB with the exception of the carboxylate peak. The composition is the ratio of the peak area at 176 ppm to the combined areas of the peaks at 176 and 180 ppm. The agreement between the elemental analysis data and n.m.r. is good (*See Table 9-1*).

Similar methods for determination of the copolymer composition by ^{13}C n.m.r. are employed for the DAAM series of copolymers (DAAM-20 is shown in *Figure 9- 3*). The DAAM copolymers range from 20 to 35 mol% DAAM comonomer in the feed. The composition of the DAAM comonomer in the final copolymer may be found by utilizing the carbonyl peaks at either 220 or 176 ppm. Similar results are found for the IPAM copolymer series (IPAM-40 is shown in *Figure 9-4*), and the ATAS (*Figure 9-5*) copolymer. For ATAS-50, although the carbonyl peaks are not completely resolved, the integration yields excellent results. Data presented in *Table 9-1* illustrate the excellent agreement in compositions from elemental analysis and d.p.m.a.s. n.m.r. measurements.

Conclusions

The data presented and the comparisons made in this study demonstrate the utility of the d.p.m.a.s. 13C n.m.r. technique for the purpose of determining copolymer compositions of solvent-swollen, high-molecular-weight acrylamide copolymers. The samples can generally be prepared in 24-48 h and require considerably less sample than do solution methods. The technique is faster than the solution method and often yields spectra with resolution similar to that obtained from solution 13C n.m.r. techniques. The method is shown to be useful for several high-molecular-weight acrylamide-based copolymers and should be applicable to a wide variety of polymers.

References

1. McCormick, C.L., Chen, G.S. and Hutchinson, B.H. J. Appl. Polym. Sci. (1982), 27, 3103.

2. Hutchinson, B.H. and McCormick, C.L. Polymer (1986), 27, 623.

3. Ganapathy, S., Badiger, M.V., Rajamohanan, P.R. and Mashelkar, R.A. Macromolecules (1992), 25, 4255.

4. Stover, H.D. H. and Frechet, J.M.J. Macromolecules (1989), 22, 1574.

5. Stover, H.D.H. and Frechet, J.M.J. Macromolecules (1991), 24, 883.

6. Blum, F.D., Dickson, J.E. and Miller, W.G. J. Polym. Sci., Polym. Chem. Edn. (1984), 22, 211.

7. Jackson, C.L. and Bryant, R.G. Biochemistry (1989), 28, 5024.

8. Guillet, S.And Delpeuch, J. J. Magn. Reson. (1980), 38, 433.

9. Cookson, D.J. and Smith, B.E. J. Magn. Reson. (1984), 57, 335.

10. Candau, F., Zekhnini, Z. and Heatly, F. Macromolecules (1986), 19, 1895.

11. Derome, A.E. 'Modern NMR Techniques for Chemistry Research', Pergamon, Oxord, (1987).

12. Elliot, D.L. PhD Dissertation, University of Southern Mississippi, (1986).

13. McCormick, C.L., Hester, R.D., Morgan, S.E. and Saffiedene, A.A. Macromolecules (1990), 23, 2124; Morgan, S.E. PhD Dissertation, University of Southern Mississippi, (1987).

14. McCormick, C.L. and Blackmon, K.P. J. Polym. Sci (A) Polym. Chem. Edn 1986, 24, 2635: Blackmon, K.P. PhD Dissertation, University of Southern Mississippi, 1987.

15. Mumick, P.S. and McCormick, C.L. Polym. Prepr. (1991), 32, 102.

16. McCormick, C.L. and Salazar, L.C. Macromolecules (1992), 25, 1896; Salazar, L.C. PhD Dissertation, University of Southern Mississippi, 1987.

Table 9-1
Feed ratios and copolymer ratios obtained from elemental analysis and 13C NMR.

CoPolymer	Mole % Comonomer in Feed	Elemental Analysis, Copolymer Composition, Mole % Comonomer	^{13}C NMR Copolymer Composition[a], Mole % Comonomer
NaAMB-5[b]	5	5.3	4.9
NaAMB-25[b]	25	22	21
NaAMB-40[b]	40	34	32
NaAMB-75[c]	75	64	62
NaAMPS-5[b]	5	4.7	3
NaAMPS-10[b]	10	9.2	8
NaAMPS-15[b]	15	13	14
NaAMPS-20[b]	20	18	17
DAAM-20[b]	20	20	20
DAAM-25[b]	25	26	26
DAAM-35[b]	35	35	35
IPAM-40[d]	40	41	41
IPAM-55[d]	55	56	53
IPAM-70[d]	70	72	68
IPAM-85[d]	86	85	82
ATAS-50[e]	50	50	48

a - 2 second recycle time, approximate error ± 4%
b - Reference 13
c - Reference 14
d - Reference 15
e - Reference 16

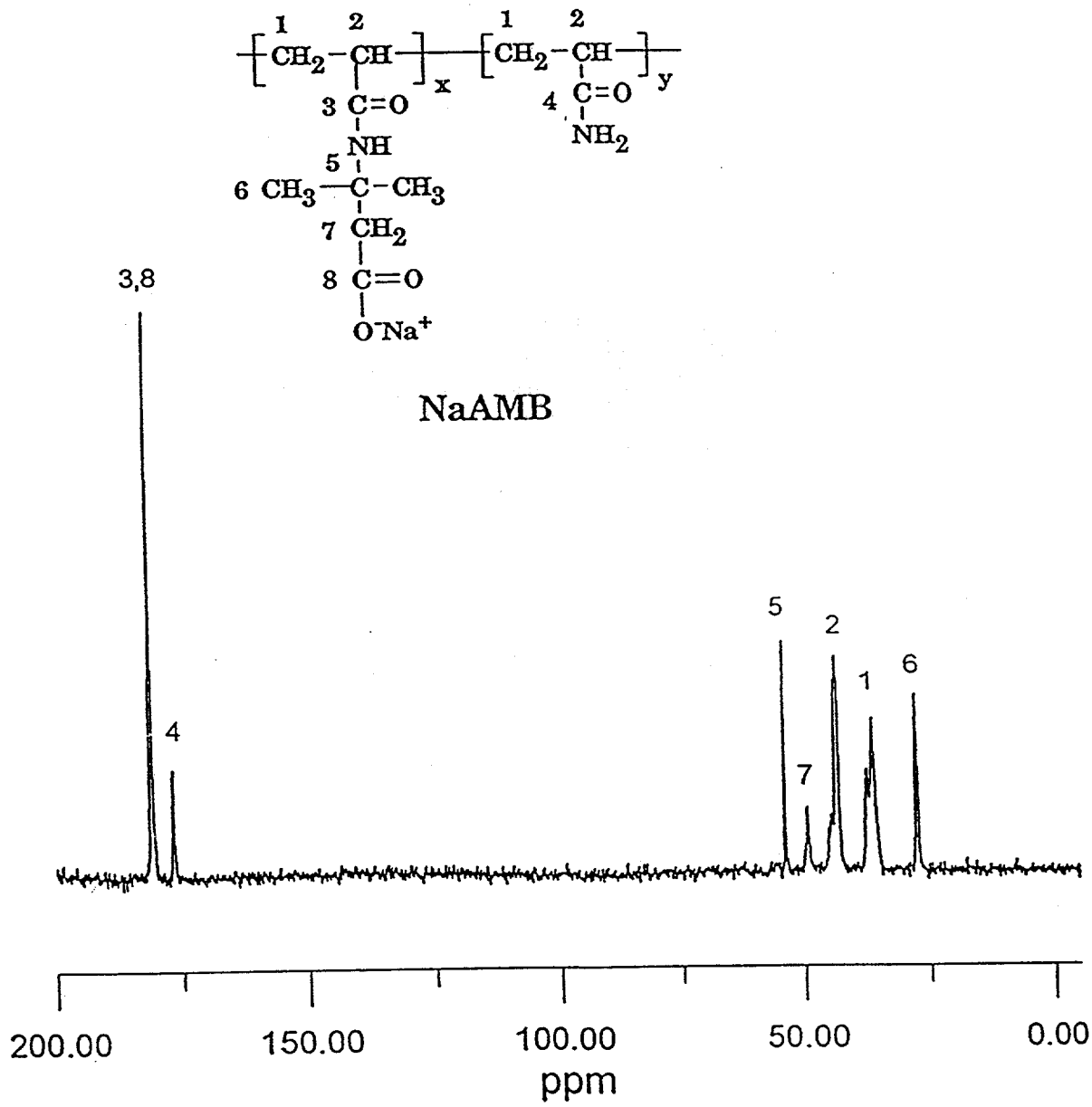

Figure 9-1. DPMAS spectrum of NaAMB-25. Assignment of the spectrum is shown along with the structure of the polymer.

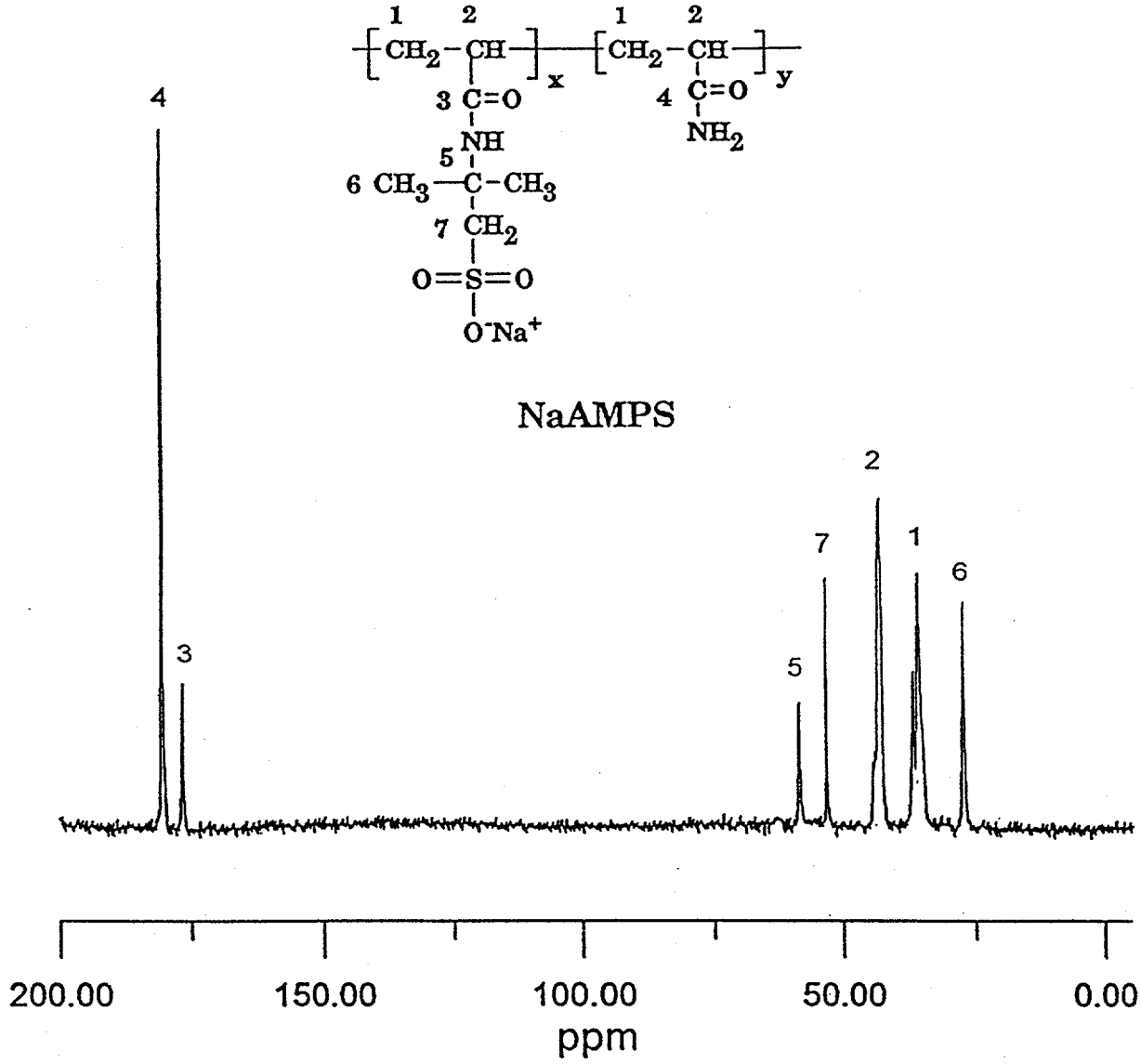

Figure 9-2. DPMAS spectrum of NaAMPS-20. Assignment of the spectrum is shown along with the structure of the polymer.

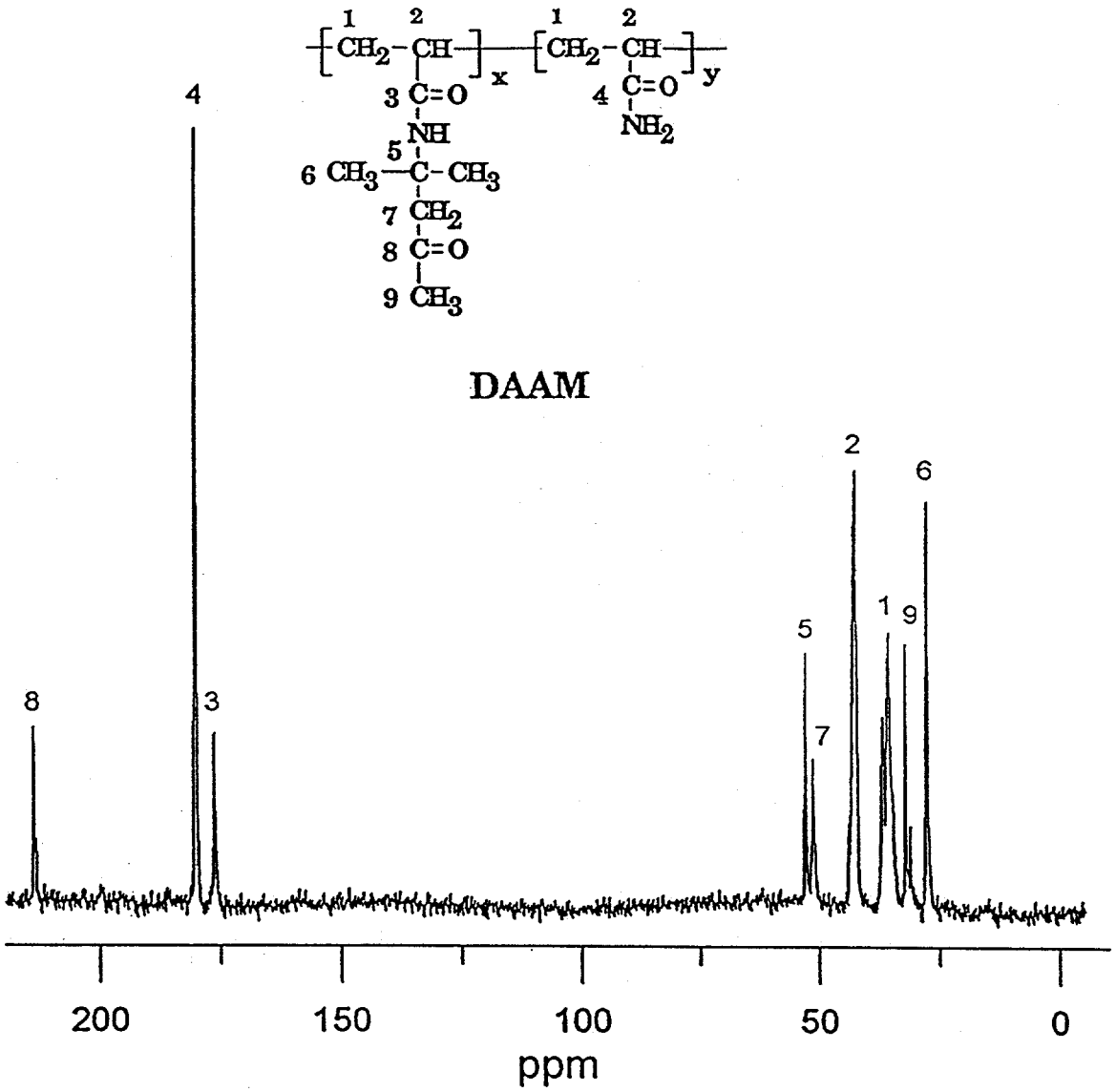

Figure 9-3. DPMAS spectrum of DAAM-20. Assignment of the spectrum is shown along with the structure of the polymer.

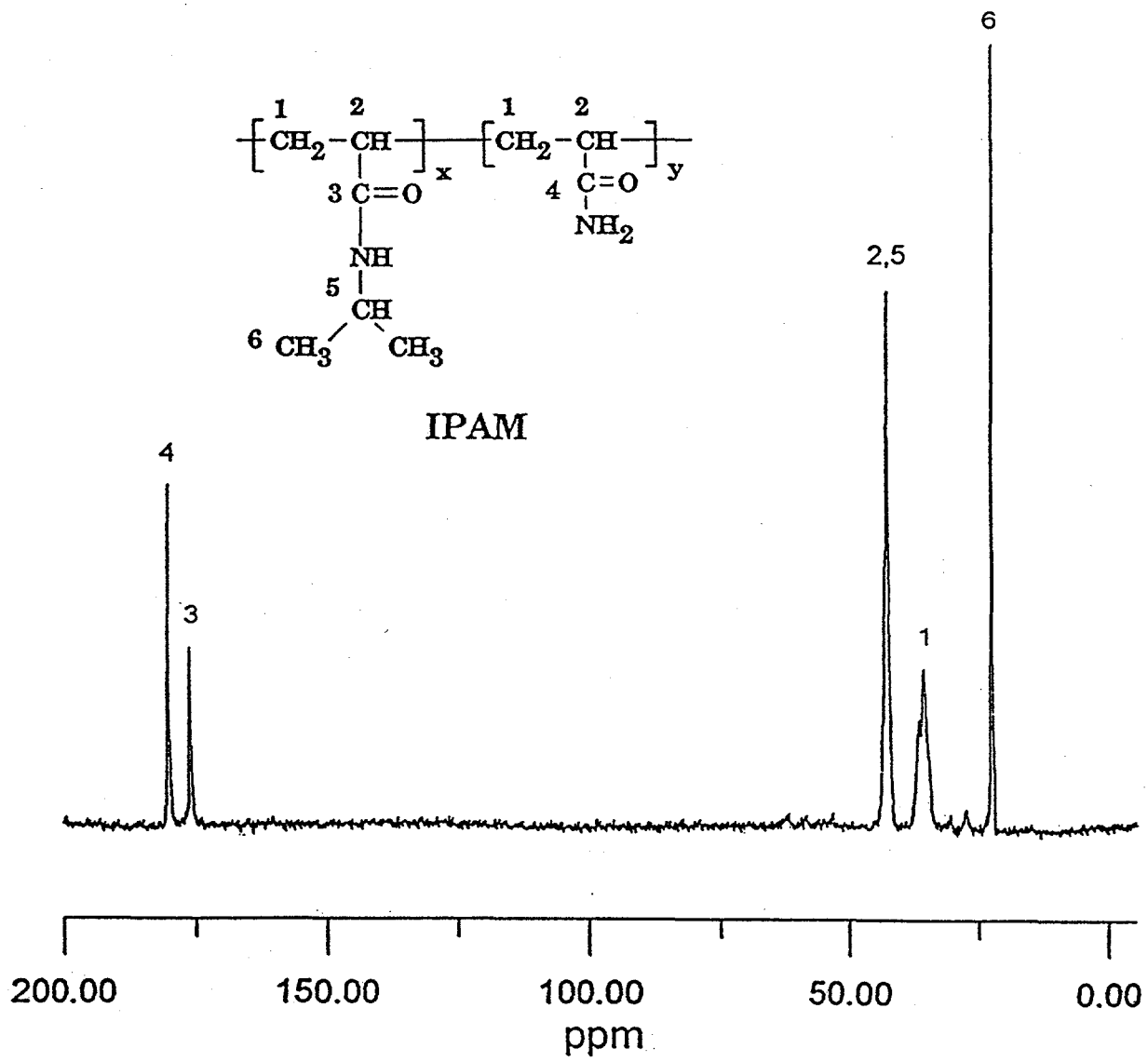

Figure 9-4. DPMAS spectrum of IPAM-40. Assignment of the spectrum is shown along with the structure of the polymer.

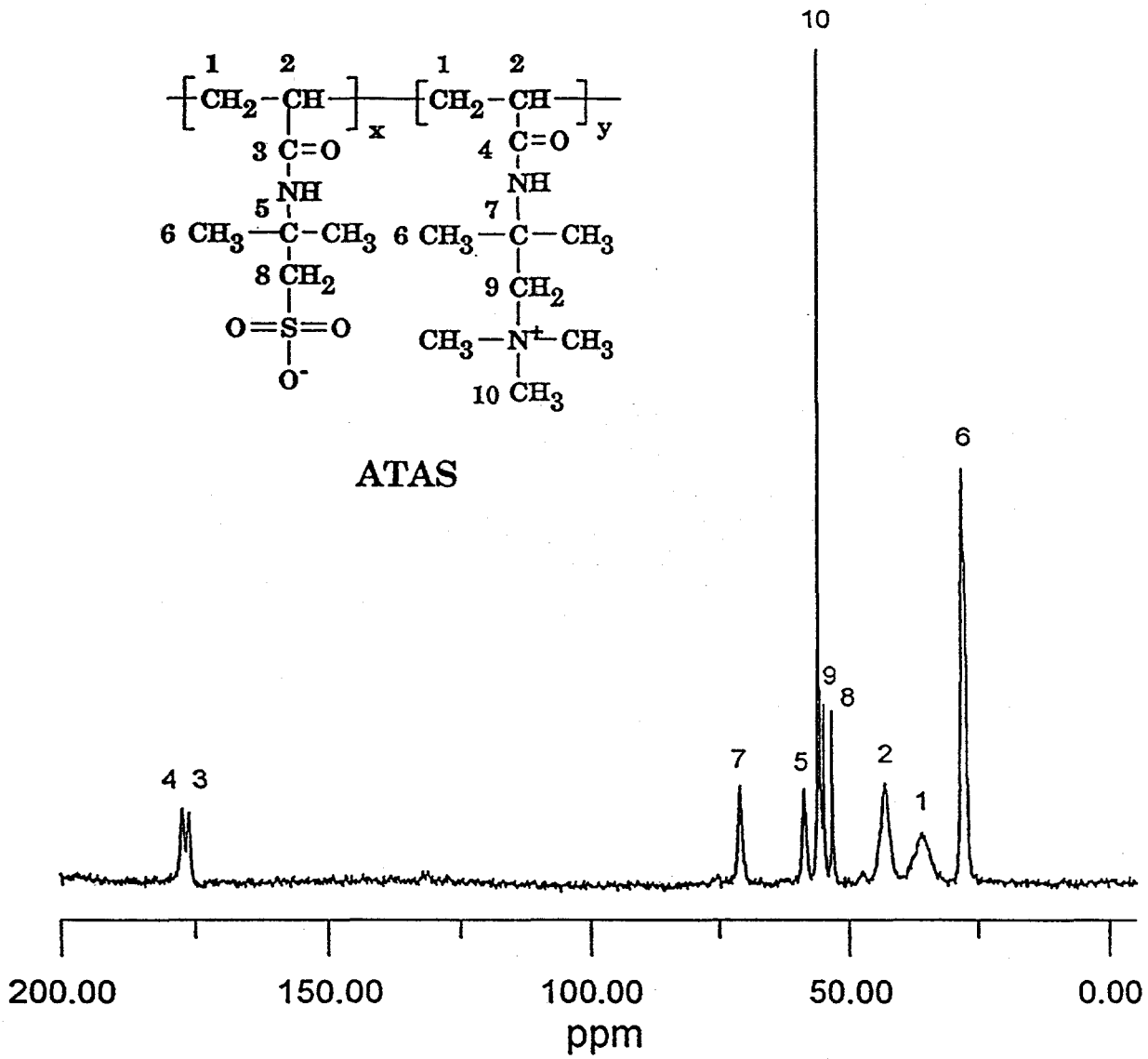

Figure 9-5. DPMAS spectrum of ATAS-50. Assignment of the spectrum is shown along with the structure of the polymer.

CHAPTER TEN: USE OF FACTORIAL EXPERIMENTAL DESIGN IN STATIC AND DYNAMIC LIGHT SCATTERING CHARACTERIZATION OF WATER SOLUBLE POLYMERS

Synopsis

When characterizing solutions of random coil polymers by static light scattering (SLS) or dynamic light scattering (DLS), linear regression is used to fit experimental data to theoretical relationships. These relationships are expressed as polynomial equations which contain two independent variables, sample concentration and scattering angle, and a response or dependent variable which is related to radiation intensities (SLS) or intensity fluctuations (DLS). The coefficients of the terms in the polynomial are used to estimate parameters such as molecular weight and polymer coil radius of gyration. One major problem during data analysis involves deciding which polynomial model is appropriate for use with the data that inherently contains a high level of random noise that is produced by the presence of dust in the solutions. Dust is an especially troublesome problem when dealing with large polymers in aqueous solutions. Polynomial models having more terms than justified are unacceptable because the coefficients of these models are excessively corrupted by the noise. Thus conclusions from unjustified models can be erroneous. This paper discusses use of a factorial experimental design technique that obtains an acceptable model for fitting light scattering data containing high levels of random noise.

Introduction

Light scattering has been used extensively in the past to characterize high molecular weight, water soluble, polymers [1,2,3,4]. After dust-free dilute polymer solutions are obtained by filtration or centrifugation, collection of scattering data is very fast and can be automated. Light scattering has no upper molecular weight limit and can be used for both organic soluble as well as aqueous soluble macromolecules. Most modern instruments are capable of performing both static and dynamic light scattering experiments.

When analyzing information on polymer solutions from both static light scattering (SLS) and dynamic or quasielastic light scattering (DLS) experimentation, linear regression is used to fit data to theoretical relationships. These relationships are usually expressed as polynomial equations. These equations contain two independent variables, sample concentration and scattering angle, and a response or dependent variable related to radiation intensities, as is the case for SLS, or apparent translational diffusion coefficients for DLS. The coefficients of the polynomials can be related to macromolecular parameters such as molecular weight, coil radius of gyration, and solvent-polymer interaction. Thus, accurate calculation of the polynomial coefficients is essential for proper interpretation of the experimental data.

A major difficulty in data analysis involves determining which polynomial model is appropriate when dealing with real data that is inherently imprecise because it contains random experimental noise. The noise level can be especially high for aqueous polymer solutions that tend to attract and retain dust. Also as the average polymer size and / or molecular weight distribution increases, solution cleanup by filtration or centrification becomes limited because the polymer molecules in solution and dust particles approach the same size. Thus, the experimenter is forced to deal with the high

uncertainly always introduced into the scattering data by a large level of noise. Under these situations a statistical approach must be applied to define the appropriate polynomial model that can be used.

As the noise level increases, statistical arguments can be used to show that only lower degree polynomials can be justified unless very large quantities of data are taken or the level of confidence for estimating coefficients is lowered to unacceptable values. Usually confidence levels are set in the 90 to 95% range to diminish both Type I and Type II errors [5]. A Type I error is one which rejects a model when it should be accepted and a Type II error is one which accepts a model when it should be rejected. Models having more terms than justified by the data are corrupted because they are fitting excess noise into the model. In this case, the model will lead the experimenter to erroneous conclusions.

This paper discusses the analysis of light scattering data by using a two variable, four level, factorial experimental design technique that employs the advantages of orthogonal polynomials. Surface analysis of the polynomial model which was justified by the experimental design will also be done using a contour plotting technique originally suggested by Zimm [6].

Light Scattering Test Model

In the case of light scattering, a good model for the experiment is a polynomial equation of the form

$$R=B_0+B_1X+B_2X^2+B_3XY+B_4Y+B_5Y^2 \qquad (1)$$

In Equation 1, R is the measured response and is dependent upon the independent variables X and Y which are set by the experimenter. Note that this polynomial is second order with respect to both independent variables and also has a term which accounts for possible interaction between the two variables. Thus, the surface described by Equation 1 can be curved. The B parameters are the coefficients which are to be estimated by fitting Equation 1 to the experimental data obtained from a set of test conditions. In light scattering, X is the square of the sin of half the scattering angle, θ, and Y is the polymer concentration, C, in the solution scattering the radiation.

$$X=\sin^2(\theta/2) \qquad (2) \qquad Y=C \qquad (3)$$

The response variable, R, measured at each test condition, depends upon the type of scattering experiment. For SLS

$$R=\frac{KC}{R_\theta} \qquad (4)$$

where K is an optical constant and R_θ is the Rayleigh ratio which is a measure of the intensity of the scattered radiation at angle θ. For DLS, R is the apparent translational diffusion coefficient, D_{app}, measured at the test condition. It is determined from a digital autocorrelation of the scattered radiation intensity variation that is produced by polymer center of mass motion.

$$R = D_{app} \qquad (5)$$

The test model proposed for light scattering is consistent with theoretical expectations for linear macromolecules that behave as random coils in solution. However, some terms in the test model may not be justified depending upon the polymer-solvent system under study and the instrument's capabilities. Indeed in some unusual cases, such as use of abnormally high solution concentrations or high scattering angles, the test model may need additional higher order terms. However, in most light scattering experiments using dilute solutions, the proposed polynomial test model should be adequate. After regression, all B coefficients not justified in the test model will be set to zero. In most cases, a simpler model, having fewer terms, will evolve after fitting the test model to the scattering data. Fitting of the test model by linear regression of data obtained from an orthogonal factorial test design is an efficient mathematical technique to estimate the values of all coefficients in the test model.

Orthogonal Factorial Test Design

When using light scattering to characterize a polymer, it is convenient to measure responses using four sample concentrations. At each sample concentration four scattering angles are used. Thus 16 test conditions are established when characterizing a polymer solution by light scattering.

The scattering can usually be conducted such that both sample concentrations and angles of measurement are equally spaced so that a factorial experimental design can be performed [7]. Independent variables can then be scaled or transformed into a coded space. For example, if X and Y are varied by spacings $2\Delta X$ and $2\Delta Y$, respectively, such that four levels exist for each variable, then the coded space variables, x and y, can be defined by Equations 6 and 7. Each coded independent variable will have four values, -3, -1, 1, and 3, which represent the four test condition levels, low, middle low, middle high, and high, respectively.

$$x = \frac{X - \bar{X}}{\Delta X} \qquad (6) \qquad y = \frac{Y - \bar{Y}}{\Delta Y} \qquad (7)$$

In the equations above $\bar{X}$ and $\bar{Y}$ are the averages of the four X and four Y values, respectively.

We can now write the following coded space test model for each of the 16 test conditions.

$$R_l = b_0 + b_1 x_l + b_2 x_l^2 + b_3 x_l y_l + b_4 y_l + b_5 y_l^2 \qquad (8)$$

We can center Equation 8 by subtracting the average of all test condition responses, $\bar{R} = b_0 + 5b_2 + 5b_5$. This gives

$$R_l - \bar{R} = b_1 x_l + b_2 (x_l^2 - 5) + b_3 x_l y_l + b_4 y_l + b_5 (y_l^2 - 5) \qquad (9)$$

We can use Equation 9 to write 16 equations that describe the 16 test conditions. These equations can then be arranged into a 4^2 factorial design (two independent variables each having four levels) to form a set of orthogonal polynomial equations. Table 10-I shows how the test conditions should be arranged to obtain a set of equations having orthogonal properties. Linear regression can then be performed on this set of equations to estimate the values of the coded coefficients in the scaled and centered test model, Equation 9.

Linear Regression in Coded Space

Matrix algebra can be used on the set of orthogonal equations formed by Equation 9 to find the vector $\underline{b}$ which has the estimated values of coded space coefficients b_1 through b_5. Coefficient b_0 can be found by recalling that $b_0 = \bar{R} - 5(b_2 + b_5)$. The matrix operation to find the vector $\underline{b}$ is given by

$$\underline{b} = (\underline{\underline{M}}^T \underline{\underline{M}})^{-1} \underline{\underline{M}}^T (\underline{R} - \bar{R}) \qquad (10)$$

where $\underline{R}$ is the response vector, $\underline{\underline{M}}$ is the matrix of coded test conditions, $\underline{\underline{M}}^T$ is the transpose of $\underline{\underline{M}}$ and $(\underline{\underline{M}}^T \underline{\underline{M}})^{-1}$ is the inverse of the product of $\underline{\underline{M}}^T$ and $\underline{\underline{M}}$. The matrix $\underline{\underline{M}}$ is shown in Table II. Each of the rows of the matrix $\underline{\underline{M}}$ describes one of the 16 test conditions. Each column of a row, starting with the second column to the left, gives values of x , $(x^2 - 5)$, x y, y , and $(y^2 - 5)$ for that test condition.

Confidence Interval for Coded Space Test Model Coefficients

The variance of the six coefficients in the vector $\underline{b}$ can be determined if the experimental standard error associated with the test conditions, s_e , can be estimated. Replications of a test condition or conditions can be used to estimate s_e. If g test conditions are truly replicated, then the variance of each set of z measurements at each test condition, v , having z -1 degrees of freedom, can be pooled to find an estimate of s_e by the following relationship [8].

$$s_e^2 = \frac{\sum_{i=1}^{g} (v_i)(z_i - 1)}{\sum_{i=1}^{g} (z_i - 1)} \qquad (11)$$

The elements on the diagonal of the variance-covariance matrix, $\underline{\underline{V}}$, contain the variances for the coefficients of vector $\underline{b}$. This matrix can be evaluated by the following operation

$$\underline{\underline{V}} = (\underline{\underline{M}}^T \underline{\underline{M}})^{-1} s_e^2 \qquad (12)$$

For example, the variances of the coefficients b_1 and b_2 , which are designated v_1 and v_2, are matrix elements $\underline{\underline{V}}_{1,1}$ and $\underline{\underline{V}}_{2,2}$, respectively. Because of the nature of an orthogonal experimental design, the covariance terms (elements not on the diagonal) in the matrix $\underline{\underline{V}}$ will be zero. No variance exists

due to interactions between coefficients. Thus the estimated standard error of each coefficient, s_j, where j varies from 1 to 5, is the square root of its variance found in matrix $\underline{V}$. However, because b_0 is calculated from the values of b_2 and b_5, its variance, v_0, must be calculated as $v_0 = 25 v_2 + 25 v_5 + \underline{\underline{V_{0,0}}}$.

A Student "t" distribution can now be used to make confidence limits on each coefficient. The $(1-\alpha)$ confidence limits for each of the six coefficients are given by $(b_j \pm t_{\alpha/2}\, s_j)$. A good value to use for the significance, α, is 0.10 (90% confidence). The tabulated value for $t_{0.05}$ at 10 degrees of freedom (16 test conditions less 6 fitted coefficients gives 10 degrees of freedom) is 1.81.

If the confidence limit for a coefficient overlaps with zero, that coefficient cannot be justified and its value can be set to zero. Thus this "t" test eliminates unjustified terms in the coded test model and prevents overfitting of the data to a model having too many parameters. If b_2 or b_5 is eliminated (set to zero) by the "t" test, then the value for b_0 and its variance, v_0, should be recalculated. Recall that $b_0 = \overline{R} - 5(b_2 + b_5)$ and $v_0 = 25 v_2 + 25 v_5 + \underline{\underline{V_{0,0}}}$.

Adjusted Correlation Coefficient

After the "t" test, a measure of how good the coded model fits the experimental data can be made by calculating the adjusted correlation coefficient, r [9]. As the fit improves, the value of r will approach one. If $\underline{R}$ is the response vector containing m values (m = 16) and having an average of $\overline{R}$, then

$$r = \sqrt{\frac{(\underline{b}^T \underline{\underline{M}}^T \underline{R} - m\overline{R}^2)}{(\underline{R}^T \underline{R} - m\overline{R}^2)}} \qquad (13)$$

Coefficients of the Real Space Test Model

After the values of the coefficients in the coded test model have been determined, then the coefficients for the real space test model can be calculated from the following relationships.

$$B_0 = b_0 - \frac{b_1 \overline{X}}{\Delta X} + \frac{b_2 \overline{X}^2}{\Delta X^2} + \frac{b_3 \overline{X}\,\overline{Y}}{\Delta X \Delta Y} - \frac{b_4 \overline{Y}}{\Delta Y} + \frac{b_5 \overline{Y}^2}{\Delta Y^2} \qquad (14)$$

$$B_1 = \frac{b_1}{\Delta X} - \frac{2 b_2 \overline{X}}{\Delta X^2} - \frac{b_3 \overline{Y}}{\Delta X \Delta Y} \qquad (15)$$

$$B_2 = \frac{b_2}{\Delta X^2} \qquad (16)$$

$$B_3 = \frac{b_3}{\Delta X \Delta Y} \qquad (17)$$

$$B_4 = \frac{b_4}{\Delta Y} - \frac{2 b_5 \overline{Y}}{\Delta Y^2} - \frac{b_3 \overline{X}}{\Delta X \Delta Y} \qquad (18)$$

After substitution of the values for coefficients B_0 through B_5, Equation 1 can be evaluated using a surface analysis technique originally developed by Zimm.

$$B_5 = \frac{b_5}{\Delta Y^2} \qquad (19)$$

Standard Error of Real Space Test Model Coefficients

The variance, $v_{u,}$ of a dependent variable, u, which is a known function of m independent variables, w_1, w_2,....,w_m, can be estimated from the variance of the independent variables v_{wi}, and the known function, f. If $u = f(w_1, w_2, ...w_m)$ then the variance of u is given by [15]

$$v_u = \sum_{i=1}^{m} \left(\frac{f}{w_i} \right)^2 v_{w_i} \qquad (20)$$

The standard error of u is the square root of its variance, v_u.

We can use the above relationship to find the variances of the coefficients of the real space model, which are calculated from Equations 14 through 19, from the variances of the coded space model coefficients, v_j. Equations 14 through 19 are the functions from which the partial derivatives of Equation 20 can be determined. Recall that the variances of the coded space coefficients were determined from Equation 12. If some of the coded test model coefficients are set to zero by the "t" test, then the variances of these coefficients should also be set to zero. If b_2 and/or b_5 were set to zero, then the values of b_0 and its variance, v_0, should be recalculated. Thereafter, the standard error of each real space model coefficient, S_j, can be found using Equation 20.

$$S_0 = \sqrt{v_0 + \frac{\overline{X}^2 v_1}{\Delta X^2} + \frac{\overline{X}^4 v_2}{\Delta X^4} + \frac{\overline{X}^2 \overline{Y}^2 v_3}{\Delta X^2 \Delta Y^2} + \frac{\overline{Y}^2 v_4}{\Delta Y^2} + \frac{\overline{Y}^4 v_5}{\Delta Y^4}} \qquad (21)$$

$$S_1 = \sqrt{\frac{v_1}{\Delta X^2} + \frac{4\overline{X}^2 v_2}{\Delta X^4} + \frac{\overline{Y}^2 v_3}{\Delta X^2 \Delta Y^2}} \qquad (22)$$

$$S_2 = \sqrt{\frac{v_2}{\Delta X^4}} \qquad (23) \qquad S_3 = \sqrt{\frac{v_3}{\Delta X^2 \Delta Y^2}} \qquad (24)$$

$$S_4 = \sqrt{\frac{v_4}{\Delta Y^2} + \frac{4\overline{Y}^2 v_5}{\Delta Y^4} + \frac{\overline{X}^2 v_3}{\Delta X^2 \Delta Y^2}} \qquad (25) \qquad S_5 = \sqrt{\frac{v_5}{\Delta Y^4}} \qquad (26)$$

Surface Analysis of the Model Equation

Using Zimm's technique, experimental measurements of scattering response, KC/R_θ for SLS or D_{app} for DLS, are plotted as the ordinate verses a compound abscissa, $\sin^2(\theta/2) + kC$. Use of the compound abscissa forces the points on the plot to be displaced from each other. This effect is due to the spacing constant k. The value of k is arbitrarily selected to provide adequate distance between the experimental data points. The set of points displays the complete response grid of the scattering experiment. When a 4^2 factorial design is used, 16 data points will form the surface response grid.

In the original Zimm technique, this grid was used to form lines of constant angles and lines of constant concentration. The lines of constant concentration were linearly extrapolated to give a set of points that had zero concentration. Also the lines of constant angles were linearly extrapolated to give a set of points that have zero angle. The straight line fitted to the zero concentration points and the straight line fitted to the zero angle points should intercept the ordinate at the same position. This common intercept is the reciprocal of the molecular weight for a SLS experiment or is the true translational diffusional coefficient for a DLS experiment. The slopes of the two straight lines can be used to find other polymer parameters.

Unfortunately linear extrapolation does not work when the data points on the Zimm plot form curves instead of straight lines. This is the usual situation when analyzing high molecular weight water soluble polymers. In this situation, the model equation developed from the 4^2 factorial design and justified by the "t" test can be used to plot the four constant concentration curves, the four constant angle curves, the zero concentration curve and the zero angle curve associated with the experimental data in the Zimm plot. Both curves will intercept the ordinate at the same position and this intersection point will be equal to the model equation coefficient B_0.

The 16 intersections of the constant concentration curves with the constant angle curves are the model equation fit points that correspond to the 16 data points on the plot. Thus, a visual understanding of the model equation fit to the experimental data can be realized by noting the placement of data points relative to curve intersections. If an experimental data point exactly corresponds to an intersection of the two curves made at the angle and concentration of that data point, then a perfect fit between the model and data exists at that test condition. The greater the deviation of a data point from its corresponding intersection point, the more poorly the model fits that test condition.

Use of the above factorial design experimentation and plotting procedures can best be demonstrated by giving three examples. In Example 1, a static light experiment was performed on a water soluble copolymer. In Example 2, the same copolymer was characterized by dynamic light scattering. Example 3 is Example 1 redone without justifying the model.

Experimental

The high molecular weight random copolymer employed in the scattering experiments was supplied by C. L. McCormick and was synthesized from acrylamide (AM) and 3-acrylamido-3-methylbutanoic acid (AMBA) monomers in the ratio of 95 to 5 as described in previous publications [10,11]. The aqueous solvent used to make the polymer solutions contained 0.514 M NaCl and had a refractive index, n, of 1.338 at 25 ^{0}C with radiation having a wavelength, λ_o, of 6328 □.

The solvent was filtered using a 0.02 micron Anotop 25 inorganic membrane manufactured by Whatman. The solvent viscosity, η_0, was 0.934 cp. Polymer solutions were made by gentle mixing for a minimum of four days. Immediately before SLS analysis the solutions were clarified by a syringe filter using a 1.0 micron Puradisc 25AS polysulfone membrane manufactured by Whatman.

Four solutions were made that had polymer concentrations of 0.04, 0.08, 0.12, and 0.16 g / liter. Light scattering experiments were performed on these solutions at 25 °C and at scattering angles of 32.3, 65, 90 and 115 degrees using a BI-2030AT goniometer equipped with a BI-DS photomultiplier and digital correlator manufactured by Brookhaven Instruments Corp. of Holtsville, NY. Duplicate measurements of intensity response, as KC/R_θ, were made for each of the 16 test conditions in SLS. Triplicate measurements of the apparent translational diffusion coefficient, D_{app}, were made for each of the 16 test conditions in DLS. The optical constant, K, used in SLS was calculated using a dn/dC value of 0.1559 ml / g for the polymer-solvent system under study. The change in the refractive index with respect to solution concentration, dn/dC, was measured using a KMX-16 differential refractometer manufactured by Chromatix Inc. of Sunnyvale, CA.

All calculations were performed on a 80486 personal computer using the program Mathcad 5.0+ manufactured by Mathsoft Inc. of Cambridge, Massachusetts. The Zimm plots were also generated with this software using a spacing constant, k, of 5000 ml / g.

All solution and 0.514 M NaCl aqueous solvent viscosity measurements were made at 25°C using a Contraves L30 rheometer. For each fluid, viscosities were determined at 3.2, 8.1, 14.9 and 27.5 sec^{-1} shear rates and then extrapolated to find the "zero" shear fluid viscosity. The "zero" shear viscosities of four copolymer solutions containing 0.125, 0.100, 0.075 and 0.050 g/liter were then used to establish the copolymer intrinsic viscosity.

Example 1 (Static Light Scattering)

The theoretical relationship between the properties of a polymer sample in solution and its light scattering characteristics is expressed by the Debye relationship [12] given by Equation 27.

$$\frac{KC}{R_\theta} = \frac{1}{M_w} + \frac{16\pi^2 n^2 R_g^2 \sin^2(\frac{\theta}{2})}{3M_w\lambda_o^2} - \frac{64\pi^4 n^4 R_g^4 \sin^4(\frac{\theta}{2})}{3M_w\lambda_o^4} + 2A_2C + 3A_3C^2 + other\ terms \qquad (27)$$

In Equation 27, M_w and R_g are the polymer weight average molecular weight and the "z" average polymer coil radius of gyration, respectively. The second and third viral coefficients, A_2 and A_3 are related to solvent-polymer interactions. Note that Equation 27 can be expressed as test model Equation 1 when we let the variables

$$R = \frac{KC}{R_\theta} \quad (28) \qquad X = \sin^2\left(\frac{\theta}{2}\right) \quad (29) \qquad Y = C \quad (30)$$

and let the B coefficients be defined as

$$B_0 = \frac{1}{M_w} \quad (31) \qquad B_1 = \frac{16\pi^2 n^2 R_g^2}{3M_w\lambda_o^2} \quad (32) \qquad B_2 = -\frac{64\pi^4 n^4 R_g^4}{3M_w\lambda_o^4} \quad (33)$$

$$B_3 = \textit{interaction coefficient} \quad (34) \qquad B_4 = 2A_2 \quad (35) \qquad B_5 = 3A_3 \quad (36)$$

Note that we have defined the "other terms" in Equation 27 as a single expression equal to the product of an interaction coefficient, B_3, and variables X and Y.

Values for X are 0.077, 0.289, 0.500, and 0.711. Thus, $2\Delta X = 0.211$ and $\bar{X} = 0.394$. Recall values for Y are 0.04, 0.08, 0.12, and 0.16 g / liter. Thus, $2\Delta Y = 0.04$ g / liter and $\bar{Y} = 0.10$ g / liter. Because of the equal separation of the values used for independent variables X and Y, we can use a 4^2 factorial design and then do a regression analysis to find estimates of the model coefficients. Thereafter we can use a "t" test to justify each coefficient of the model.

Scattering experiments were performed according to the design shown by Table 10-I. The responses, KC/R_θ in moles per gram, to the test conditions are shown in Table 10-III. Two measurements were taken at each condition. The average at each test condition of the two measurements was used to form the response vector, $\underline{R}$, and is shown in the last column of Table III. Because two response measurements were taken at each test condition, Equation 11 could be used to estimate the average experimental error, s_e, associated with a response to a test condition. The s_e value obtained was 5.15×10^{-8} mole per gram. The average of all responses, $\bar{R}$, was 6.92×10^{-7} mole per gram. Thus the standard experimental error is about 7% of the average response.

The coded and scaled test model, Equation 9, can now be solved for the b coefficients using Equation 10. The results, vector $\underline{b}$, are shown in Table IV along with the upper and lower 90% confidence limits. The limits were calculated by solving for the matrix $\underline{\underline{V}}$ and then calculating the limits $(b_j \pm t_{0.05} s_j)$ after finding the s_j values from the square root of the $\underline{\underline{V}}$ diagonal elements.

Inspection of Table IV shows that coefficients b_3 and b_5 are not significantly different from zero and thus their values and variances will be set to zero in subsequent calculations. Because b_5 was set to zero, b_0 and s_0 were recalculated as 7.21×10^{-7} and 2.06×10^{-8}, respectively. Equations 14 through 19 can now be used to find the test model B coefficients. Equations 31, 32 and 34 can be used to find the polymer parameters M_w, R_g and A_2.

Equation 20 can be used to find the standard error of the polymer parameters from the functions described by Equations 31, 32 and 34. If S_{MW}, S_{Rg}, and S_{A2} are the standard error of the molecular weight, radius of gyration and second viral coefficient, respectively, then

$$S_{MW} = \frac{S_0}{B_0^2} \qquad (37) \qquad S_{A2} = \frac{S_4}{2} \qquad (38)$$

$$S_{Rg} = \frac{\lambda_o}{8\pi n}\sqrt{3B_0B_1S_{MW}^2 + \frac{3S_1^2}{B_0B_1}} \qquad (39)$$

The B coefficients, the polymer parameters and all standard errors are listed in Table V.

Figure 1, a Zimm plot, shows the average response for each test condition as "X" symbols which are superimposed onto the curves constructed from the test model. Curves of constant angle are shown solid, curves of constant concentration are shown dashed, and the extrapolated zero concentration and zero angle curves are both shown doted. The plot shows that the fit of the model equation to the experimental data is adequate. The adjusted correlation coefficient, r, calculated from Equation 13, has a value of 0.997 which also indicates that the model gives a good fit to the data.

Example 2 (Dynamic Light Scattering)

The apparent translational diffusional coefficient, D_{app}, obtained by DLS is related to the true diffusional coefficient, D_{true}, by the relationship

$$D_{app} = D_{true} + \alpha \sin^2\left(\frac{\theta}{2}\right) + \beta \sin^4\left(\frac{\theta}{2}\right) + \chi C \sin^2(\theta/2) + \delta C + \xi C^2 \qquad (40)$$

The coefficients, $D_{true}, \alpha, \beta, \chi, \delta, \xi$, are related to polymer-solvent properties. The parameters δ and ξ are usually referred to as the second and third diffusional viral coefficients. They are related to the interactions between solvent and polymer. The parameter D_{true} is the diffusional coefficient in the limit of zero polymer concentration and zero scattering angle and is related to the hydrodynamic polymer coil radius, R_h, by the Stokes-Einstein equation.

$$R_h = \frac{k_B T}{6\pi \eta_0 D_{true}} \qquad (41)$$

In Equation 41, k_B is the Boltzman constant, T is the absolute temperature, and η_0 is the solvent viscosity. For random coil polymers in solution, the coefficients α and β are expected to be related to D_{true} and R_g by the following relationships [13]

$$\alpha = \frac{16\pi^2 n^2 D_{true} R_g^2}{5\lambda_0^2} \qquad (42) \qquad \beta = \frac{-128\pi^4 n^4 D_{true} R_g^4}{5\lambda_0^4} \qquad (43)$$

The coefficients δ and ξ are related to D_{true} and the polymer intrinsic viscosity, $[\eta]$.

$$\delta = \kappa D_{true}[\eta] \qquad (44) \qquad \xi = \upsilon D_{true}[\eta]^2 \qquad (45)$$

The proportionality constants, κ and υ, are expected to have values of 1.56 and -6.83, respectively [14]. Jamieson [1] has suggested that κ may have a lower value of 0.58.

Equation 40 can be expressed as test model Equation 1 when we let the variables be defined as

$$R = D_{app} \qquad (46) \qquad X = \sin^2\left(\frac{\theta}{2}\right) \qquad (47) \qquad Y = C \qquad (48)$$

and let the B coefficients be defined as

$$B_0 = D_{true} \qquad (49) \qquad B_1 = \alpha \qquad (50) \qquad B_2 = \beta \qquad (51)$$

$$B_3 = \chi \qquad (52) \qquad B_4 = \delta \qquad (53) \qquad B_5 = \xi \qquad (54)$$

Values for X, $2\Delta X$, $\overline{X}$, Y, $2\Delta Y$, and $\overline{Y}$ are the same as in the example for SLS and thus a 4^2 factorial design and "t" test can be applied as in Example 1. The DLS responses, D_{app} values in cm^2 / sec, are shown in Table VI. Three measurements were taken at each of the 16 test conditions. The average at each test condition of the three measurements was used to form the response vector, $\underline{R}$, and is shown in the last column of Table VI. As in the SLS example, an experimental error, s_e, was calculated to be 1.47×10^{-9} cm^2 / sec. The average response, $\overline{R}$, was 3.13×10^{-8} cm^2 / sec. Thus the standard experimental error is about 5% of the average response.

The coded and scaled test model, Equation 9, can now be solved for the b coefficients using Equation 10. The results, vector $\underline{b}$, are shown in Table VII along with the upper and lower 90% confidence limits calculated by solving for the matrix $\underline{\underline{V}}$ and then calculating the limits $b_j \pm t_{0.05} s_j$ after finding the s_j values from the $\underline{\underline{V}}$ diagonal elements.

Inspection of Table VII shows that coefficients b_3, b_4 and b_5 are not significantly different from zero and thus their values and variances will be set to zero in subsequent calculations. Because b_5 was set to zero, b_0 and s_0 were recalculated as 3.39×10^{-8} and 5.86×10^{-10}, respectively. Equations 14 through 19 can now be used to find the test model B coefficients. Next Equations 49 and 41 can be used to find D_{true} and the hydrodynamic polymer coil radius, R_h. The polymer coil

radius of gyration, R_g, can be calculated from Equation 42.

As in Example 1, Equation 20 can be used to find the standard error of the polymer parameters from the functions described by Equations 41, 42 and 49. If S_D, S_{RG}, and S_{Rh} are the standard error of the true diffusion coefficient, dynamic radius of gyration and hydrodynamic radius, respectively, then

$$S_D = S_0 \qquad (54) \qquad S_{Rh} = \left(\frac{k_B T}{6 \pi \eta_o} \right) \frac{S_0}{B_0^2} \qquad (55)$$

The B coefficients, the polymer parameters and all standard errors are listed in Table VIII.

$$S_{RG} = \frac{\lambda_o}{8 \pi n} \sqrt{\frac{5 S_1^2}{B_0 B_1} + \frac{5 B_1 S_0^2}{B_0^3}} \qquad (56)$$

Figure 2 is the Zimm plot for the DLS example. The fit of experimental data is shown to be adequate. The adjusted correlation coefficient, r, calculated from Equation 13, has a value of 0.994 which also indicates that the model gives a good fit to the data.

Example 3 (Sls with Unjustified Model)

If data analysis is done without performing a "t" test to remove unjustified terms in the model, results can be misleading. This is demonstrated by Example 3 which is a reanalysis of the SLS data of Example 2 without using model justification. In this example, all terms of the coded model are retained after regression. The Zimm plot, Figure 3, shows an excellent fit of the unjustified model to the data. Also the adjusted correlation coefficient has a value of 0.998 which indicates a better fit than the model of Example 1. However, the molecular parameters calculated for Example 3 (Mw = 3.1 x 10^7 g / mole , Rg = 4700 , and A2 = 9.1 x 10^{-4} ml mole / g^2) are significantly larger than determined in Example 1 (Mw = 1.2 x 10^7 g / mole , Rg = 2900 , and A2 = 2.7 x 10^{-4} ml mole / g^2). These molecular parameters are too large to be consistent with the intrinsic viscosity measured for this polymer - solvent system, 17.0 dl / g. Thus, without model justification erroneous conclusions can be obtained when analyzing light scattering data.

Conclusions

The data analysis technique detailed above which employs a factorial experimental design can be used to establish a light scattering model which is statistically justified. Calculations are straightforward and can be easily programmed. The model can thereafter be used to estimate macromolecular parameters such as polymer coil size, viral and diffusional coefficients, and molecular weight. In addition, confidence intervals can be found for the polymer parameters estimated from the model.

REFERENCES

1. Patterson, P.M. and A. M. Jamieson, *Macromolecules, 18,* 266, 1985.

2. Skouri, M., J. P. Munch, S. J. Candau, S. Neyret, and F. Candau, *Macromolecules, 27,* 69, 1994.

3. Zhou, Z and B. Chu, *Macromolecules, 24,* 2025, 1994.

4. Borochov, N. and H. Eisenburg, *Macromolecules, 27,* 1440, 1994.

5. Wine, R. L., *Statistics for Scientists and Engineers*, Prentice-Hall, N.J., 215, 1964.

6. Zimm, B. H., *J. Chem. Phys., 16*, 1099, 1948.

7. Hicks, C. R., *Fundamental Concepts in the Design of Experiments*, Holt, Rinehart and Winston, N.Y., 95, 1964.

8. Box, G. P., W. G. Hunter, J. S. Hunter, *Statistics for Experiments,* John Wiley & Sons, N.Y., 319, 1978.

9. Draper, N. R. and H. Smith, *Applied Regression Analysis,* 2nd Edition, John Wiley & Sons, N.Y., 91, 1981.

10. McCormick, C. L. and K. P. Blackmon, *J. Poly. Sci., Poly. Chem., A24,* 2635, 1986.

11. McCormick, C. L., K. P. Blackmon, and D. L. Elliott, *J. Poly. Sci., Poly. Chem, A24,* 2619, 1986.

12. Tanford, C., *Physical Chemistry of Macromolecules,* John Wiley & Sons, N.Y., 275, 1961.

13. Peitzsch, R. M., M. J. Burt, and W. F. Reed, *Macromolecules, 25,* 806, 1992.

14. Schmitz, K.S., *An Introduction to Light Scattering by Macromolecules,* Academic Press, Inc., N.Y., 181, 1990.

15. Mellor, J. W., *Higher Mathematics for Students of Chemistry & Physics,* Longman, Green & Co., London, 530, 1926.

TABLE 10-I
4^2 EXPERIMENTAL FACTORIAL DESIGN

Test Condition Number	Coded Level For Independent Variable x	Coded Level For Independent Variable y
1	-3	-3
2	-3	-1
3	-3	1
4	-3	3
5	-1	-3
6	-1	-1
7	-1	1
8	-1	3
9	1	-3
10	1	-1
11	1	1
12	1	3
13	3	-3
14	3	-1
15	3	1
16	3	3

TABLE 10-II
Matrix M

	x	$x^2 - 5$	xy	y	$y^2 - 5$
1	-3	4	9	-3	4
1	-3	4	3	-1	-4
1	-3	4	-3	1	-4
1	-3	4	9	3	4
1	-1	-4	3	-3	4
1	-1	-4	1	-1	-4
1	-1	-4	-1	1	-4
1	-1	-4	-3	3	4
1	1	-4	-3	-3	4
1	1	-4	-1	-1	-4
1	1	-4	1	1	-4
1	1	-4	3	3	4
1	3	4	-9	-3	4
1	3	4	-3	-1	-4
1	3	4	3	1	-4
1	3	4	9	3	4

TABLE 10-III
Example 1 (SLS) Responses

Test Condition	Measurement 1 mole / g x 10^7	Measurement 2 mole / g x 10^7	Average Response mole / g x 10^7
1	2.60	2.15	2.38
2	2.53	2.67	2.60
3	2.81	2.97	2.89
4	3.10	2.81	2.96
5	5.55	4.75	5.15
6	5.43	5.50	5.47
7	5.84	6.26	6.05
8	6.29	5.62	5.96
9	9.68	7.21	8.45
10	8.60	8.31	8.46
11	9.06	9.12	9.09
12	9.25	7.99	8.62
13	11.28	9.07	10.18
14	10.66	10.33	10.50
15	10.84	11.37	11.11
16	11.62	10.10	10.86

TABLE 10-IV
Example 1 (SLS) Coded Test Model Coefficents

Coefficient	Estimated Value*	Standard Error**	Confidence Limits	
			Upper	Lower
b_0	7.34×10^{-7}	2.61×10^{-8}	7.81×10^{-7}	6.87×10^{-7}
b_1	1.34×10^{-7}	5.76×10^{-9}	1.45×10^{-7}	1.24×10^{-7}
b_2	$- 5.90 \times 10^{-9}$	3.22×10^{-9}	-7.45×10^{-11}	-1.17×10^{-8}
b_3	1.63×10^{-11}	2.57×10^{-9}	4.68×10^{-9}	-4.64×10^{-9}
b_4	1.11×10^{-8}	5.76×10^{-9}	2.15×10^{-8}	6.51×10^{-10}
b_5	-2.52×10^{-9}	3.22×10^{-9}	3.30×10^{-9}	-8.35×10^{-9}

* $b_0 = \overline{R} - 5 (b_2 + b_5)$ ** $s_0 = \sqrt{25v_2 + 25v_5 + V_{\equiv}}$

TABLE 10-V
Example 1 (SLS) Test Model Coefficients and Polymer Parameters

Coefficient	Estimated Value	Standard Error	Polymer Parameter	Estimated Value	Standard Error
B_0	8.3×10^{-8}	6.3×10^{-8}	Molecular Weight, M_w	1.2×10^7 g / mole	0.9×10^7 g / mole
B_1	1.7×10^{-6}	2.4×10^{-7}	Radius of Gyration, R_g	2900 Å	1100Å
B_2	-5.3×10^{-7}	2.9×10^{-7}	---	---	---
B_3	0	---	---	---	---
B_4	5.5×10^{-4}	2.9×10^{-4}	Second Virial Coefficient, A_2	2.7×10^{-4} ml-mole / g^2	1.4×10^{-4} ml-mole / g^2
B_5	0	---	---	---	---

TABLE 10-VI
Example 2 (DLS) Responses

Test Condition	Measurement 1 cm^2 / sec x 10^8	Mesurement 2 cm^2 / sec x 10^8	Measurement 3 cm^2/ sec x 10^8	Average Response cm^2/ sec x 10^8
1	1.95	2.05	1.85	1.95
2	1.81	1.75	1.81	1.79
3	1.36	1.79	1.84	1.67
4	1.88	1.91	1.83	1.87
5	3.04	3.02	2.96	3.00
6	3.01	3.00	2.97	2.98
7	3.09	3.02	2.97	3.03
8	2.85	3.00	2.88	2.91
9	3.80	3.80	3.77	3.79
10	3.74	3.65	3.72	3.71
11	3.62	3.68	3.60	3.63
12	3.65	3.64	3.62	3.63
13	3.92	4.10	4.18	4.07
14	3.61	4.18	4.28	4.03
15	4.14	4.24	4.17	4.18
16	4.11	3.23	4.13	3.82

TABLE 10-VII
Example 2 (DLS) Coded Test Model

Coefficient	Value*	Standard Error**	Confidence Limits	
			Upper	Lower
b_o	3.38×10^{-8}	7.44×10^{-10}	3.52×10^{-8}	3.25×10^{-8}
b_1	3.66×10^{-9}	1.64×10^{-10}	3.96×10^{-9}	3.37×10^{-9}
b_2	-5.18×10^{-10}	9.16×10^{-11}	-3.52×10^{-10}	-6.83×10^{-10}
b_3	-2.49×10^{-11}	7.33×10^{-11}	1.08×10^{-10}	-1.58×10^{-10}
b_4	-2.15×10^{-10}	1.64×10^{-10}	8.18×10^{-11}	-5.11×10^{-10}
b_5	5.57×10^{-12}	9.16×10^{-11}	1.71×10^{-10}	-1.60×10^{-10}

* $b_0 = \overline{R} - 5(b_2 + b_5)$ **$s_0 = \sqrt{25v_2 + 25v_5 + V_{\equiv}}$

Table VIII
Example 2 (DLS) Test Model Coefficients and Polymer Parameters

Coefficient	Estimated Value	Standard Error	Polymer Parameter	Estimated Value	Standard Error
B_0	1.3×10^{-8}	1.5×10^{-9}	True Diffusional Coefficient, D_{true}	1.3×10^{-8} cm^2 / sec	1.5×10^{-9} cm^2 / sec
B_1	7.1×10^{-8}	6.7×10^{-9}	Radius of Gyration, R_g	2000 Å	150Å
B_2	-4.6×10^{-8}	8.2×10^{-9}	Hydrodynamic Radius , R_h	1800 Å	210Å
B_3	0	---	---	---	---
B_4	0	---	---	---	---
B_5	0	---	---	---	---

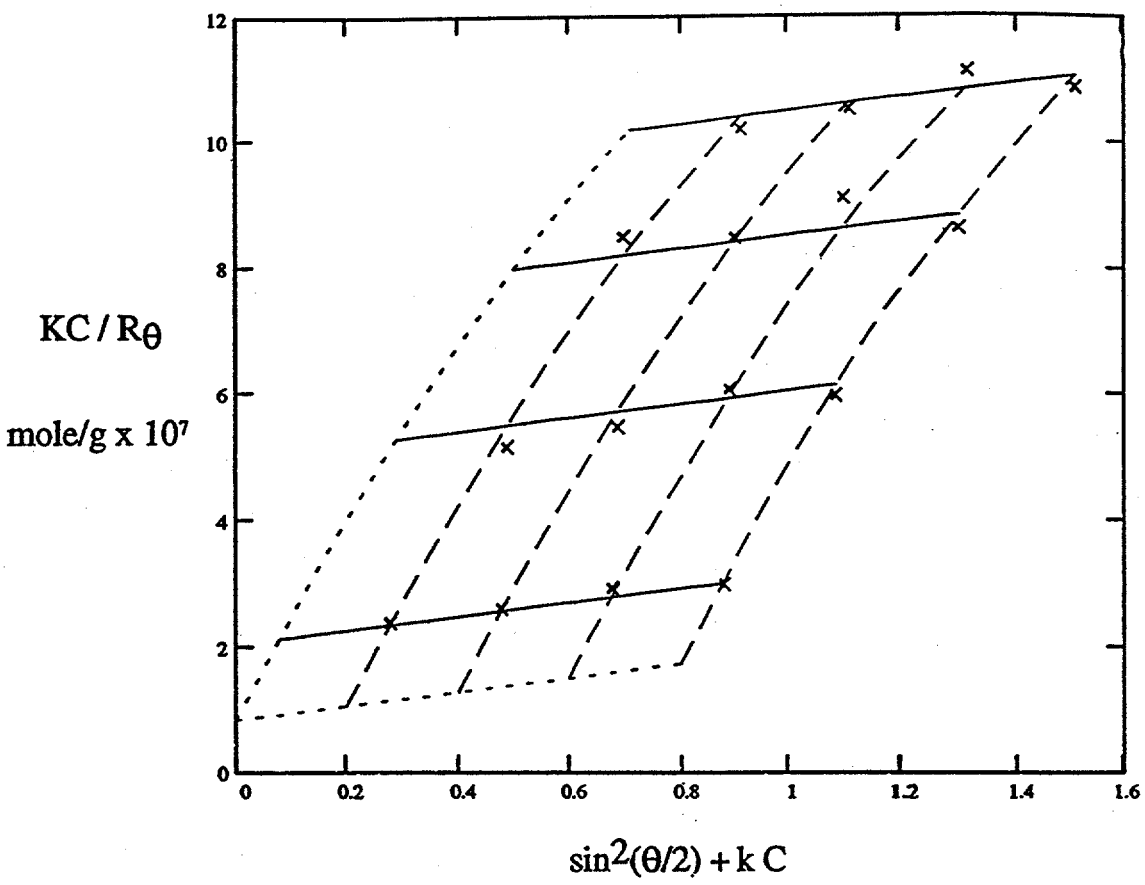

Figure 10-1: Zimm Plot for Example 1(SLS)

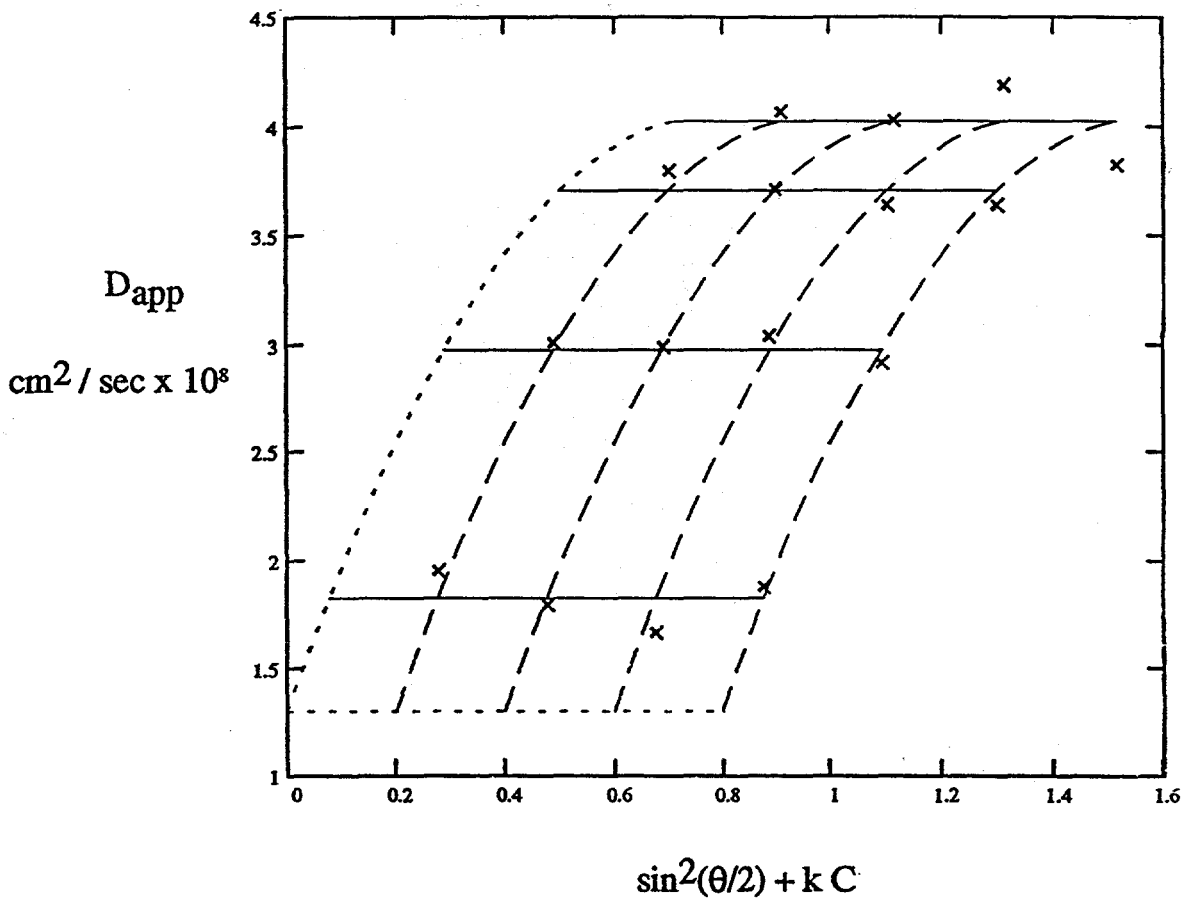

Figure 10-2: Zimm Plot for Example 2 (DLS)

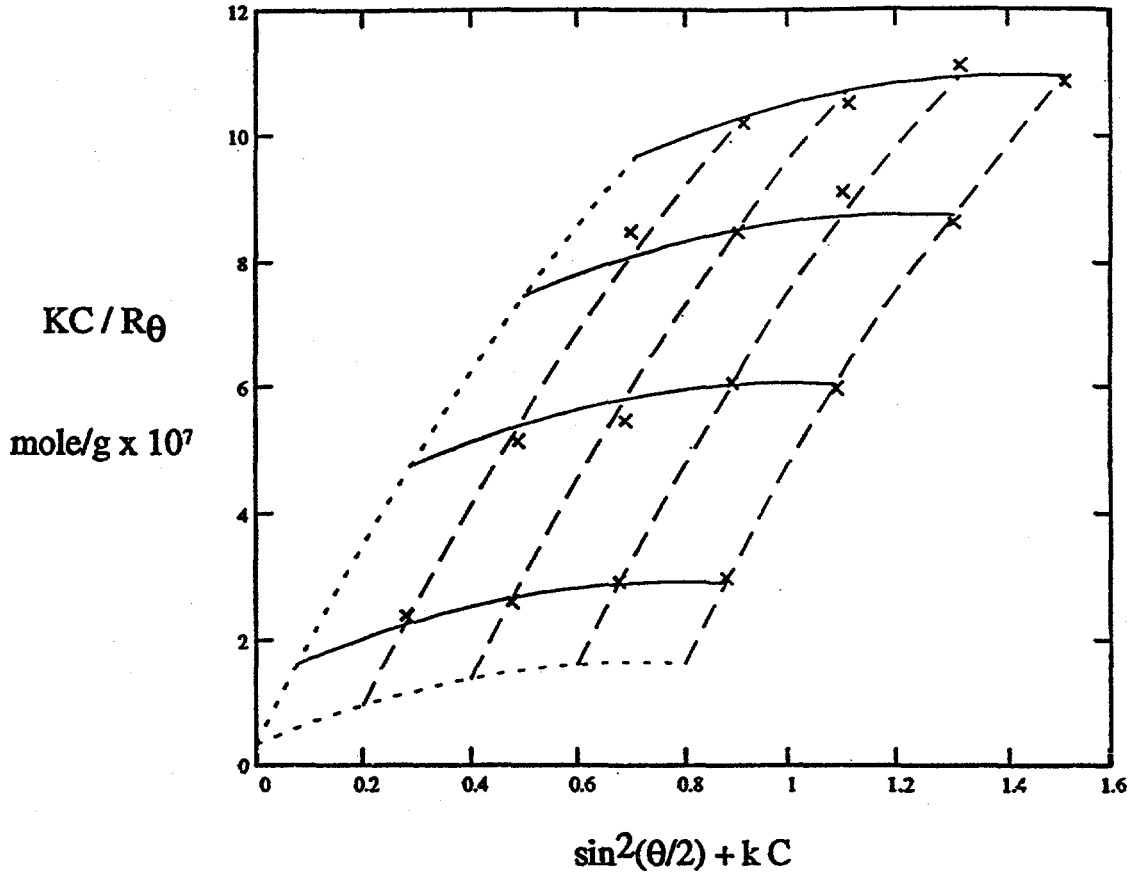

Figure 10-3: Zimm Plot for Example 3 (SLS)

CHAPTER ELEVEN : POROUS MEDIUM ELONGATIONAL RHEOMETER STUDIES OF NaAMB / AM COPOLYMER SOLUTIONS

Abstract

A porous media elongational rheometer was constructed in this laboratory [4]. It was used to compare the fluid flow properties of AM / NaAMB copolymer solutions and acrylamide homopolymer solutions in beds of solid spheres. The extensional flow properties of the polymer solutions in the porous medium were characterized by plotting Normalized Flow Resistance as a function of the Deborah number [5,6]. The Normalized Flow Resistance indicates the extent of polymer coil elongation during flow through the converging and diverging cavities of the porous medium. The Deborah number characterized the fluid extensional flow field in the porous media and was defined as the ratio of polymer coil response time to the extensional flow field process time. Plots of this type, which will be referred to as Durst plots, were constructed for all polymer types. Of all polymers examined using the Durst plotting technique, the AM / NaAMB 80 / 20 copolymer solutions had the largest resistance to extensional flow. This copolymer is an excellent candidate for use as an advanced EOR polymer.

Introduction

When using a polymer solution to flood an oil reservoir the displacing fluid should have a high resistance to flow within the porous medium. High flow resistance increases movement of residual oil to a producing well and thus enhances oil recovery. However, to be economical, the water soluble polymers used as displacing fluids must have a high resistance to flow when added in very small quantities to an aqueous solvent. Fluid resistance results from polymer coil molecular distortions and extensions during flow through the small and tortuous channels of the porous medium. Polymer solution behavior in complex porous media can be modeled using packed beds of solid spheres.

As polymer coils in solution pass through a bed of packed spheres of uniform diameter, d, they travel through a continuous and interconnected series of converging-diverging cavities. As the fluid travels through this geometry it will continually accelerate and then decelerate as it passes from cavity to cavity. As the fluid flow is increased, fluid acceleration and deceleration forces will compel the polymer coils to extend and then contract or recover from each extension. The number of coil extensions and recovery cycles is equal to the number of cavities passed through by the polymer.

Each coil extension-recovery cycle will convert some fluid kinetic energy into heat. This energy conversion created by the polymer coils extending and recovering will be sensed as a higher solution pressure drop across the bed, ΔP, as compared to the pressure drop of a solvent flowing through the bed at the same flow conditions or bed Reynolds Number, R_e. This fluid pressure increase is expressed as a Normalized Flow Resistance, ψ.

The Normalized Flow Resistance, ψ, is directly related to the amount of energy converted to heat by the polymer coils as they travel through the packed bed and are continually extended and contracted. Thus Durst Plots, which show the Normalized Flow Resistance versus Deborah number, show the efficiency with which polymer coils convert kinetic energy to heat as a function of flow conditions, porous media geometry, and polymer properties and concentration.

The Normalized Flow Resistance, ψ, measures solution flow resistance in a porous medum under conditions specified by the Reynolds and Deborah Numbers. It is calculated from the friction factor of the solution, f, and the friction factor of the solvent, f_s, measured at the same bed Reynolds number. The Deborah number, De, is the product of the polymer coil response time, τ, and the average fluid extension rate, ε, which depends upon average fluid velocity and the pore geometry. These dimensionless parameters are defined by the relationships given below.

$$D_e = \varepsilon \tau \tag{1}$$

$$\psi = \frac{f - f_s}{f_s [\eta] C} \tag{2}$$

$$Re \equiv \frac{v d \rho}{\eta_s (1 - \phi)} \tag{3}$$

$$\varepsilon = \frac{\sqrt{2}}{\phi} \frac{v}{d} \tag{4}$$

$$\tau = \frac{\eta_s [\eta] M}{RT} \tag{5}$$

$$f \equiv \frac{d \phi^3}{v^2 (1 - \phi) \rho} \frac{\Delta P}{\Delta l} \tag{6}$$

As shown in the above equations, the nature of the porous medium is specified by the diameter of the spherical particles, d, forming a bed having porosity, ϕ. The fluid flow resistance through the bed is measured by the pressure drop per unit length of bed, $\Delta P/\Delta \ell$. Flow conditions through the bed are defined by the average fluid velocity, v. This velocity is based on the cross sectional area of an empty bed. The fluid velocity within the pore channels within the bed would be the empty bed velocity divided by the bed porosity. Solution properties of shear viscosity, η_s, and density, ρ, are also used in the dimensionless groups. The coil response time, τ, can be estimated from the intrinsic viscosity of the polymer, $[\eta]$, its molecular weight, M, and the temperature, T.

Past experimental work has shown that as the Deborah Number approaches unity a maximum solution flow resistance develops and after that is maintained at higher Deborah Numbers [5]. The maximum in the Normalized Flow Resistance is expected to be only a function of polymer molecular weight, macromolecular structure and the concentration of polymer coils in solution.

Experimental

Polymers

The high molecular weight random copolymers used in this study were supplied by C. L. McCormick. They were synthesized from acrylamide (AM) and 3-acrylamido-3-methylbutanoic acid (AMBA) monomers in the ratio as described in previous publications [1,2]. Four copolymers in the solid form were supplied having AM/ NaAMB monomer ratios of 5/95, 10/90 (two samples of different molecular weights), and 20/80. One acrylamide homopolymer was also supplied. The aqueous solvent used to make all polymer solutions contained 0.514 M NaCl and had a viscosity of 0.934 cp at 25 ° C. Polymer solutions were made by gentle mixing of polymer and solvent for a minimum of four days.

Solutions of these copolymers were analyzed using static and dynamic light scattering characterization techniques [3] to find coil sizes, molecular weights and Viral coefficients. A low shear Contravis rheometer was used to estimate each solution intrinsic viscosity in the limit of zero shear rates. Table I lists polymer properties and the calculated dilute solution coil response times for each polymer.

Porous Media Rheometer

The porous media rheometer constructed for this study is shown in Figure 1. Pressurized nitrogen gas forces polymer solution or solvent out of a 1000 ml sample reservoir through one of two porous media flow cells. The fluid flow rate was controlled by adjusting the nitrogen gas pressure with a Victor 0 to 200 psi, single stage, pressure regulator. Both flow cells were 1 cm diameter cylinders having a 12 cm length. The cells were packed with uniform diameter solid glass spheres manufactured by Cataphote Inc. Cell # 1 contained 297 micron diameter glass spheres. Cell # 2 contained 149 micron diameter glass spheres. Both packed beds had a porosity, ϕ, of 0.367. Fluid from a flow cell was directed into a flask that was placed upon a Mettler PM4000 balance. The fluid mass throughput was measure by recording the change in mass on the balance with respect to time.

The glass spheres were retained within the flow cells at each end by three polypropylene screens having mesh sizes of 149, 390, and 149. A threaded retaining plug, having 25 through holes, each having a diameter of 0.07 cm, was used at each flow cell end to compress the screens against the glass spheres. Each cell end was capped with a Swagelock SS-400-1-6ST fittings.

Pressure probes were positioned 10 cm apart in both packed beds. Each probe was a 0.159 cm diameter stainless steel tube that had two 0.09 mm wide by 4.2 mm long slit openings. The probes were positioned within the cells such that the slit centered the packed bed. The fluid pressure difference across the probes in each cell was measured using a Validyne DP15 differential pressure transducer with a number 48 diaphragm. The pressure transducers were previously calibrated by applying a hydraulic force across the transducers using a series of known weights. The electrical signals from a pressure transducer (bed fluid pressure drop) and the balance (mass of fluid) were recorded each second by a Camile, model 2000, process controller. The controller graphically displayed both signals as a function of time.

After fluid was forced through the rheometer system by fixing a nitrogen gas pressure, steady state conditions were detected when the Camile real-time plots of flow rate and pressure drop versus time were constant. This usually required about one minute. After the system reached steady state, the pressure drop across the packed bed and the flow rate was averaged for 30 seconds. These averages were then recorded. Thereafter a new nitrogen gas pressure was then set to force fluid through the rheometer at a different mass throughput and the above procedure repeated.

Usually about 12 throughput conditions were used to characterize the porous media flow properties of the solvent. Thereafter polymer solution was forced through the rheometer system over the same range of bed Reynolds numbers. Laminar fluid flow conditions were maintained in all tests by always having a bed Reynolds numbers less than 10.

After the polymer solution flow properties were measured, solvent was again forced through the rheometer. This was done to determine if any polymer had been retained in a packed bed. If the porous medium flow properties of the second solvent were significantly greater than the first solvent then additional solvent was forced through the rheometer until the second solvent offered the same porous medium flow resistance as the first solvent. This purging of a flow cell with solvent assured that the packed bed was free of polymer and thus could not affect the rheometer measurements on subsequent polymer solutions. After three sets of data were collected (solvent before polymer solution, polymer solution, and solvent after polymer solution), they were imported into a Mathcad 5.0 document where data analysis calculations were performed.

Results

Durst Plots

As shown by the Durst plots of Figures 11-2 and 11-3, all polymer solutions show the same generally expected ψ versus D_e relationship when using either cells # 1 or # 2. Recall that cell # 1 and cell

2 have uniform packed spheres with diameters of 297 and 149 microns, respectively. In these packed beds, a converging-diverging channel geometry exists over a distance scale that corresponds to the diameter of a sphere. This geometry forces the fluid velocity to accelerate and decelerate as it passes through the porous media and this produces cyclic extensional and compressional strains on the polymer coils.

As shown by both Figures, at Deborah numbers less than 0.1, ψ values are usually less than 4. As the Deborah number increases above 0.1, the ψ values increase to a maximum at a Deborah number of about 0.5. However, in contrast to previous observations [5] the ψ parameter decreases as the Deborah Number increases to values greater than 0.5. This reduction in the Normalized Flow Resistance at higher Deborah numbers is probably due to the diminished ability of polymer coils to convert kinetic energy to heat as they are extended and compressed at faster rates. At faster fluid flow conditions the polymer coils are not able to follow in concert with the rapidly changing local fluid flow fields because insufficient time is available for coil deformation during fluid acceleration and coil recovery during fluid deceleration. As a consequence, less total coil extension and compression is experienced each cycle and thus less energy is converted into heat by the macromolecules. Therefore the solution will have less resistance to flow through the porous medium at higher Deborah numbers.

Effects of Polymer Molecular Weight

When the polymer has a low molecular weight, very large fluid velocities are needed in a porous medium to achieve a Deborah Number greater than 0.1. This can be shown by using Figures 2a and 2b to compare the flow performance of low and high molecular weight NaAMB/AM copolymers. For these two copolymers to have the same Deborah Number flow conditions the fluid velocity of the low molecular weight copolymer has to be about 20 times larger than the high molecular weight copolymer. This is because for equal Deborah numbers the fluid velocities must scale to the ratio of the inverse of each copolymer response time (7.8 msec / 0.4 msec ≈ 20).

These results show that low molecular weight polymers would not have significant extensional flow resistance in reservoirs because the fluid velocities at typical flooding conditions away from the injection well are too low to cause coil extension. In contrast, a high molecular weight copolymer coil can be extended in the porous medium at much lower fluid velocity and therefore is better candidate for reservoir flooding.

As shown by Equation 2, the Normalized Flow Resistance, ψ, is directly proportional to the difference between solution and solvent friction factors, $f - f_s$, and is also inversely proportional to the product of the dimensionless concentration of polymer coils in solution, and solvent friction factor. The dimensionless concentration of polymer coils is the product of the polymer's mass concentration and its intrinsic viscosity, $C[\eta]$. Thus ψ is a measure of the increase in solution flow resistance as compared to solvent per dimensionless concentration of polymer coils in solution. Because higher molecular weight polymers have larger intrinsic viscosities than lower molecular weight polymers (coils occupy more volume per unit mass polymer) then less high molecular weight polymer mass is needed to have the same dimensionless concentration. Thus

less mass of a high molecular weight polymer is needed to achieve the same Normalized Flow Resistance, ψ, when compared to lower molecular weight polymer.

Effects of Copolymer Monomer Composition

Polymer molecular structure is also an important factor influencing solution flow resistance. Figures 3a through 3b show Durst plots of three different NaAMB / AM copolymers. The molecular weights of all three copolymers are about the same; however, the difference in copolymer monomer composition has greatly affected the expansion of the polymer coils. The NaAMB / AM 20 / 80 copolymer having 20% NaAMB monomer has an intrinsic viscosity of 46 dl / g. This intrinsic viscosity is 2.5 times greater than the other two copolymers. Also as shown by Table I, the 20 / 80 copolymer has macromolecular coils that are much larger in diameter than the other two copolymers. The 20 / 80 monomer composition has greatly expanded the polymer coils in solution.

When compared to the 3.3 million molecular weight AM homopolymer of Figure 2c, the 14 million molecular weight 20 / 80 copolymer of Figure 3c has a coil response time which is 26 times greater (26 msec versus 1 msec). Thus even at very low porous media fluid velocities the 20 / 80 polymer coils will experience elongation and therefore have a large resistance to flow.

Effects of Polymer Concentration

As shown by Figures 11-2 and 11-3, all the Durst plots, no matter the copolymer composition, are displaced upward as the copolymer concentration decreases. Figure 4 shows that the maximum in the Normalized Flow Resistance, ψ_{max}, of a Durst plot for any polymer solution has the following dependence on dimensionless polymer coil concentration, C [η].

$$\ln \psi_{max} = \alpha - \beta [\eta] C \qquad (7)$$

The values for α and β depend upon the copolymer type. The α parameter is the value of $\ln(\psi_{max})$ in the limit of zero polymer concentration. These parameters are important in predicting polymer performance when flooding a reservoir. A high α value suggests that the polymer solution would have a high fluid flow resistance in the porous medium even under the dilute conditions found at large distances away from an injection well. A large β value indicates a large decrease in the Normalized Flow Resistance as the polymer concentration increases. Near the injection well the polymer solution is concentrated. Thus a large β value would mean that less injection pressures would be required to force the polymer solution into the reservoir. Table II lists the α and β values for the copolymers used in this study. The NaAMB / AM 20 / 80 copolymer has properties that suggest it would be a superior reservoir flooding polymer.

General Flow Behavior of All Polymer Solutions

All the Durst plots have the same general relationship as given by Equation 8.

$$\psi = \exp(\alpha - \beta\,[\eta]C)\,\sin\left(\frac{\pi D_e}{2\gamma}\right) \qquad 0 < D_e < 2\gamma \qquad (8)$$

As shown by Equation 8, the polymer coils are greatly restricted from extension as the polymer concentration increases. Thus the Normalized Flow Resistance, ψ, decreases with increasing polymer concentration. The γ parameter used in Equation 8 is the Deborah number value when the Normalized Flow Resistance, ψ, is a maximum. As shown by Table II, most of the polymer system studied had a γ value between 0.4 and 0.8.

Conclusions

All the Durst plots show the same general behavior regardless of polymer type. At Deborah numbers less than about 0.1, the Normalized Flow Resistance is very low which indicates that almost no polymer coil extension and recovery is occurring under these conditions. At Deborah numbers between 0.1 and 0.8, the Normalized Flow Resistance increases to a maximum but then decreases as the Deborah number increases to higher values. This suggests that the degree of polymer coil expansion and recovery is at first accelerating under these conditions, then reaches a limit at a Deborah number of about 0.6. Above this Deborah number the polymer coils are probably not able to completely recover all of the large extensional strains developed during the first extension-recovery cycles and thus have less potential to extend in subsequent extension-recovery cycles. Therefore, at higher Deborah numbers the coils travel through the bed in a more extended state. They will have less and less recoverable extension as they travel from cavity to cavity. At very high Deborah Numbers, the polymers travel through the bed in a highly extended state, do not extend or recover as they pass from cavity to cavity, and no fluid kinetic energy is converted to heat. Thus, the Normalized Flow Resistance should decrease to zero in the limit of high Deborah numbers.

Of all the polymers examined, the NaAMB / AM 20 / 80 copolymer solutions had the greatest porous media flow resistance. This is because the polymer coils of these macromolecular structures are greatly expanded and can elongate and recover in extensional flow fields having low average fluid velocities.

Summary

In summary, use of high molecular weight, highly expanded copolymers (such as the NaAMB / AM 20 / 80 shown in Figure 3c) versus lower molecular weight polymers that are not greatly expanded (such as the AM homopolymer shown in Figure 2c) has a dual advantage in reservoir flooding. Solutions of larger molecular weight macromolecules with expanded polymer coils not only require less polymer mass for a given fluid flow resistance but this resistance is experienced at lower flow rates through the porous media. They are effective flooding agents even at low concentrations. Thus the 20 / 80 copolymer has a significant economic advantage.

References

1. McCormick, C. L. , K. P. Blackmon, *J. Poly. Sci., Poly. Chem., A24,* 2635, **1986.**

2. McCormick, C. L., K. P. Blackmon, D. L. Elliott, *J. Poly. Sci., Poly. Chem, A24,* 2619, **1986.**

3. Hester, R. D. and C. L. Flesher, Chapter 10 of this Report, **1994.**

4. McCormick, C. L. and R. D. Hester, "Responsive Copolymers for Enhanced Petroleum Recovery," DE-AC22-92BC-14882, Quarterly Technical Progress Report, June 22, **1993.**

5. Durst, F. and R. Haas, *Rheol. Acta.* **1981**, *20*, 179.

6. Hester, R. D., L. M. Flesher, C. L. McCormick, "Polymer Solution Extensional Viscosity Effects During Reservoir Flooding," 9th Symposium on Improved Oil Recovery, *Proceedings, Volume 2*, 447, April, **1994.**

Table 11-1
NaAMB/AM Copolymer Solution Properties at 25 °C Using 0.514 M NaCl Aqueous Solvent

Copolymer Monomer Molar Ratio	Intrinsic Viscosity	Diffus-ional Coeff.	Hydo-dynamic Radius	Radius of Gyration	Weight Average Mol. Weight	Second Viral Coeff.	Polymer Coil Response Time
NaAMB : AM	$[\eta]$	$D_{true} \times 10^8$	R_h	R_g	$M \times 10^6$	$A_2 \times 10^4$	τ
dimensionless	dl / g	cm^2 /sec	Å	Å	g / mole	ml mole / g^2	sec x 10^3
0 : 100	7.2	--	--	--	3.3	--	1.0
5 : 95	17	1.3	1800	2950	12	2.8	8.3
10 : 90	4.8	--	--	--	1.9	--	0.4
10 : 90	18	5	460	--	11	--	7.8
20 : 80	46	0.68	3400	3700	14	3.1	26.2

Table 11-2
α, β and γ Values for Solution Flow in Cell #1

Copolymer Monomer Molar Ratio NaAMB : AM	α value	β value	γ value
0: 100	3.18	3.85	0.5
05: 95	3.68	0.88	0.3
10 : 90	3.38	1.22	0.6
20 :80	4.36	0.91	0.6

Figure 11-1. Porous Media Elongational Flow Rheometer System

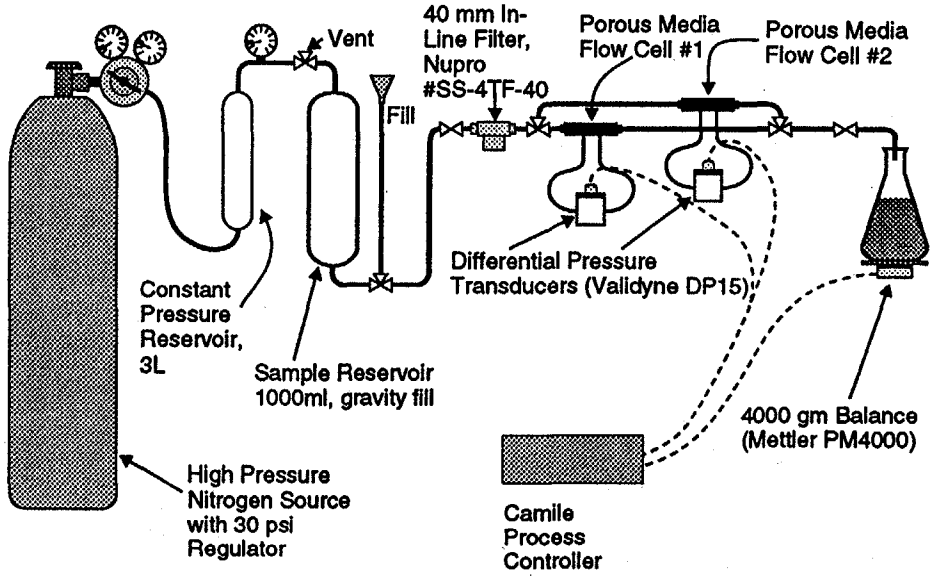

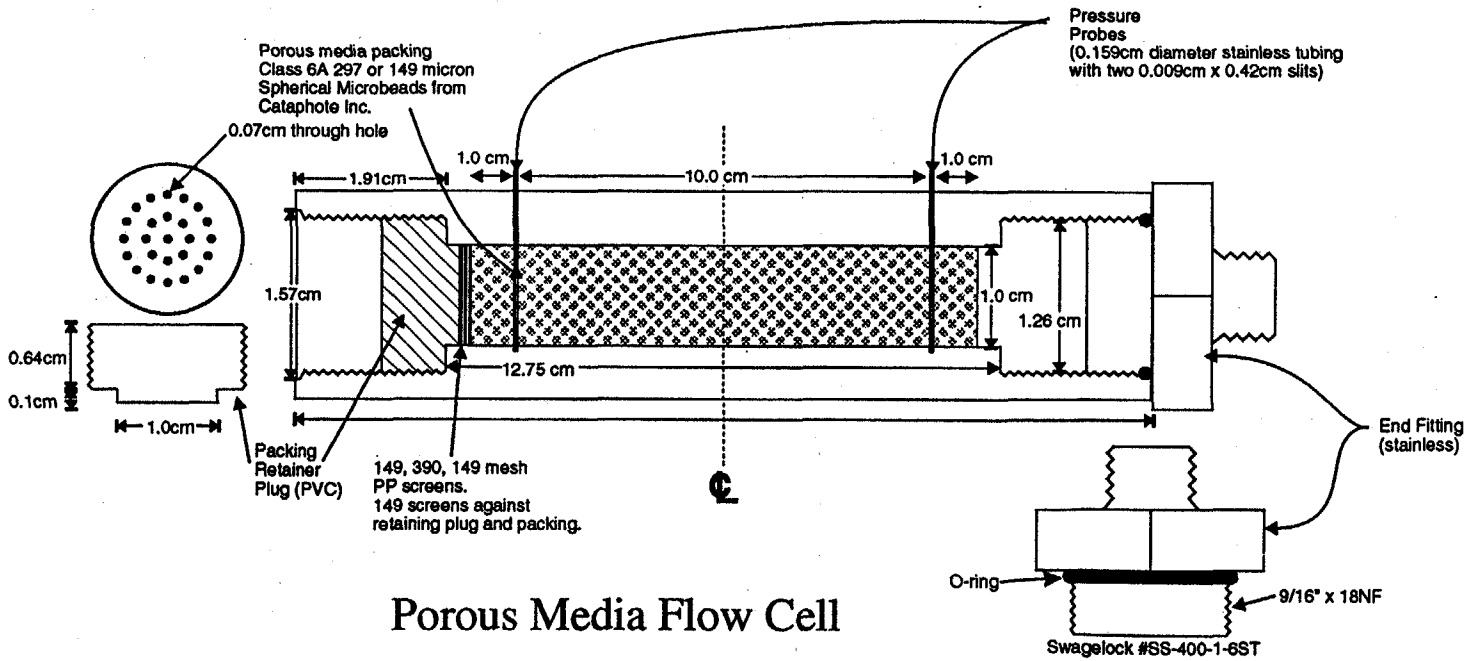

Porous Media Flow Cell

Figure 11-2. Flow Resistance of 3-Acrylamido-3-Methylbutanoic Acid--Acrylamide (Mole Ratio of 1:9) Copolymers and Polyacrylamide Homopolymer Solutions

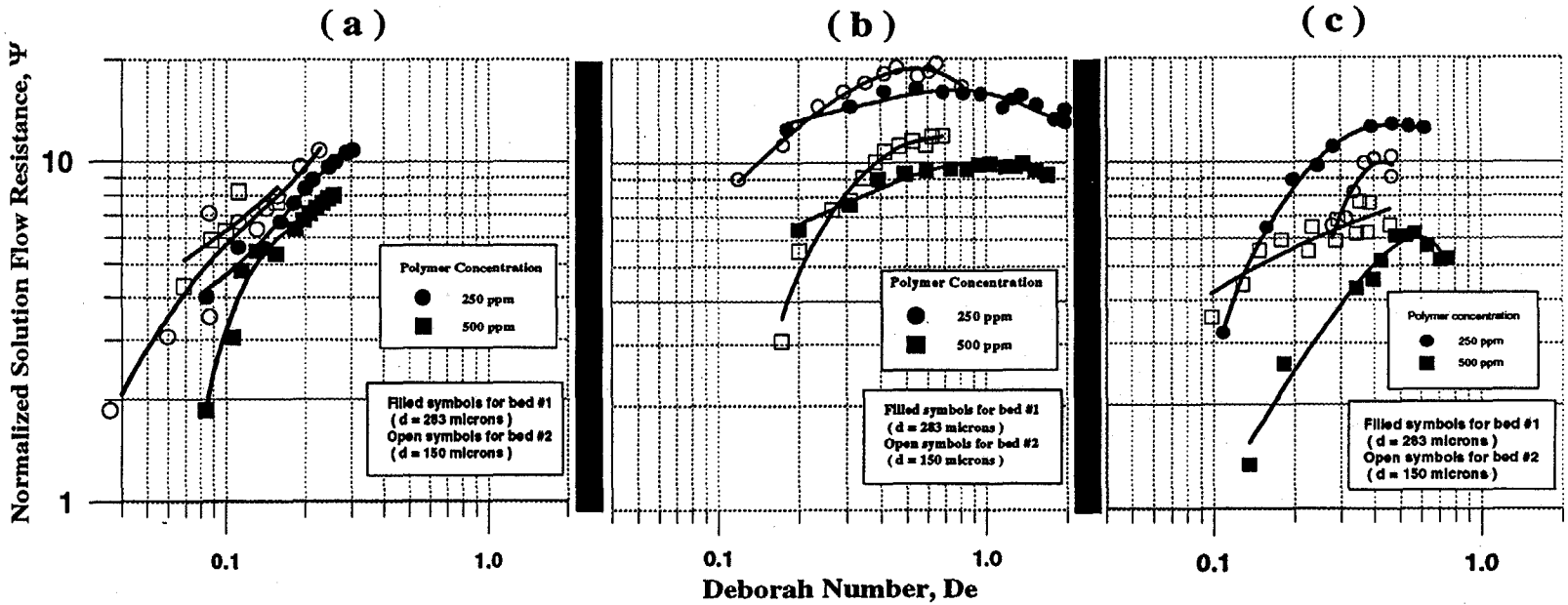

NaAMB/AM 10/90 Copolymer in 0.5 M NaCl solvent
Weight average molecular weight = 1.9 x 10^6 g / mole
Intrinsic viscosity = 4.8 dL / g
Polymer Coil Response Time = 0.4 millisec

NaAMB/AM 10/90 Copolymer in 0.5 M NaCl solvent
Weight average molecular weight = 10.9 x 10^6 g / mole
Intrinsic viscosity = 17.7 dL / g
Polymer Coil Response Time = 7.8 millisec

AM Homopolymer in 0.5 M NaCl solvent
Weight average molecular weight = 3.3 x 10^6 g / mole
Intrinsic viscosity = 7.2 dL / g
Polymer Coil Response Time = 1.0 millisec

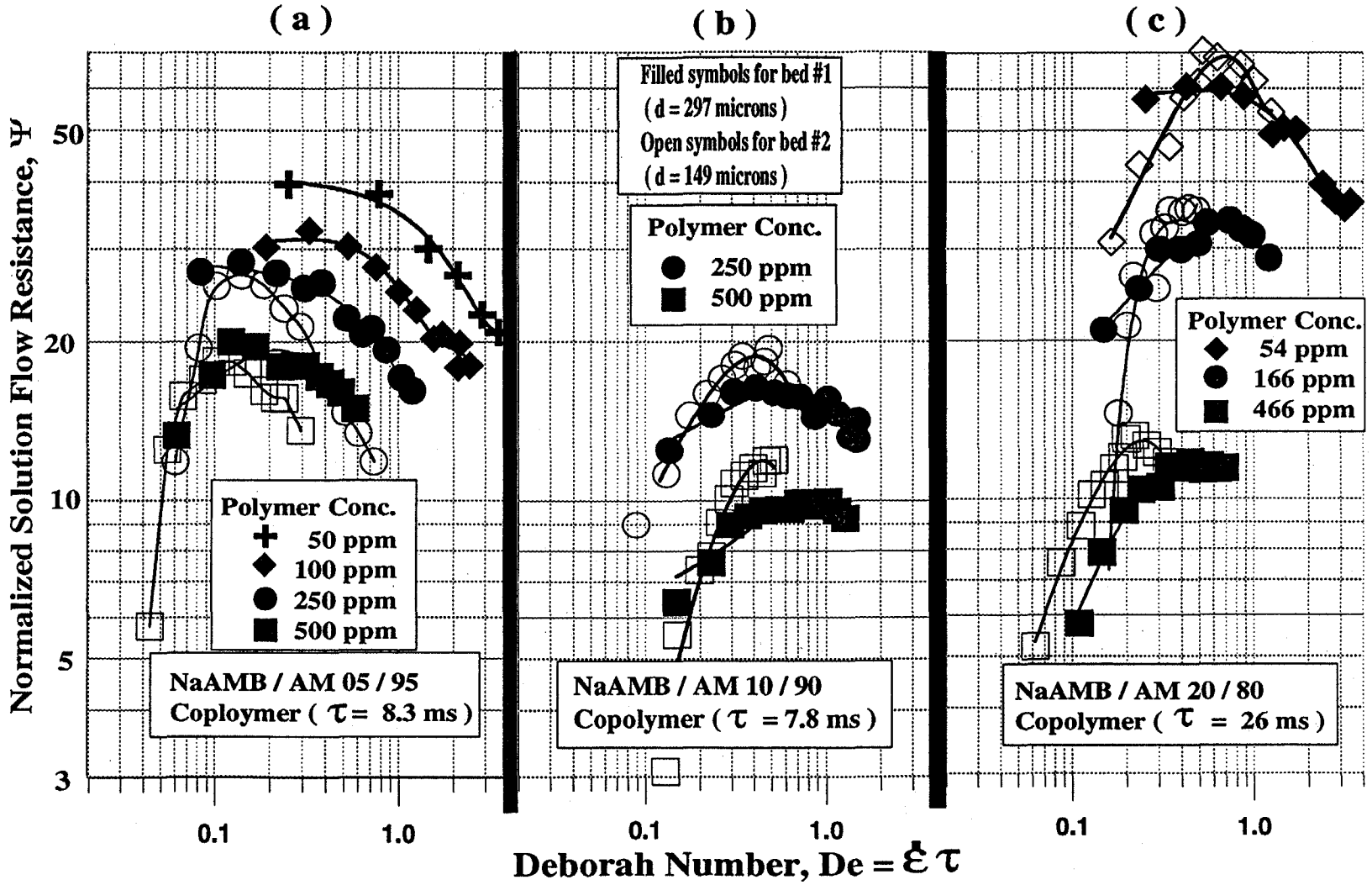

Figure 11-3. Durst Plots Showing Flow Resistance of 3-Acrylamido-3-Methylbutanoic Acid--Acrylamide Copolymer Solutions Through Packed Beds at 25 °C

°C

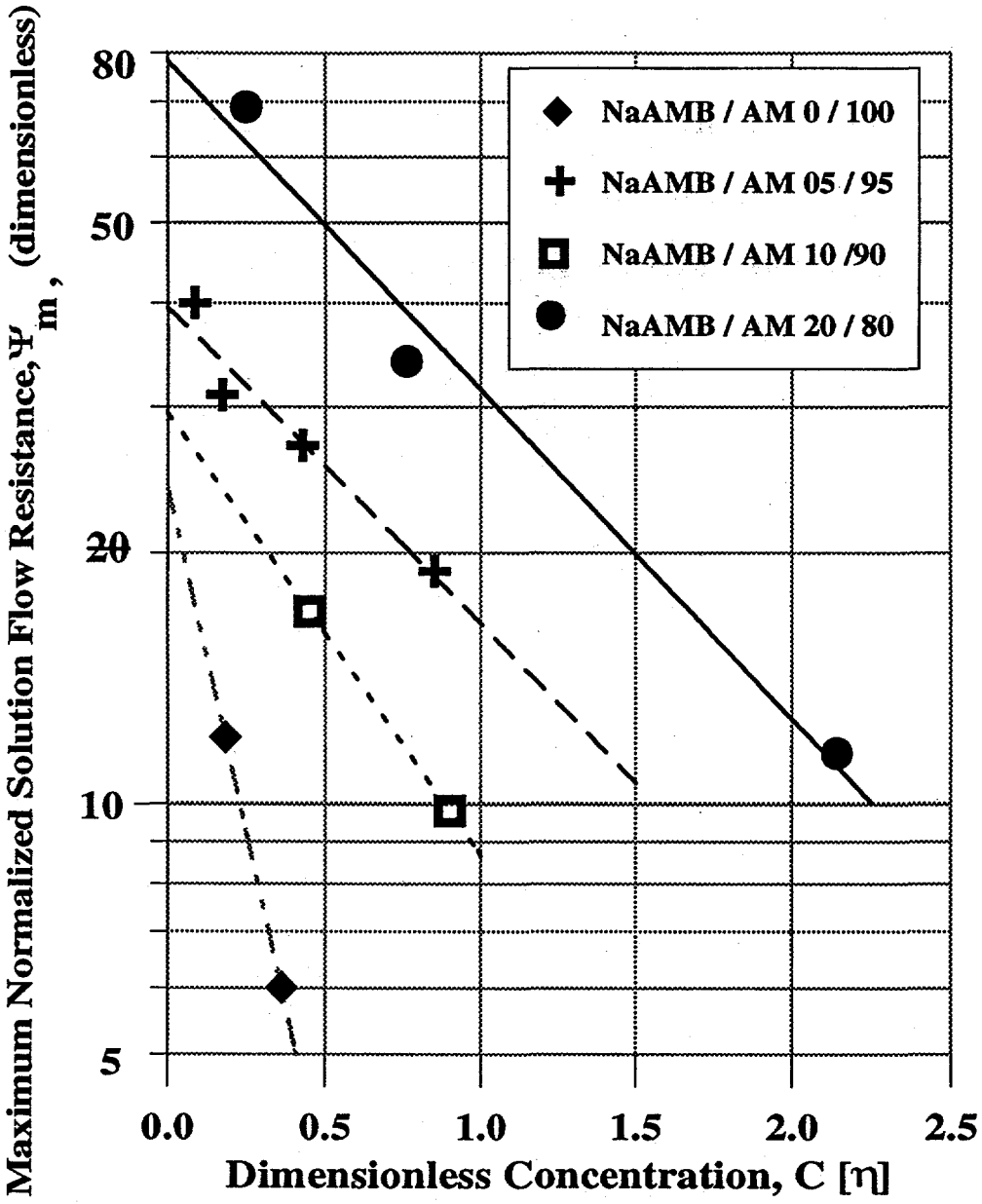

Figure 11-4. Dependence of the Maximum Normalized Flow Resistance on Dimensionless Polymer Concentration

☆U.S. GOVERNMENT PRINTING OFFICE: 1995 - 660-029/20018